MODELING AND CONTROL OF PASSIVE CHILLED BEAMS WITH UNDERFLOOR AIR DISTRIBUTION OF VENTILATION IN OFFICE BUILDINGS IN HUMID CLIMATES

A Dissertation

by

VANITA KISHORE NEGANDHI

Submitted to the Office of Graduate and Professional Studies of
Texas A&M University
in partial fulfillment of the requirements for the degree of

DOCTOR OF PHILOSOPHY

Chair of Committee, Charles H. Culp
Committee Members, David E. Claridge
Jeff S. Haberl
Louis Tassinary
Head of Department, Ward V. Wells

August 2015

Major Subject: Architecture

ABSTRACT

This dissertation presents the results of a study to determine the operational control, energy performance and comfort conditions associated with passive chilled beams for office buildings in a humid climate and to develop a method for the modeling of passive chilled beams with a ventilation system and underfloor air distribution (UFAD).

For the analysis, a 606,900 ft^2 commercial office building in ASHRAE climate zone 3A with passive chilled beams and a ventilation system with UFAD was selected as the case-study building. In the first step, measured data from the building was used to develop a calibrated whole-building energy analysis model in EnergyPlus 8.1. The energy model also implemented methods to model the controls found in a passive chilled beam system with underfloor air distribution. A simplified steady-state energy model was also developed for the validation of the EnergyPlus model and for energy use prediction.

In the second step, two methods of optimization for the operational control strategies were tested: a simplified rule-based optimization and a model-based predictive control optimization. The influence of these two approaches to optimization on HVAC energy savings and thermal comfort were found to be within 2% of each other.

Finally, summertime stratification measurements were taken in the offices and were combined with a CFD model of a single zone in Star CCM+ 9.04 to establish temperature and airflow profiles in the zones. These comfort studies were conducted for the cooling season only and showed that the thermostat setpoints are not fulfilled in the

exterior zones in summer and chilled beam and ventilation system interact with each other and have an adverse effect on the overall system energy efficiency.

The results of the research show that if properly controlled, a passive chilled beam system with a parallel ventilation system has the potential for HVAC savings of 14-24% over standard VAV systems in office buildings in humid climates. All of the HVAC energy savings come from fan and reheat energy. Energy savings are affected by latent loads and ventilation requirements in the zones and the potential for the use of an economizer. Indoor humidity levels are also higher with a passive chilled beam system than a standard VAV system. Independent control of the volume of air supplied by the ventilation system and the supply air temperature is necessary to achieve the predicted energy savings.

Lastly, the summertime zone comfort studies reveal that the presence of the UFAD ventilation system hinders the natural downward plumes from the chilled beams and the presence of the chilled beam system inhibits stratification in the zones. Because of the lower ventilation flow rates associated with the chilled beams, there is significant increase in the temperatures in the supply plenums.

DEDICATION

To my father

ACKNOWLEDGEMENTS

I would like to thank several people without whose support this dissertation would never be completed. First and foremost, I am indebted to my advisor, Dr. Charles Culp for his guidance and support during the entire duration of my Ph.D. In addition to lending his expertise and knowledge to my research, he has also been a mentor in my professional development and has pushed me to challenge myself at every step of the way. I would also like to acknowledge my committee members, Dr. David Claridge, Dr. Jeff Haberl and Dr. Louis Tassinary for their valuable inputs that have enhanced the quality of my research.

I am grateful to Steve Connelly at Command Commissioning and the building operation personnel at the case-study building for assisting me with my data collection and patiently answering all my questions. Acknowledgements also go out to the Energy Systems Laboratory, the CRS Center and the Energy Institute at Texas A&M University for their significant financial support.

Next, I would like to thank my friends at ESL for being the perfect sounding board for my sometimes confused ideas, my father for teaching me to strive to be the best person I could ever be, my mother for the endless nights she stayed awake with me while I completed my assignments and my sister for always being the voice of reason. Lastly, I am forever grateful to my husband, for believing in me even when things kept going awry and for being my best friend and emotional support.

NOMENCLATURE

k	turbulence energy
ε	dissipation rate of turbulence energy
y_i	data used for the calibration
$\hat{y}_i$	mean of the measured data
EE	elementary effects
μ_i	mean of the elementary effects
σ_i	standard deviation of the elementary effects
U_1, U_2, s1,s2	user-defined constants used for the optimization penalty function
P_{beam}	beam cooling output per unit length
K	beam heat transfer coefficient
$v\rho$	room air mass flow rate across beam
Q_{in}	room air volumetric flow rate per unit length of beam
A	beam coil surface area per coil length
α_0	free area of the beam in plan view per unit beam length
Q_{pr}	supply air flow rate per unit length of beam
ω	beam water velocity
K_{in}	coefficient of induced air through the beam
ΔT	difference between the room air temperature and average beam water temperature

K_1, n, n1, n2, n3, α	chilled beam coefficients based on beam geometry
P_w	beam water side cooling power
P_{air}	beam air side cooling power
$Q_{w,beam}$	water mass flow rate per beam
L_{beam}	length of beam
$T_{w,in}$	beam inlet water temperature
$T_{w,out}$	beam outlet water temperature
N	CO_2 generation rate per person
$C_{setpoint}^{t}$	zone air CO_2 concentration setpoint
C_∞	CO_2 concentration in the outside air
P_z	number of persons in the zone
$m_{OA,z}$	outside air mass flow rate
$\dot{m}_{inf}$	infiltration air mass flow rate
C_z^t	zone air CO_2 concentration at current timestep
V_z	zone volume
C_{CO2}	CO_2 capacity multiplier
C_{zi}	CO_2 concentration in the zone air being transferred to the zone
$\sum_{i=1}^{N_{sl}} kg_{mass_{sched}}$	sum of scheduled internal CO_2 loads
$V_{OA,v}$	volume of outside air to fulfill ventilation requirements
$V_{SA,v}$	volume of supply air to fulfill ventilation requirements
$V_{OA,l}$	volume of outside air to fulfill latent requirements

$T_{ZA,sp}$	zone temperature setpoint
$T_{SA,sp}$	supply air temperature setpoint
$T_{CC,sp}$	cooling coil leaving temperature setpoint
ΔT_{RF}	temperature rise across the return fan
ΔT_{SF}	temperature rise across the supply fan
$Q_{z,l}$	zone latent load
$HR_{ZA,sp}$	zone humidity ratio setpoint
$HR_{SA,sp}$	supply air humidity ratio
q''_{LWX}	net longwave radiant exchange flux between zone surfaces
q''_{LWS}	longwave radiation flux from equipment
q''_{SW}	net shortwave radiation flux from lights
q''_{sol}	transmitted solar radiation flux
q''_{conv}	convective heat flux to zone air
q''_{ki}	conduction flux through wall
$q_{i,j}$	longwave radiation exchange between surfaces
$F_{i,j}$	longwave radiative coefficient
h_c	convection coefficient
Z_o	outside CTF coefficient
Z_j	inside CTF coefficient
ϕ	flux CTF coefficient
Y	cross CTF coefficient
δ	timestep

Abbreviations

CTF	Conduction Transfer Function
HVAC	Heating, Ventilating and Air-Conditioning
SDVAV	Single-Duct Variable Air Volume
VAV	Variable Air Volume
CV	Constant Volume
DOAS	Dedicated Outdoor Air System
UFAD	Underfloor Air Distribution
AHU	Air Handling Unit
FCU	Fan Coil Unit
CRAC	Computer Room Air Conditioning
COP	Coefficient of Performance
MEP	Mechanical, Electrical and Plumbing
OA	Outside Air
SA	Supply Air
RA	Return Air
MA	Mixed Air
BA	Bypass Air
EA	Exhaust Air
DBT	Dry-Bulb Temperature
RH	Relative Humidity
Pr.	Pressure

DP	Dew Point
SP	Setpoint
TMY	Typical Meteorological Year
AMY	Actual Meteorological Year
EMCS	Energy Management Control System
CFD	Computation Fluid Dynamics
RTD	Resistance Temperature Detector
NMBE	Normalized Mean Bias Error
CV(RMSE)	Coefficient of Variation of Root Mean Square Error

TABLE OF CONTENTS

Page

LIST OF FIGURES

Page

LIST OF TABLES

Page

CHAPTER I

INTRODUCTION

1.1. Background

The role of the Heating, Ventilating and Air-Conditioning (HVAC) system in buildings is three-fold; to heat and cool spaces for thermal comfort, to provide adequate outside air to fulfill ventilation requirements and to exhaust unwanted air from a zone. The cooling of spaces can include both sensible cooling for temperature control and latent cooling for moisture control. In traditional HVAC systems, all these diverse requirements such as cooling, heating, moisture removal and ventilation are tackled at the same time by a single air-based system (ASHRAE 2012). Typically, return air from the zones is mixed with a certain percentage of outside air for ventilation and is then cooled to around 55°F for moisture removal. Supply air volume control and reheat (if necessary) are used for temperature control at the zone level (Roth et al. 2002, ASHRAE 2012). This approach to air conditioning in buildings has been well documented and is effective at achieving comfort conditions in buildings (Grondzik 2007, Kreider 2010). However, it can also be energy intensive, especially when latent loads are high (Brandemuehl and Katejanekarn 2004), and sometimes does not guarantee required ventilation rates for individual zones in the building (Chamberlin et al. 1999).

Over the past decade, in the pursuit of the next level of energy efficiency in buildings, there has been growing interest in alternate approaches to heating, cooling and ventilation. One of the prominent areas of HVAC research that has re-emerged has been

the decoupling of the various functions of the HVAC system and the utilization of separate equipment to fulfill each requirement individually with greater efficiency than a single combined HVAC system (Mumma 2001, Khattar and Brandemuehl 2002, Morris 2003). This approach typically involves a dedicated ventilation system that handles both ventilation and latent loads and a separate system that handles heating and sensible cooling (Mumma 2001). Chilled beams, which are exposed water-cooled coils located directly in spaces and supplied with chilled or hot water, have often been employed as the sensible cooling and heating system (Roth et al. 2007). There are several types of chilled beams; passive two-pipe beams, active two-pipe beams, active four-pipe beams, active beams with VAV primary air and even radiant chilled ceilings, walls and floors (Rumsey 2010). Figure 1.1 shows the possible configurations that can be specified while designing an HVAC system with chilled beams and a parallel ventilation system. Chilled beams require no additional fans and exchange energy with the spaces solely through natural or induced convection resulting in fan power savings (Roth et al. 2007, Rumsey 2010). In a space equipped with chilled beams, the quantity of primary air supplied to the spaces is 50-60% lower than an equivalent VAV system, resulting in fan and reheat energy savings. Chilled beams also employ higher supply chilled water temperature and, as a result, can use the return water from the primary ventilation system for sensible cooling. This results in a higher temperature difference between the return and supply chilled water and a more efficient chiller performance. Due to all these reasons, chilled beams have been reported to have energy savings in the 15-40% range (Roth et al. 2002).

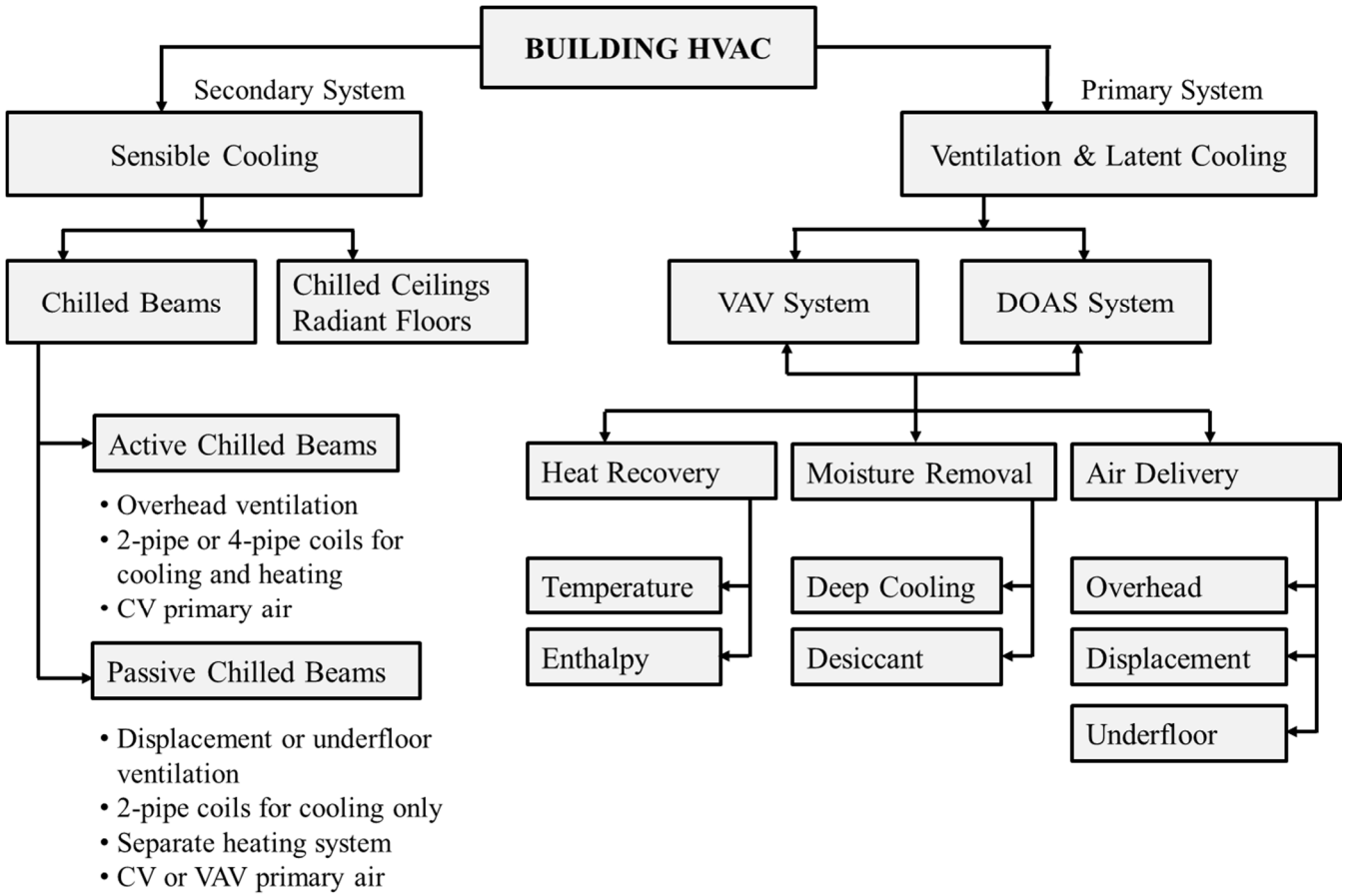

Figure 1.1: Components in a Decoupled Ventilation and Sensible Cooling System (compiled from Mumma (2001), Roth et al. (2007) and Virta et al. (2007))

However, there are challenges associated with the design, implementation, performance and operation of chilled beams in buildings. These systems aren't always more energy efficient than VAV systems. They can consume more energy in buildings with high latent loads and ventilation requirements (Stetiu 1998, Novoselac and Srebric 2002, Stein and Taylor 2013). Operational strategies for humidity control may also be energy intensive and compromise thermal comfort (Vangtook and Chirarattananon 2006). Optimization of operational control to achieve greater energy savings is currently in the research realm (Mossolly et al. 2008, Ge et al. 2011) and information on implementation and performance in real buildings is scarce. Humid climates pose additional challenges such as condensation risks, humidity control, inadequate cooling during the peak of summer and draughts causing discomfort at lower beam temperatures (Vangtook and Chirarattananon 2006).

Another major challenge is adequate whole-building energy simulations of these systems (Betz et al. 2012). The systems are time-consuming to model and a high level of expertise in energy simulation software is required. In addition, many whole-building energy simulation programs are unable to model the various permutations of the systems discussed in Figure 1.1 with advanced operational controls to reasonably predict energy use (Betz et al. 2012). Stratification, if employed, is not factored into chilled beam energy calculations. Induced chilled beam airflow estimates that play a major part in the designing of chilled beams and comfort conditions in the spaces require separate CFD models (Koskela et al. 2010, Nelson 2012).

1.2. Research Objectives

Given the challenges associated with the chilled beams discussed in Section 1.1, the three major objectives of this research were to:

- Analyze operational control strategies, energy performance and comfort conditions for passive chilled beams in a real building in a humid climate using measured data. Determine the conditions under which a chilled beam system is more energy efficient that an equivalent VAV system.
- Develop a detailed whole-building energy analysis model in a widely available hourly simulation program for passive chilled beams with an outside air ventilation system and underfloor air distribution. Develop a simplified, steady-state energy model based on first principles for more rapid energy use prediction with acceptable accuracy.
- Propose new operational control strategies that can be implemented in a building EMCS and document their effect on energy savings through simulations.

These objectives were achieved in the following steps:

1. A literature review of chilled beams, dedicated ventilation systems, and air distribution methods that are applicable to humid climates was conducted.
2. A real building with chilled beams in a humid climate was used as a case-study for the research. Measured data was collected from the case-building and included physical building and HVAC system descriptions, load characteristics, sequences of operation, EMCS trend data for the zones, Air Handling Units (AHU) and plant and zonal air stratification measurements.

3. A detailed calibrated energy analysis model of the building was developed in EnergyPlus. A simplified steady-state energy model based on first principles was also developed for more rapid energy use prediction. The models have the capability to control the ventilation system based on outside air requirements and humidity control. Effects of Underfloor Air Distribution (UFAD) such as increase in supply and return plenum temperature and zonal air stratification on the energy balance was also included. Thermal comfort predictions included temperature and humidity estimates at different load conditions.
4. The energy use of the building under varying loads and operational conditions was compared to an equivalent VAV system baseline and an ASHRAE 90.1 code-compliant building.
5. Optimization strategies were developed for the building. They included the following steps:
    a. A sensitivity analysis of the operational control variables obtained from the literature was conducted to rank them by their impact on energy use.
    b. Energy saving optimization strategies were proposed, considering the interactions between the ventilation system and the chilled beams.
    c. The impact of these strategies on energy use and comfort was documented.

1.3. Significance of the Study

This research is significant because it adds to our understanding of the issues associated with the operation of chilled beams in real buildings in humid climates. It is

especially important because it focuses the following topics that have not been addressed in current literature:

- Development of a simulation-based method for predicting whole-building energy use for buildings with both passive chilled beams with UFAD ventilation. Development of a steady-state method to estimate energy use using minimal input information without sacrificing the interactions between the various sub-components of the total HVAC system.
- Clarification of building loads and operating conditions under which chilled beams are more energy efficient than VAV systems in humid climates.
- Ranking of the control variables in a passive chilled beam system that have the most significant impact on the building energy use. Recommendations for the optimization of these control variables and the effect of these controls on space comfort conditions.
- Clarification of summertime zone comfort conditions in real buildings and interactions between the ventilation system and the chilled beams through stratification measurements and CFD-based models.

1.4. Limitations of the Study

The research was conducted within the following boundaries:

- The study is focused on office buildings with a specific HVAC system configuration: passive chilled beams and a ventilation system with underfloor air distribution.
- The study was carried out in a specific climate zone 3A, i.e. a warm and humid climate. The strategies proposed apply to other climates, but energy savings estimates will vary.

- Key assumptions for the energy analysis model include isothermal zone surfaces, single zone node temperatures, pressure and humidity.
- The proposed operational strategies only address hourly response times for the various components in the HVAC system. Real-time system interactions are not explored.

1.5. Organization of the Dissertation

This dissertation is organized into nine chapters:

Chapter I introduces the research and includes a background outlining the need for the research, the research objectives and expected contributions from the study.

Chapter II documents existing literature relevant to the research and identifies areas that have not yet been explored. The topics of the literature reviewed include: an overview on chilled beams, dedicated ventilation systems and air distribution methods, energy use and thermal comfort for chilled beam systems, operation and control for chilled beams, chilled beam modeling and control optimization used in building HVAC systems.

Chapter III describes the methodology applied in this research. It includes the building data collection, development of the calibrated EnergyPlus model, the simplified energy model, modeling of the real building controls and the method to optimize strategies for the HVAC system.

Chapter IV includes details of the simulation modeling of the primary system and the chilled beams and details of the calibration of the EnergyPlus model to the building energy use.

Chapter V includes simplified numerical models for demand control ventilation, primary system control, underfloor air distribution and the chilled beams.

In Chapter VI, the energy use of the building is evaluated against an equivalent VAV system and an ASHRAE 90.1 code-compliant model of the building. The influence of factors such as ventilation rates, latent loads in the building and climatic conditions on potential energy savings is also discussed.

Chapter VII provides details of the control optimization process and the resulting energy savings and thermal comfort conditions. The control optimization process includes the sensitivity analysis of the operational control parameters and the results of the rule-based and the model-based optimization.

Chapter VIII includes measured temperature profiles in the zones. These temperature measurements are supplemented by the results of the CFD model which also provides the airflow profiles in the zone. This chapter also documents the interactions between the two systems and their effect on system performance and thermal comfort.

Chapter IX presents the conclusions of this research and includes recommendations for operation and energy use prediction of chilled beams in humid climates.

CHAPTER II

LITERATURE REVIEW

The literature review relevant to this research can be divided into 5 categories:

1. decoupled ventilation with water-based sensible cooling;
2. energy use and thermal comfort of chilled beams in buildings;
3. operational strategies used for chilled beams;
4. tools used to model energy use and thermal comfort for chilled beams with parallel outside air ventilation systems; and
5. optimization methods in building HVAC control.

2.1 Decoupled Ventilation and Water-Based Sensible Cooling Overview

Typically, in a zone being conditioned by parallel water and air systems, the latent and sensible loads are decoupled such that the ventilation system supplies the required outside air and controls space humidity and the water based system meets the sensible load (Mumma 2001, Roth et al. 2002). Section 2.1.1 and 2.1.2 provide an overview of the two main sub-systems; chilled beam cooling and heating, and the dedicated ventilation system.

2.1.1 Chilled Beam Cooling and Heating

The general principle behind chilled beam cooling and heating is the use of chilled or hot water to move heat to and from the zones and heat transfer to the space occurs by convection and radiation. Depending on the percentage of radiant heat transfer to the space, the systems can be classified as radiant or convective. In chilled beams (both active

and passive), heat transfer from the space to the beam is largely convective (either natural or induced convection), while in chilled ceilings or radiant slabs and floors, heat transfer is both radiant and convective with a 40/60% radiant/convection capacity split (Roth et al. 2002, ASHRAE 2012).

Chilled beams reduce the need to condition and deliver air to spaces for sensible heating and cooling by utilizing chilled water coils that transfer heat from the spaces via convection and radiation. Passive chilled beams are typically cooling coils that are suspended from the ceiling and use natural convection to exchange heat with the air that comes in contact with them. Active chilled beams, on the other hand, have built-in ventilation nozzles which supply ventilation air through the beams to the space. The ventilation supply air provides additional forced convection that induces room air through the beams to achieving greater cooling capacity (Roth et al. 2007, Rumsey 2010). Chilled beams provide sensible cooling and have to be used with separate ventilation systems to fulfill outside air requirements and latent cooling (Roth et al. 2007). A passive chilled beam system will typically be combined with an underfloor or displacement distribution of the ventilation system so as not to interfere with the beam plumes and the reduction in the cooling capacity of the beams (Virta et al. 2007). Figure 2.1 and Figure 2.2 show the typical components of a passive chilled beam system with a parallel ventilation system and underfloor air distribution. Active chilled beams have in-built ventilation nozzles, which allow them to use the typical overhead ventilation distribution. Studies suggest that chilled beams have the potential to reduce HVAC energy use by 25-30% due to reduction in air moving power and higher evaporator temperature of the chiller supplying water to

the chilled beams (Roth et al. 2002, Virta et al. 2007). Energy use studies of overall parallel air-water HVAC systems will be discussed in Section 2.2.

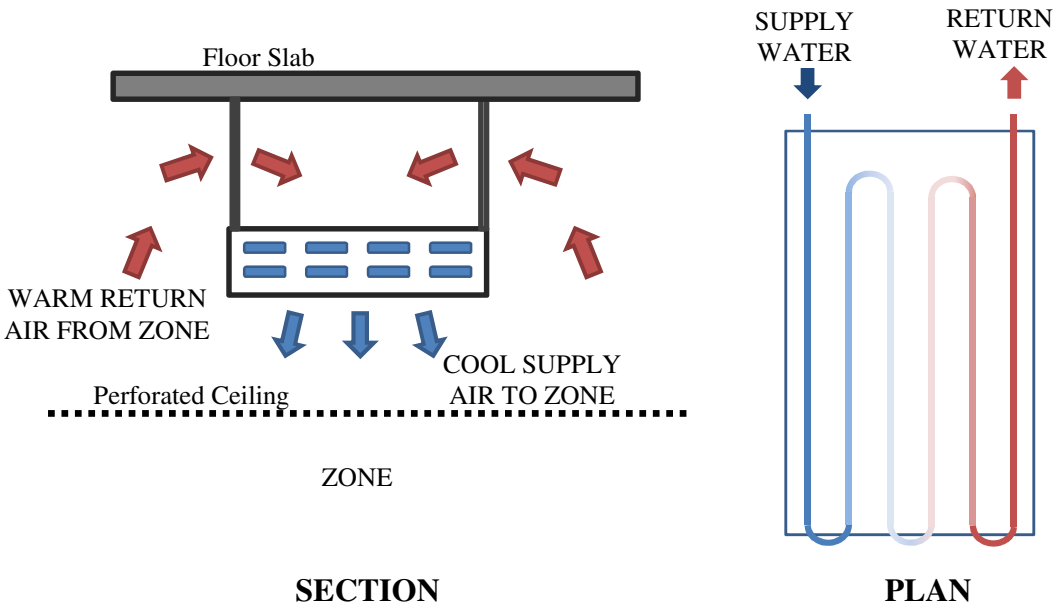

Figure 2.1: Detail of a Typical Passive Chilled Beam Showing Direction of Air and Water Flow

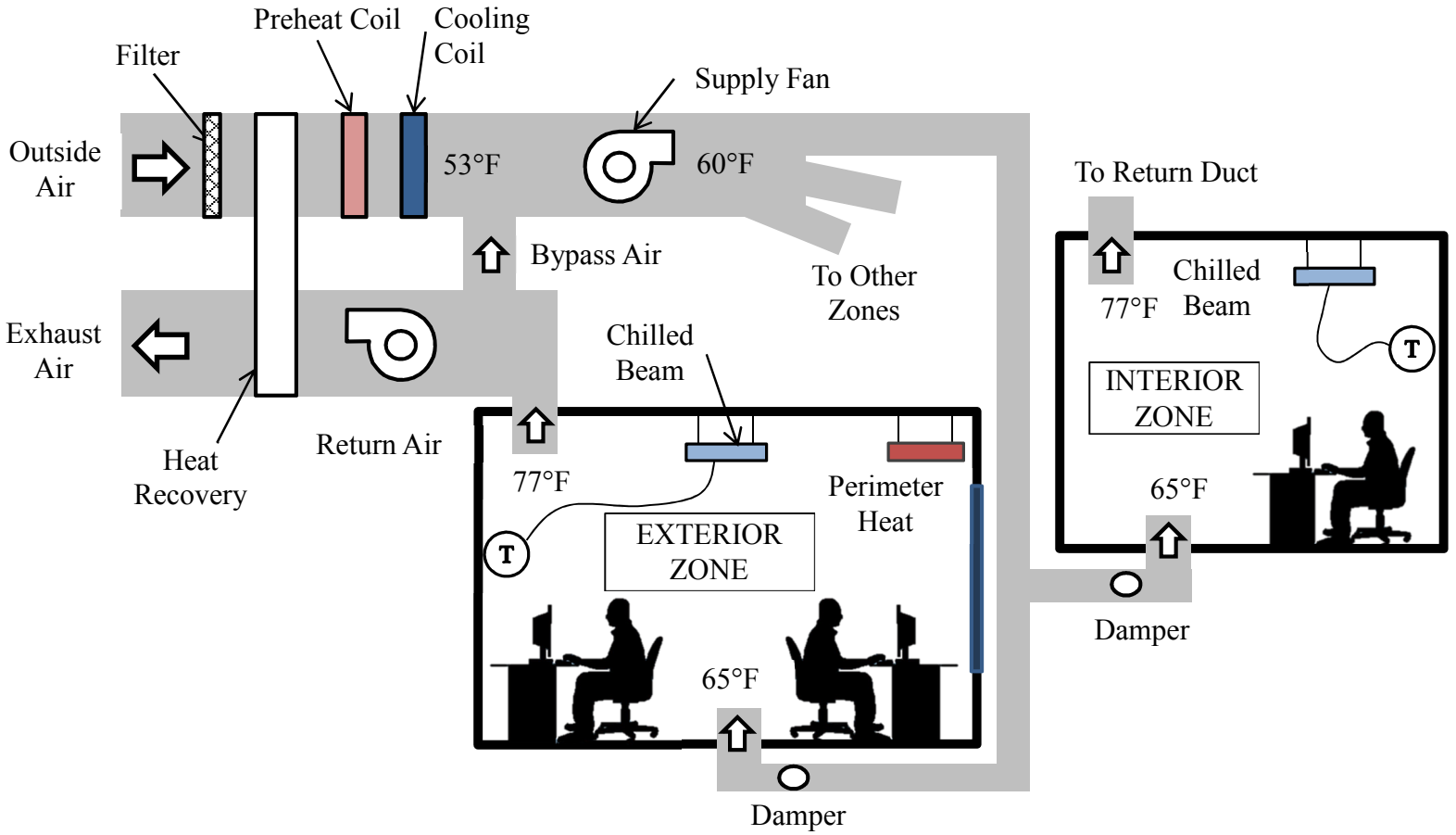

Figure 2.2: Components of a Typical Passive Chilled Beam System with a Parallel Ventilation System and Underfloor Air Distribution of Ventilation Air

Valance cooling units, a predecessor of chilled beams, are similar to chilled beams with two or four-pipe units that are mounted in architectural enclosures above windows near the ceilings in the zones. They are identical to chilled beams with hydronic coils supplied with chilled or hot water and cool or heat the zone air through induction without fans or blowers. However, unlike chilled beams, in valance units, latent cooling of the air is also allowed and drain pans are used to collect condensation. In addition, outside air can also be potentially drawn into the units from the windows to fulfill ventilation requirements (McGuinness 1960, Lechner 2001). Valance units have been used for both residential and smaller commercial buildings and are preferred for building retrofits as no ductwork and AHU units in the building are required (McGuinness 1964). However, there are risks of mold forming in the drain pans of the valance cooling units from the condensate water accumulated (Lechner 2001).

Chilled ceilings and radiant floors are similar to chilled beams but radiation is a more significant mode of heat transfer in these systems. Chilled ceilings have lower cooling capacities than chilled beams and are often combined with ventilation systems that deliver air through displacement ventilation to avoid draughts and thermal discomfort at cooling loads higher than the capacity of the chilled ceilings (Virta et al. 2007, Ghaddar et al. 2008). Chilled ceilings have slower response time to changes in building loads than chilled beams, but response times are also related to the structure and mass of the slab with the embedded chilled pipes (Babiak et al. 2009).

Comfort analysis is an important aspect of the design, implementation and operation of chilled beams. Studies have been conducted to assess factors influencing air

distribution and temperature profiles in buildings with chilled beams, chilled ceilings or radiant floors. Design considerations such as placement of beams relative to heat sources, windows and obstructions to airflow patterns influence both chilled beam performance and space comfort (Melikov et al. 2007, Zboril et al. 2007, Koskela et al. 2010, Nelson 2012). However, knowledge about the impact of operational setpoints on thermal comfort conditions in the spaces is limited. Loudermilk (2009) discusses best practices for operational control to avoid thermal discomfort but there is a lack of information on effects of control parameters such as air and water temperature, flow rate and velocity on local airflows and temperature profiles in spaces.

2.1.2 Ventilation Systems and Air Delivery Methods

In addition to sensible cooling provided by the chilled beams, a zone also requires humidity control (latent cooling) and a predetermined amount of outside air for ventilation as specified by ASHRAE 62.1 (2013). This can either be achieved by a parallel VAV system or a DOAS. A DOAS uses 100% outside air with no mixing of return air and supplies conditioned outside air directly to zones based on their individual ventilation requirements (Mumma 2001, Morris 2003). In such a parallel decoupled air-water configuration, building loads tend to be split up between the systems such that the ventilation system takes care of the latent load and a small part of the sensible load and the supplementary chilled beam system takes care of most of the sensible load (Mumma 2001, Morris 2003). Using a DOAS has four benefits; humidity control in each zone, required ventilation air is provided directly to each zone, energy savings in the range of 10-17% and the potential to use heat recovery to pre-condition outside air (Mumma 2001,

Khattar and Brandemuehl 2002, Morris 2003). However, it is important to note that these benefits can also be achieved by using a ventilation-only DOAS sized for latent cooling in parallel with a conventional VAV system sized for sensible cooling (Roth et al. 2002).

There are three major components in a DOAS (see Figure 1.1); heat recovery from the exhaust air to pre-condition the entering outside air, the air-conditioning system and the method of air delivery to the spaces (Mumma 2001, Morris 2003). If the exhaust air exiting the building has more favorable temperature and humidity than the outdoors, it is possible to recover both heat and moisture from this exhaust air to precondition incoming ventilation air (ASHRAE 2012). This is achieved by utilizing either temperature or enthalpy based energy recovery ventilators. There are several configurations for heat recovery such as air-to-air cross flow heat exchangers, rotary wheels, heat pipes, run-around loops and thermosiphons among others (ASHRAE 2012). Studies show that operational control for heat recovery ventilators can strongly influence energy savings obtained and may even increase energy use if control strategies are incorrectly applied (Zhou et al. 2007, Rasouli et al. 2010). This is especially true when opportunities exist for economizer operation (Deru et al. 2005, Pless and Torcellini 2005).

Conditioning of the outside air in a DOAS is typically identical to a conventional constant or variable air volume system, i.e. dehumidification is achieved by cooling the supply air up to the temperature (typically 55°F) at which it contains the amount of moisture required to maintain zone relative humidity of 50-55%. Solid or liquid desiccant dehumidification processes have also been used for dehumidification of air in ventilation-only systems (Lowenstein et al. 1998, Dai et al. 2001, Liu et al. 2006). Roth et al. (2002)

discuss the disadvantage of desiccant dehumidification which is the need for a heat source to reactivate the desiccant. Due to this, the system coefficient of performance (COP) is typically less than 1. As a result, this configuration works if latent loads are very high and either solar or low-grade sources of heat are available for regeneration. However, advanced and hybrid configurations for desiccant systems are capable of achieving better efficiencies and possibly being an alternative to vapor compression cycle cooling and dehumidification (Roth et al. 2002).

Delivery of ventilation air to the zones can occur in two ways. Typically, supply air is delivered from ceiling diffusers at higher velocity and lower temperatures (based on cooling load and required humidity control) to achieve satisfactory mixing of supply and zone air and uniform zone temperature (ASHRAE 2012). Another method that is also used, especially with passive chilled beams to increase the cooling capacity of the combined system, is supplying air from outlets at or near the floor (Ghaddar et al. 2008). This method delivers ventilation air directly to the occupied zone and prevents mixing of ventilation air with zone air. The cooler ventilation air displaces the warmer zone air upward and the natural stratification and upward movement of the air is considered effective at ventilation and contaminant control (Skistad et al. 2002, Bauman 2003). The height of the stratification layer in the zones, if controlled well, can improve the ventilation effectiveness of the HVAC system to a maximum of 1.2, requiring 20% lesser ventilation air. Since this ventilation air is delivered directly at the floor level in the occupied zone, a higher supply air temperature and lower supply air velocity can also be used. Due to these reasons, UFAD air distribution can result in both cooling and fan energy savings (Bauman

2003). This method of air delivery can be used with most HVAC system combinations with similar benefits: VAV systems with UFADs, chilled beams or chilled ceilings with displacement ventilation and radiant floors with displacement ventilation among others (Bauman 2003). Bauman and Webster (2001) discuss the three approaches in UFADs to supplying air to the zone; a pressurized plenum and passive floor registers, a non-pressurized plenum with fan-powered, active, locally controlled floor registers, and underfloor ducts that supply air to floor terminal devices. Pressurized plenums are most commonly used and require low plenum static pressure so air delivery to the space occurs by natural buoyancy at low velocities and stratification is achieved. However, they are prone to leakage and subsequent energy waste (Bauman 2003). Locally controlled floor registers provide individualized comfort, but air stratification or overall controls are difficult to predict and local fan energy use may increase (Bauman 2003). Underfloor ducts systems are easiest to control but have the added cost of underfloor duct installation (Bauman 2003).

2.2 Energy Use and Thermal Comfort in Buildings with Chilled Beams and Parallel Ventilation Systems

The comparative energy performance and resulting feasibility of chilled beams with a parallel ventilation system versus a VAV system is strongly dependent on climate, building loads and ventilation requirements. Research studies address this issue parametrically and try to ascertain the conditions under which chilled beams and DOAS become the more energy efficient alternative to VAV systems. Stetiu (1998) conducted parametric studies for radiant cooling systems with separate ventilation systems in 11

locations in the United States and concluded that the radiant systems have energy saving potential in all locations. Potential savings are higher for hot and dry climates and lower for cold and moist climates. However, Stetiu also concludes that if the ventilation air required for dehumidification is a large portion of the cooling and fan energy consumption of the all-air system, then there will be no energy saving from switching to a parallel radiant system. Some of the drawbacks of this study are that the baseline VAV system and the radiant system are modeled in two separate simulation software (DOE-2 and RADCOOL, respectively), and only single zone energy analysis calculations are conducted.

Niu et al. (1995) compared chilled ceilings with constant volume systems in Hong Kong, a subtropical hot and humid climate, and concluded that chilled ceilings have energy saving potential of almost 44%. Vangtook and Chirarattananon (2006) conducted a similar study for chilled ceilings in Thailand (also a subtropical hot and humid climate) and showed similar energy savings, but found that chilled ceilings are inadequate at providing required cooling during the hottest times of the year. They also showed that at lower ceiling temperatures, there is a risk of higher convection air velocity in spaces. Bahman et al. (2009) conducted both experimental and simulation studies in Kuwait and concluded that chilled ceilings with displacement ventilation are more energy efficient than conventional VAV systems only at 100% outside air requirements. Novoselac and Srebric (2002) also emphasize that ventilation rates, ratio of the total cooling load removed by the ventilation system and operational control determine energy savings achievable with cooled ceilings and displacement ventilation systems. Imanari et al. (1999) conducted

energy studies for an office building in Tokyo, Japan with radiant chilled ceiling panels and estimated energy savings of 10% over a VAV system. They also conducted occupant surveys that indicate that the occupants prefer the radiant chilled ceiling system in terms of comfort. Antonopoulos et al. (1998) also showed similar savings (13%) for radiant ceiling plans through experimental studies. Since the climate in both these studies (Antonopoulos et al. 1998, Imanari et al. 1999) is similar to that found in southern United States with hot and humid summers and mild winters, the energy savings obtained by them are likely to be similar.

Most of these and other energy comparison studies conducted for chilled beams with ventilation systems (Niu et al. 1995, Matsuki et al. 1999, Hao et al. 2007) are based on experimental or simulation models. While such systems have been implemented in buildings (Rumsey and Weale 2007, Chowdhury et al. 2008, Weidner et al. 2009, Penny 2012) real building energy use data for demonstration of operational benefits and energy performance comparison are difficult to obtain.

2.3 Operation and Controls for Chilled Beams with Parallel Ventilation Systems

Typically, for a combined chilled beam and DOAS or VAV system, room temperature is controlled by varying water flow rate or water temperature through the chilled beam (Mumma and Jeong 2005, Loudermilk 2009). Monitoring of zone air and dew point temperature along with condensate monitoring on the chilled beam and chilled water supply pipe is essential to avoid condensation on the beams. It is also essential to keep chilled water supply temperature above space dew point temperature and maintain space dew point temperature within a range of ±2ºF at all times (Mumma and Jeong 2005,

Loudermilk 2009, Schurk 2012). If building loads can be predicted, a demand-based operational strategy can also be utilized to control the chilled beam and ventilation system (Loudermilk 2009, Schurk 2012).

Mumma and Jeong (2005) provide detailed control logic schematics for a DOAS system with a ceiling cooling panel system (similar to chilled ceilings). They recommend a constant volume ventilation system with provisions for building pressure monitoring. The building is also recommended to be slightly pressurized to avoid infiltration and also ensure that the zone air is returned to the heat recovery unit instead of being lost to exfiltration. Overall, they recommend simple conservative controls such as varying supply air temperature, high chilled ceiling water temperature and fixed supply air to avoid infiltration, condensation and unstable operation. These recommendations are reinforced by Alexander and Rourke (2008) and Loudermilk (2009). However, the impact of the control strategies on the energy use of the building especially in humid climates is not explored. Loudermilk (2009) also briefly explores the added dimension of influence of the chilled beam controls on occupant thermal comfort and room air distribution. For example, in active chilled beams, beam discharge air is a mixture of primary air and induced zone air and is typically warmer than that of all-air systems. To account for this higher discharge air temperature, a higher discharge airflow rate is required, but this can contribute to greater draft risks in the zone.

For underfloor air distribution (UFAD) of ventilation air, the main control parameters are supply air temperature, airflow rate and plenum/duct static pressure (Bauman 2003). With UFADs, since air is supplied directly to the occupied zone, higher

supply air temperatures (typically 60-65ºF) are required to avoid cold feet and cold floors (Bauman and Webster 2001, Bauman 2003). UFADs also encourage stratification of air for contaminant control and ventilation effectiveness (Bauman and Webster 2001), but ASHRAE comfort requirements (ASHRAE 2010b) restrict the vertical air temperature difference in a zone. In order to fulfill these conflicting conditions, a certain range of supply airflow rates is required when the space is occupied (Webster et al. 2002, Bauman 2003). It is important to note that stratification can only be partly controlled by supply airflow rate and is influenced by other factors such as heat sources and obstructions to airflow (Webster et al. 2002). Pressure setpoints of the plenum/duct in UFADs are typically much lower (0.5-1.0 in. W.G.) and additional fan savings can be achieved by applying a static pressure reset during periods of lower loads (Bauman 2003, Stein and Taylor 2005).

As more of these systems are being implemented, optimization of operational control has potential for further research in order to increase energy savings while maintaining comfort (Mossolly et al. 2008, Ge et al. 2011). Ge et al. (2011) developed a model-based optimal control strategy using genetic algorithms to predict supply air temperature, humidity ratio and supply chilled water temperature for a DOAS system with chilled beams and liquid desiccant system. An external optimization processor was linked to the TRNSYS model of the building to evaluate the energy savings potential of the optimal controls. Mossolly et al. (2008) compared several optimization strategies for a chilled ceiling with displacement ventilation control including varying ceiling temperature, ventilation supply temperature, and ventilation supply flow rate. The optimal

control strategy was obtained using multi-objective genetic algorithms with a prediction period of 60 minutes. The predicted performance of the system was validated by experimental studies and estimates energy savings of 15% over the baseline system with no optimization. These studies show that optimization has potential for energy savings in decoupled ventilation systems, but implementation of these optimization methods in existing building energy management control systems has yet to be explored.

2.4 Chilled Beam Modeling

Many whole-building energy analysis programs have built-in models to estimate capacity and energy use in buildings with chilled beams. However, there are issues associated with all of them (Betz et al. 2012). For the purpose of this research, five whole-building energy analysis programs; eQuest 3.64 with the DOE 2.2 simulation engine, EnergyPlus 8.1, TRNSYS 17, Trane TRACE and IDA Indoor Climate and Energy 4.0 were reviewed to evaluate their ability and approach to modeling chilled beams with separate ventilation systems. These programs were selected based on the following criteria: they are widely used and have been validated, they have a chilled beam model, they are currently under development and offer ongoing support, they have the capability to model building loads, HVAC systems and equipment and they provide detailed energy use reporting.

The eQuest 3.64 (Hirsch & Associates 2010) simulation program is an easy to use but powerful tool which provides detailed hourly energy analysis of most of the state-of-the art technologies used in buildings today . However, the program lacks a chilled beam model so an approximation using an induction unit system is typically used (Betz et al.

2012). The program also lacks the flexibility required for modeling atypical ventilation systems used with chilled beams (Betz et al. 2012), the capability to conduct zone airflow calculations, thermal comfort analysis and dynamic (or quasi-dynamic) simulations (Crawley et al. 2008).

EnergyPlus 8.1 (U.S.DOE 2012b) is a modular energy analysis tool that combines the features of BLAST and DOE 2 and gives advanced users flexibility to configure and simulate non-traditional HVAC systems and building control (Crawley et al. 2008). The chilled beam model in EnergyPlus is a quasi-empirical model developed by chilled beam manufacturer Halton Oy (Livchak and Lowell 2012). The model depends on a series of either user-defined or default coefficients to model beam capacity and energy use (Bauman et al. 2011). However, limitations in EnergyPlus are on the air and water-side modeling of the system such as combining UFADs with chilled beams, a VAV DOAS, modeling of secondary water loops for the chilled beams and the zone-level control of the ventilation air based on factors other than temperature (such as humidity or zone CO_2 levels) (Betz et al. 2012).

TRNSYS 17 (TRaNsient SYstem Simulation Program) (UWM 2012) is a transient simulation tool that models HVAC systems as a series of components which are mathematical models that are either built into the program or can be input by the user thus giving the user flexibility to develop their own HVAC configuration and components (Crawley et al. 2008). The TRNSYS chilled beam model is also empirical and details of this model are proprietary. Like EnergyPlus, the TRNSYS model also relies on a series of manufacturer-specific input parameters (Bauman et al. 2011). The energy balance of the

model also includes the radiant component of the chilled beam. TRNSYS also offers the greatest flexibility in terms of the air and water side temperature and flow. However, developing complex building models for chilled beams in TRNSYS are often time and cost prohibitive and validation of the chilled beam model is not available (Betz et al. 2012).

TRACE 700 6.3 (TRANE 2014) has four calculation phases: Design, System, Equipment and Economics and is extensively used for the design, sizing and cost calculations of systems in new buildings (Crawley et al. 2008). TRACE offers models for advanced system configurations such as VRFs, UFADs and chilled beams. However, the TRACE chilled beam model is based on a user-defined value for beam capacity and is activated only when the primary system is unable to meet zone loads (Betz et al. 2012). On the air and water-side, the program has the same limitations as EnergyPlus such as an inflexible AHU and water loop configuration. TRACE also lacks the ability to provide zone-level hourly reports (Betz et al. 2012).

IDA-ICE (Indoor Climate and Energy) 4.0 (EQUA 2012) is a modular simulation tool where the user specifies tolerances to control the accuracy of the solution and the entire mathematical model and calculations for the simulation are available for inspection by the user (Crawley et al. 2008). The IDA chilled beam model requires a user-defined input for beam conductivity (K) and an exponent for the logarithmic temperature difference between the beam water and the zone air (Bauman et al. 2011). Airflow modeling in IDA-ICE includes non-CFD based hybrid ventilation and multi-zone airflow estimation. However, IDA ICE is partial to HVAC systems associated with the Northern European engineering culture (Crawley et al. 2008).

CFD is typically used for detailed simulation of zone airflows in buildings with chilled beams. The type of model used to solve the CFD equations that describe the motions of the fluids in the space (in this case, air) is dependent on the type of flow. Several studies have been conducted to evaluate the methods for room air turbulence modeling, surface boundary conditions, mesh sizing and simplification of geometries for chilled beam modeling (Chen and Xu 1998, Srebric and Chen 2002, Chen et al. 2007, Srebric et al. 2008). The physics model that has been extensively used and validated in room airflows (Nielsen 1998, Cehlin and Moshfegh 2002, Nelson 2012) is the standard k-ε model (Launder and Spalding 1974). In this model, two differential equations are solved to calculate the turbulent viscosity and the dependent variables for the equations are the turbulence energy k and the dissipation rate of turbulence energy ε.

2.5 Building HVAC Control Optimization

Achieving optimal control involves modification of the operation of the building HVAC system such that the energy use or operating cost of the equipment is minimized and satisfactory indoor environmental quality is maintained (Wang 2010). The optimization process is typically conducted in 2 steps; 1) predicting the sensitivity of the control variables; 2) developing a control strategy that can change in response to the changes the building in order to reduce energy while maintaining comfort (Hopfe 2009).

2.5.1 Sensitivity Analysis Review

Generally, sensitivity analyses for quantifying the impact of any measurable inputs or variables on the desired output are classified as local and global sensitivity analyses

(Yıldız and Arsan 2011). Local sensitivity methods are applicable if the relationship between the variable and output is linear and the interaction between variables is not important (Hopfe 2009, Yıldız and Arsan 2011). On the other hand, global sensitivity analyses account for interactions between variables and non-linear responses. They are also more computationally intensive but can rank and quantify both the input and output uncertainties. They can be conducted by modifying all variables at once, and are capable of conducting uncertainty analysis for each iteration of the model (Hopfe 2009, Yıldız and Arsan 2011). Screening tools are a type of global analyses that are used to identify and rank the variables that contribute significantly to the outputs rather than quantifying the sensitivity of all the variables. Since screening tools are also global analyses, they can be used when input variables are interdependent and can distinguish linear and non-linear variables. They are typically used for preliminary analysis since they are less computationally intensive and lack the ability to perform uncertainty analysis (Hopfe 2009, Yıldız and Arsan 2011).

The Morris method (Morris 1991, Campolongo et al. 2004) is widely used to screen factors in models of large dimensionality (which is typical with a building). It is an iterative experimental plan that consists of randomized 'one-factor-at-a-time' experiments: the impact of changing one factor at a time is evaluated in turn. There are two sensitivity measures for each factor; an estimate of the mean of the distribution and an estimate of the standard deviation of the mean. A high value of the mean indicates an input factor with an important overall influence on the output. A high value of the standard deviation

indicates the factor is involved in interaction with other factors or one whose effect is nonlinear (Morris 1991).

2.5.2 Building Control Optimization Review

Wang (2010) discusses several optimal control methods that are currently used in intelligent buildings today, including rule-based, model-based and model-free and hybrid controls. Rule-based controls include simplified heuristic reset controls based on engineering judgment and prior knowledge of the HVAC systems used (Liu et al. 2002). Model-based controls involve developing a model that represents the actual system and the use of optimization algorithms at each sampling interval to compute the optimal control (Ellis et al. 2006, Bengea et al. 2013). The models involved in model-based control can be either physical simulation models, grey-box models or black-box models (Wang 2010). Performance-map based controls are simplified model-based controls in which a matrix of results generated from simulations of the building over different operating conditions are used in the real building (Wang 2010, Coffey 2011). Model-free controls are typically built into intelligent building EMCS systems such as reinforcement learning systems or expert systems. Their ability to detect optimal solutions and the time they take to 'learn' are dependent on the knowledge database available and they typically do not respond well to unusual situations. Hybrid controls use a combination of model-based controls or even model-based and model-free methods to achieve optimal solutions (Wang 2010).

Simplified rule-based controls are widely discussed for HVAC applications and can provide energy savings, improved thermal comfort and are widely implemented in

buildings (Liu et al. 2002). Several operational strategies and resulting energy savings have been extensively documented such as; supply air temperature and static pressure reset (Zhu et al. 1998, Wei et al. 2000, Engdahl and Johansson 2004), optimized supply and outside air volume based on loads (Liu et al. 2001, Liu et al. 2002), optimized economizer operation (Joo and Liu 2003, Zhou et al. 2010) chilled and condenser water temperature reset (Ardehali and Smith 1997, Seidl 2008), optimized HVAC start-up, shut-down and operation schedules and optimized chiller and boiler staging among others (Liu et al. 2002).

Model-based predictive control methods are capable of providing optimal solutions that respond to the changes in the building and the climate, but are computationally intensive and difficult to implement in existing EMCS systems (Ellis et al. 2006). The process involves the development of a building model (which can either be a simplified mathematical model or a whole-building simulation) which is used in parallel with a search algorithm to predict optimal setpoints (Ellis et al. 2006, Bengea et al. 2013). Optimization algorithms can be either simplified linear solutions or non-linear solutions, the latter providing better results for HVAC applications (Hopfe 2009, Ge et al. 2011). Linear optimization (Hanafy 2012), NGSA-II (Emmerich et al. 2008), genetic algorithms (Mossolly et al. 2008) among others (Wetter and Polak 2005, Ellis et al. 2006, Bengea et al. 2013) have been explored for HVAC control in building simulations.

Applicability of model-based controls to real buildings is limited because of computational requirements and difficulty in implementation (Ellis et al. 2006). As a result, a reasonable approximation includes the development of a matrix of optimized

control points over different operating conditions of a real building. The matrix is developed offline from simulations of the building and is then used to control operation of the real building (Coffey 2011).

2.6 Conclusions from Literature Review

The literature review provides an overview of chilled beams with parallel ventilation systems, their energy performance, factors affecting energy use, operational control strategies, approaches to optimization and simulation tools used for predicting energy use and thermal comfort.

Section 2.1 documented the various components that could be used as part of a decoupled ventilation and chilled beam cooling and heating system. Chilled beams, chilled ceilings and radiant floors are water-based conditioning systems that use either chilled water or hot water, and exchange sensible heat with a space through convection and radiation. Chilled ceilings and chilled beams have lower cooling capacities and are combined with displacement ventilation or underfloor air distribution to increase cooling capacity especially in hot and humid climates. Dedicated outdoor air systems are the parallel 100% outside air ventilation systems that are designed to handle all of the ventilation and latent loads in a space. A DOAS will always include heat recovery for the preconditioning of the outside air. Dehumidification is achieved by deep cooling of the supply air, but desiccant dehumidification is also sometimes used. Delivery of ventilation air to a space can be either through ceiling mixed ventilation or displacement ventilation where air is supplied at floor level, i.e. directly to the occupied zone. This allows natural

stratification, displacement of the warmer zone air upward, lower supply air velocity and temperature and is considered effective at contaminant control.

Section 2.2 documented the energy use studies for chilled beams with parallel ventilation systems. The studies indicate that potential savings are higher in hot and dry climates and lower in cold and moist climates. Building ventilation rates, the ratio of the total cooling load removed by the ventilation system and operational control also strongly influence energy savings achievable with chilled ceilings/beams and parallel ventilation systems. The review of the literature reveals a lack of real building energy use data for demonstration of operational benefits and energy performance comparison. It also reveals a lack of data on effects of air and water temperature, flow rate and velocity on local airflows and temperature profiles in spaces.

Section 2.3 documented operational controls for chilled beams with decoupled ventilation systems. The studies reveal a preference for a simple and conservative approach to control in real building. The studies also show that optimization has potential for energy savings in decoupled ventilation systems, but there is need to develop simple strategies that can be implemented into the existing building energy management control system (EMCS) without unstable operation. There is also a need to understand the effect of altered building operation on temperature, humidity and airflow profiles in spaces.

Section 2.4 documented five simulation tools for estimating whole-building energy use: eQuest, EnergyPlus, TRNSYS, TRACE and IDA ICE. It also discusses the CFD models used in literature to calculate room airflows. These tools were evaluated for their ability to model chilled beams and the associated systems. All the chilled beam

models require a series of user-defined inputs based on actual chilled beam geometry in order to model beam capacity and energy use. Several issues were also identified with the air and water-side systems associated with chilled beams. These issues combined with the high level of expertise and time required to adequately estimate whole building energy use for such systems make the design and implementation of chilled beams more challenging.

Section 2.5 provided an overview of sensitivity analysis and optimization methods that are currently used. Sensitivity analyses methods include local sensitivity methods and global sensitivity analysis. Local sensitivity methods are applicable if the relationship between the variable and output is linear and the variables are independent. Global sensitivity analyses can be conducted by modifying all variables at once, and are capable of conducting uncertainty analysis for each iteration of the model. Screening tools are a form of global sensitivity analyses that identify and rank the variables that contribute significantly to the outputs. Optimization methods include heuristic rule-based controls, model-based controls, model-free controls and hybrid controls. Simplified rule-based controls and demand-based controls are most commonly used due to the ease in implementation in real buildings and energy savings. Model predictive controls are also beginning to be investigated in the quest for zero-energy buildings (Ellis et al. 2006, Bengea et al. 2013).

CHAPTER III

RESEARCH METHODOLOGY

This chapter documents the methodology used in the research. In Section 3.1, the process for the development of the simulation model of the building is discussed. Section 3.2 outlines the method for evaluating the energy use of the building model. Details of the process used to develop the optimization strategies for the building operation are documented in Section 3.3. In Section 3.4, the stratification measurements taken to evaluate the zone level comfort conditions in the building is described. Finally, 3.5 summarizes the research methodology.

3.1. Development of the Energy Model

The development of the energy model of the building consisted of three steps;

1. Energy data was collected from the case-study building and inputs were established for the EnergyPlus simulation model.
2. A process for modeling the operation of the passive chilled beams and the UFAD system in EnergyPlus was developed.
3. A simplified steady state model was also developed for validation and quick energy use predictions.

The building physical data was collected from as-built architectural and MEP drawings of the building. Walkthroughs of the building and HVAC systems were conducted to verify accuracy of the drawings. Because the HVAC systems are equipped with sensors that are monitored through the building automation system, trends were setup

for critical sensor points to establish day-to-day building operation and schedules. Trends were collected for October 15-31, 2013, January 15-31, 2014 and July 5-19, 2014. The sensors in the building are on a yearly calibration cycle, so random verification checks were conducted to confirm sensor accuracy. The details of the verification checks are presented in Table A.1 (Appendix A). Baseline comfort measurements (temperature and CO_2 levels) were also taken in the offices, lobbies and cafeteria, details of which are presented in Table A.2 (Appendix A). Overall building operation was established through the functions programmed into the EMCS. The number of people in the offices were estimated based on the number of desks multiplied by average occupancy levels of 95%[1]. The occupancy levels in the gymnasium, cafeteria and lobby were estimated using the values from Deru et al. (2011). Occupancy profiles were estimated from the CO_2 trends in the building. Lighting levels (W/ft^2) were initially based on values specified in Standard 90.1 (ASHRAE 2004). Lighting schedules were estimated based on building walkthroughs at different times during the weekdays and weekends. Equipment levels (W/ft^2) and schedules were initially estimated based on engineering judgment and hourly building demand data and were modified during the calibration process. Section 4.1 provides details of the building envelope, zoning, occupants, lighting and equipment loads, HVAC equipment description, the existing HVAC operation and the measured energy use data.

[1] Occupancy levels were based on conversations with the building management and operators

The inputs from the actual building were used to develop a simulation model in EnergyPlus 8.1.0.008. This model was then calibrated using the electricity and demand data obtained from the case-study building. The statistical comparison techniques outlined in Guideline 14 (ASHRAE 2002) were used to calibrate the simulation model to the available measured energy data. This method requires the calculation of two statistical indices, the coefficient of variation of the root mean square error (CV (RMSE)) and the normalized mean bias error (NMBE). The acceptance criteria for calibrated models are a CV (RMSE) within ±15% and NMBE within ±5% when using monthly measured energy data.

$$\mathrm{CV(RMSE)(\%)} = \left(\frac{\sum_{i=1}^{n}(y_i - \hat{y}_i)^2}{n-1}\right)\left(\frac{100}{\bar{y}}\right) \quad 3.1$$

$$\mathrm{NMBE\ (\%)} = \left(\frac{\sum_{i=1}^{n}(y_i - \hat{y}_i)}{n-1}\right)\left(\frac{100}{\bar{y}}\right) \quad 3.2$$

The calibrated model represents a reasonable approximation of the real building behavior and was used to test the control strategies discussed in the next steps. Section 4.2 provides details of the calibration of the simulation model.

Both the chilled beam system and the ventilation system in the building is controlled by the zone thermostat and this approach can lead to unstable operation. As a result, a modified operation was modeled based on recommended chilled beam controls in literature (Loudermilk 2009, Schurk 2012). In the modified operation, the delivered supply air to the zones is controlled by zone ventilation or humidity requirements instead of temperature. To model this in EnergyPlus, the EMS module was used to develop a process to replicate the control. Details of this can be found in Section 4.4.

A simplified steady-state energy model of the building was also developed to compare with the results obtained in the EnergyPlus model. This involved equations for demand controlled ventilation, SDVAV AHU configuration with bypass air for reheat, estimation of supply and return plenum temperatures and the energy supplied from the passive chilled beam. The model also includes zone temperature and humidity calculations.

3.2. Building Energy Use Evaluation

The next step was to verify the energy performance of the building. Two additional models were developed for the comparative energy use analysis of the building. The first model (labeled as VAV) was a building with identical physical characteristics and a modified HVAC system with VAV AHUs and overhead mixing ventilation. The HVAC plant sizing, efficiencies and operation were kept the same as the real building. The second model (labeled as ASHRAE) was an ASHRAE 90.1 (ASHRAE 2004)[2] code-compliant model of the building. The calibrated building (labeled as CALIB) and the building with the modified chilled beam operation (labeled as MCB) was compared with the VAV and ASHRAE model to establish energy savings if any from the chilled beam system. Figure 3.1 shows the differences between the four building models used in the energy evaluation.

[2] The building was designed to comply with ASHRAE Standard 90.1-2004 minimum requirements.

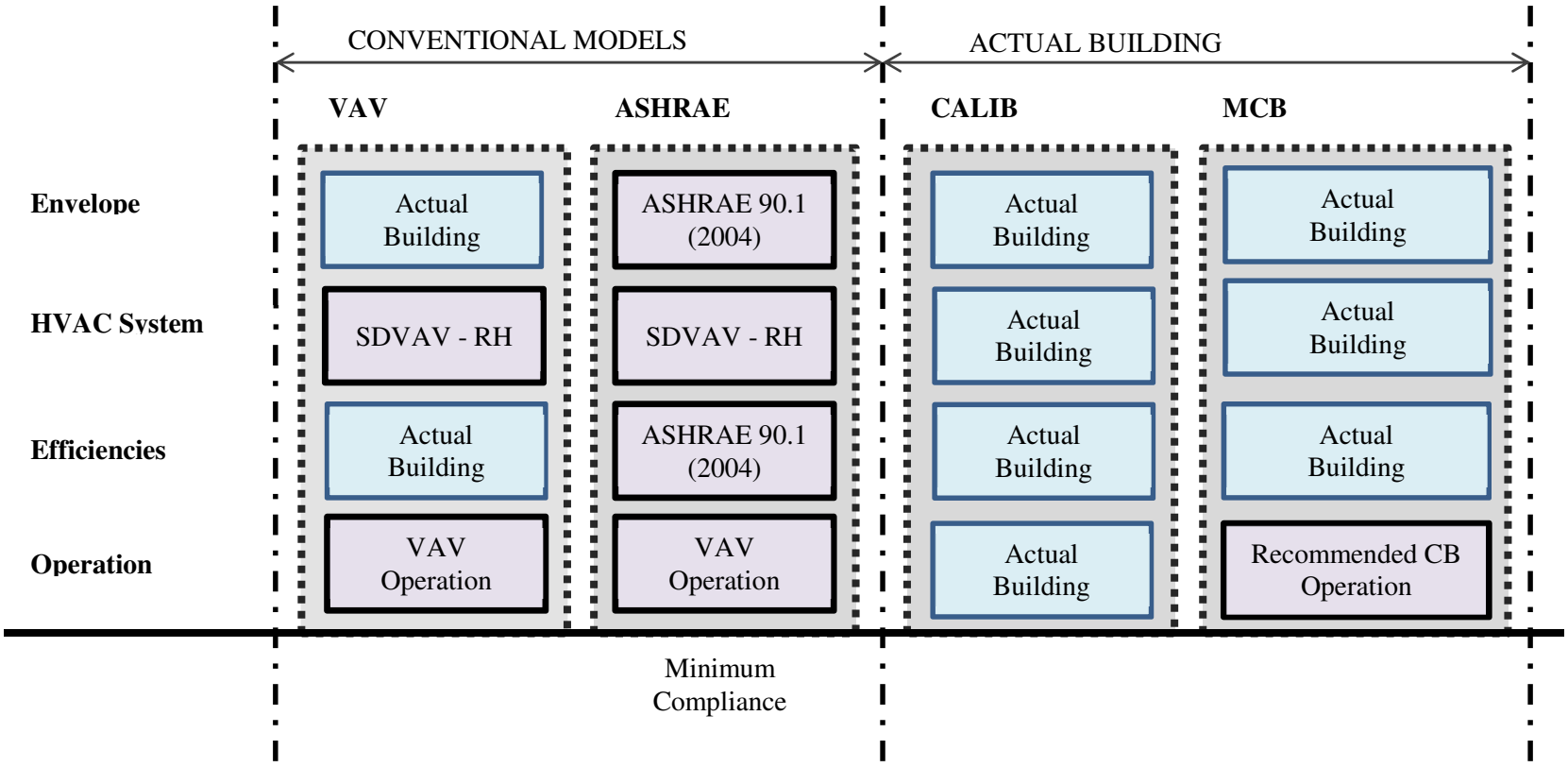

Figure 3.1: The Four Building Models Used for the Energy Use Evaluation

Table 3.1: Differences between the Calibrated Building, the Equivalent VAV System Model and the ASHRAE 90.1 (2004) Compliant Model

Characteristics	'CALIB' & 'MCB' model	'VAV' model	'ASHRAE' model
Exterior Wall	First Floor U=0.055 Btu/hr-ft^2-°F	First Floor U=0.055 Btu/hr-ft^2-°F	U = 0.124 Btu/hr-ft^2-°F
	Second Floor U = 0.060 Btu/hr-ft^2-°F	Second Floor U = 0.060 Btu/hr-ft^2-°F	
	Top Floor U = 0.085 Btu/hr-ft^2-°F	Top Floor U = 0.085 Btu/hr-ft^2-°F	
Windows	U-factor = 0.46 Btu/hr-ft^2-°F	U-factor = 0.46 Btu/hr-ft^2-°F	U-factor = 0.57 Btu/hr-ft^2-°F
	SHGC = 0.25	SHGC = 0.25	SHGC = 0.25
Fan Static Pressure Setpoint[3]	Supply Fan = 1.20 in.W.G. (Equal to actual building)	Supply Fan = 3.50 in.W.G.[4]	Supply Fan = 3.50 in.W.G.[4]
	Return Fan = 0.75 in.W.G. (Equal to actual building)	Return Fan = 2.00 in.W.G.	Return Fan = 2.00 in.W.G.
Cooling Coil Leaving Temperature[3]	53°F	55°F	55°F
Supply Air Temperature[3]	62°F	55°F	55°F
Supply Plenum[3]	Yes (Underfloor)	No (Overhead terminal units and ducted supply diffusers)	No (Overhead terminal units and ducted supply diffusers)
Zone Air Distribution for Ventilation Effectiveness	1.0	1.0	1.0
Return Plenum	Yes	Yes	Yes
Heating System[3]	Separate heating terminal units in the return plenums (heating coil efficiency = 0.85)	SDVAV terminal units with reheat (heating coil efficiency = 1.00)	SDVAV terminal units with reheat (heating coil efficiency = 1.00)
Airside System Sizing	Equal to actual building	Sized for ASHRAE 99.6% design day conditions. Sizing Parameter = 1.2	Sized for ASHRAE 99.6% design day conditions. Sizing Parameter = 1.2
Waterside System Sizing	Equal to actual building	Equal to actual building	Equal to actual building
Chiller COP	Water Cooled = 0.558 kW/Ton	Water Cooled = 0.558 kW/Ton	Water Cooled = 0.577 kW/Ton
	Air Cooled = 1.3kW/Ton	Air Cooled = 1.3kW/Ton	Air Cooled = 1.135kW/Ton
Cooling Tower	Equal to actual building	Equal to actual building	Equal to actual building

[3] Modifications were made only to the UFAD AHUs (AHU4A1, 5B1 and 5C1)
[4] Based on Deru et al. (2011)

Table 3.1 lists the differences between the CALIB and MCB model, the VAV model and the ASHRAE model. For this comparative analysis, the AMY weather data used in the calibrated model was replaced with the TMY3 weather data as it includes typical weather conditions over longer periods of time and is considered appropriate for a comparative energy analysis.

A parametric study was also conducted by varying the latent and sensible loads in the space to understand their effect on the energy savings potential of the chilled beam system. Loads were varied by modifying internal plug loads and occupancy in the zones. The occupancy levels increase both ventilation and latent loads in the building. Chapter VI documents the details and the results from the comparative energy use evaluation.

3.3. Building Control Optimization

Development of optimization strategies for operational control consisted of three steps;

1. A sensitivity analysis of operational control parameters was conducted for the MCB and the VAV system.
2. Simplified rule-based optimization strategies were developed for the MCB system.
3. A process was outlined to develop and model a simulation assisted optimization strategy that can be eventually implemented in the building. The results of this strategy was compared with the one developed in step 2.

First, a sensitivity analysis was conducted on both the MCB and the VAV models to rank the operational control parameters based on their influence on the energy use of the building. From the literature review, operational control parameters for the MCB model such as outside air flow rate, cooling coil leaving temperature, supply air

temperature, supply air flow rate, chilled water temperature, chilled beam water temperatures, chilled beam flow rates and zone temperatures were identified. For the VAV model, the control parameters identified were outside air flow rate, supply air temperature, supply air flow rate, chilled water temperature, economizer operation and zone temperatures. Since the supply air flow rate, chilled beam water temperature and chilled beam flow rate are dependent control variables, they were omitted from the sensitivity analysis. The Morris method was used as the screening tool for the sensitivity analysis. Five (5) inputs (n) were selected for the MCB and VAV models with 6 values (R) for each input for a total of R(n+1) simulation runs for each model. Table 3.2 documents the values used for each parametric input. In order to cover the entire range of possibilities for the simulation, the values were selected based on reasonable minimum and maximum values seen in buildings for each input.

Table 3.2: Control Input Parameters for the Sensitivity Analysis for the MCB and VAV Models

MCB MODEL								
(n)	**Parameter**	**Units**	**(R)**					
Input			**Base**	**Run 1**	**Run 2**	**Run 3**	**Run 4**	**Run 5**
1	Outside Air Volume (OAv)	cfm	22,288	23,461	25,063	27,006	29,179	32,022
2	Zone Temperature (Tz)	°F	69.0	70.4	71.8	73.2	74.6	76.0
3	Cooling Coil Leaving Air Temperature (Tcc)	°F	50.0	51.6	53.2	54.8	56.4	58.0
4	Supply Air Temperature (Tsa)	°F	55.0	56.4	57.8	59.2	60.6	62.0
5	Chilled Water Supply Temperature (Tchw)	°F	44.0	45.0	46.0	47.0	48.0	49.0

Table 3.2 (continued): Control Input Parameters for the Sensitivity Analysis for the MCB and VAV Models

VAV MODEL								
(n)	Parameter	Units	(R)					
Input			Base	Run 1	Run 2	Run 3	Run 4	Run 5
1	Outside Air Volume (OAv)	cfm	22,288	23,461	25,063	27,006	29,179	32,022
2	Zone Temperature (Tz)	°F	69.0	70.4	71.8	73.2	74.6	76.0
3	Supply Air Temperature (Tsa)	°F	53.0	54.8	56.6	58.4	60.2	62.0
4	Economizer Control (Econ)	hours	4,274	3,781	2,666	1,812	946	0
5	Chilled Water Supply Temperature (Tchw)	°F	44.0	45.0	46.0	47.0	48.0	49.0

The process involved running a simulation to an initial set of inputs (base). A random input was then modified by a value Δ (run 1, input 1) and the elementary effect (EE) of that input value (Δ) was calculated by using Equation 3.3 where f(x) is the HVAC energy use. This step was repeated until all the inputs were modified (run 1, inputs 2-5). This modified model was then used as the base run for the next set of values (run 2-5, inputs 1-5) and the process was repeated till all the runs were complete. Elementary effects were calculated for heating, cooling and total HVAC energy use. The mean (Equation 3.4) and standard deviation (Equation 3.5) of all the elementary effects for each input were then calculated. A high value of the mean indicates an input with an important overall influence on the output. A high value of the standard deviation indicates the input is involved in interaction with another input or the effect of the input on the output is nonlinear. The control inputs that had the most influence on the energy use in the building were then selected for the optimization process. Section 7.1 documents the results of the sensitivity analysis.

$$EE_{i,R} = \frac{f(x_1, \ldots, x_i + \Delta_i, \ldots, x_n) - f(x_1, \ldots, x_i, \ldots, x_n)}{\Delta_i} \quad 3.3$$

$$\mu_i = \frac{\sum_r^R |EE_{i,R}|}{R} \quad 3.4$$

$$\sigma_i = \frac{\sum_r^R (EE_{i,R} - \mu_i)^2}{R} \quad 3.5$$

Based on the results of the sensitivity analysis, outside airflow rate, cooling coil leaving temperature and chilled water supply temperature were selected as the control input parameters for the optimization process. For the rule-based optimization process, a simple reset was proposed based on dehumidification requirements in the building. The main assumption in this optimization strategy is that the airside system is always less efficient than the chilled beam system and is to be controlled only to fulfill minimum ventilation or latent load requirements. If humidity in any of the zones exceeded the maximum humidity setpoint, a 'dehumidify' mode was initiated that reset the control setpoints for the airside system. Four scenarios were examined; constant-volume outside air with fixed coil leaving air temperature, constant-volume outside air with varying coil leaving air temperature, variable-volume outside air with fixed coil leaving air temperature and variable-volume outside air with varying coil leaving air temperature. These scenarios were modeled in EnergyPlus and the resulting HVAC energy use and comfort conditions were documented and compared. The results from this step are documented in Section 7.2.

The above strategy achieves the goal of lower HVAC energy use, but it is important to verify if there are other optimum solutions to the minimization of HVAC energy use problem. The best way to do this is to link the simulation model to an

optimization algorithm to solve for minimum energy use. This approach is used in model predictive control that can be potentially implemented in buildings. Figure 3.2 shows the general flow diagram for online model predictive control strategy as implemented real-time in a building. This is an ongoing process in which real building conditions such as internal loads and outside air conditions are fed to a simulation model of the building which is linked to an optimization tool. The control outputs that results in least energy use are then calculated for the next timestep and are eventually implemented in the building. This approach is preferred if an integrated solution for a complex building system with several components is required. This approach is also preferred if a system is non-typical and rule-based solutions are not available or not tested. A chilled beam system fulfills both these criteria and, as a result, is a good candidate for online model predictive control.

However, the major issue with the real-time implementation of model predictive control is the time and computational capacity required to run the optimization. Depending on the input conditions and the control points required to be controlled, the optimization can take anywhere between a few hours to several days. A solution to this issue proposed by Coffey (2011) is to run the optimization offline and preferably before its implementation in the building. It involves the generation of optimal control points for a given grid of building conditions and a development of a performance table of controls that can be then implemented online in the building. This method was adopted for the development of the optimization control used in this research. Figure 3.3 shows the flow diagram for this optimization and the inputs and outputs used in the research.

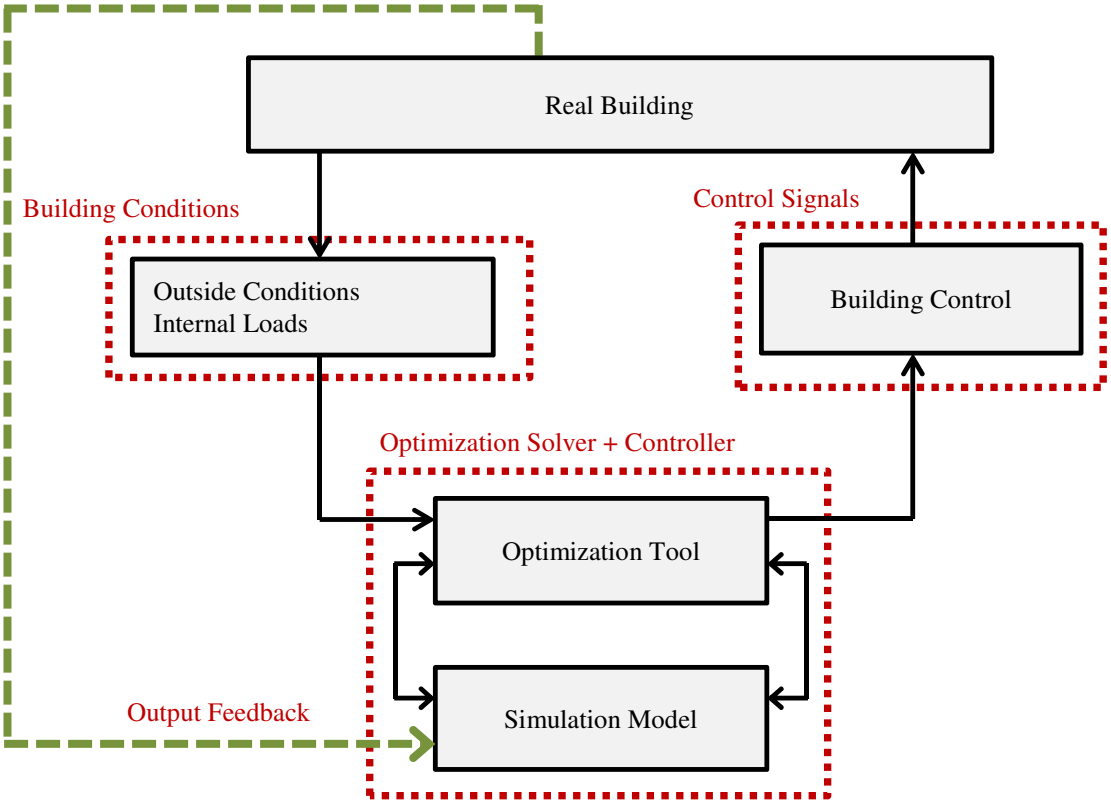

Figure 3.2: Typical Data Flow Diagram for Online Model Predictive Control

GenOpt® (Wetter 2011) was used as the optimization program for the minimization of HVAC energy use. GenOpt® was linked to the EnergyPlus model of the building which calculated the building HVAC energy. A grid of inputs was set up to cover a wide range of possible building operation conditions. The grid was developed by varying outside air temperature, humidity and internal loads in the offices. The grid of conditions for the outside air temperature was developed by dividing the minimum and maximum range of temperatures for a TMY year into 4 periods; cold, cool, warm and hot. The average low and high humidity for each temperature range is established as a grid for

outside air humidity. For the internal loads, the occupancy, lighting and equipment schedules (fraction of peak) were modified to create a grid for maximum, minimum and average internal loads.

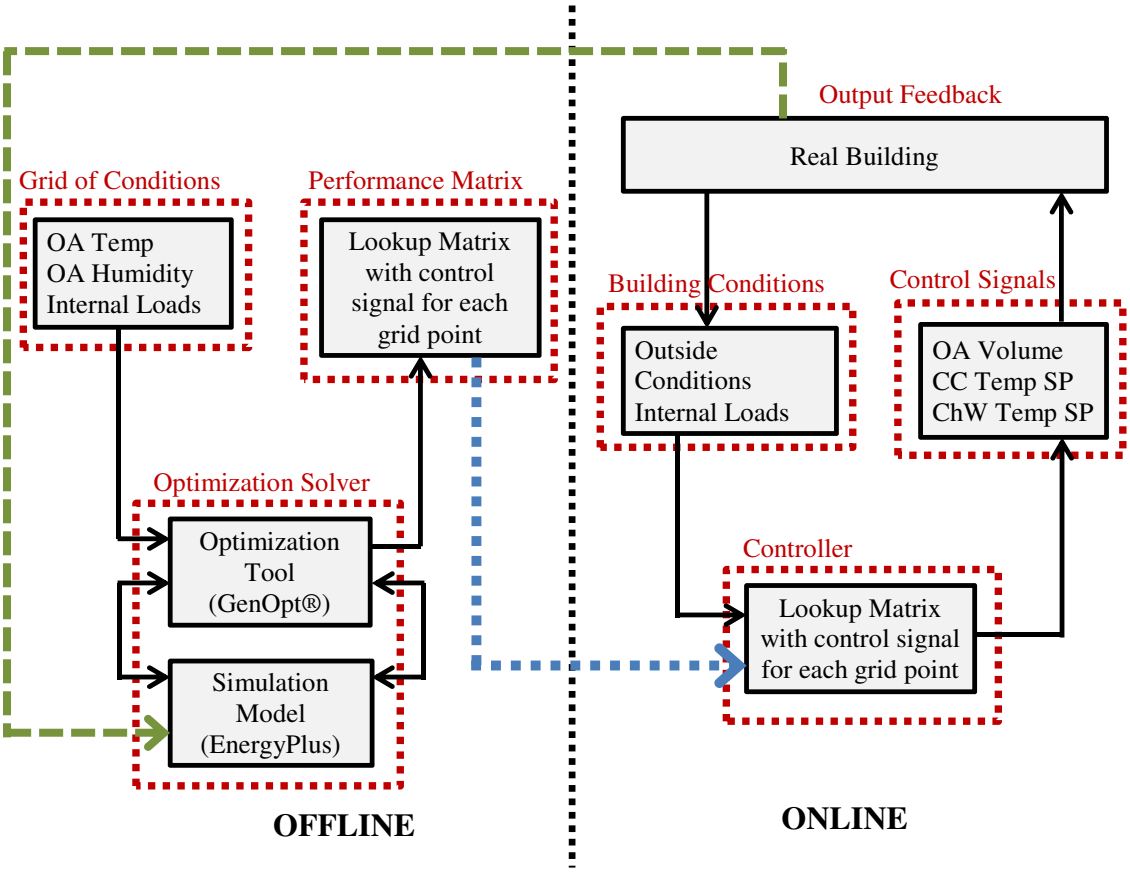

Figure 3.3: Data Flow Diagram for the Modified Model Predictive Control Used in the Research (Adapted from Coffey (2011))

Table 3.3 shows the values used for the grid points in the lookup matrix. Because humidity is not a factor in 'cool' and 'cold' conditions, only a single average value was used for outside air humidity. From the table, we can see that there are 18 grid points and

optimal controls were developed for each grid point in the matrix. The density of the grid is a tradeoff between accuracy and computational time. For each grid point, the parameters that were optimized were the volume of outside airflow, cooling coil leaving temperature and chilled water temperature. A minimum and maximum value was added as limits to each parameter to avoid unrealistic solutions. Table 3.4 documents the limits used.

Table 3.3: Grid of Building Conditions used for the GenOpt® Optimization

OA Temp	OA Humidity	Office Loads		
		People	Lights	Equipment
°F	lbw/lba	Fraction of peak		
30.40	0.0034	0.85	0.95	0.88
		0.50	0.78	0.74
		0.10	0.60	0.58
50.38	0.0067	0.85	0.95	0.88
		0.50	0.78	0.74
		0.10	0.60	0.58
70.36	0.0062	0.85	0.95	0.88
		0.50	0.78	0.74
		0.10	0.60	0.58
	0.0133	0.85	0.95	0.88
		0.50	0.78	0.74
		0.10	0.60	0.58
90.34	0.0134	0.85	0.95	0.88
		0.50	0.78	0.74
		0.10	0.60	0.58
	0.0181	0.85	0.95	0.88
		0.50	0.78	0.74
		0.10	0.60	0.58

Table 3.4: Control Parameter Limits Used in the GenOpt® Optimization

Control Parameter	Minimum Value	Maximum Value	Initialization Value
Volume of Outside Air	AHU4A1 = 8,300 cfm	AHU4A1 = 39,670 cfm	AHU4A1 = 14,316 cfm
	AHU5B1 = 13,000cfm	AHU5B1 = 61,740cfm	AHU5B1 = 23,212cfm
	AHU5C1 = 10,000cfm	AHU5C1 = 43,000cfm	AHU5C1 = 15,736cfm
Cooling Coil Leaving Air Temperature	45°F	70°F	53°F
Chilled Water Temperature	44°F	58°F	44°F

A penalty function was added to the HVAC energy use if the zone temperature and humidity setpoints were not being maintained. The temperature and humidity constraints were implemented using Equations 3.6, 3.7 and 3.8. The 'Modified HVAC Energy Use' was used as the cost function to be minimized in GenOpt®.

$$\text{Temp Constraint} = U_1 \times (\text{Max Zone Temp} - \text{Zone Temp Stpt})^{s1} \quad (3.6)$$

$$\text{Humidity Constraint} = U_2 \times (\text{Max Zone Hum} - \text{Zone Hum Stpt})^{s2} \quad (3.7)$$

$$\text{Modified HVAC Energy Use} = \text{Plant} + \text{Heating} + \text{Fans} + \text{Temp Constraint} + \text{Humidity Constraint} \quad (3.8)$$

The values for U_1 and U_2 were 50 and for s1 and s2 was 5. These values were estimated through trial and error to give a sufficiently high penalty value that is at least equivalent to the actual HVAC energy use (in joules) when the temperature or humidity exceeds the setpoint by 1°C or 1% RH. Appendix C.3 documents the EnergyPlus EMS program used to calculate the temperature and humidity constraints.

The actual optimization was conducted using two algorithms, a Generalized Pattern Search (GPS) algorithm and a Particle Swarm Optimization (PSO) algorithm. This hybrid approach combines the global approach of the PSO algorithm with the convergence properties of the GPS algorithm. Additionally, because the hybrid algorithm does not rely on the gradient of the problem being optimized, it is effective when the solution is noisy or irregular. The hybrid algorithm initially runs a Particle Swarm Optimization (PSO) for a user-defined set of iterations. Using the results of the PSO algorithm as the starting point, the Hooke-Jeeves Generalized Pattern Search (GPS) algorithm is initiated to locate the lowest cost function value. The PSO algorithm (Eberhart and Kennedy 1995, Wetter 2011) is a global optimization algorithm that optimized a problem by moving possible solutions (also known as particles) in the total space of solutions and uses both their relative local and global positions to achieve the optimization. The particle positions are initiated by using a random number generator that covers the total solution space uniformly. In the next iterations, the particles are moved in the space by updating the values for the particle position vector and velocity using simple mathematical formulae. The Hooke-Jeeves algorithm (Hooke and Jeeves 1961, Wetter 2011) uses the output of the PSO algorithm as the initial iteration point for the optimization. At this point, each variable that needs to be optimized is given an increment value (in both directions) and the solutions are compared. If the cost function is minimized, the new value is used as the initial point and the process is repeated. If no minimization is achieved, the step length is reduced and the process is repeated till the solution converges. Appendix C.1 provides the details of the variables and equations used for the PSO and Hooke-Jeeves algorithm.

The outputs of the optimization process were used to generate a controls lookup matrix that can be implemented in the real building. For this research, the lookup matrix was implemented in the EnergyPlus model of the building and the HVAC energy use and comfort conditions were evaluated. Section 7.3 documents the results from this step.

3.4. Zone Level Comfort Analysis

Stratification measurements were taken in the offices to establish temperature and airflow patterns in the zones. The measurements were conducted by installing temperature sensors in the supply plenum, return plenum, at the chilled beam entry, chilled beam exit and at varying heights in the office zone. Stratification measurements were taken for an interior office zone and an exterior office zone.

Figure 3.4 shows the position of the temperature sensors in the zones. Two sets of measurements were taken, one when the chilled beams were on and one when only the UFAD system was operational. 5-minute temperature measurements were taken in summer for a period of two weeks from a period of July 5th to July 19th 2014 for the interior zones and from July 19th to August 2nd 2014 for the exterior zones. Concurrently, trends were also collected from the building EMCS system for the AHU supply air temperature and setpoints, chilled beam water temperature and zone thermostat setpoints and temperature to document the operating conditions that influence the temperatures in the zones.

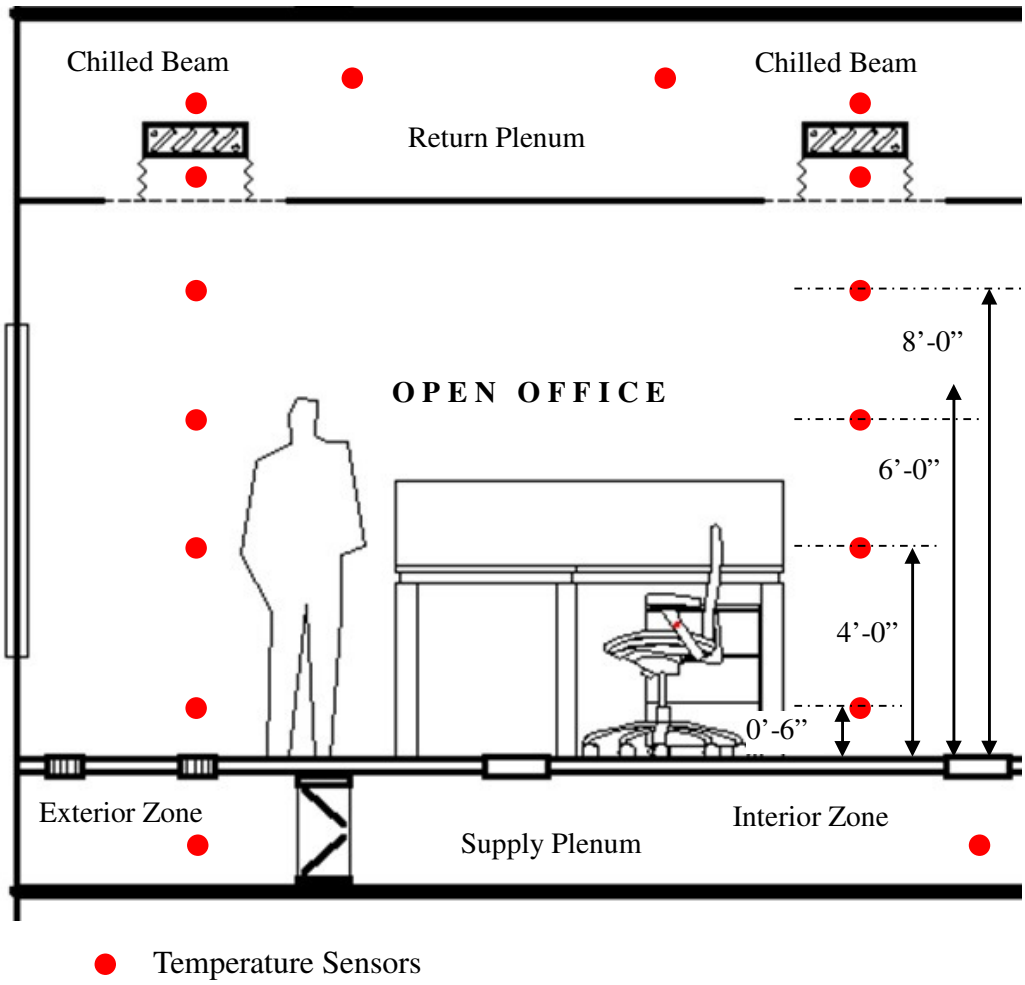

Figure 3.4: Section through the Chilled Beams Showing Location of the Temperature Sensors in the Interior and Exterior Zones for the Stratification Measurements

HOBO U12 data loggers were used for the zone temperature measurements. These data loggers were calibrated before they were installed in the building. The calibration process for the data-loggers was conducted in two steps. In the first step, 3 RTD sensors were calibrated to the ice-point and boiling-point of distilled water. In the second step, the calibrated RTD sensors were then used to calibrate the temperature data loggers. Both the

RTD sensors and the data loggers were placed in an insulated refrigerator and air temperature measurements were taken at cool, ambient and warm conditions. Based on the difference between the temperature measurements of the RTD sensors and the data loggers, an offset was applied to each of the data loggers. The details of the ice-bath, boiling point measurements, the refrigerator setup and the logging devices used in the calibration are described in Kim (2006) and Ugursal (2010). Appendix B documents the ice-point and boiling-point measurements for the RTD sensors and the offsets applied to the 7 data loggers after the calibration process.

A CFD model of a single interior zone was also developed in Star CCM+ 9.04 to supplement the zone temperature measurements and to estimate the zone airflows. The CFD model is based on the method developed by Nelson (2012), but the major assumptions of the model are documented here. The standard k-ε model was used to calculate the turbulent flows. The chilled beam in the CFD model was simulated as a porous region with a porosity of 0.62. The chilled beam was also modeled as a heat sink with a cooling capacity of 250 Btu/hr-Lft which is lower than the maximum beam capacity of 280 Btu/hr-Lft. The inlet and outlet interface between the passive chilled beam and the room was specified as an in-place interface that exchanges fluid and heat freely with the room. The walls of the chilled beam was specified as a baffle boundary that restricts heat transfer between these surfaces and the rooms. This replicates the actual chilled beam where heat exchange takes place only at the inlet and the outlet of the beam.

The walls of the zone were specified as walls with a surface temperature of 73°F (the average temperatures of the zone). The zone floor and return plenum ceiling were

specified as walls with surface temperatures of 68°F. Three diffusers were specified in the zone floor as velocity inlets with velocities of 50ft/min. A pressure outlet was also specified in the return plenum. Four persons were modeled in the zone with heat fluxes of 409 Btu/hr each. Eight computer monitors were also modeled with heat fluxes of 137 Btu/hr each. The total area of the zone was 300 ft^2, hence the total loads in the zone was 9.1 Btu/hr-ft^2 which is lower than the maximum loads of 15 Btu/hr-ft^2 recommended for passive chilled beams. Figure 3.5 shows the zone CFD model showing the inlets, outlets and boundaries.

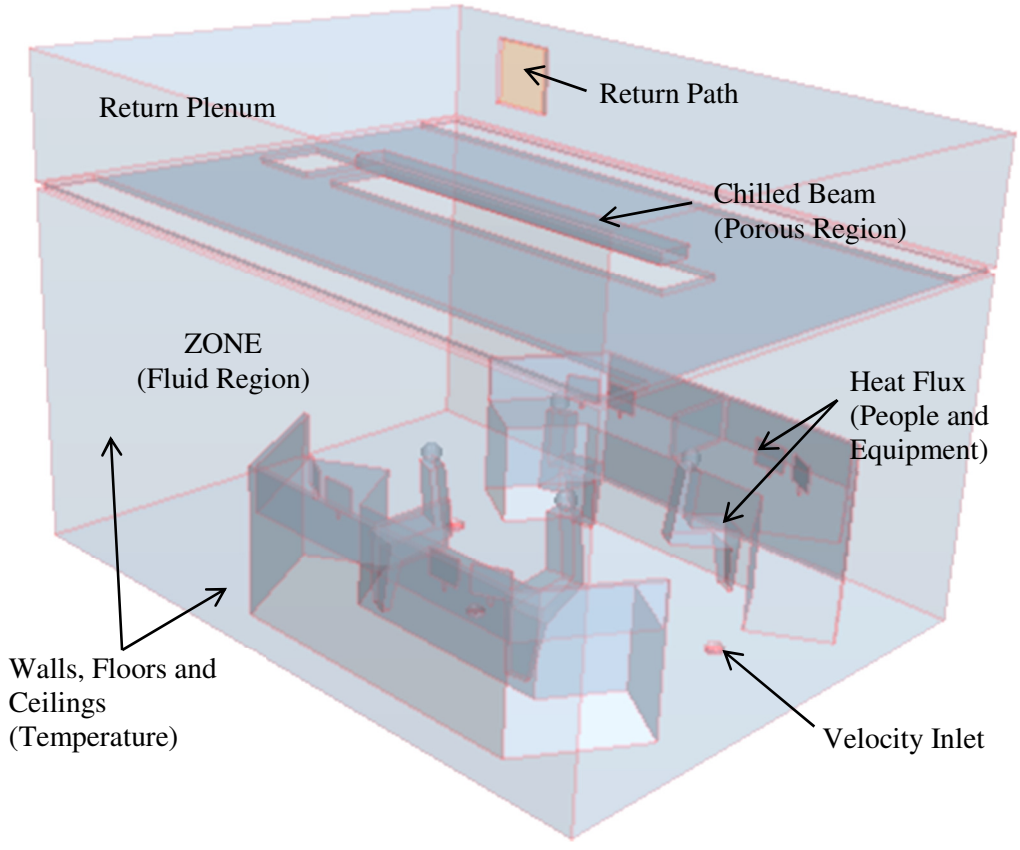

Figure 3.5: View of the Zone CFD Model Showing Inlets, Outlets and Boundaries

An unstructured polyhedral meshing scheme was used with a single prism layer as the first cell along the boundaries. The density of the grid was incrementally reduced to establish grid independence. Figure 3.6 shows the mass flow rate at the pressure outlet for the total cells in the volume mesh. It shows that the mass flow rate does not change significantly for number of cells greater than 1,000,000. Figure 3.7 shows the final volume mesh of 1,040,268 cells that was used for the CFD model. The parameters for the mesh are documented in Table 3.5.

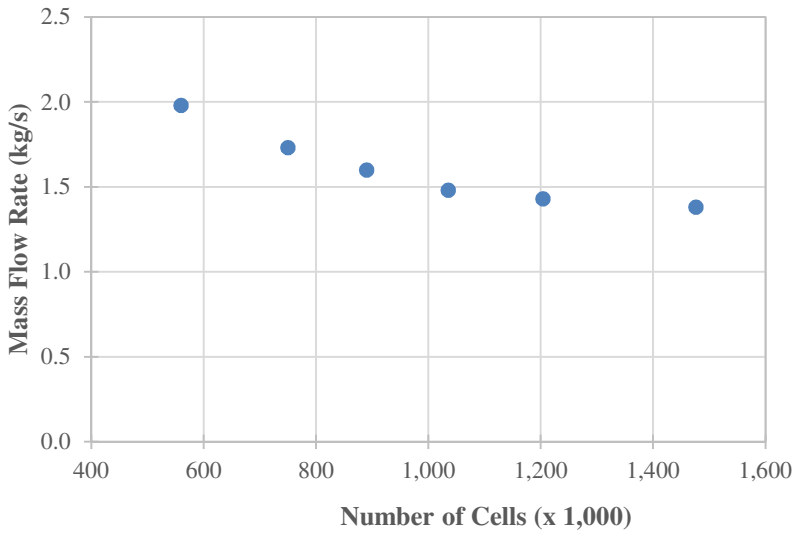

Figure 3.6: Grid Dependence Test showing the Mass Flow Rate at the Plenum Outlet for the Different Densities of the Volume Mesh

Table 3.5: Mesh Parameters for the Final Volume Mesh

Number of Cells	1,040,268
Base Size	10 cm
Number of Prism Layers	1
Prism Layer Thickness	5 cm
Surface Growth Rate	1.3
Minimum Surface Size	2.5 cm
Target Surface Size	5 cm
Beam Area Mesh Size	5 cm
Beam, Inlet and Outlet Surface Size	5 cm

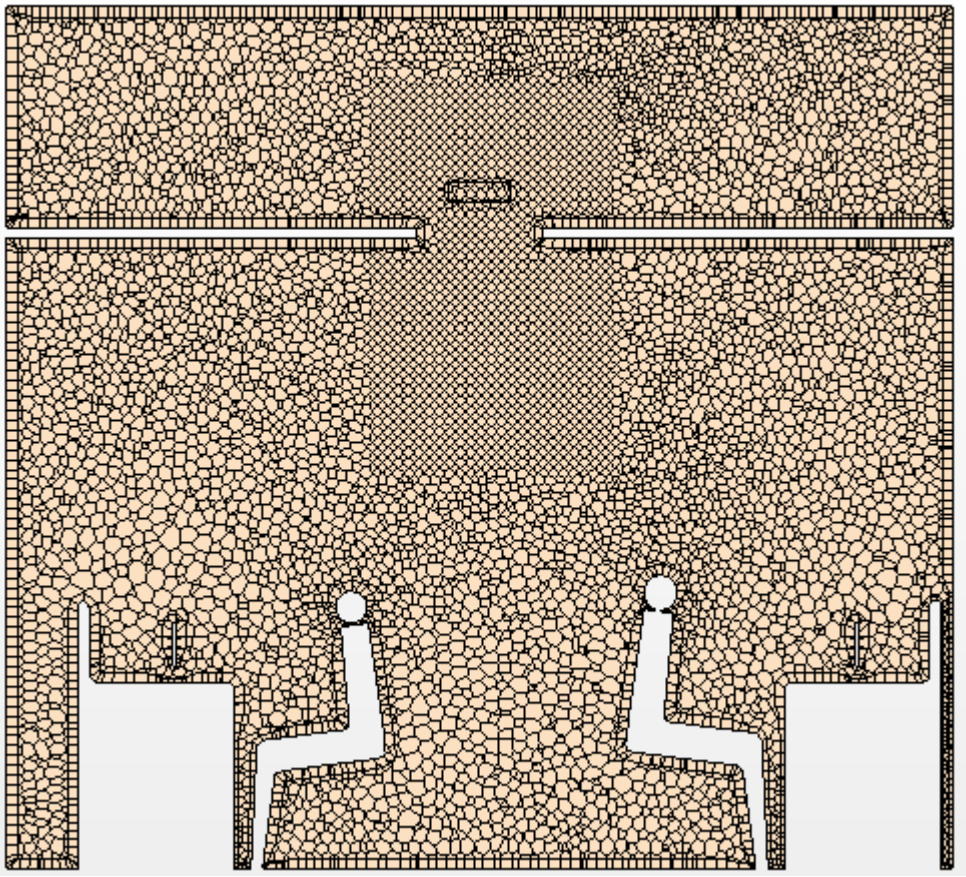

Figure 3.7: Cross-Section of the Final Volume Mesh (1,040,268 Cells)

3.5. Summary of Methodology

In summary, the methodology applied in the research consisted of 4 major steps:

- Development of an energy model for chilled beams and UFADs
    - Building data was collected for the case-study building with chilled beams and UFADs and inputs were established for the EnergyPlus simulation model.
    - A process for modeling the operation of the passive chilled beams and the UFAD system in EnergyPlus was developed.
    - A simplified steady state model was developed for validation and quick energy use predictions.
- Energy use evaluation of passive chilled beams
    - The energy use of the building was compared to an equivalent VAV system baseline and an ASHRAE 90.1 code-compliant building.
    - A parametric study was also conducted by varying the latent and sensible loads in the space to understand their effect on the energy savings potential of the chilled beam system.
- Development of optimization strategies for operational control of passive chilled beams
    - A sensitivity analysis of operational control parameters was conducted for the chilled beam and the equivalent VAV system.
    - Simplified rule-based optimization strategies were developed for the chilled beam system.

- A process was outlined to develop and model a simulation assisted optimization strategy that can be eventually implemented in the building. The results of this strategy was compared with the simplified rule-based optimization strategies developed.

- Zone level comfort analysis for passive chilled beams with UFADs
  - Stratification measurements were taken in the offices to establish temperature profiles in the zones.
  - A CFD model was developed of a single interior zone in the building. The model included the passive chilled beam as a heat sink, the velocity inlets, the heat sources such as people and computers and the return plenum with the pressure outlet.

The comfort analysis conducted provided insight into the zone airflow patterns and the thermal effect of the chilled beam and UFAD system on each other.

CHAPTER IV

ENERGY MODEL DESCRIPTION

In this chapter, Section 4.1 contains the building description including the envelope, zoning, occupants, lighting and equipment loads, HVAC equipment description, details of the existing HVAC operation and the measured energy use data for the building. Section 4.2 documents the assumptions for the EnergyPlus simulation model. Section 4.2 contains details of the step-by-step process used to calibrate the simulation model to the building energy data. Section 4.4 documents the modeling of the modified control for the chilled beams based on recommended operation. Finally Section 4.5 includes the observations from the development and calibration of the building simulation model.

4.1. Case-Study Building Description

The case-study building[5] is a 606,900 ft^2, 4 story LEED Gold rated commercial office building in the Dallas-Fort Worth area[6]. The building includes open-plan offices, conference areas, training areas, break areas, a cafeteria, kitchen and a fitness center. The offices are heated and cooled by a passive chilled beam system with a parallel VAV ventilation system, underfloor air distribution and perimeter electric heating. The cafeteria, kitchen, lobby and mechanical areas are equipped with standard VAV systems with overhead mixing ventilation.

---

[5] Conditioned floor area

[6] A non-disclosure agreement has been signed with the owners of the case-study building to withhold the exact location, name and occupants of the building.

4.1.1. Building Physical Description

The case-study building is divided into 3 wings with a total of 515,338 ft^2 of office area (including conference and break areas), a cafeteria and kitchen on the ground level (29,371 ft^2 total), a fitness center on the first floor (10,567 ft^2), semi-conditioned penthouse mechanical rooms (45,571 ft^2), and a ground level service area with the central plant room, electrical rooms, data centers, generator rooms and loading/storage areas (44,126 ft^2).

4.1.1.1. Building Envelope

The building has three types of exterior wall systems. The first floor wall system has a 6" steel stud wall (with cavity insulation) on the inside, an 8" filled concrete block wall in the middle and a stone cladding finish on the outside. The second and third floor wall system is a 6" steel stud wall (with cavity insulation) on the inside and an exterior insulation and finish system (EIFS) wall on the outside. The top floor wall is a floor-to-ceiling window glazing system with a 4" steel stud insulated plenum wall and an exterior aluminum fascia panel. The building has an overall window-wall ratio of approximately 39%[7]. The building windows are air filled double pane glass with low-e coating on the inside surface of the outer glass. The building roof has a 6" ceiling concrete slab with batt insulation in the space between the ceiling slab and the exterior sheet metal pitched roof. The building slab-on-grade floor is a 6" concrete slab with no exterior insulation. The office floors are raised access floor systems with a rigid structural grid and lay-in steel

[7] Window-wall area was calculated for the conditioned floor area

floor with a carpet finish. Infiltration was assumed in the zones and supply and return plenums. Figure 4.1 shows the exterior images of the building. Table 4.1 provides details of the building envelope as modeled.

Figure 4.1: Exterior Images of the Case-Study Building

Table 4.1: Building Envelope Specifications[8]

Component	Construction	Assembly Details	Source
Floors			
Exterior Floor	Slab-on-grade floor with 6" heavy-weight concrete	U-2.25[9] Btu/hr-ft^2-°F	As-built drawings
Interior Office Floor	Raised steel UFAD floor, carpet with carpet pad over floor	-	
Walls			
First Floor Wall	6" exterior stone veneer with 8" filled concrete block backup, 5/8" exterior sheathing, 2x6 steel studs with R-19 cavity insulation and 5/8" interior gypsum board	U=0.058[9] Btu/hr-ft^2-°F	As-built drawings
Second/Third Floor Wall	2" exterior EIFS system with 1/2" backup sheathing, 5/8" exterior sheathing, 2x6 steel studs with R-19 cavity insulation and 5/8" interior gypsum board	U=0.063[9] Btu/hr-ft^2-°F	As built drawings

[8] Data in highlighted cells was modified during the calibration process
[9] Values calculated by EnergyPlus

Table 4.1 (continued): Building Envelope Specifications[8]

Component	Construction	Assembly Details	Source
Top Floor Wall	Alum fascia panel, 1/2" exterior sheathing, 2x4 steel studs with R-13 cavity insulation	U=0.085[9] Btu/hr-ft^2-°F	As-built drawings
Windows			
Exterior windows	Low-E, argon filled double pane glazing system; aluminum frame with thermal break	U=0.46[9] Btu/hr-ft^2-°F; SHGC=0.57[9]	As-built drawings
Roofs			
Exterior Roof	6" heavy-weight concrete with R-13 cavity insulation, exterior sheet metal roof	U=0.034[9] Btu/hr-ft^2-°F	As-built drawings; ASHRAE 90.1 (2004) requirements

Infiltration values were assumed to be 0.4 cfm/ft^2 @ 0.3 in.W.G. of above-grade envelope area based on Deru et al. (2011) when the fans are off. This was converted to a pressure of 0.016 in.W.G. assuming a flow exponent of 0.65.

4.1.1.2. Zoning

The building zoning for the energy model was simplified based on use, space loads and the HVAC systems. The building was modeled as office areas, a gymnasium, a kitchen, a cafeteria, three penthouse mechanical areas, a ground level service area and a reception/lobby area. The office areas were divided by wing and floor with each floor subdivided into two zones, an interior zone and an exterior zone. Each office zone was also modeled with a supply UFAD plenum and a return plenum. The cafeteria and gymnasium were also subdivided into an interior zone and an exterior zone each. The service areas on the ground level in the building include a central plant, server rooms, electric rooms, loading areas and storage areas with several FCUs, CRAC units and a plant AHU. These areas were simplified into a single zone with a single supply AHU. Figure

4.2, Figure 4.3 and Figure 4.4 show the physical simulation model of the building. Table 4.2 documents details of the building zones as modeled.

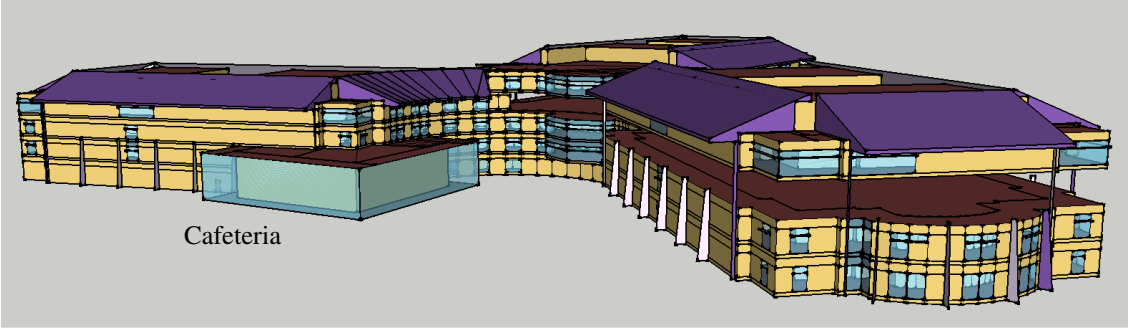

Figure 4.2: South-West View of the Building Energy Model (showing the cafeteria)

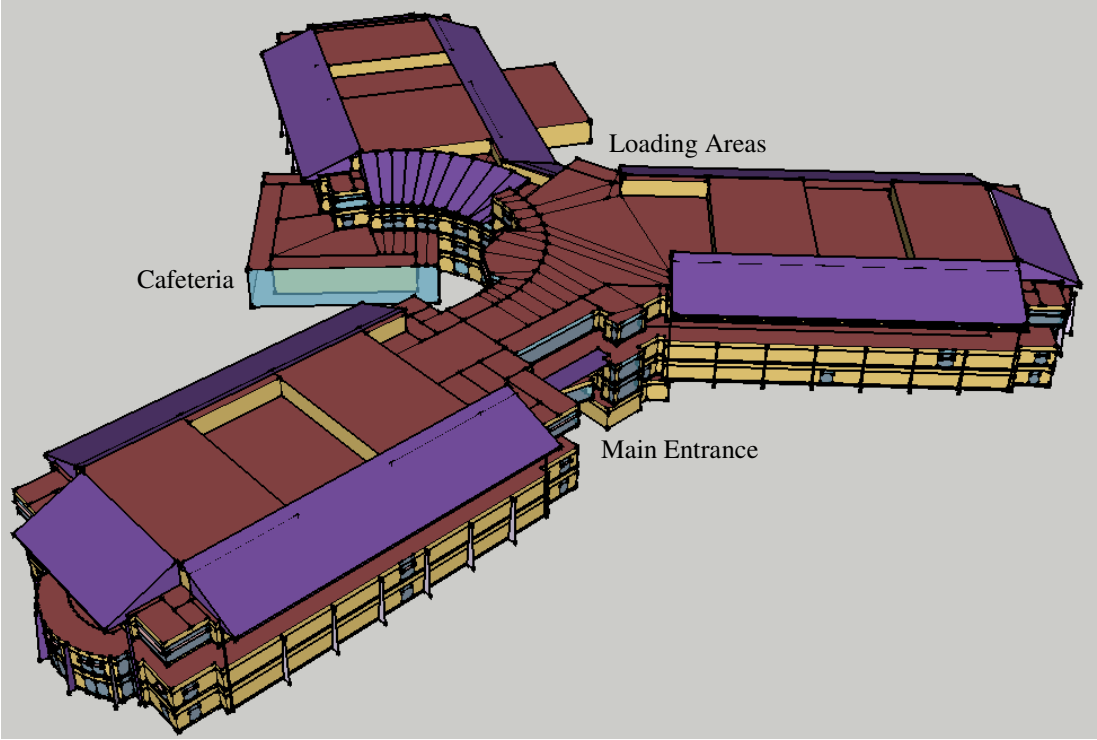

Figure 4.3: South-East View of the Building Energy Model (showing the main building entrance)

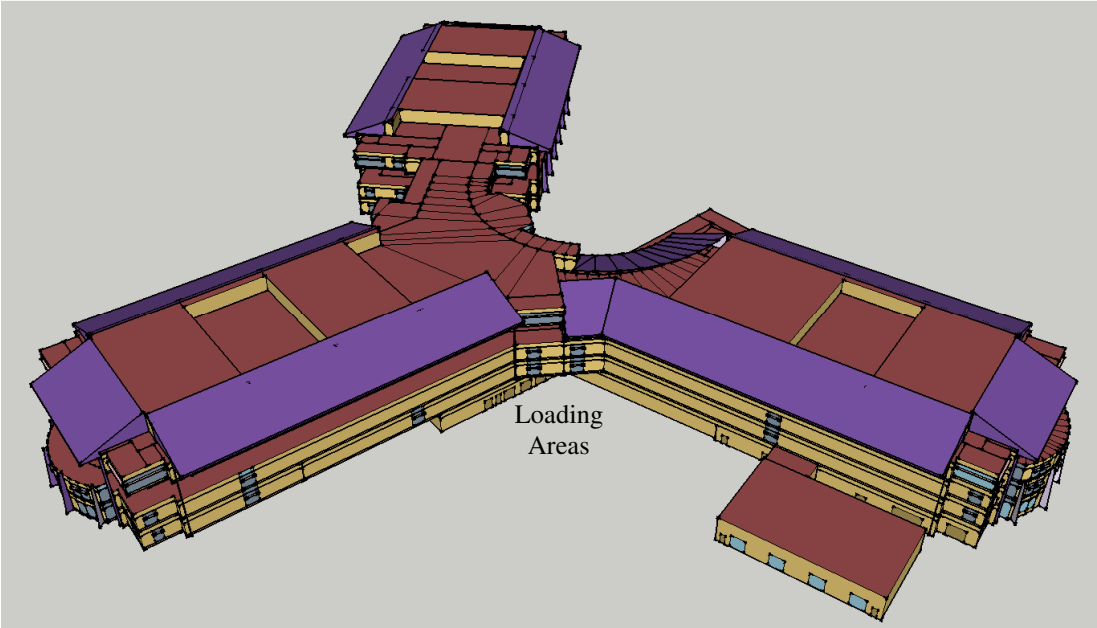

Figure 4.4: North-East View of the Building Energy Model (showing the loading areas and the exterior emergency generator room)

4.1.2. Occupancy, Lighting and Equipment Loads

The occupancy, lighting and equipment details for the various zones in the building are documented in Table 4.2. Figure 4.5 and Figure 4.6 show the weekday and weekend occupancy, lighting and equipment profiles as modeled in the initial simulation. The details of process used to estimate these values are discussed in Section 3.1.

Table 4.2: Zone and Interior Loads Modeled in the Building[10]

Program	Zone	Area (ft^2)	Occupancy (ft^2/person)	LPD (W/ft^2)	Equipment (W/ft^2)
Service Area	Ground floor mechanical room	44,126	-	0.5	1.2
Cafeteria	Exterior zone	14,232	30	1.0	0.5
	Interior zone	10,132			
Kitchen	Ground floor kitchen	5,003	200	1.8	7.5
Lobby	First floor main lobby	7,497	200	1.4	0.4
Offices	Wing A first floor exterior zone	12,681	187	1.0	1.0
	Wing A first floor interior zone	33,716			
Gymnasium	Wing B first floor exterior zone	3,042	36	1.4	1.0
	Wing B first floor interior zone	7,525			
Training Areas	Wing B first floor exterior zone	8,213	150	1.0	1.0
	Wing B first floor interior zone	31,257			
Offices	Wing C first floor exterior zone	11,746	127	1.0	1.0
	Wing C first floor interior zone	30,252			
	Wing A second floor exterior zone	12,681	137	1.0	1.0
	Wing A second floor interior zone	33,874			
	Wing B second floor exterior zone	16,160	179	1.0	1.0
	Wing B second floor interior zone	41,149			
	Wing C second floor exterior zone	11,746	347	1.0	1.0
	Wing C second floor interior zone	30,252			
	Wing A third floor exterior zone	12,307	163	1.0	1.0
	Wing A third floor interior zone	33,072			
	Wing B third floor exterior zone	16,160	179	1.0	1.0
	Wing B third floor interior zone	41,149			
	Wing C third floor exterior zone	11,746	347	1.0	1.0
	Wing C third floor interior zone	30,252			
Offices	Wing B fourth floor exterior zone	15,777	146	1.0	1.0
	Wing B fourth floor interior zone	40,347			
	Wing C fourth floor exterior zone	11,372	118	1.0	1.0
	Wing C fourth floor interior zone	29,450			
Penthouses	Wing A mechanical room	17,451	-	0.3	-
	Wing B mechanical room	14,185	-	0.3	-
	Wing C mechanical room	13,935	-	0.3	-

[10] Data in highlighted cells was modified during the calibration process

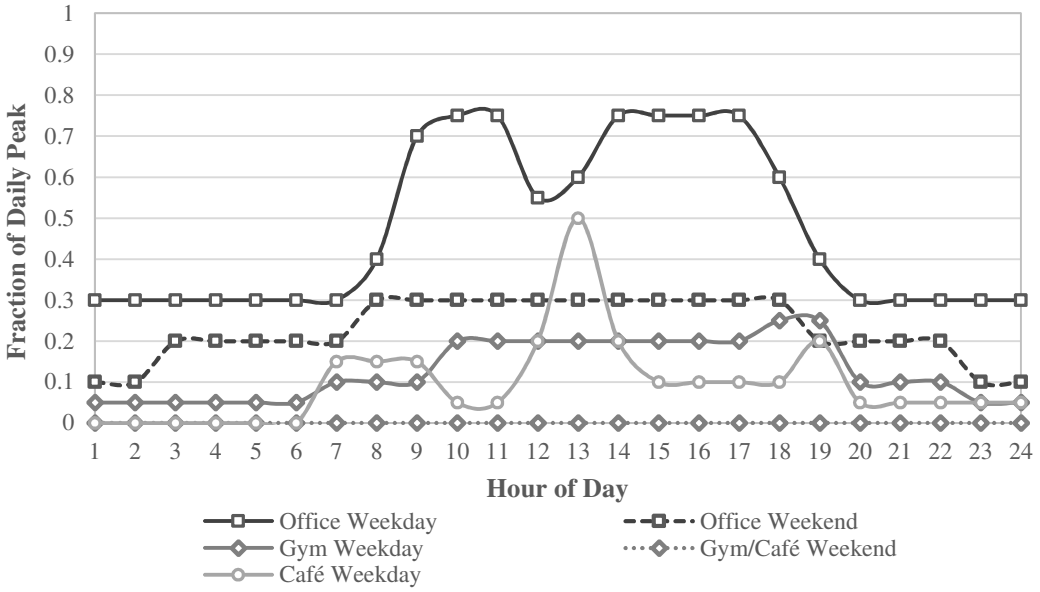

Figure 4.5: Occupancy Profiles Modeled in the Initial Simulation[11]

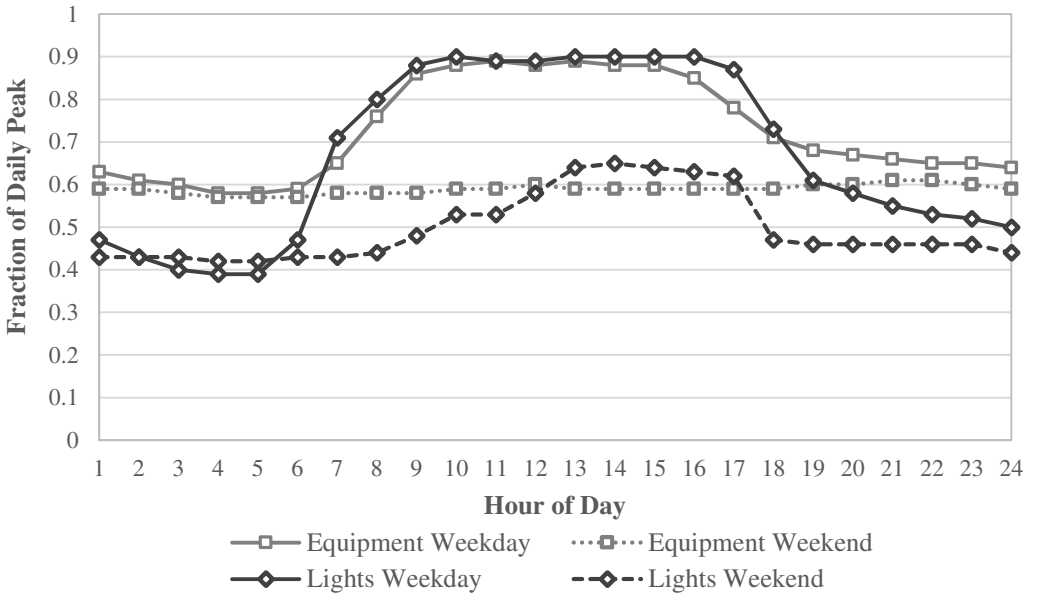

Figure 4.6: Equipment and Lighting Profiles Modeled in the Initial Simulation[11]

[11] Occupancy, lighting and equipment profiles were modified during the calibration process

4.1.3. HVAC Equipment Description

The offices in the building are heated and cooled by a VAV ventilation system with underfloor air distribution (UFAD). Supplemental cooling is provided at the zone level by passive chilled beams. Heating is provided only in the exterior zones by terminal heating boxes installed in the return plenum. The cafeteria, kitchen and lobby equipment are standard VAV systems with overhead zone supply and mixing ventilation. Figure 4.7 shows the interior images of the office spaces showing the UFAD diffusers and the chilled beam.

Figure 4.7: Interior Images of the Office Spaces Showing the UFAD Diffusers and the Chilled Beams

The building equipment consists of 15 VAV AHUs, 1 CV AHU, 17 FCUs, 4 CRAC units, 3 centrifugal variable-speed water-cooled chillers, 1 screw air-cooled chiller, 3 variable-speed cooling towers, 1 water-side heat-exchanger, 4 chilled water pumps, 3

condenser water pumps, 3 chilled beam pumps (one for each wing) and 2 heat-exchanger pumps.

4.1.3.1. Air Handling Units

For the offices in the building, 4 VAV AHUs feed a central supply shaft in each wing, which in turn feed the underfloor airways on each floor. This arrangement was simplified in the energy model. The 4 AHUs were modeled as a single AHU per wing. Figure 4.10 shows the configuration for the UFAD AHUs. The cafeteria, kitchen and lobby are conditioned by an AHU each and were modeled as installed. Figure 4.11 shows the configuration for the VAV AHUs. The plant room on ground floor houses the water-cooled chillers and is conditioned by a CV AHU. The other service areas on the ground floor are conditioned by the FCUs and the CRAC units. All these areas were modeled as a single zone with a single CV AHU. All the airside equipment was sized as installed. Table 4.3 documents sizes, flows and efficiencies of the airside equipment as modeled.

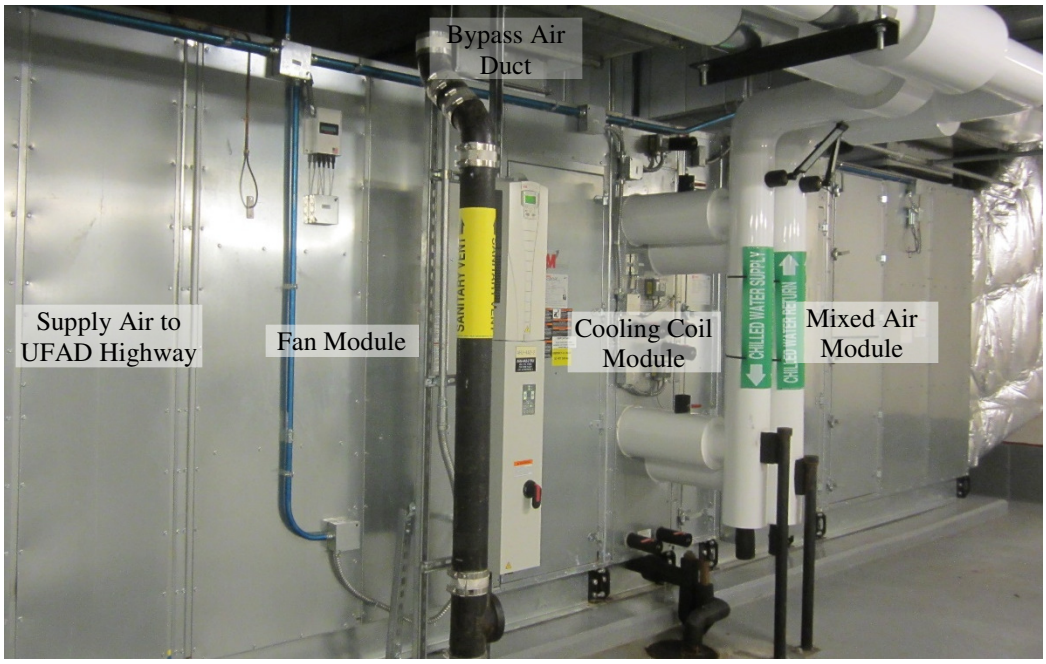

Figure 4.8: AHU 4A2-2 (Typical UFAD AHU)

Figure 4.9: Outside Air Intakes for AHUs 5B1-1 and 5B1-2 (Typical UFAD AHU)

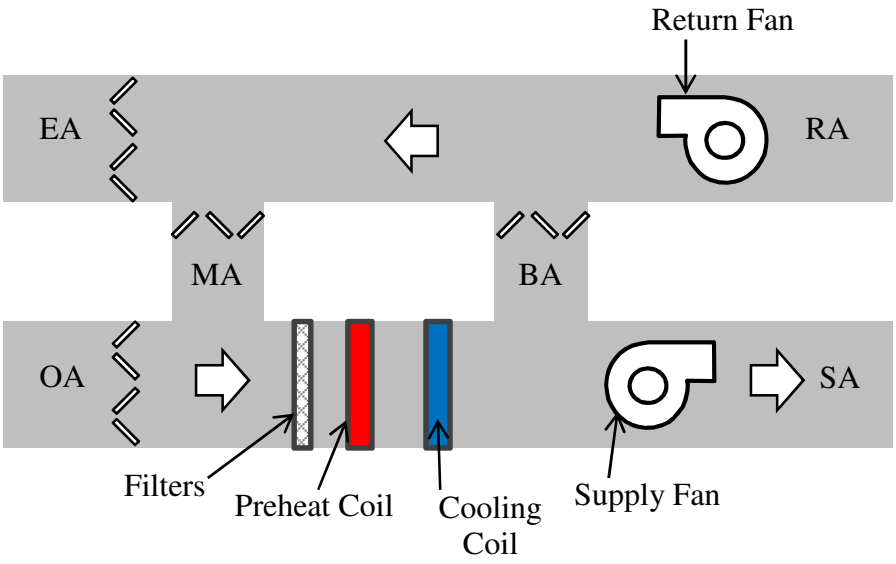

Figure 4.10: Typical UFAD AHU Configuration

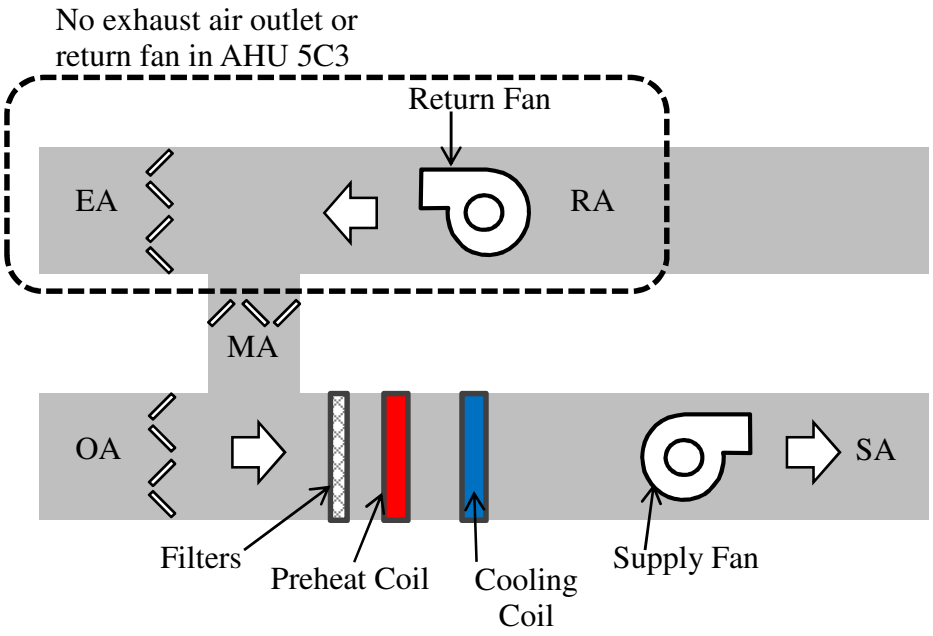

Figure 4.11: Typical VAV AHU Configuration

Table 4.3: AHU Details as Modeled[12]

AHU	Type	Serves	Schedule	Max Supply Airflow	Min Outside Air	Cold Deck Temp SP	Supply Air Temp SP	CB Temp SP	UFAD Plenum Pr. SP	Fan Specifications			
										Size	Static Pr.	Fan Eff.	Motor Eff.
				cfm	cfm	°F	°F	°F	in.W.G.	HP	in.W.G.		
4A1	VAV/ UFAD	Wing A Offices	24x7	150,000	10,000	53	62	62	0.02-0.04	240	1.20	0.65	0.9
										120	0.75	0.65	0.9
5B1	VAV/ UFAD	Wing B Offices	24x7	200,000	12,000	53	62	62	0.02-0.05	300	1.20	0.65	0.9
										160	0.75	0.65	0.9
5C1	VAV/ UFAD	Wing C Offices	24x7	200,000	12,000	53	62	62	0.02-0.05	300	1.20	0.65	0.9
										160	0.75	0.65	0.9
4A3	VAV	Café	3:00am-10:00pm	40,000	1,800	-	55	-	-	60	1.20	0.65	0.9
										30	0.75	0.65	0.9
4A4	VAV	Kitchen	3:00am-10:00pm	25,000	200	-	55	-	-	40	1.20	0.65	0.9
										30	0.75	0.65	0.9
5C3	VAV	Lobby	3:00am-1:00am	15,000	500	-	55	-	-	20	2.00	0.65	0.9
CP1	CV	Service Areas	24x7	7,000	0	-	-	-	-	-	-	0.65	0.9

[12] Data in highlighted cells was modified during the calibration process

4.1.3.2. Zone Equipment

At the zone level, each office zone was modeled with 2 supply terminal units; the VAV UFAD supply plenum and the passive chilled beam terminal unit (with no supply air). The heating terminal units in the building are constant volume and were modeled as unit heaters. Figure 4.12 shows the zone equipment in the office spaces. Terminal units in the cafeteria, lobby and kitchen were modeled as standard VAV units. The lobby area was modeled with terminal reheat, the cafeteria was modeled with baseboard heating and the kitchen is not equipped with zone heating. The zone level equipment was sized based on ASHRAE Design Day (99.6%) conditions instead of using the actual zone equipment sizes because the modeled zones are a simplification of the actual building zones.

Stratification achieved in a UFAD system plays an important role in the energy balance in the zones and can be modeled in EnergyPlus using a simplified room air model (Liu 2006). However, the presence of chilled beam system hinders stratification and lowers the ventilation effectiveness of the underfloor air distribution system. A more mixed temperature profile is obtained as a result, and was modeled as such in EnergyPlus. Details of the temperature profiles in the offices with the UFAD and chilled beam system operating are discussed in Chapter VIII.

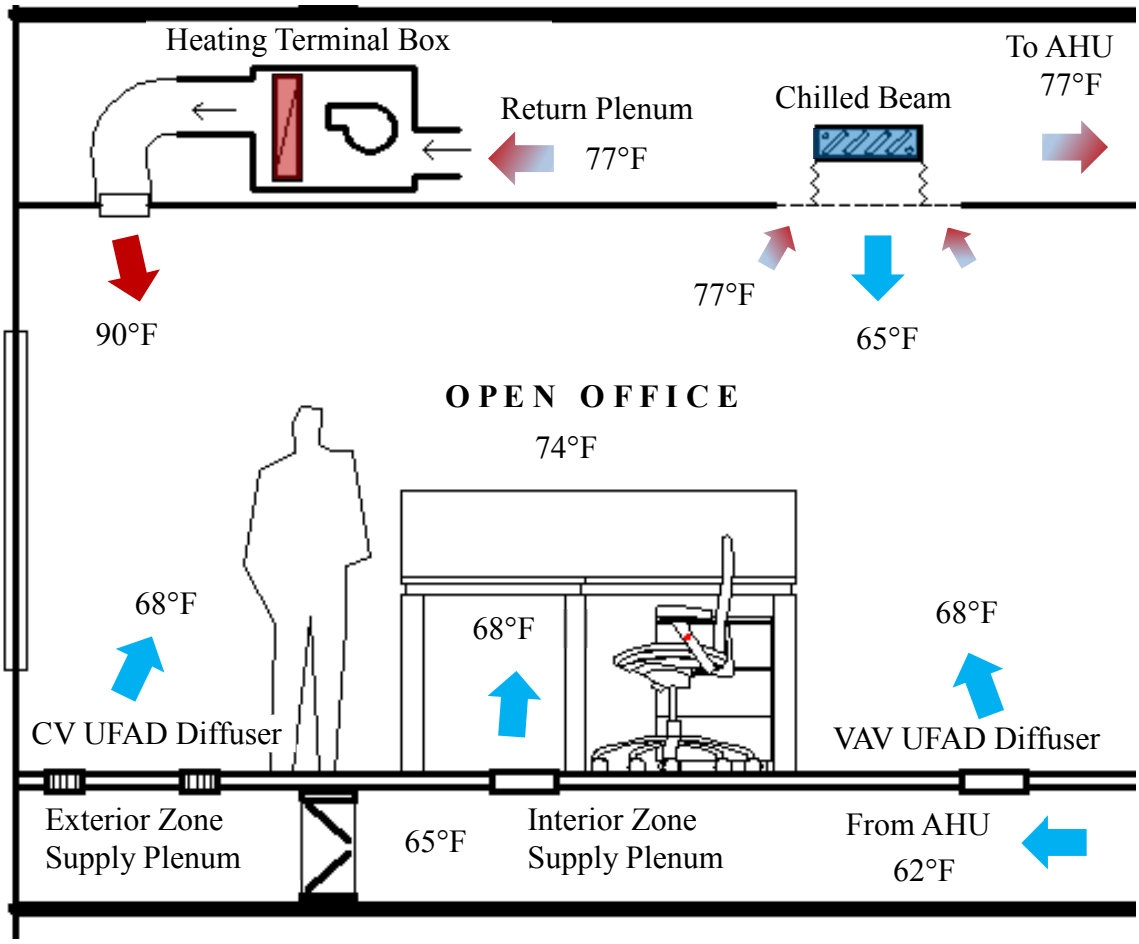

Figure 4.12: Section showing Zone Equipment in the Office Spaces in the Building (Typical for Spaces with a UFAD/Chilled Beam System)

4.1.3.3. Plant Equipment

The waterside system was modeled as installed with some accommodations for the limitations of EnergyPlus. The chilled water pumps in the actual building are series inlet branch pumps that switch on and off along with the associated chiller. This configuration if modeled in EnergyPlus causes issues when switching between the air-cooled chiller and the water-cooled chillers. As a work-around, the chilled water loop was modeled as a bank

of parallel return water pumps that still switch on and off along with the corresponding chiller. The same modeling approach was used for the condenser water pumps. Figure 4.15 shows the configuration for the modeled chilled water and condenser water supply loops. The chilled beams in the building are supplied with return chilled water from the AHUs. A mixing valve is also included to blend supply chilled water if required to meet the chilled beam water setpoint. This configuration was approximated in EnergyPlus by modeling each chilled beam loop with a heat exchanger that couples the chilled water demand loop with the chilled beam supply loop and provides chilled water to the chilled beams. All the plant equipment was sized as installed. Table 4.4 documents sizes, flows and efficiencies of the waterside equipment as modeled. Chiller curves for chillers in EnergyPlus that were similar in make, type, size and efficiency to the actual building were used in the model.

Figure 4.13: Water Cooled Chillers and Chilled Water Pumps in the Building

Figure 4.14: Cooling Towers and Condenser Water Pumps in the Building

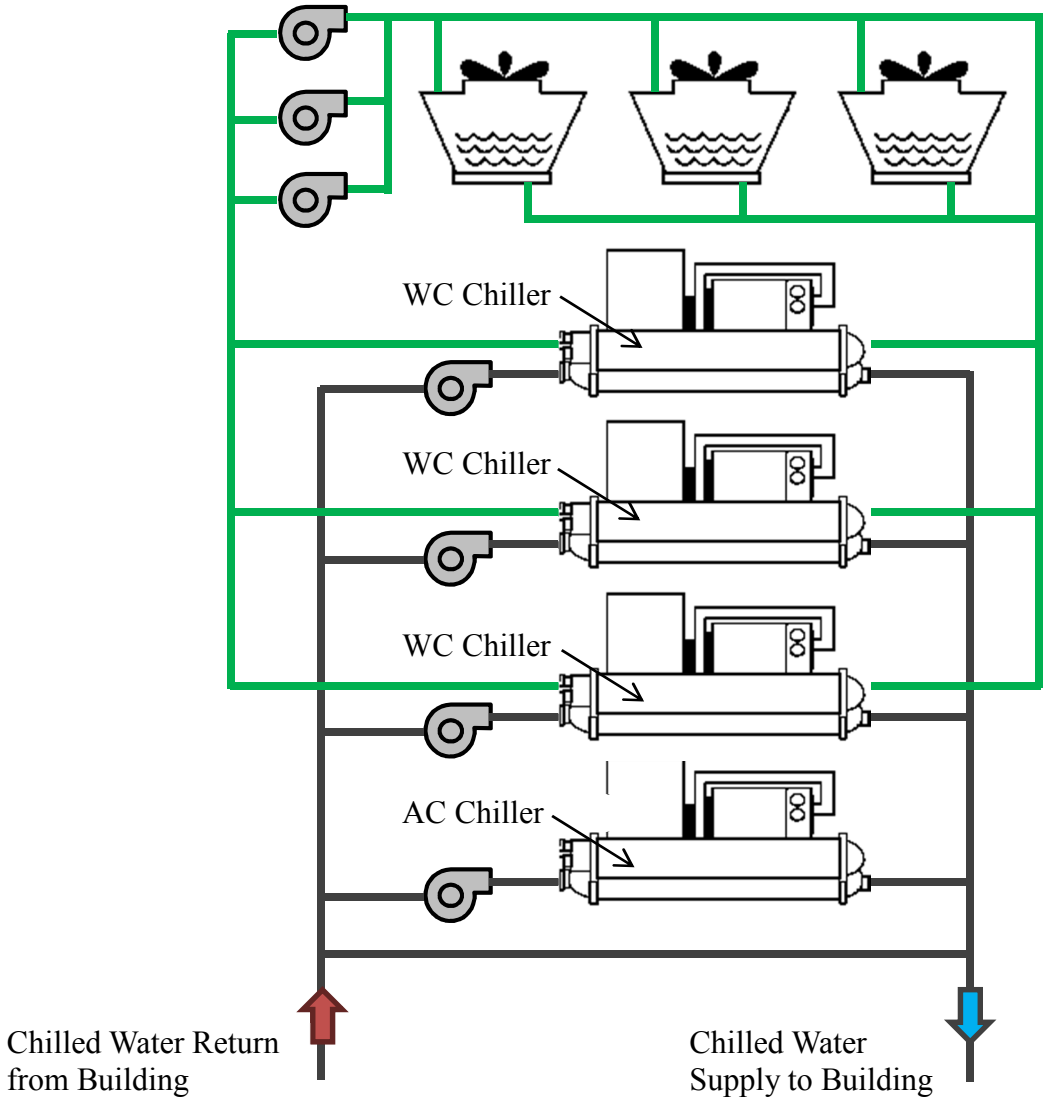

Figure 4.15: Plant Loop Configuration as Modeled in EnergyPlus

Table 4.4: Plant Equipment as Modeled in EnergyPlus[13]

Equipment	Description	Quantity	Flow Rate	Rated Output	Power Input	Max Efficiency
Chillers						
WC Chiller	Centrifugal water cooled chiller with variable speed pumps	3	1045 gpm 2100 gpm	700 Tons	394 kW	0.558 kW/ton
AC Chiller	Screw air cooled chiller with constant speed pumping	1	458 gpm	300 Tons	450 kW	1.465 kW/ton
Cooling Towers						
Cooling Tower	2 variable speed fans per tower, constant speed pumps	3	2100 gpm	700 Tons	30 (2) HP	-
Chilled Beams Heat Exchanger						
Heat Exchanger	Cross flow mixed fluid-to-fluid heat exchanger	3 (1 per wing)	390 gpm 640 gpm 520 gpm	-	-	-
Pumps				**Head**	**Size**	**Pump Eff.**
WC Chiller	Variable speed	3	1045 gpm	150 ft	60 HP	0.8
Cooling Tower	Constant speed	3	2100 gpm	100 ft	75 HP	0.8
Chilled Beams	Variable speed	3	390 gpm 640 gpm 520 gpm	100 ft 100 ft 90 ft	20 HP 25 HP 20 HP	0.8

4.1.4. Building Operation

4.1.4.1. AHU Control

The quantity of outside air to all the AHUs in the building is controlled by the CO_2 levels in the building, i.e. the outside air dampers modulate to maintain return air CO_2 levels on each floor of each wing below 900ppm. This demand controlled ventilation is subject to minimum outside airflow setpoints (see Table 3) and is overridden during

[13] Data in highlighted cells was modified during the calibration process

economizer operation. The economizers operate between 35-60°F and have differential enthalpy control, i.e. the economizers are activated only when the outside air enthalpy is 0.25Btu/lb_a less than that of the return air. The preheat coil leaving temperature and cooling coil leaving temperature is maintained at a constant setpoint all through the year. For the UFAD AHUs, the supply air temperature to the zones is higher than the cooling coil leaving temperature. The return air bypass dampers are modulated (see Figure 4.10) and the cooled supply air is mixed with the return air to achieve a supply air temperature setpoint of 62°F. The exhaust air dampers are controlled to maintain a building pressure setpoint of 0.05in.W.G. Table 4.3 documents the control setpoints for the AHUs in the building.

4.1.4.2. Zone Equipment Operation

The UFAD supply air is the primary source of cooling in the offices. The supply diffusers in the pressurized UFAD plenum modulate to maintain zone cooling temperature setpoints. Because of the expected uncontrolled leakage from the pressurized plenum to the zone, a minimum supply flow to the zones is not specified. At present, the chilled beams are switched on manually for approximately 2 months of the year. When operational, the chilled beams are controlled to a supply water temperature setpoint that is maintained at a value that is 3°F higher than the dewpoint temperature of the return air plenum. The chilled beam supply water pumps modulate to meet a fixed differential pressure setpoint in each wing. In heating mode, the heating terminal unit fans in the return plenums of the exterior zones are activated and recirculate return air to the zones. If the heating temperature setpoints are still not met, the 2-stage electric heating coils in the

terminal units are then activated. Figure 4.16 shows the overall control of the zone equipment in the offices.

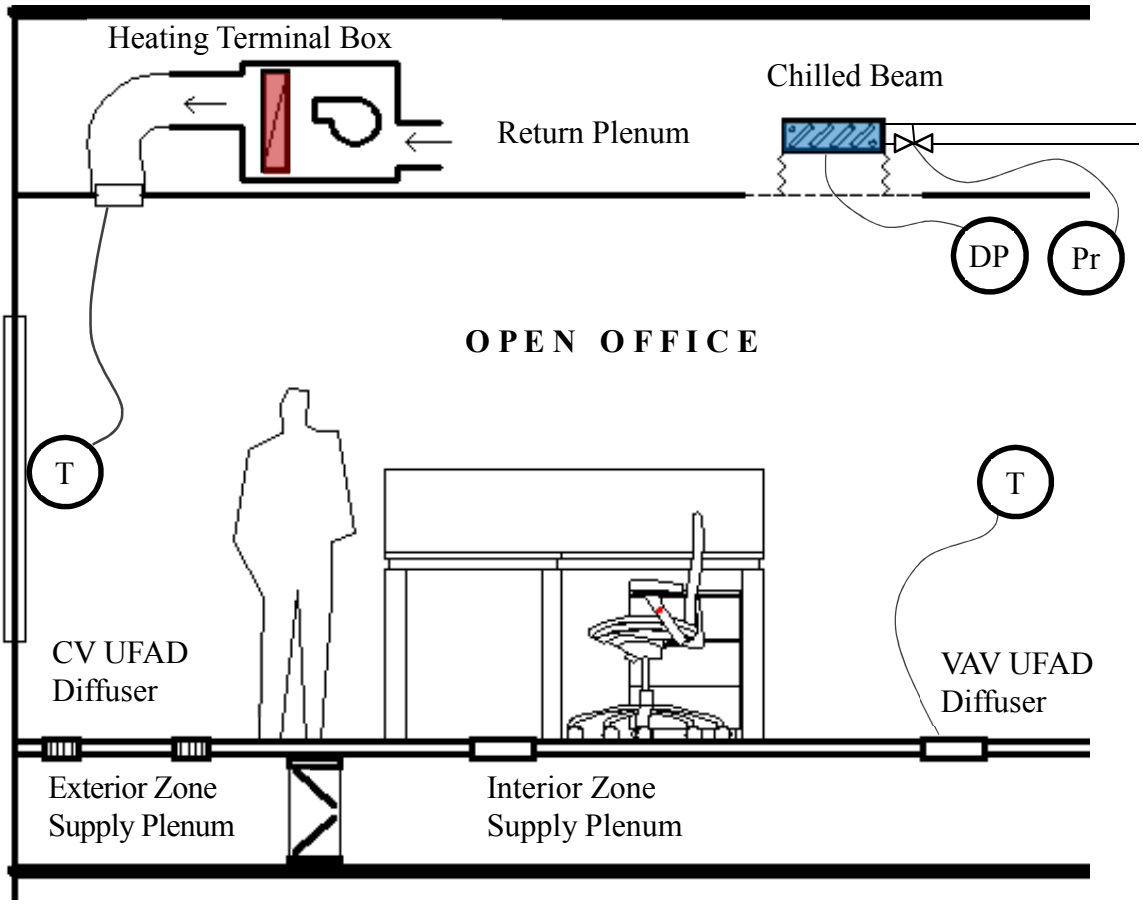

Figure 4.16: Control of the Zone Equipment in the Offices

4.1.4.3. Plant Operation

The chillers operate to maintain a constant chilled water supply temperature setpoint of 43°F throughout the year. During the cooling season, the water-cooled chillers are operated and staged for uniform loading and the air-cooled chiller is only used as a

backup for the critical spaces (i.e. data centers) in the building. However, at low load conditions, the water-cooled chillers and cooling towers are turned off and the air-cooled chiller is operated to meet the entire building load. This was modeled as an outside air temperature based schedule, i.e. at outside air temperatures below 50°F, the air-cooled chiller is made available and the water-cooled chiller is turned off. The chilled water pumps are operated to maintain the differential pressure setpoint for each wing in the building. The condenser water temperature setpoint is maintained at the outside air wet bulb temperature plus 2°F. The condenser water pumps are sequenced to operate with each respective chiller.

4.1.5. Measured Energy Data

The building is all electric with natural gas used only for domestic hot water and kitchen equipment. The entire building, including a detached multi-level parking garage is on a single electric meter. Hourly demand data available for the parking garage shows a daily demand range variation of 35-90kW but a relatively consistent average monthly demand of 70kW over the period of a year. Since we are primarily interested only in monthly calibration, the average monthly parking garage energy use was deducted from the utility bills to arrive at the monthly electric use for the building.

The building has been operational since January 2010 but was partially occupied through December 2011. In addition, there were several issues with HVAC operation because of the complex nature of mechanical systems. Due to these reasons, the data prior to mid-2012 is unreliable for calibrating the energy use model. Figure 4.17 and Figure 4.18 present the time series plots of electricity use and demand for the building. The period

from August 2012 to July 2013 has consistent occupancy and HVAC operation patterns and was used for calibrating the energy model. Figure 4.19 and Figure 4.20 show the electricity and demand use as a function of outside air temperature. They show a significant outlier for the February-March 2013 period even though demand stays consistent for this period. Random samplings of electric demand for February and March 2013 also show no significant variations for these months when compared to other months with similar outside air temperatures. This could be because of a possible faulty meter reading for this time period.

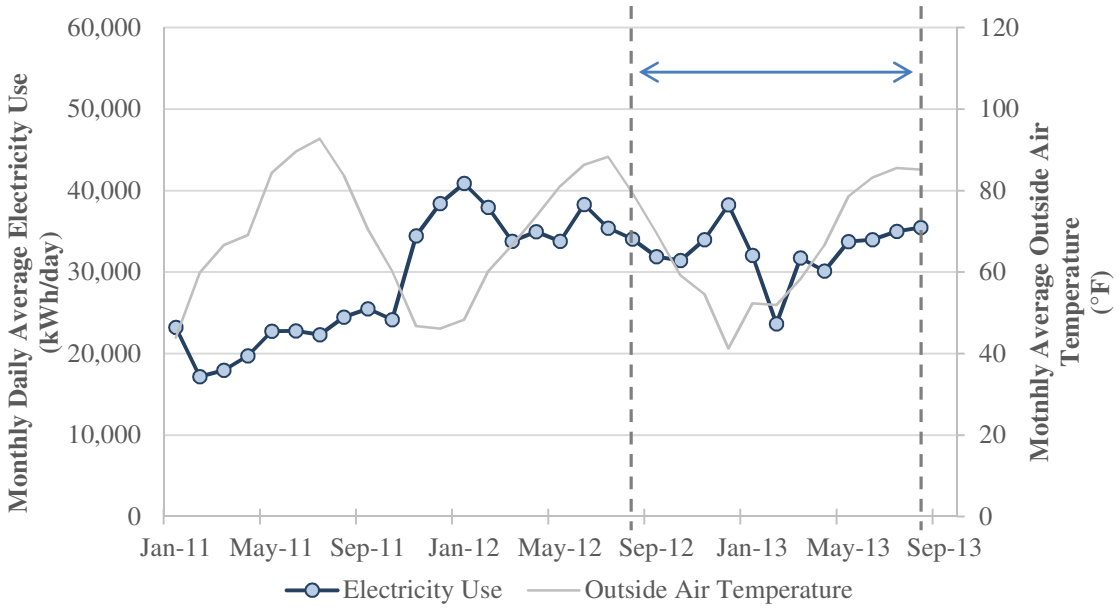

Figure 4.17: Monthly Electricity Use in the Building from January 2011 to August 2013

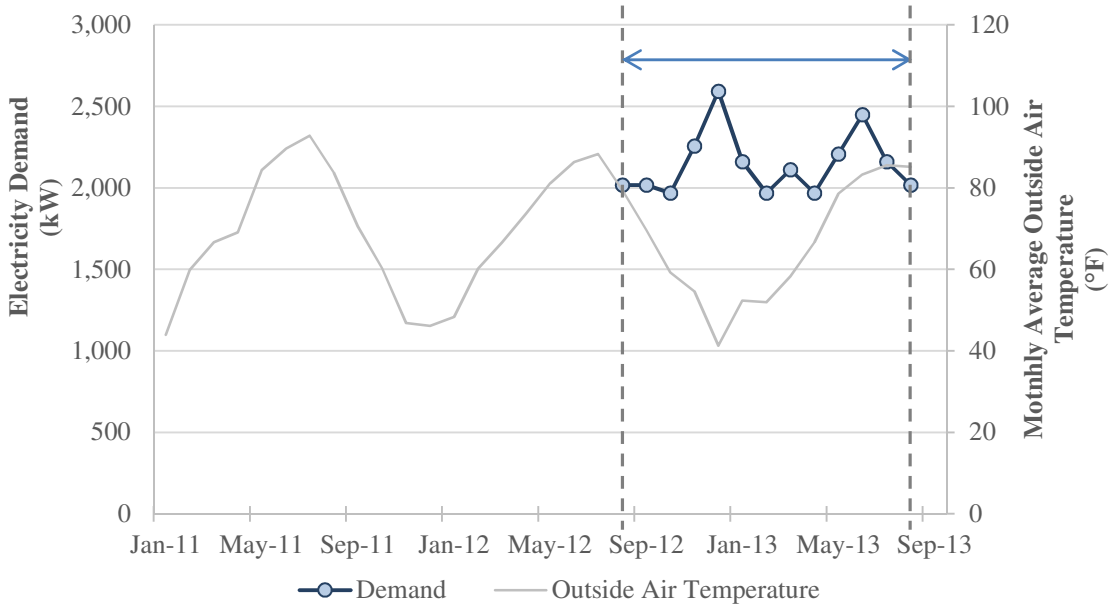

Figure 4.18: Monthly Electricity Demand in the Building from August 2012 to August 2013

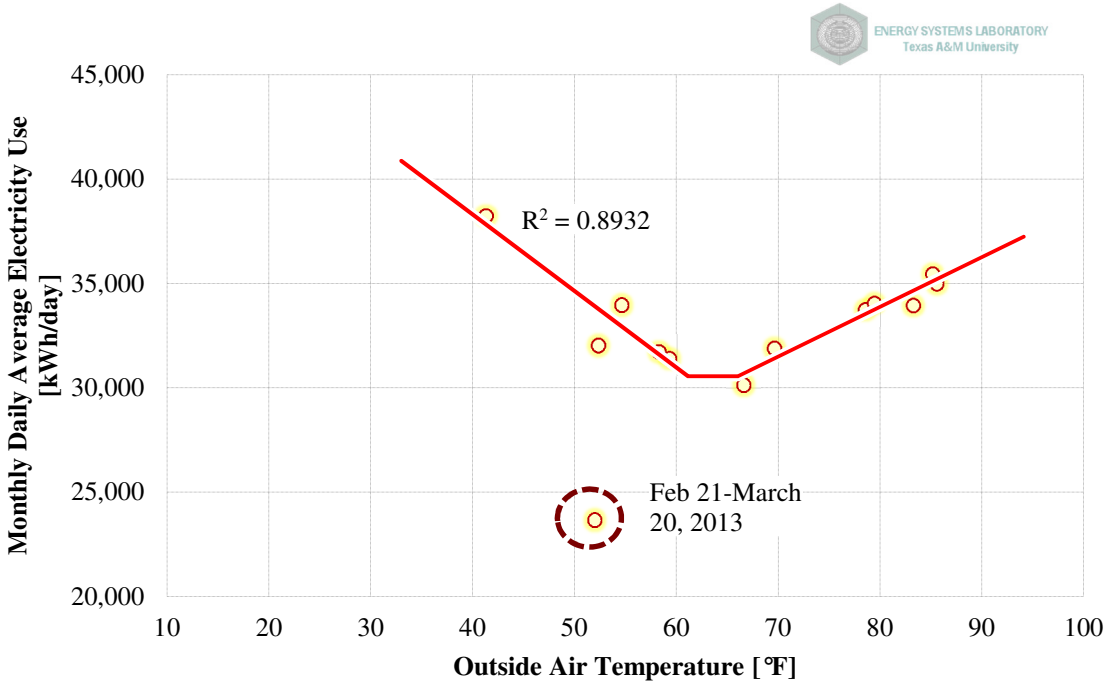

Figure 4.19: Monthly Electricity Use from August 2012 to August 2013 as a Function of Outside Air Temperature

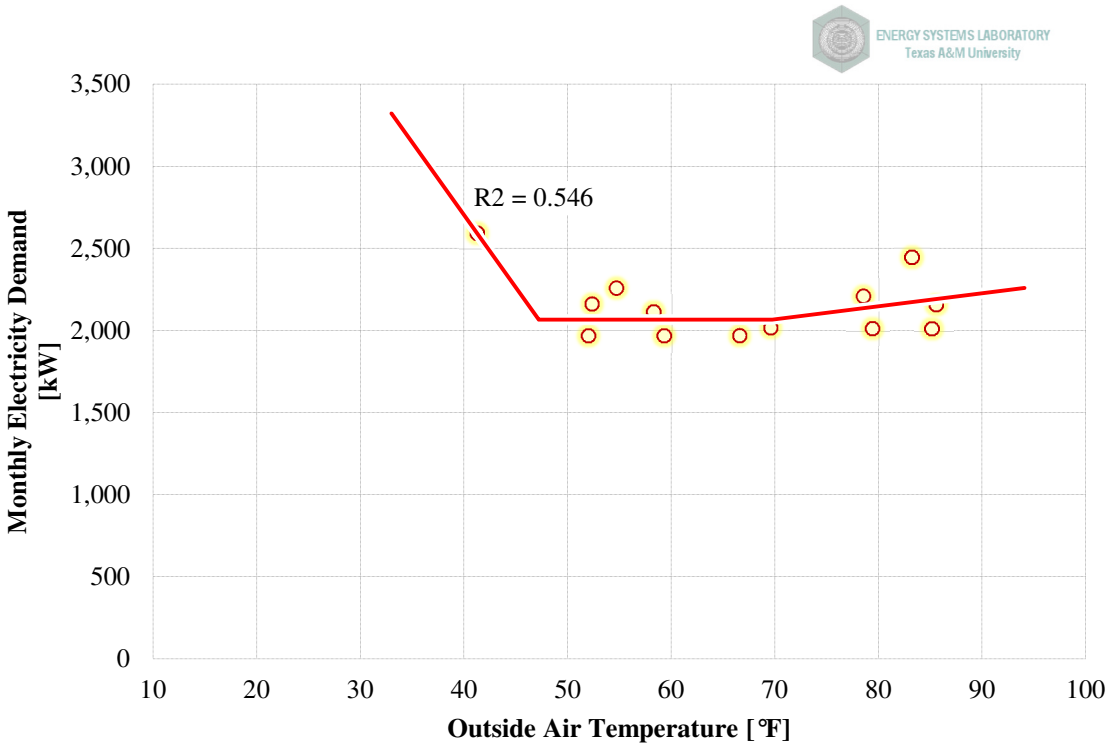

Figure 4.20: Monthly Electricity Demand from August 2012 to August 2013 as a Function of Outside Air Temperature

Utility monthly data was the only data available. However, random samplings of electricity demand were documented by the building operators and were made available for the period from October 2012 to December 2013. These were plotted against outside air temperature and are presented in Figure 4.21. They show an electric demand range from 1,000 to 2,500 kW with peak demand occurring in the heating months.

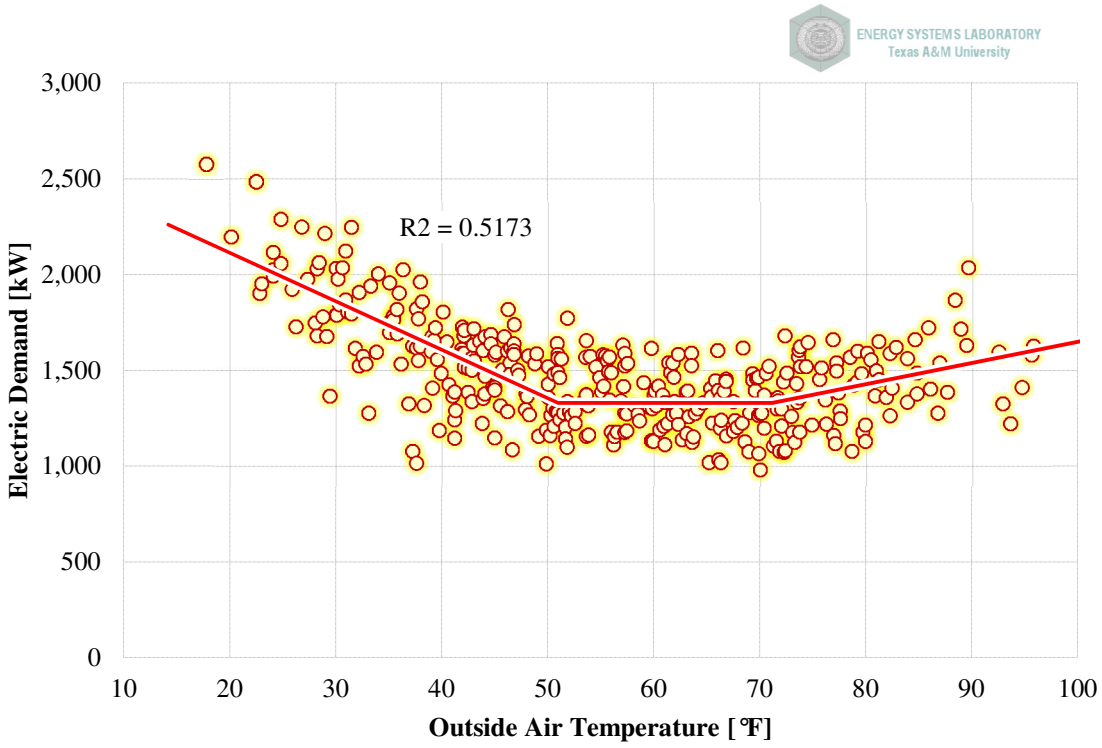

Figure 4.21: Electricity Demand from August 2012 to December 2013 as a Function of Outside Air Temperature

4.2. EnergyPlus Model Assumptions

The three HVAC components that are atypical in this building are the demand controlled ventilation, the underfloor air distribution and the passive chilled beams. This section details how these components are modeled in EnergyPlus.

The quantity of outside air in the building varies to maintain the CO_2 concentration in the spaces at a certain setpoint. The Indoor Air Quality Procedure (IAQP) in ASHRAE (2010a) recommends either a steady-state or dynamic mass-balance analysis to establish flow rates. In EnergyPlus, the flow rates are modeled by calculating outside air

requirements and CO_2 concentrations for each zone dynamically at each timestep using Equation 4.1.

$$\sum_{i=1}^{N_{zones}} \dot{m}_{OA,z}\left(C_{\infty} - C_{setpoint}^{t}\right) = \left[\sum_{i=1}^{N_{zones}} \dot{m}_i + \dot{m}_{inf}\right] * \left[C_{setpoint}^{t} - C_z^{t-\delta t} * \exp\left(-\frac{\sum_{i=1}^{N_{zones}} \dot{m}_i + \dot{m}_{inf}}{\rho_{air} V_z C_{CO2}} \delta t\right)\right] * \left[1 - \exp\left(-\frac{\sum_{i=1}^{N_{zones}} \dot{m}_i + \dot{m}_{inf}}{\rho_{air} V_z C_{CO2}} \delta t\right)\right]^{-1} - \left(\sum_{i=1}^{N_{sl}} kg_{mass_{sched\ load}} * 10^6 + \sum_{i=1}^{N_{zones}} m_i C_{Zi} + m_{inf} C_{\infty}\right) \quad (4.1)$$

The chilled beam model is an empirical model developed by the equipment manufacturer Halton-Oy. The model is a convection-only model and the radiant effect of the chilled beam is ignored. The model can be used for both passive and active chilled beams and consists of Equations 4.2 to 4.5. The coefficient of induced air (K_{in}) is used only when active chilled beams are required to be modeled and is considered to be zero in case of passive chilled beams.

$P_{beam} = A * K * \Delta T$	Beam cooling output per unit length	4.2
$K = \propto * \Delta T^{n1} * v\rho^{n2} * \omega^{n3}$	Coil heat transfer coefficient	4.3
$v\rho = \left(\frac{Q_{in}}{\propto_0}\right) \rho_{air}$	Room air mass flow rate across coil	4.4
$Q_{in} = K_1 * \Delta T^{n} + K_{in} * Q_{pr}$	Room air volumetric flow rate across coil	4.5

α, α_0, A and water pipe diameter are product specific coefficients and are related to the geometry of the chilled beam. Default values provided in EnergyPlus for these

coefficients yield cooling capacities that are less than 50% of the capacities provided by the chilled beam manufacturer (Figure 4.22). Therefore, it is necessary to have information about the chilled beam geometry for reasonably accurate sizing and energy use estimates.

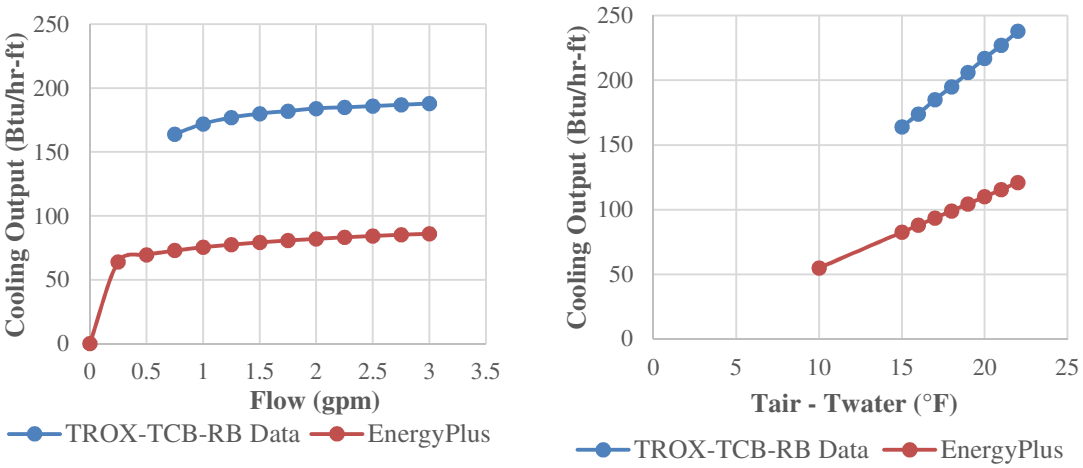

Figure 4.22: Chilled Beam Cooling Capacities (EnergyPlus vs. Chilled Beam Manufacturer's Data)

In the overall HVAC system, the chilled beam is modeled as a terminal unit similar to a four-pipe induction terminal unit and Equations 4.6 and 4.7 are solved iteratively at each timestep to calculate the cooling delivered and water outlet temperature.

$$P_w = Q_{w,beam} * c_{p,w} * (T_{w,out} - T_{w,in}) \quad 4.6$$

$$P_{air} = K * A * \Delta T * L_{beam} \quad 4.7$$

There are two major requirements for the UFAD modeling; the internal zone-level heat balance should account for the heat exchange between the supply/return plenums and the zone; non-uniform room air temperatures that occur in the zone should be factored into

the heat balance. Both these requirements are satisfied by EnergyPlus. The internal heat balance in a zone takes into account the conduction through the zone walls, the convective heat exchange with the zone air, the longwave radiation exchange between the surfaces that are 'seen' by the zone (estimated based on direct view factors), the longwave radiation from other internal sources such as thermal mass and equipment and the shortwave radiation from solar and internal sources (see Figure 4.23). Equations 4.8 to 4.11 solve for the longwave radiation exchange between surfaces, interior convection, conduction to the inside face of the wall and inside face heat balance respectively. The longwave radiation from the interior equipment is estimated as a radiative/convective split which is then distributed to the surfaces of the zone.

$$q_{i,j} = A_i F_{i,j}\left(T_i^4 - T_j^4\right) \quad 4.8$$

$$q''_{conv} = h_c(T_s - T_a) \quad 4.9$$

$$q''_{ki}(t) = -Z_o T_{i,t} - \sum_{j=1}^{nz} Z_j T_{i,t-j\delta} + \sum_{j=1}^{nz} Y_j T_{o,t-j\delta} + \sum_{j=1}^{nq} \phi_j q_{ki,t-j\delta} \quad 4.10$$

$$q''_{LWX} + q''_{SW} + q''_{LWS} + q''_{ki} + q''_{sol} + q''_{conv} = 0 \quad 4.11$$

A grey interchange model developed by Hottel (1967) is used to estimate the longwave radiative coefficient $F_{i,j}$ between two surfaces i and j. The convective coefficient h_c is calculated based on the convection model selected for the simulation. For this research, the TARP inside surface algorithm (Walton 1983) was used. The conduction coefficients, Y, Z and ϕ are conduction transfer function (CTF) coefficients for each construction type calculated using the state space method (Ceylan and Myers 1980, Ouyang and Haghighat 1991).

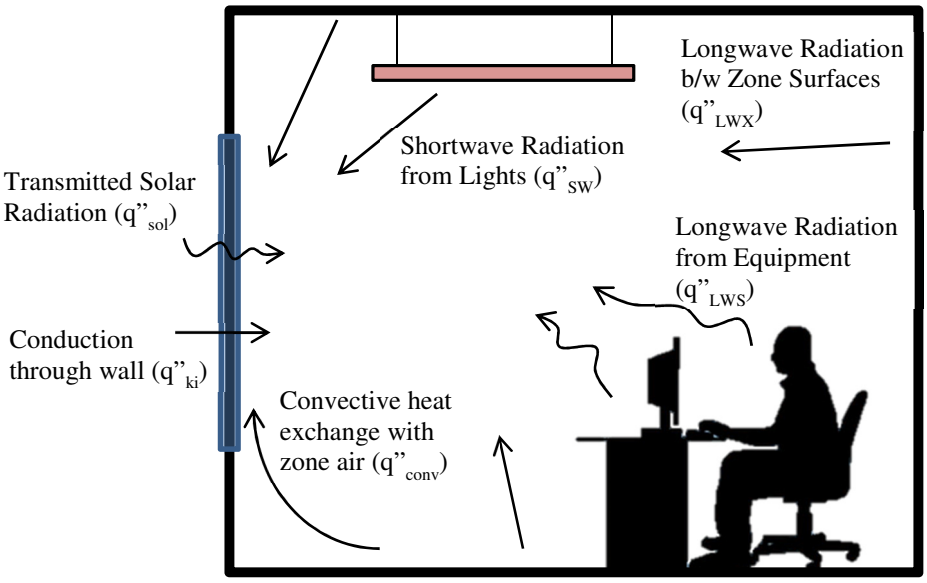

Figure 4.23: Zone Heat Balance Control Volume Diagram

The non-uniform zone temperatures seen in a UFAD system are estimated using the model developed by Lin and Linden (2005). The In this model the zone is subdivided into 2 subzones (occupied and upper subzone) and each layer is assumed to have a single average temperature. The boundary between the two subzones is modeled as an infrared transparent surface with no convection at the top and bottom. The height of the boundary layer is recalculated at each timestep and as a result, the sections of the zone surfaces are reassigned to each subzone and the heat balance is performed for the subzones at each timestep. The stratification height is calculated by a plume-layer model that depends on two major criteria, the buoyancy flux of the heat source and the momentum flux of the

UFAD jets. The model is defined for multiple heat sources and multiple diffusers and separate models are included for interior and exterior zones.

4.3. Calibration Procedure

The statistical comparison techniques documented in Section 3.1 were used to calibrate the EnergyPlus simulation model to the available measured energy data. Figure 4.24 shows the results of the monthly energy use of the initial simulation compared with the measured energy use data for the period from September 2012 to August 2013. It shows that the initial simulation model predicts energy use approximately 16% below the measured energy use. Simulated energy use in the heating seasons (November to February) were also 27% lower than the measured data. With a CV (RSME) of 19.48% and NMBE of 17.84%, several modifications are necessary in order to consider the simulation model a reasonable representation of the building.

The changes made to the energy model were a combination of observations and new information made available during subsequent walkthroughs and discussions with the building operators. Some of the changes such as modeling of the miscellaneous equipment and the reduction of the heating coil efficiencies were included during the calibration process because they more closely represent the actual building conditions.

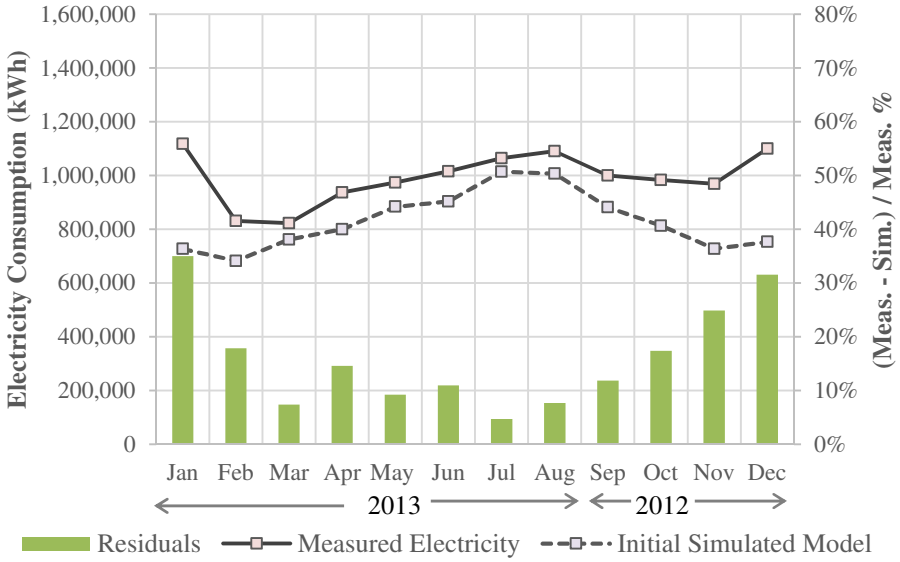

Figure 4.24: Comparative Monthly Energy Use for the Initial Simulation with the Measured Electricity Usage Data from September 2012 to August 2013[14]

4.3.1. Revise Occupancy, Lighting and Equipment Schedules

Lighting and equipment schedules in the building were modified based on walkthroughs in the building during the weekdays and weekends. Some of the lighting occupancy sensors in the offices were found to be malfunctioning during the building walkthroughs. The lights in the lobbies, circulation areas, cafeteria and training spaces were also found to be operational 24x7. The daily demand data also shows very little variation between day and night, implying consistent internal loads 24x7. These observations were factored into the lighting and equipment schedules of the model. Occupancy schedules for the offices were estimated from the trend data of the CO_2 levels

[14] Energy use for the months of Sep – Dec 2012 was placed at the end to show a full year's worth of data

in the zones. Occupancy schedules for the other zones were estimated based on building walkthroughs at different times during the weekdays and weekends. Figure 4.26 and Figure 4.27 shows the revised occupancy, lighting and equipment schedules used in the energy model. The revised schedules increased both heating and cooling energy and brought the simulated energy consumption to within 10% difference of the measured data (see Figure 4.25). It also reduced the CV(RMSE) from 19.48% to 14.58% and NMBE from 17.84% to 10.51%.

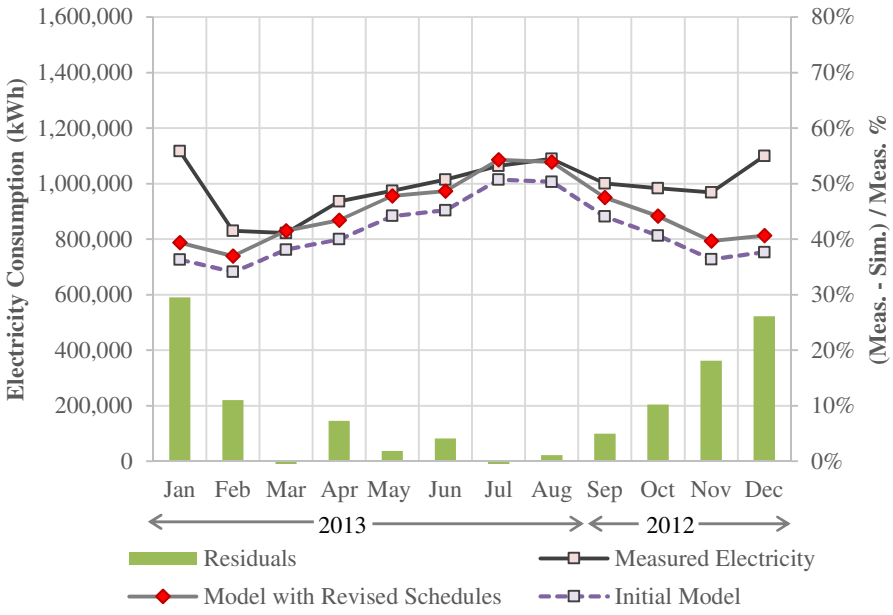

Figure 4.25: Comparative Monthly Energy Use for the Initial Model, the Model with the Revised Schedules and the Measured Electricity Usage Data

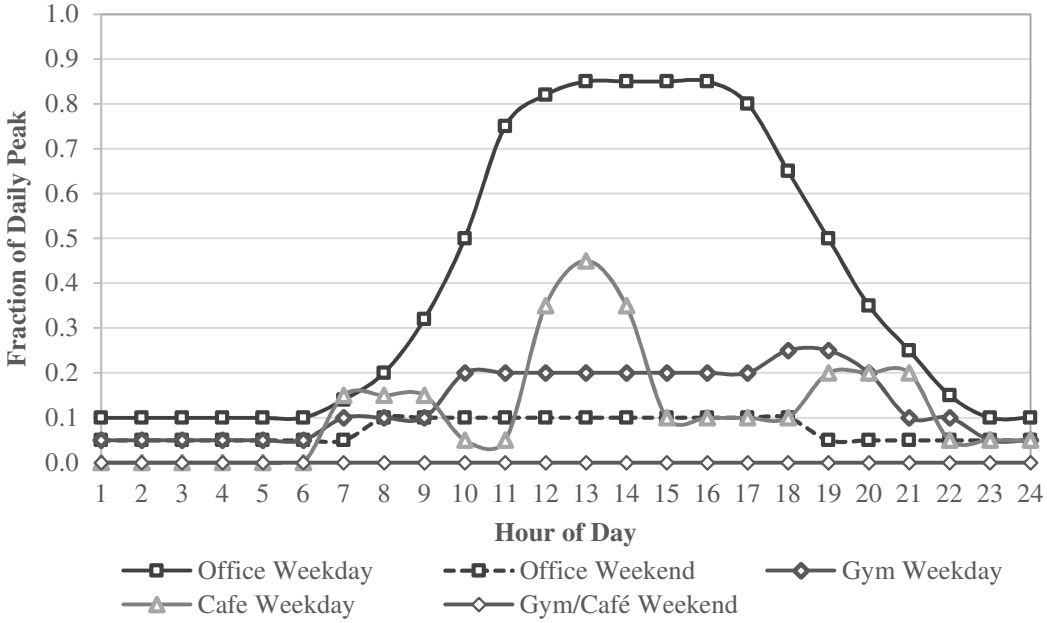

Figure 4.26: Occupancy Profiles Modeled in the Calibrated Simulation

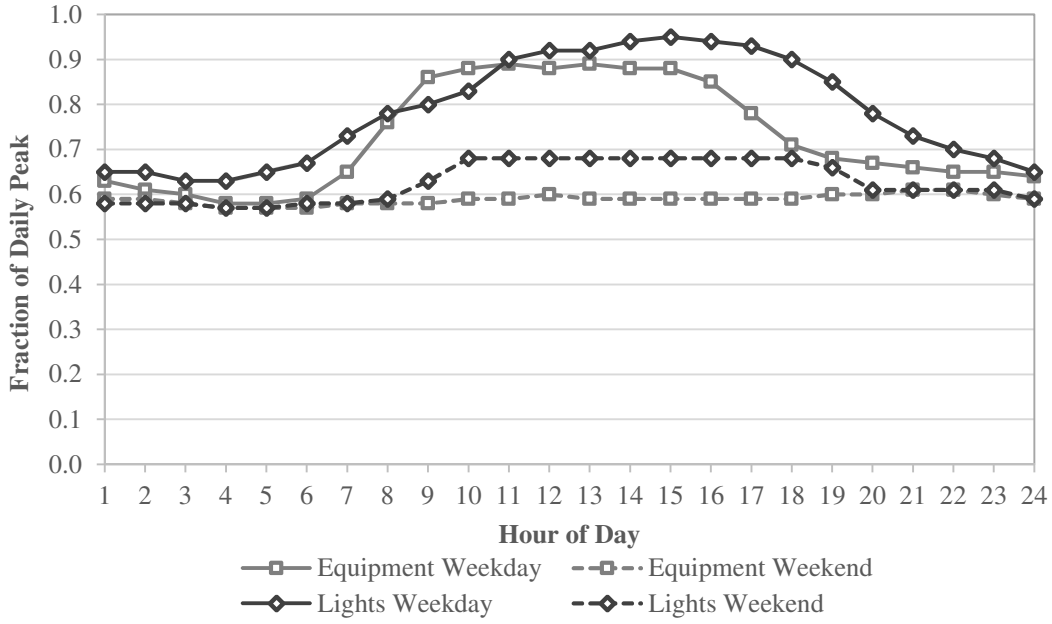

Figure 4.27: Equipment and Lighting Profiles Modeled in the Calibrated Simulation

4.3.2. Model Miscellaneous Zone Equipment

A review of the EMCS control sequences and trend data showed that the kitchen make-up air units and exhaust fans were were operating 24x7. Because the make-up air units are large (7,000 CFM total, 28% of the AHU capacity) and have a heating coil for pre-treatment of air, they will have an impact on the energy use in the model. As a result, the kitchen make-up air units and exhaust fans were also included in the simulation model.

Unit heaters and cooling equipment in the penthouses and mechanical rooms were the other supplementary equipment that were also modeled. Ventilation fans in the electrical rooms, toilets, break rooms and stairwells were ignored. These modifications marginally increased only the heating energy used in the simulation model (see Figure 4.28) and reduced the CV (RMSE) from 14.58% to 13.25% and NMBE from 10.51% to 9.31%.

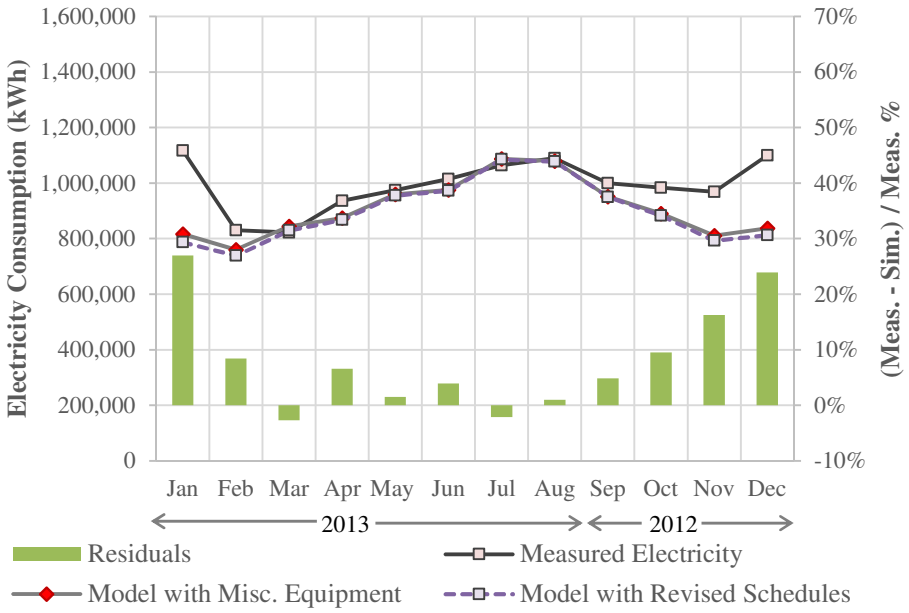

Figure 4.28: Comparative Monthly Energy Use for the Model with the Revised Schedules, Model with the Misc. Equipment and the Measured Electricity Usage Data

4.3.3. Increase Zone Minimum Airflow Fraction

In zones with underfloor air distribution, the minimum zone airflow fraction is specified to be zero because uncontrolled leaks into the zones from the pressurized supply plenum are unavoidable and provide the minimum supply air to the zones (Bauman et al. 2008). This uncontrolled airflow to the zones was estimated as a minimum zone supply flow fraction of 0.1 in the initial model. However, in this building, all the UFAD floor diffusers are VAV units with dampers controlling supply air. There is approximately one (1) floor diffuser per person in the offices, resulting in over 2,500 diffusers in the offices with mechanical moving parts that are prone to leakage and failure. Failure occurs very frequently as confirmed by the building operators. As the result of these observations, the

zone minimum flow fraction was increased to 0.2. This modification further increased the heating energy consumption in the simulation model such that it more closely matched the measured data (see Figure 4.29). The cooling energy use did not change significantly, but the CV (RMSE) was reduced from 13.25% to 10.4% and NMBE from 9.31% to 6.6%.

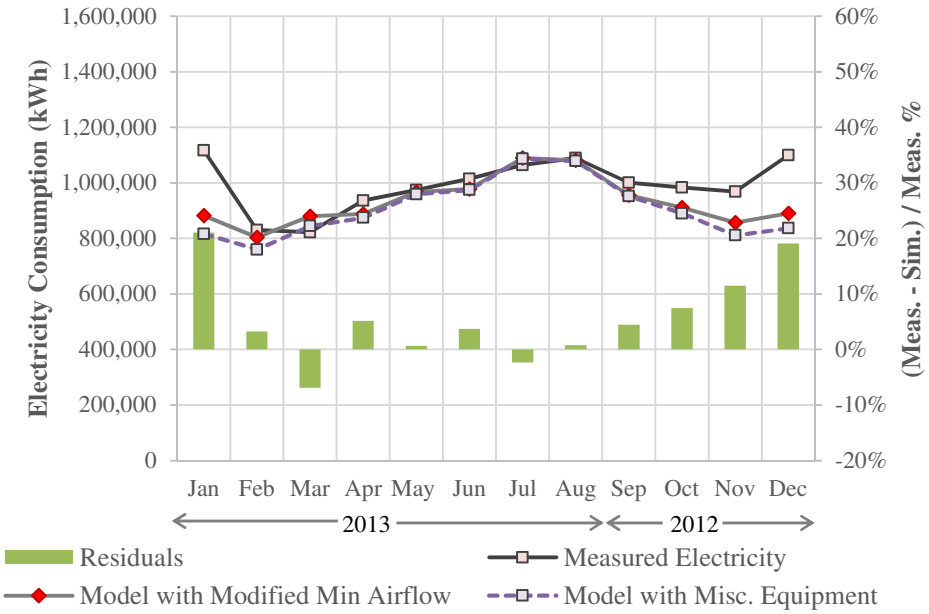

Figure 4.29: Comparative Monthly Energy Use for the Model with the Misc. Equipment, Model with the Modified Minimum Airflow Fraction and the Measured Electricity Usage Data

4.3.4. Change Window Properties

The window properties used for the initial simulation model were U-values of 0.46 Btu/h-ft^2-°F and SHGC of 0.57. However, in order to comply with ASHRAE 90.1 (2004) requirements for windows in climate zone 3A the SHGC of the windows was modified to 0.25. This modification reduced the cooling energy use with no significant impact on the

heating energy use (see Figure 4.30) and increased the CV (RMSE) and NMBE values of the model from 10.4% and 6.6% to 11.16% and 8.86% respectively. However, because the modified windows more accurately represent the actual building conditions, they were included in the calibrated model.

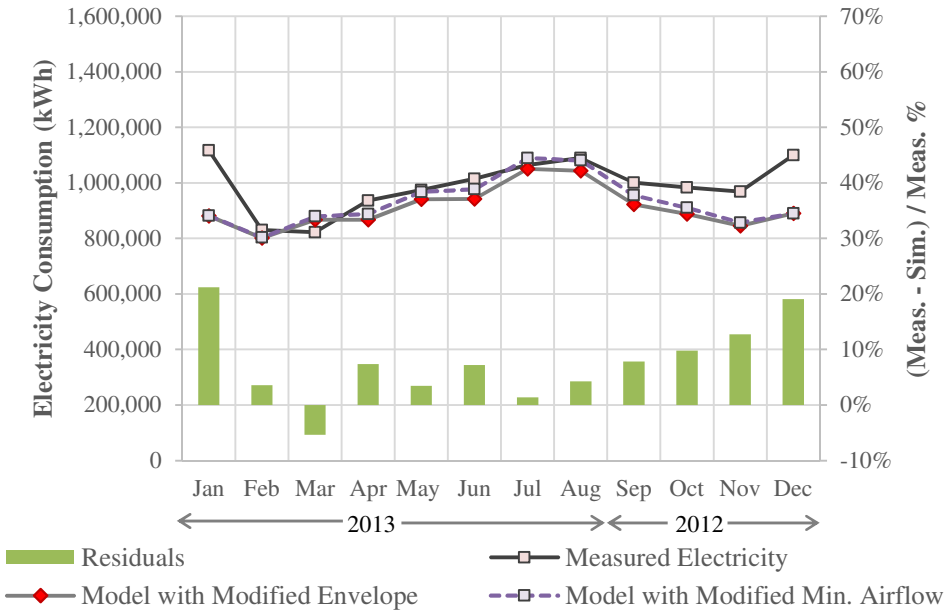

Figure 4.30: Comparative Monthly Energy Use for the Model with the Modified Minimum Airflow Fraction, Model with the Modified Envelope and the Measured Electricity Usage Data

4.3.5. Increase Minimum OA Flow

In the initial simulation model, the minimum OA flow was estimated based on the design documents and the EMCS sequence of operation. However, a review of the outside airflow trend data showed that there seemed to be substantial measured OA flow (>1,000 CFM) through each of the flow stations even when the OA dampers were reported as

closed. To account for this excess outside air, the minimum OA was increased to 13,500 cfm, 17,000 cfm, 15,000 cfm and 2,500 cfm for AHUs 4A1, 5B1, 5C1 and 4A3 respectively. The increased OA increased both heating and cooling energy use and brought the simulated energy consumption to 93% of the measured data (see Figure 4.31). It also resulted in a lowered CV(RMSE) and NMBE values from 11.16% to 10.55% and 8.86% to 7.65% respectively.

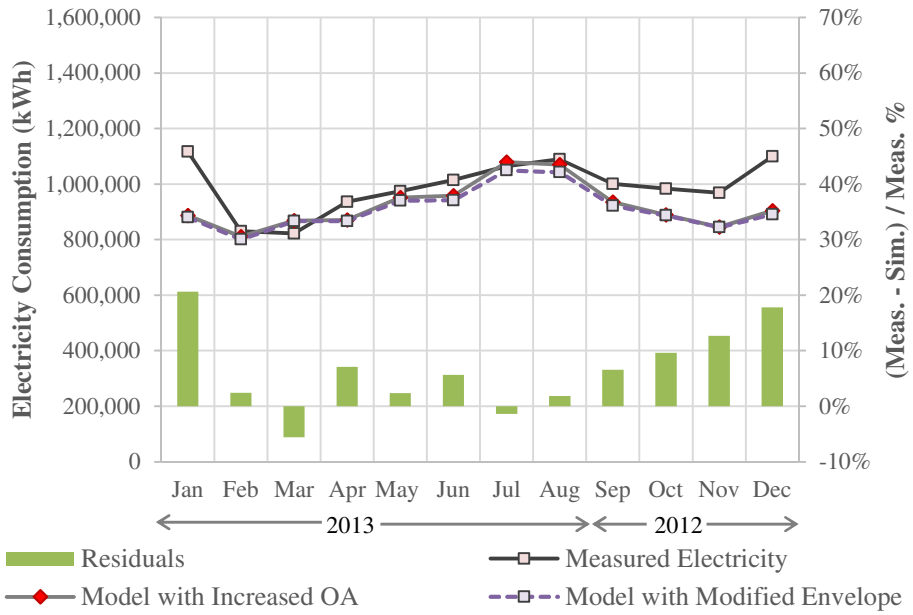

Figure 4.31: Comparative Monthly Energy Use for the Model with the Modified Envelope, Model with the Increased Outside Air and the Measured Electricity Usage Data

4.3.6. Modify Equipment Loads in the Offices

In the initial simulation, average plug loads of 1.0 W/ft^2 were estimated in the offices. However, in the actual building, due to high efficiency EnergyStar® equipment,

this value had been overestimated. In addition, constant plug loads in the data center were not modeled in the initial simulation. Based on information obtained from the building owners and operators, the data center has a constant plug load of approximately 280,000W. As a result, the plug loads in the offices were reduced to 0.65W/ft^2 and a constant plug load of 280,000W was added to the ground floor that houses the data centers. These modifications drastically improved the calibration fit of the simulation model with the measured data, reducing the CV (RMSE) from 10.55% to 6.77% and the NMBE from 7.65% to 0.6%. The total simulated energy use was also within 1% of the measured energy use (Figure 4.32).

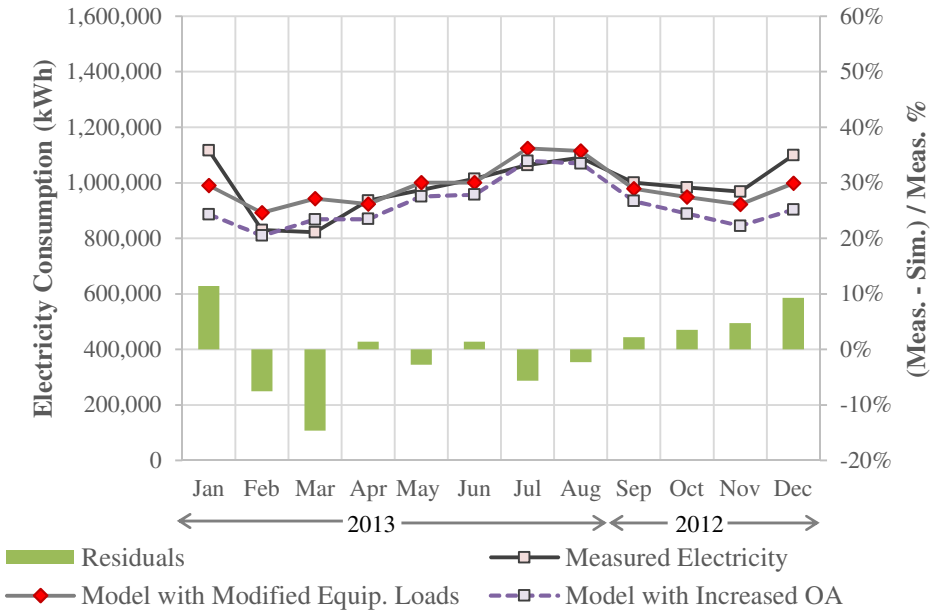

Figure 4.32: Comparative Monthly Energy Use for the Model with the Increased Outside Air, Model with the Modified Equipment Loads and the Measured Electricity Usage Data

4.3.7. Reduce Heating Coil Efficiency

In a UFAD system, the supply air gains heat from the zones as it travels through the supply plenum to the UFAD diffusers. This is a common phenomenon that has been widely documented (Webster et al. 2008, Schiavon et al. 2011, Lee et al. 2012) and can be acceptable since the heat lost to the zones assists in cooling them. However, air travelling through the return plenum also loses heat due to heat exchange between the return plenum and supply plenum of the floor above. This heat exchange largely depends on the slab construction and the air velocities through the return plenum. This heat transfer is considered undesirable as it raises the air temperature of the supply air plenum on the floor above, and unnecessarily reduces the temperature of the return air and wastes energy. This phenomenon was confirmed by stratification measurements in the offices (see Chapter VIII) and is modeled in EnergyPlus (Figure 4.33) only if the plenum and zone surfaces are correctly specified as being adjacent to each other.

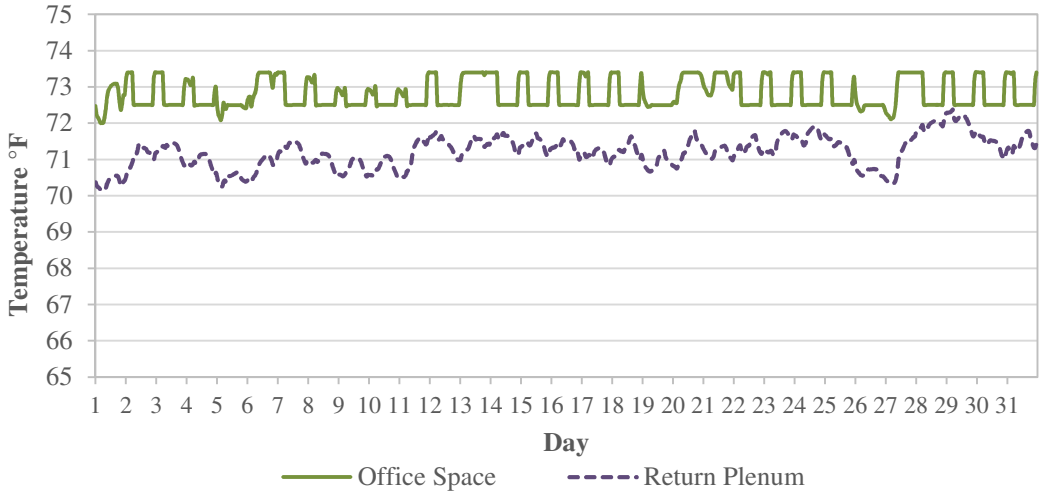

Figure 4.33: Modeled Temperature Difference between the Office Zones and Return Plenum for January 2013

In the building, terminal boxes with heating coils are placed in the return plenums and use the air from the return plenum to heat the zones in heating mode. For the initial model, the heating terminal boxes were modeled as zone heaters that reheat and recirculate zone air instead of return plenum air. However, as seen in Figure 4.33, the zone air temperature is approximately 2°F higher that the return plenum air temperature. This results in an incorrect estimation of the heating in the spaces. In order to more accurately model the actual heating conditions, the heating efficiency of the coils in the office zones was reduced to 0.85. This modification predictably increased the heating energy use (Figure 4.34) and reduced the CV (RMSE) from 6.77% to 6.46% and the NMBE from 0.6% to -0.07%. It also reduced the difference between the total simulated energy use and measured energy use to within 0.1%.

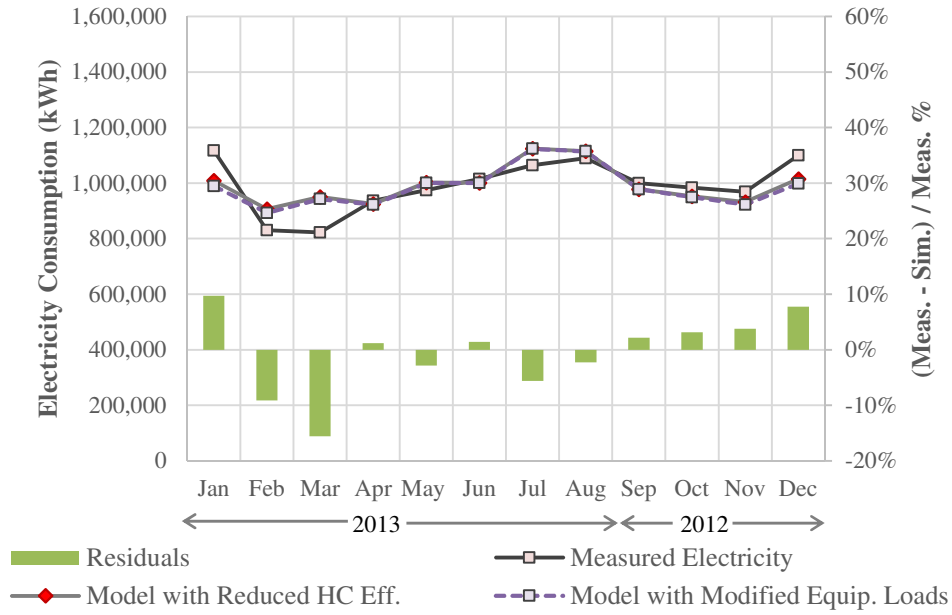

Figure 4.34: Comparative Monthly Energy Use for the Model with the Modified Equipment Loads, Model with the Reduced Heating Coil Efficiency and the Measured Electricity Usage Data

4.3.8. Change Thermostat Setpoints

The zone thermostats were modified to 71.6°F in winter and 73.4°F in summer. The setbacks modeled during unoccupied hours were also removed based on a review of the EMCS sequence of operation and the trend data obtained from the zones. This modification increased the heating energy use (Figure 4.35) and reduced the CV (RMSE) of the model from 6.46% to 6.22%, but also increased the NMBE from -0.07% to -0.89%.

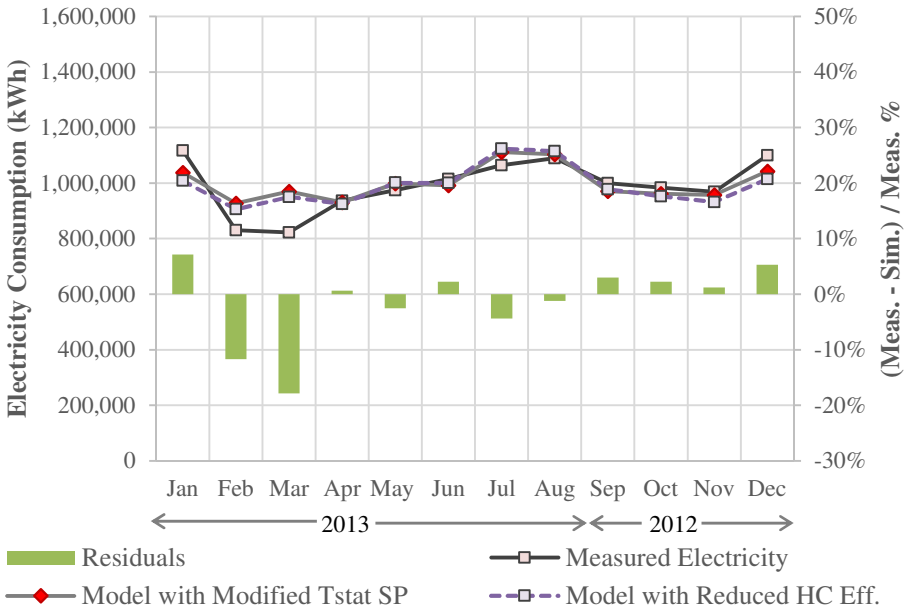

Figure 4.35: Comparative Monthly Energy Use for the Model with the Reduced Heating Coil Efficiency, Model with the Modified Thermostat Setpoints and the Measured Electricity Usage Data

4.3.9. Change Weather Data

The TMY3 weather data from the closest weather station, the Fort-Worth Alliance airport was used for the initial simulation. This weather data is appropriate to predict average energy use and design HVAC and renewable energy equipment, but is not recommended for calibrating simulations to real-time energy use data for specific years (Wilcox and Marion 2008). So, in order to improve the accuracy of the simulation model, Actual Meteorological Year (AMY) data for 2012 and 2013 was reformatted into the TMY3 format and used for the simulation. The AMY data was obtained from White Box Technologies (2014) and is a combination of the archived Integrated Surface Hourly (ISH) data base maintained by the National Climatic Data Center (NCDC) and calculated solar

radiation data. The solar radiation data is calculated using the Zhang-Huang Model (Zhang et al. 2002) to estimate global-horizontal solar radiation, the ASHRAE Clear Sky Model (Powell 1982) to estimate hourly profiles and the Gompertz Function Model to calculate the direct normal radiation. Where available, monthly total global horizontal radiation are calibrated against measured satellite-derived monthly totals.

Figure 4.36 shows the difference (delta-T) between the TMY and AMY dry-bulb temperatures. Figure 4.38, Figure 4.39 and Figure 4.39 show the daily and monthly TMY and AMY dry-bulb temperatures and humidity ratios for the Fort-Worth Alliance Airport. They show that the temperature difference between the AMY and TMY data are significant (up to ±40°F) at the daily level and the variations average out for monthly data. Therefore, if daily measured data is available, it is important to use AMY data for accurate calibration. Since for the case-study building, only monthly measured data was available, changing the weather data had a minor impact on the calibration fit of the simulation model. After this modification, the CV (RMSE) changed from 6.22% to 6.39% and the NMBE changed from -0.89% to 1.13%.

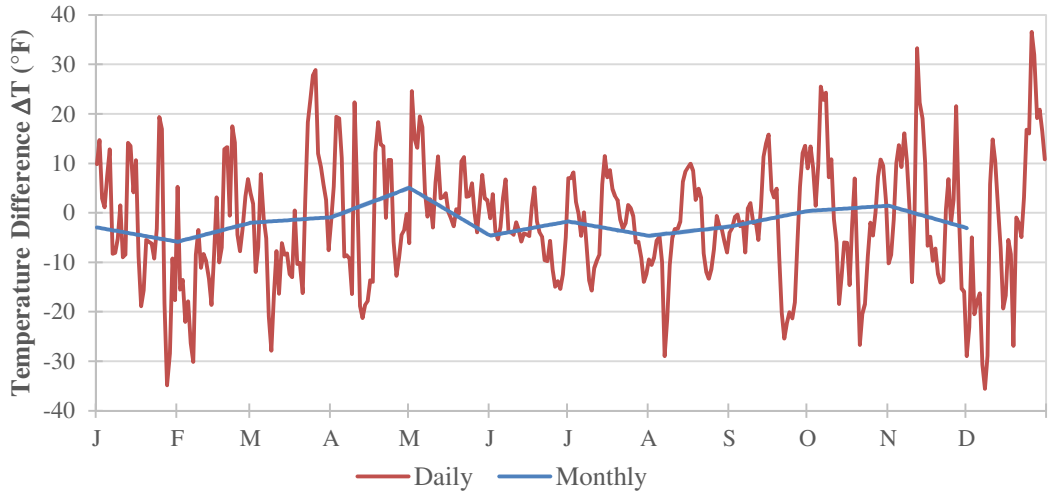

Figure 4.36: Dry-Bulb Temperature Difference (ΔT) between Typical Meteorological Year (TMY) and Actual Meteorological Year (AMY-2013) Data for the Fort-Worth Alliance Airport

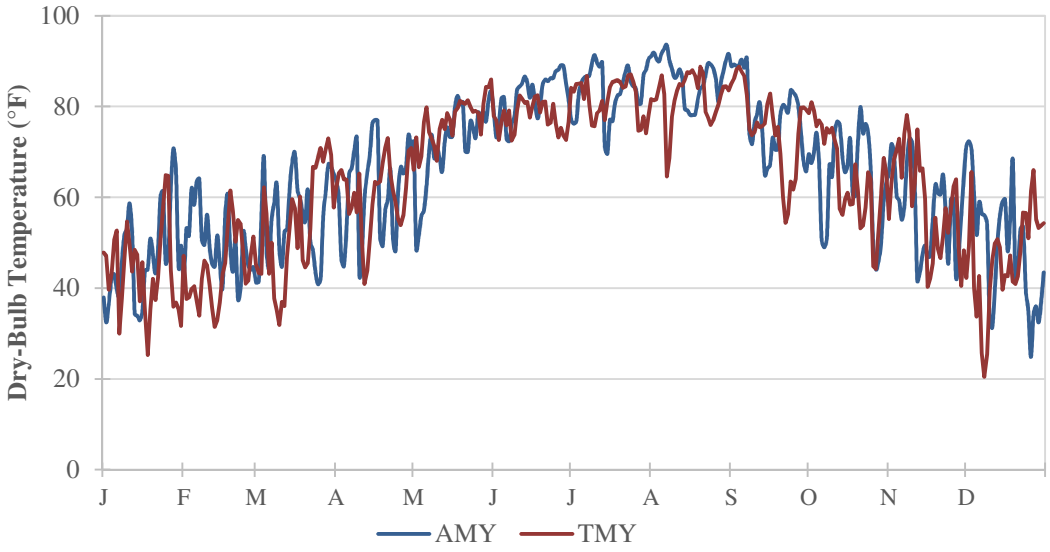

Figure 4.37: Daily Average Typical Meteorological Year (TMY) and Actual Meteorological Year (AMY-2013) Dry-Blub Temperatures for the Fort-Worth Alliance Airport

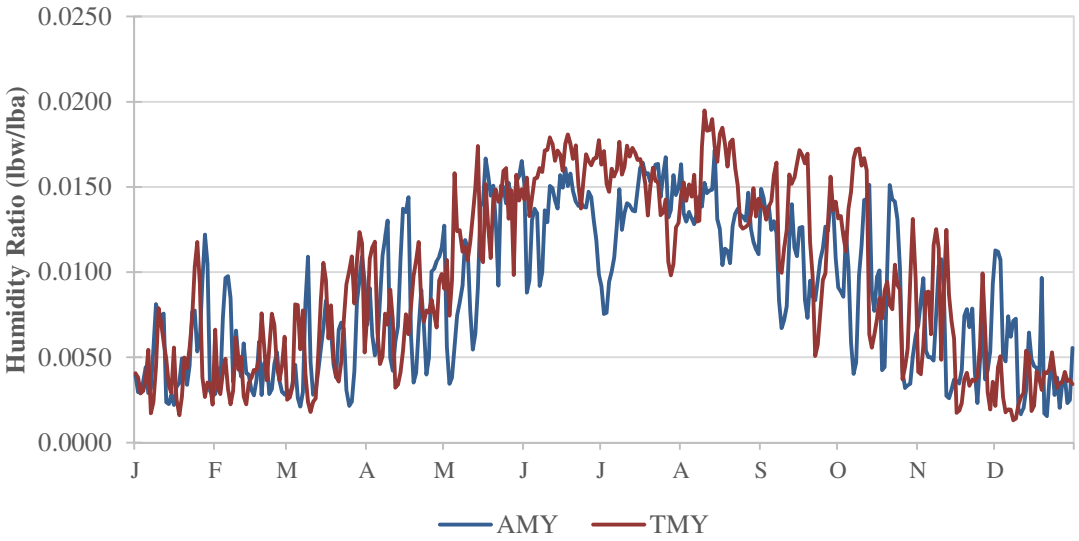

Figure 4.38: Daily Average Typical Meteorological Year (TMY) and Actual Meteorological Year (AMY-2013) Humidity Ratios for the Fort-Worth Alliance Airport

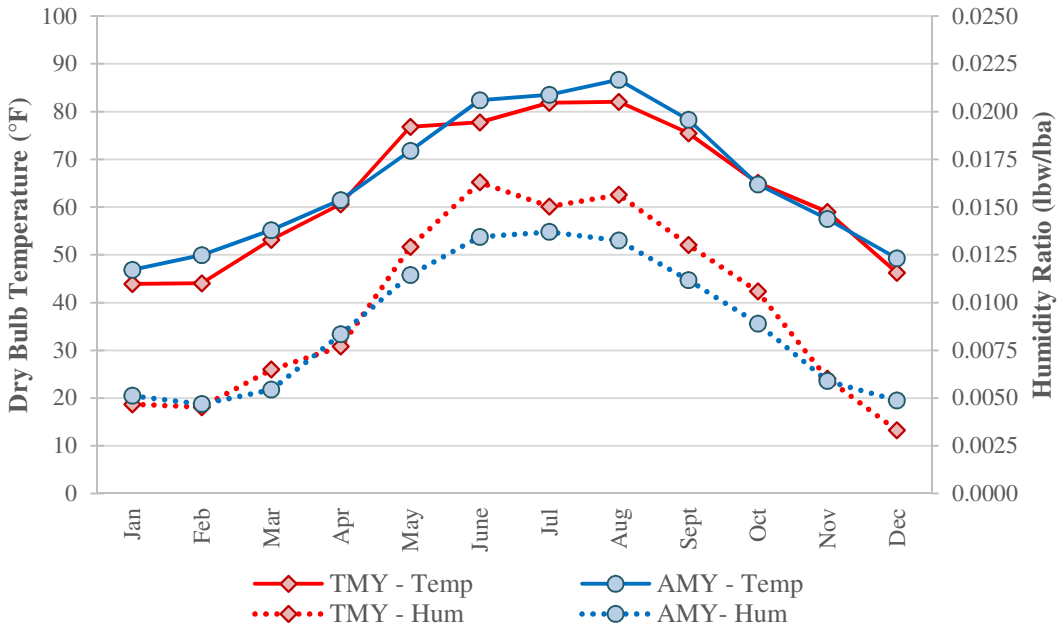

Figure 4.39: Monthly Average Dry-Blub Temperature and Humidity Ratios for Typical Meteorological Year (TMY) and Actual Meteorological Year (AMY-2013) for the Fort-Worth Alliance Airport

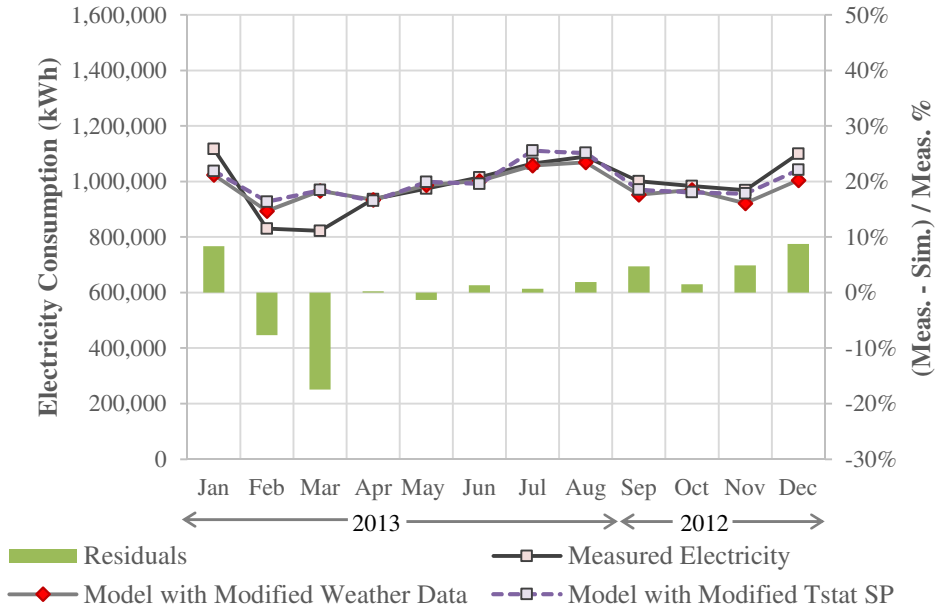

Figure 4.40: Comparative Monthly Energy Use for the Model with the Modified Thermostat Setpoints, Model with the Modified Weather Data and the Measured Electricity Usage Data

4.3.10. Change Chiller Efficiency and Chiller Schedule

In this step, the chiller efficiency for the air-cooled chiller was changed to 1.3kW/ton. The outside air temperature at which the building switches from the water-cooled chillers to the air-cooled chillers was also increased from 50°F to 60°F based on feedback from the building operators. This modification changed the CV (RMSE) of the model from 6.39% to 6.36% and the NMBE from 1.13% to 0.86%. The annual energy consumption for the simulation model was also 99.7% of the measured energy data. Figure 4.41 shows the changes in the CV (RMSE) and NMBE values for each step of the calibration process.

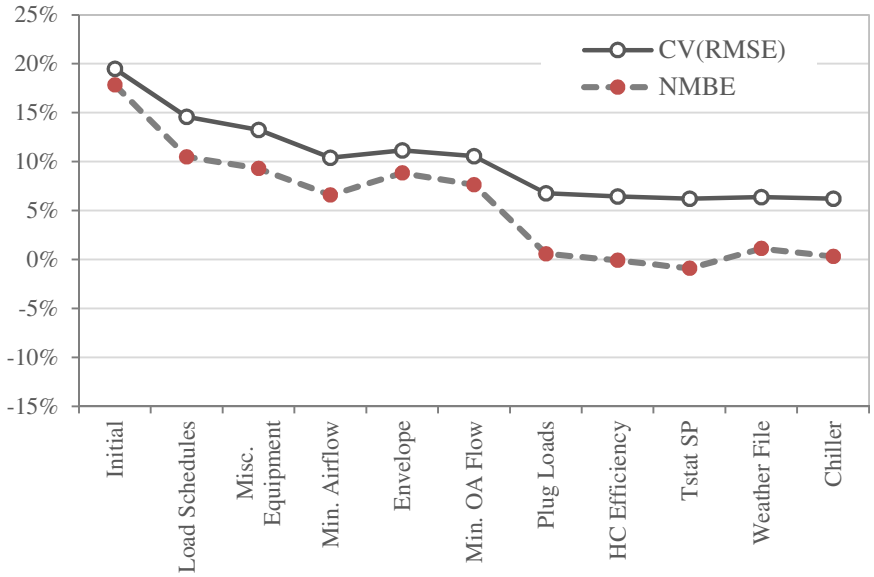

Figure 4.41: CV (RMSE) and NMBE Values for Each Step of the Calibration

Table 4.5: CV (RMSE), NMBE and Residuals for Each Step of the Calibration

Calibration Step	CV (RMSE)	NMBE	Residuals
Initial Model	19.49%	17.84%	16.35%
Modified Load Schedules	14.58%	10.51%	9.63%
Addition of Misc. Equipment	13.25%	9.31%	8.53%
Increased Minimum Airflow	10.40%	6.60%	6.05%
Modified Envelope	11.16%	8.86%	8.12%
Increased OA Flow	10.55%	7.65%	7.01%
Modified Equipment Loads	6.77%	0.60%	0.55%
Reduced Heating Coil Efficiency	6.46%	-0.07%	-0.06%
Modified Thermostat Setpoints	6.22%	-0.89%	-0.82%
Modified Weather Data	6.39%	1.13%	1.03%
Modified Plant Equipment	6.22%	0.33%	0.30%

At this step, the physical data, HVAC equipment and operation input in the simulation model were found to be satisfactorily representative of the actual building conditions. The calibration statistical indices were also found to be within the recommended ranges for a calibrated simulation (ASHRAE 2002). Figure 4.42 shows the results of the monthly energy use of the calibrated simulation compared with the measured energy use data for the period from September 2012 to August 2013. It shows residuals for all the months except March 2013 to be lower than 10%. The simulated energy use for March 2013 is 17% higher than the measured energy used data, but this is possibly because of the faulty measured energy consumption data from Feb 21st to March 20th discussed in Section 4.1.5. Based on these results, the simulation model was considered to be calibrated and a reasonable representation of the actual building conditions.

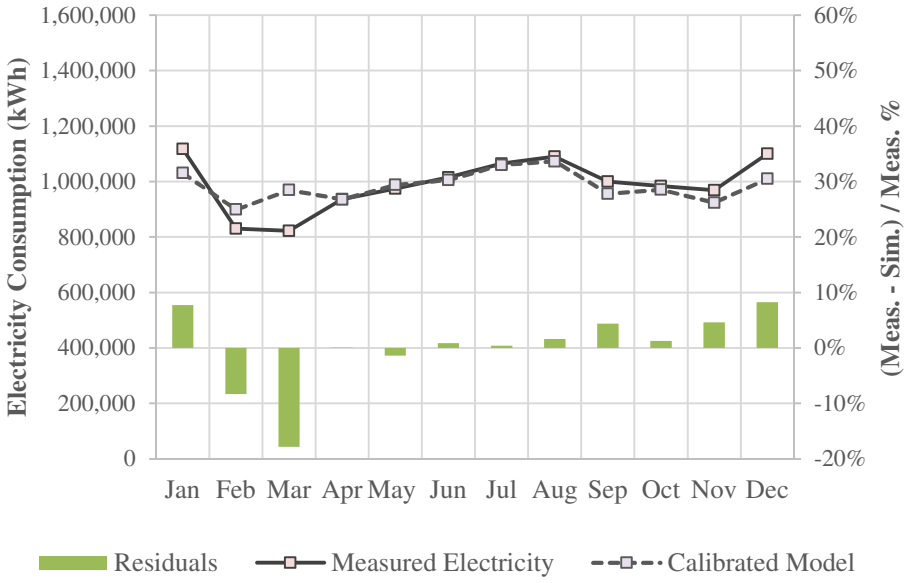

Figure 4.42: Comparative Monthly Energy Use for the Calibrated Simulation with the Measured Electricity Usage Data from September 2012 to August 2013

At this stage, it is important to mention that there are inherent uncertainties associated with calibrated simulations. The uncertainties can arise from a variety of sources; external uncertainties such as improper input parameters and model assumptions, discrepancies in weather and building schedules or operational data and user errors; internal uncertainties such as model simplification, algorithms used for heat and mass transfer and coding errors. It is very difficult to calculate actual uncertainties in large complex models of buildings such as the case-study building used, but ASHRAE Guideline 14 (2002) recommends that the level of uncertainty for energy savings estimates be less than 50% of the annual reported savings at a confidence level of 68%. Studies estimating savings uncertainties for calibrated models have reported savings uncertainties that range from 10-35% and the uncertainties are dependent on amount and duration of

measured data available and the weather dependency of the available data (Effinger et al. 2009, Sun and Baltazar 2013). These uncertainty estimates should be kept in mind while interpreting the energy savings discussed in Chapters 6 and 7.

4.4. Modified Chilled Beam Operation

Typically, in HVAC systems with chilled beams and a separate ventilation system, the quantity of conditioned air delivered to the spaces is controlled to meet either space latent loads or ventilation requirements, whichever is greater. Since ventilation requirements are linked to occupancy levels, they are typically predictable throughout the year. On the other hand, latent loads are linked to both people and infiltration and can vary throughout the year. In a humid climate like Dallas, infiltration can also be a significant factor (upto 50% of non-peak latent loads) in summer. Actual infiltration in the building is a variable quantity that is difficult to measure or estimate. As a result, 2 infiltration values were investigated; one for a reasonably well-sealed pressurized building and one for an average leaky building (Persily 1998, Deru et al. 2011). Figure 4.43 and Figure 4.44 show the latent loads in wing 'A' in January, April July and October due to people and infiltration for infiltration values of 0.4cfm/ft^2 and 1.5cfm/ft^2. They show that in a leaky building, latent loads can be approximately 20% more than a well-sealed, pressurized building.

Figure 4.45 and Figure 4.46 show the amount of outside air required to meet ventilation and latent loads in wing 'A' at infiltration values of 0.4cfm/ft^2 and 1.5cfm/ft^2 respectively. The ventilation requirements are calculated to maintain maximum zone CO_2 levels of 900ppm. The latent requirements are calculated to maintain maximum zone

humidity ratios from 0.0097 to 0.010 lbw/lba (maximum relative humidity of approximately 57% to 60%). They suggests that when the cooling coil is in dehumidifying mode (i.e. wet), latent requirements are greater than ventilation requirements. Figure 4.45 also shows that if space humidity control requirements are more stringent, the outside air required may be too large, which negates any energy savings potential of the chilled beams. In such a situation, heat recovery for the outside air, a run-around coil for the bypass air or a mixed air ventilation system may be necessary. A comparison between Figure 4.45 and Figure 4.46 shows that on a average, a leaky building can require at least 40% more dehumidified outside air to fulfill latent load requirements than a well-sealed pressurized building. This reaffirms that the first step in a well-designed and operated chilled beam system is a sealed an pressurized envelope.

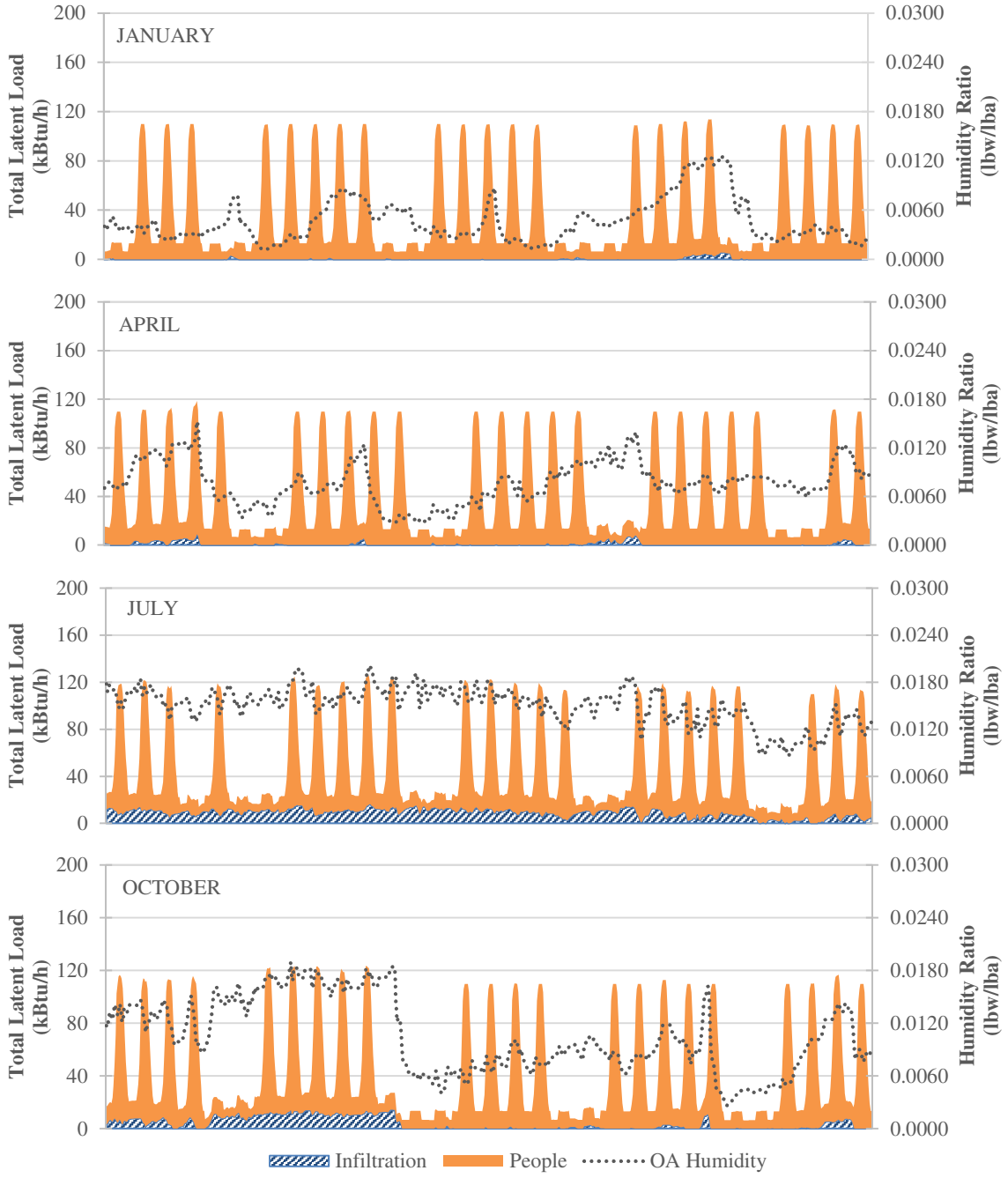

Figure 4.43: Total Latent Loads in the Wing 'A' Offices in January, April, July and October at Infiltration Levels of 0.4cfm/ft^2

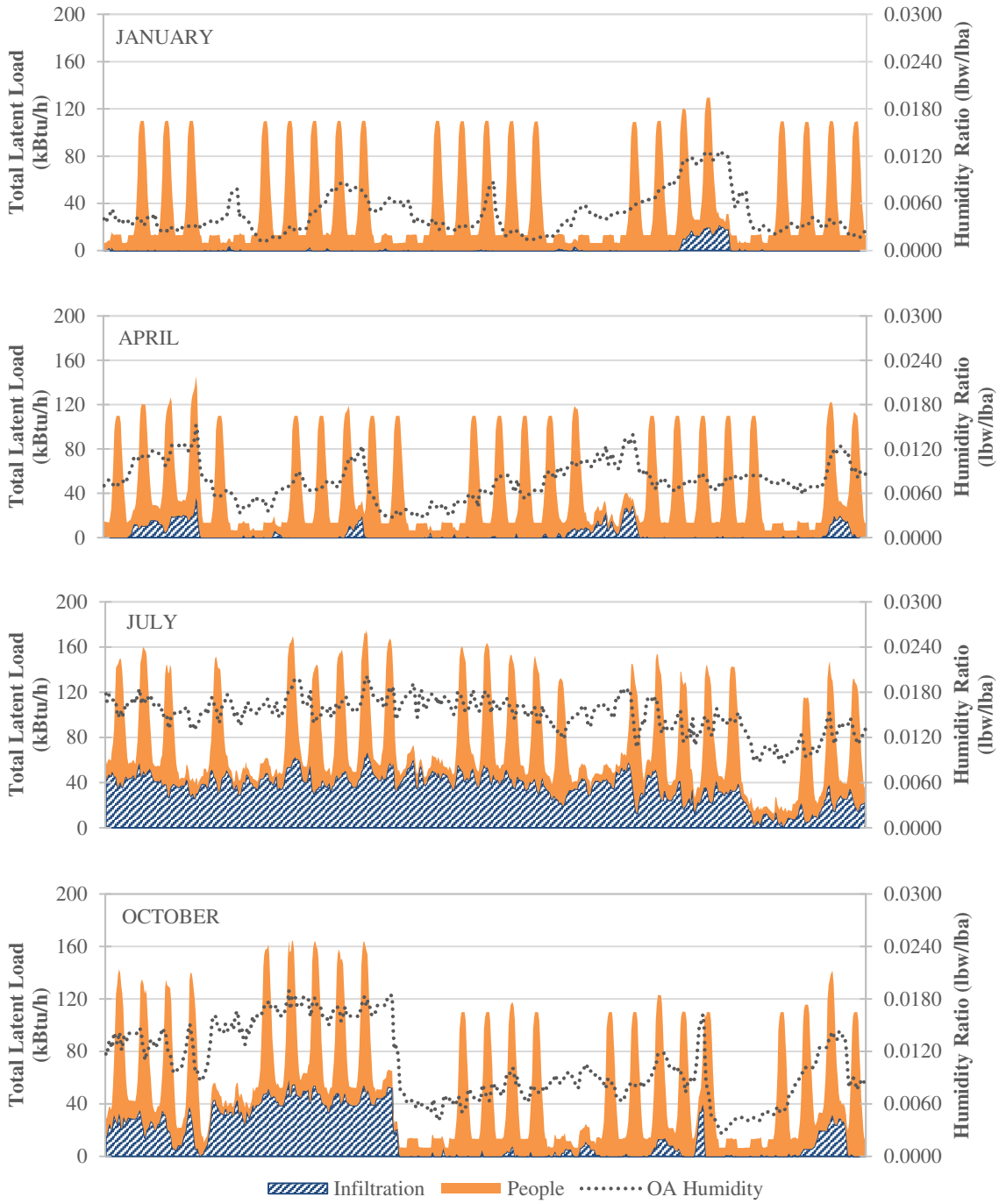

Figure 4.44: Total Latent Loads in the Wing 'A' Offices in January, April, July and October at Infiltration Levels of 1.5cfm/ft^2

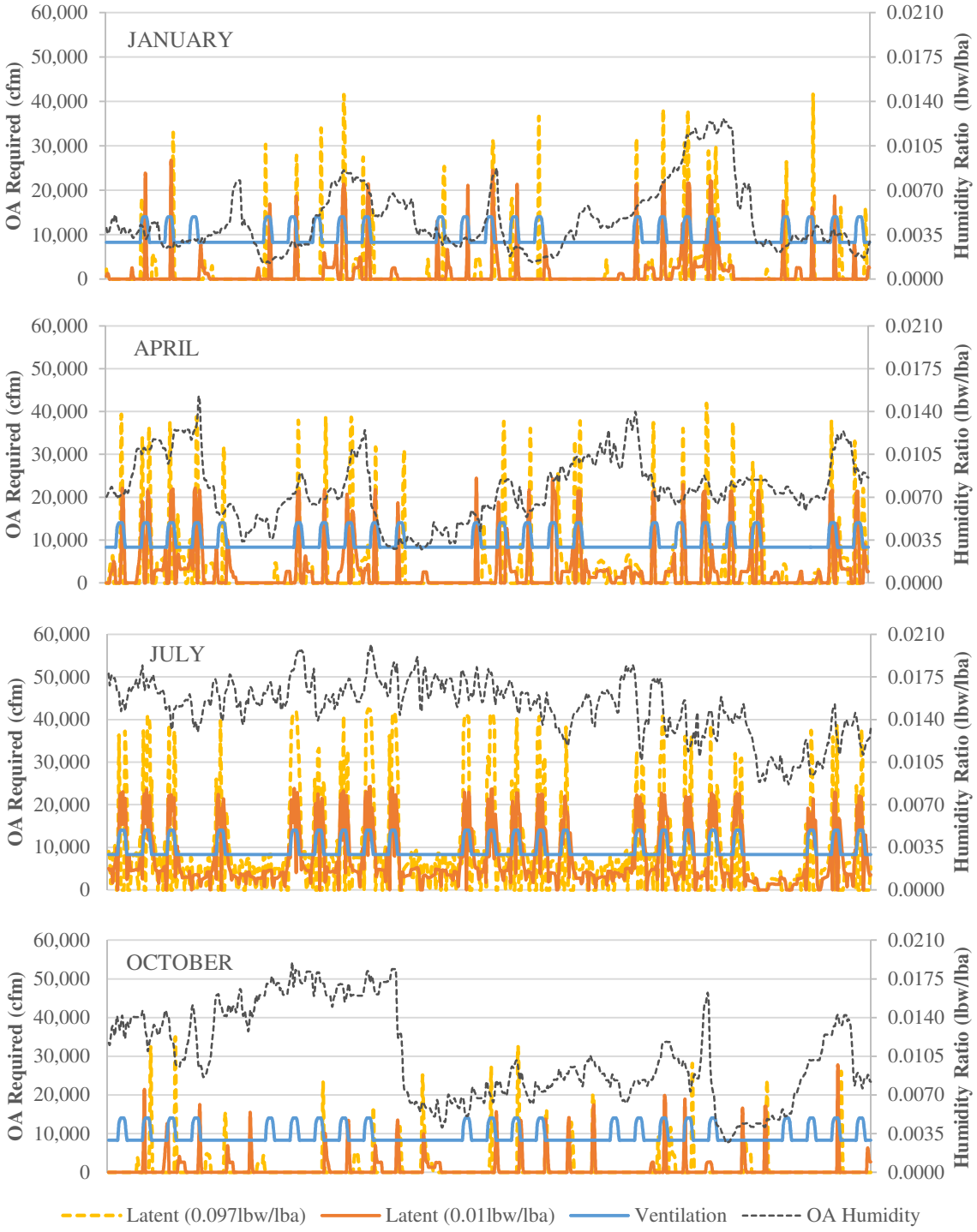

Figure 4.45: Outside Air Required to Fulfill Ventilation and Latent Loads in the Wing 'A' Offices at Infiltration Levels of 0.4cfm/ft^2

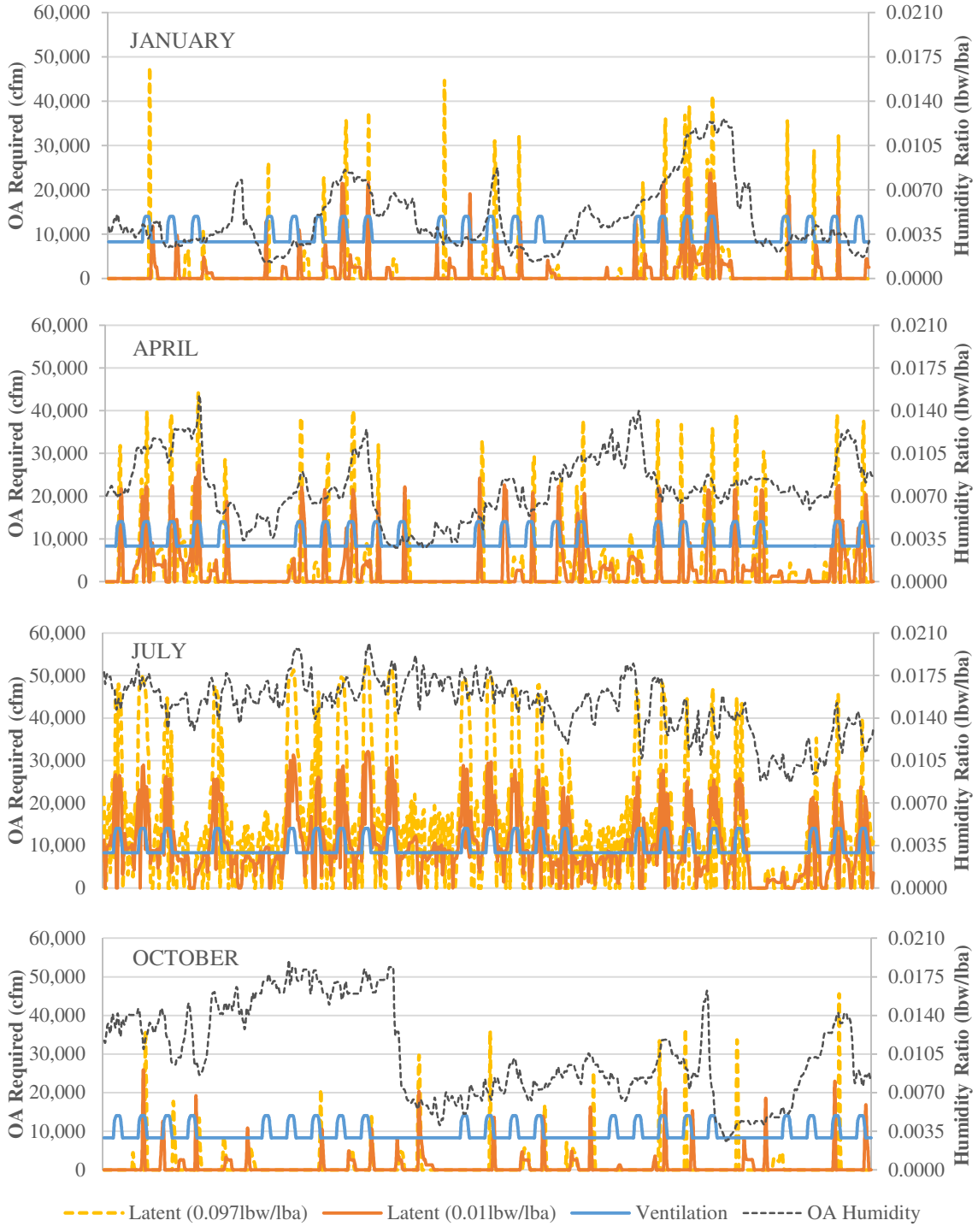

Figure 4.46: Outside Air Required to Fulfill Ventilation and Latent Loads in the Wing 'A' Offices at Infiltration Levels of 1.5cfm/ft^2

As discussed in Section 4.1.4, the AHU and terminal unit airflow in the building is controlled by the zone thermostats and the chilled beam water flow is controlled to a differential pressure setpoint in each wing. This approach can lead to unstable operation due to the interactions between the two systems and also has a potential for overcooling and thermal comfort problems. In order to avoid these issues, a modified control sequence based on the outside air requirements discussed above is proposed for the AHU (Figure 4.48 and Figure 4.48). This sequence allows the AHU to be run as a partial DOAS unit. The outside air damper is controlled by maximum zone CO_2 levels, but is subject to an override if the return air humidity ratio exceeds a humidity ratio setpoint of 0.01 lbw/lba. The AHU return air damper (see Figure 4.10) is kept closed and the bypass air damper is modulated to maintain a supply air setpoint of 62°F. The cooling coil is controlled to maintain a leaving temperature of 53°F. This control sequence ensures that both ventilation and latent requirements are met for all hours with a VAV operation. On the chilled beam system side, the beam supply water temperature is maintained at 3°F above the zone dewpoint and the chilled beam water flow is varied to meet zone thermostat requirements.

Unfortunately, all the AHU and terminal unit supply air controls in EnergyPlus are linked only to the zone thermostats. The chilled beam model is designed to run only with a constant volume DOAS. There are provisions for the bypass air that reheats the supply air in a UFAD/displacement ventilation setup but supply air volume control is only associated with building sensible loads. If the default systems and controls in EnergyPlus are used, whole building energy estimates and zone thermal comfort evaluations will be

inaccurate. Therefore, in order to model a reasonable approximation of the control sequence discussed, the Energy Management System (EMS) option is used. The EMS is designed to replicate an actual building EMCS and overrides the system controls based on feedback from the simulation outputs. However, the EMS only performs high-level controls, such as setpoint overrides and system availability overrides. Low-level controls such as PID control of dampers and valves are not possible in the EMS setup.

Figure 4.49 (modified from Figure 4.10) shows the air-side loop of the UFAD AHUs as modeled in EnergyPlus. The entire AHU excluding the return and supply fans is modeled as an outdoor air system and the bypass air damper is modeled as the outdoor air mixer. Thus the supply side of the airloop has only 3 components, the return fan, the outdoor air system and the supply fan. Three sets of programs are written in the EMS module to control the outside air flow, the supply airflow and the chilled beam water temperature. The outdoor air requirements are initially set based on CO_2 levels in the zones. If the humidity ratio in any of the zones is greater than 0.01 lbw/lba, an override is setup to increase the outside air. The adjusted amount of outside air is calculated based on Equation 4.12. The supply air flow is controlled by overriding the AHU supply fan flow rate based on Equation 4.13. These two equations are iteratively solved inside the HVAC system loop. The chilled beam water temperature setpoint is set to be 3°F higher than the highest zone dewpoint temperature and is subject to a minimum of 58°F. The three EMS programs for the chilled beam water temperature setpoint, outside air volume and supply air volume are documented in Appendix C.4, C.5 and C.6 respectively.

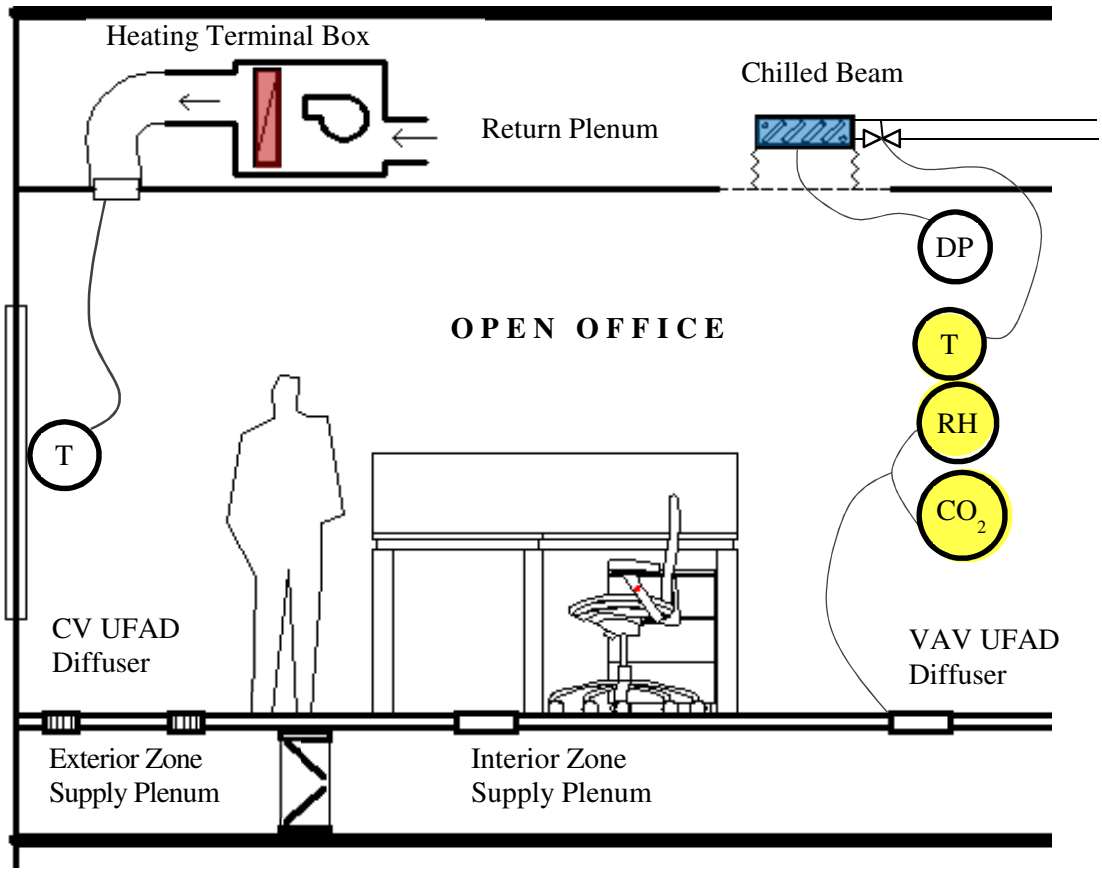

Figure 4.47: Modified Control Diagram for the Airside System (Typical for UFAD AHUs)

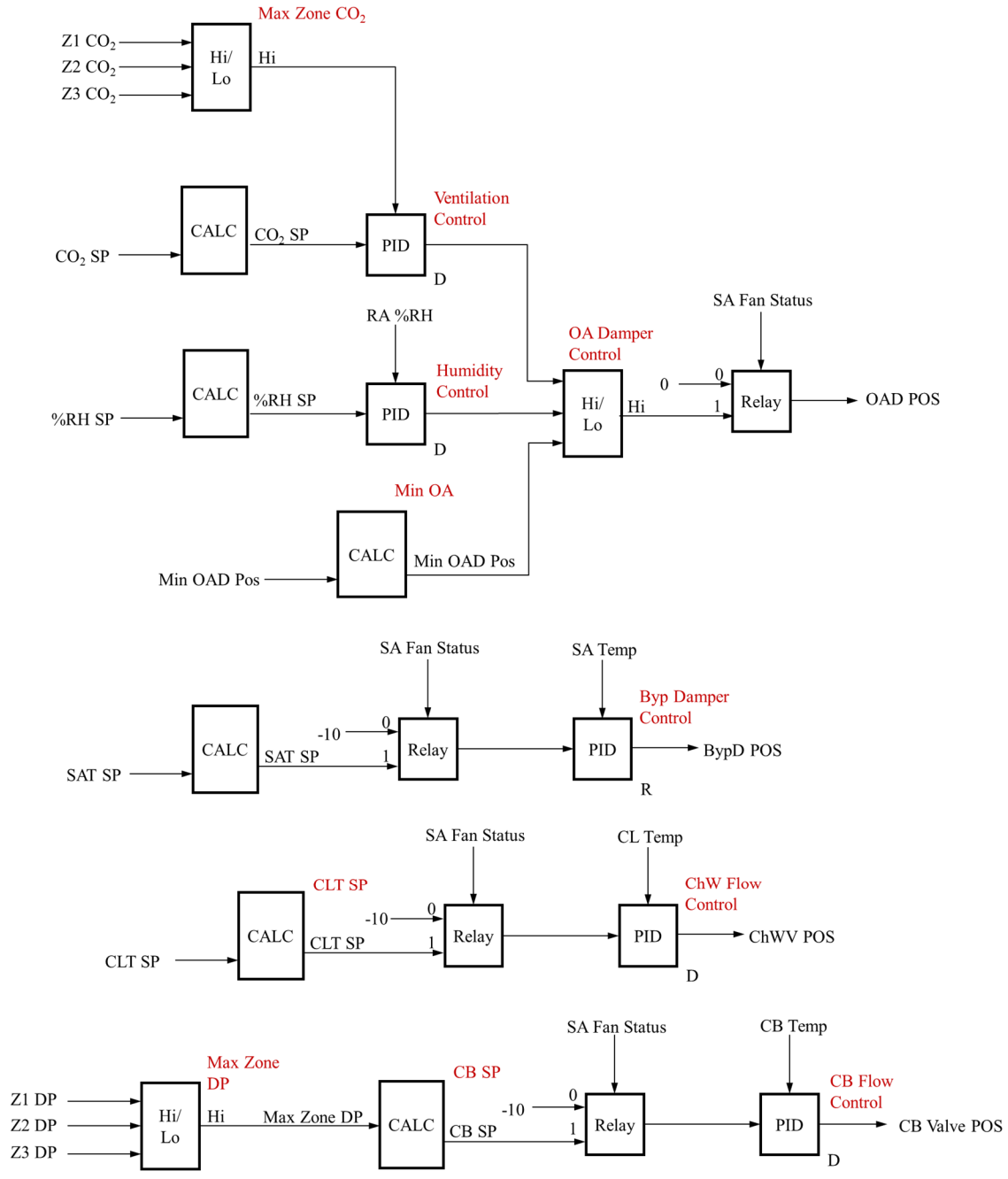

Figure 4.48: Modified Control Diagram for the Airside System as implemented in the EnergyPlus EMS (Typical for UFAD AHUs)

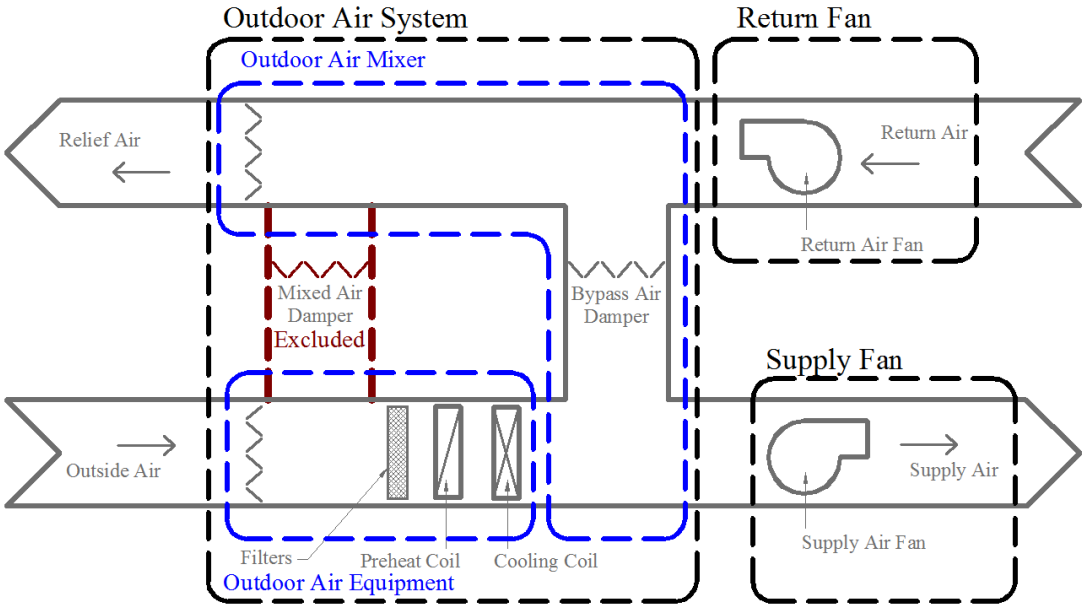

Figure 4.49: Typical UFAD AHU Configuration in EnergyPlus Modified for Operation with Passive Chilled Beams

$$V_{OA,l} = \frac{\sum_{z=1}^{n} Q_{z,l} * \left(T_{ZA,sp} + \Delta T_{RF} - \left(T_{SA,sp} - \Delta T_{SF}\right)\right)}{4840 * \left(HR_{ZA,sp} - HR_{SA}\right) * \left(T_{ZA,sp} + \Delta T_{RF} - T_{CC,sp}\right)} \quad 4.12$$

$$V_{SA,v} = \frac{\left(T_{SA,sp} + \Delta T_{RF} - T_{CC,sp}\right) * V_{OA,v}}{T_{ZA,sp} + T_{RF} - \left(T_{SA,sp} - \Delta T_{SF}\right)} \quad 4.13$$

4.5. Summary and Observations

In this chapter, an energy model of the building was created using EnergyPlus 8.1.0.008. The initial model was created using inputs obtained from the as-built drawings, control drawings, sequences of operation, building walk-throughs, comfort baseline measurements, discussions with building operators, system trend data and control programming data. Other references such as Standard 90.1 (ASHRAE 2004) and Deru et al. (2011) were also used when building data was not available.

The energy model was then calibrated using monthly electricity data obtained from the case-study building. Several parameters were modified during the calibration process and the impact of each parameter on the statistical indices CV (RMSE) and NMBE were evaluated. The revised load schedules, minimum zone airflow fractions and peak equipment plug loads had the most significant impact on the calibration fit of the model. The CV (RMSE) and NMBE of the initial simulation model were 19.48% and 17.84% respectively. The CV (RMSE) and NMBE of the final calibrated model were 6.36% and 0.86% respectively.

Because the controls set in place for the chilled beams in the building are different from the controls recommended in literature, a modified chilled beam operation was proposed and a process to model this control was developed.

The following observations were made during the development and calibration of the EnergyPlus model:

- In all-electric buildings with a single electric meter, lighting, equipment and plug loads play an important role in the accurate modeling of energy use in the building. Total equipment loads along with location and scheduling of these loads need to be carefully documented through building walkthroughs and demand energy meters in order to create a simulation model with sub-metered heating and cooling data that is representative of the real building.
- Using meteorological weather data for the actual year during which energy use data was collected instead of TMY weather data does not significantly improve the

calibration of the model if monthly energy data is used, but may have a significant impact for hourly calibrations.

- Larger miscellaneous equipment such as kitchen make-up air units and exhaust, if operated continuously, can play a significant role in the energy use of a building and need to be included in a calibrated simulation model to account for their energy consumption.
- Irregular operation, manual overrides and faults in the building need to be modeled to account for their effect on energy use. These faults can be determined by collecting trend data for the building if available and spot checks of the sensors, dampers and valves in the building.
- The case-study building has a larger perimeter to interior zone ratio (approximately 0.39) than an equivalent rectangular building (approximately 0.25). Even with a larger perimeter zone ratio, modification in the building envelope played a minor role in the calibration of the simulation model.
- In spaces with UFADs, if thermal heat gain in the supply plenum and heat loss in the return plenum is not modeled, it can result in predicted cooling, fan and heating consumption that is lower than the actual energy use. However, if the zone heating components are in the supply plenum, the predicted heating consumption will be higher than the actual heating energy.
- The quantity of conditioned air supplied to the zones in buildings with chilled beams determines the number of hours the chilled beams will be used. If the airside system is controlled through the zone thermostats or is oversized, the chilled beams will see

little or no use and any energy saving potential from the chilled beams will not be realized.

- Outside air requirements can be large (almost twice the ventilation requirements) if strict humidity control is required in a building negating any potential savings from the chilled beams. In such a scenario, heat recovery for the outside air will be necessary and alternative measures for latent cooling may have to be explored.
- Latent loads in a leaky building can be 20% higher than a well-sealed pressurized building due to infiltration. Ventilation volumes required to fulfill these additional latent loads can be more than 40% higher than that required in a well-sealed pressurized building with low infiltration.
- EnergyPlus can only model chilled beams with overhead constant volume supply air. It also does not provide an option to control the air and water side systems in the zones separately. This makes it difficult to model passive chilled beams which are typically combined with underfloor or displacement ventilation. If the default systems and controls are used, whole building energy estimates and zone thermal comfort evaluations will be inaccurate.
- There are some inherent assumptions in the modeling of chilled beams/UFADs in EnergyPlus.
    - The chilled beam model is a convection-only quasi-empirical model which requires information about the physical characteristics of the chilled beam used. Radiant cooling, if any, provided by the chilled beam is ignored.

- Default coefficients used in EnergyPlus yield chilled beam cooling capacities that are less than 50% of the capacities provided by the chilled beam manufacturers.
- For the UFAD system, the supply and return plenums must be accurately physically described to adequately estimate supply and return plenum temperatures. EnergyPlus does estimate both the conduction heat transfer between the supply and return plenums and the radiant heat transfer from the warm ceiling to the cooled floor. Stratification models, which are also quasi-empirical plume equations for interior and exterior zones, are provided to estimate sub-zone temperatures in a UFAD setup.

- There are real-time operation and maintenance issues such as the malfunctioning of the VAV UFAD diffusers and the incorrect zoning and piping of the chilled beams.
  - If a single VAV UFAD diffuser is provided for approximately 150 ft^2 of office space, this results in over 3,000 diffusers with moving parts that are prone to regular damage and failure.
  - The chilled beams are piped in series for the exterior and interior zones and separate flow control is not possible. Because the exterior and interior zones have different cooling/heating requirements, this leads to overcooling in the interior zones and undercooling in the exterior zones. This issue needs to be taken into consideration during the design of the chilled beams.

CHAPTER V

SIMPLIFIED NUMERICAL BUILDING MODEL

In this chapter, a simplified numerical building model is proposed to estimate the energy use for a building with passive chilled beams and underfloor air distribution without the use of a whole building energy analysis software. This model is based on hourly steady-state calculations for each component of the HVAC system. As discussed in Section 4.2, the three atypical components of the system are the demand controlled ventilation, the underfloor air distribution and the passive chilled beams.

The ventilation system supplies the amount of air required to meet the maximum of the ventilation and latent load requirements. Therefore, both ventilation and latent load requirements are calculated at each timestep and the maximum of the two values are used as the outside air volume for that timestep.

The outside air required for ventilation is calculated from Equation 5.1 which is based on required CO_2 concentrations in the space, CO_2 generation per person depending on physical activity levels and the CO_2 concentration of the ventilation air. The CO_2 generation rate for people is assumed to be 0.0000237259 cfm/Btu-hr of activity. For office people, activity levels of 1.2 met are assumed, which translates to 409 Btu/hr of heat generation. The CO_2 concentration in the outside air is assumed to be 400 ppm. The CO_2 concentration setpoint in the space is assumed to be 900 ppm.

The supply air volume required for ventilation is then calculated using Equation 5.2.

$$V_{OA,v} = \frac{N}{C^{t}_{setpoint} - C_{\infty}} \times \sum_{z=1}^{n} P_z \quad (5.1)$$

$$V_{SA,v} = \frac{\left(T_{ZA,sp} + \Delta T_{RF} - T_{CC,sp}\right) * V_{OA,v}}{T_{ZA,sp} + \Delta T_{RF} - \left(T_{SA,sp} - \Delta T_{SF}\right)} \quad (5.2)$$

The latent loads in the office spaces are only from people and infiltration. The ratio of latent to sensible heat generation from people is assumed to be 0.365 (equal to the ratio used in EnergyPlus). The infiltration loads in the spaces are calculated for infiltration values of 0.06 cfm/ft^2 of above grade wall area. Infiltration is assumed in the zones, supply plenums and return plenums. The supply and outside air required for the latent loads in the zones is then calculated by Equations 5.3 and 5.4.

$$V_{SA,l} = \frac{\sum_{z=1}^{n} Q_{z,l}}{4840 * (HR_{ZA,sp} - HR_{SA})} \quad (5.3)$$

$$V_{OA,l} = \frac{V_{SA,l} * \left(T_{ZA,sp} + \Delta T_{RF} - \left(T_{SA,sp} + \Delta T_{SF}\right)\right)}{T_{ZA,sp} + \Delta T_{RF} - T_{CC,sp}} \quad (5.4)$$

$$V_{OA,actual} = \mathrm{Max}\,(V_{OA,v}, V_{OA,l}) \quad (5.5)$$

Figure 5.1 shows the volumes of supply air computed for Wing 'A' in EnergyPlus and by Equations 5.1 to 5.5 for the months of January, April, July and October. It shows that when ventilation requirements are higher, the calculated supply air volumes are lower than EnergyPlus values. When latent requirements are higher, the calculated and EnergyPlus values are very close. On an average, the difference between the supply air volumes computed in EnergyPlus and by the simplified numerical model is less than 4%.

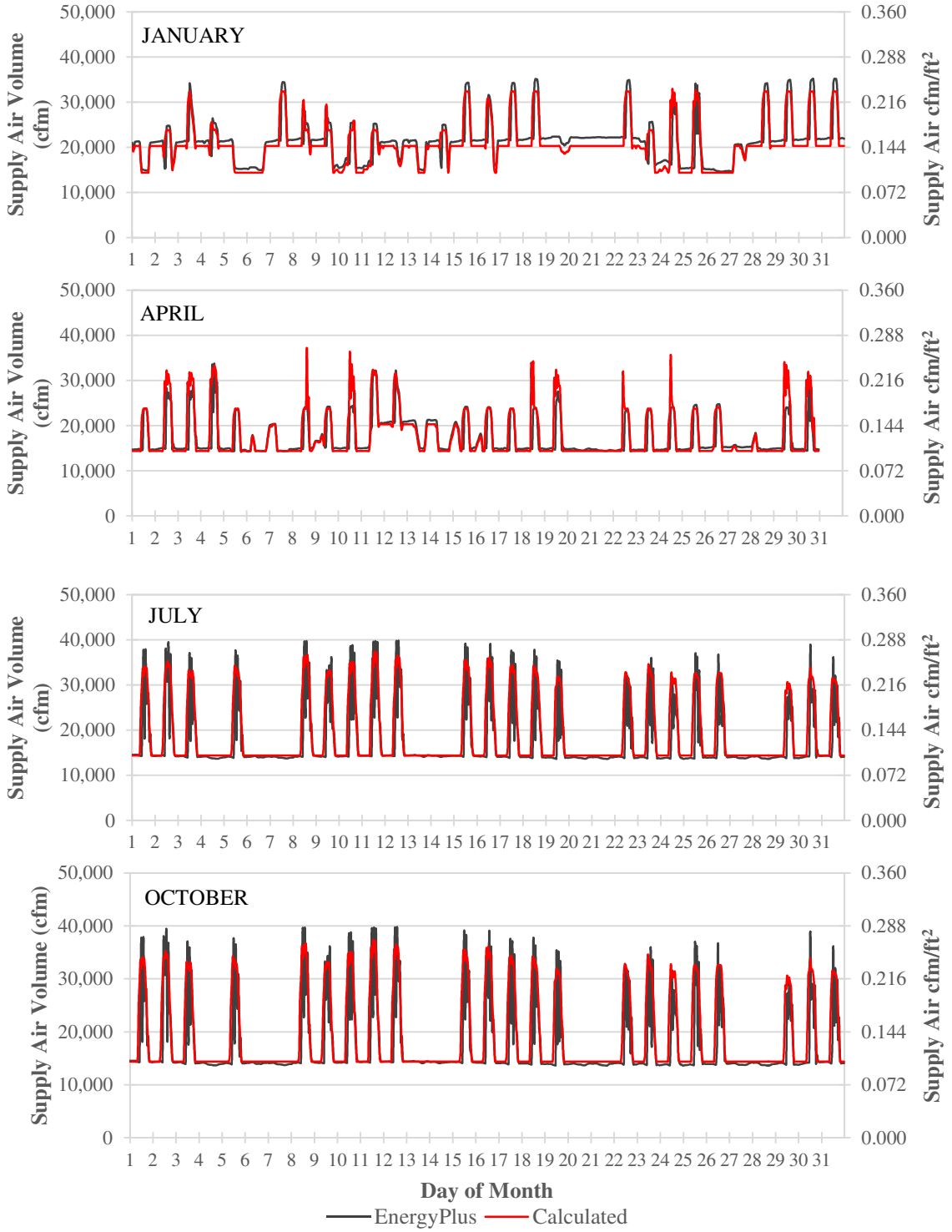

Figure 5.1: Supply Air Volumes for Wing 'A' as Computed in EnergyPlus and by the Simplified Numerical Model for January, April, July and October

For the estimation of the heat transfer to the supply and return plenums, a simplified statistical model documented in Schiavon et al. (2011) was used. The method uses simple regression coefficients to convert the loads associated with an overhead mixing ventilation system to that of a UFAD system. The loads are then split by ratio between the supply plenum, the zone and return plenum. Figure 5.2 shows the schematic flow diagram of the process used to estimate the ratios of buildings loads transferred to the supply and return plenums. These values are then used to estimate the temperatures in the supply and return plenums.

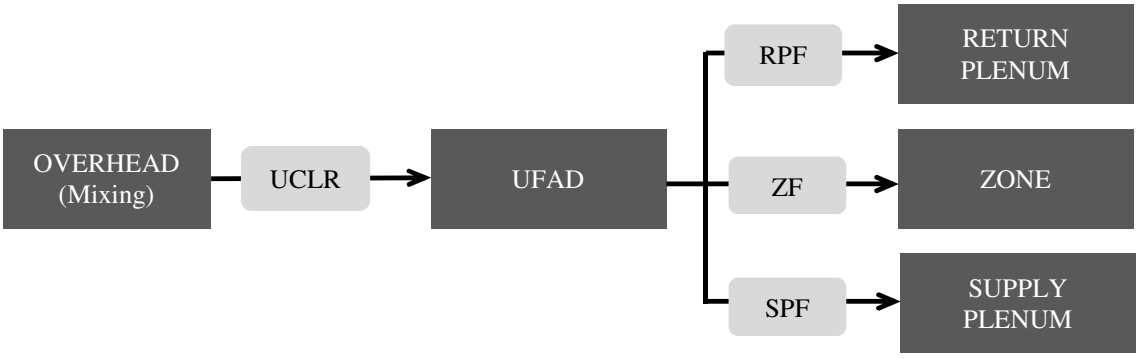

Figure 5.2: Schematic Flow Diagram of the Process Used to Estimate the Ratios of Buildings Loads Transferred to the Supply and Return Plenums in a UFAD System (Adapted from Schiavon et al. (2011))

Equations 5.6 to 5.9 show the calculations for the UFAD Total Cooling Load Ratio (UCLR) as a ratio of the total cooling load of an overhead mixing system, the ratio of the cooling removed by the supply plenum (SPF), the return plenum (RPF) and the zone (ZF).

$$UCLR = 0.9528 + C_1 + C_2 \quad (5.6)$$

$$SPF = (0.6179 + C_3 + C_4 + C_5)^2 \quad (5.7)$$

$$RPF = C_6 \quad (5.8)$$

$$ZF = 1 - SPF - RPF \quad (5.9)$$

The UCLR coefficients C_1 and C_2 depend on the floor level of the zone and the orientation of the zone. C_3 is a function of the zone type (interior or perimeter), C_4 depends on the floor level and C_5 depends on both the floor level and the zone type. The return plenum coefficient C_6 is a function of the floor level. Figure 5.3 shows the supply plenum temperatures for an interior zone in Wing 'A' for the month of August as calculated by EnergyPlus and the simplified numerical model. They are within 3% of each other even though the temperatures calculated by the numerical model are consistently lower than that of the EnergyPlus model.

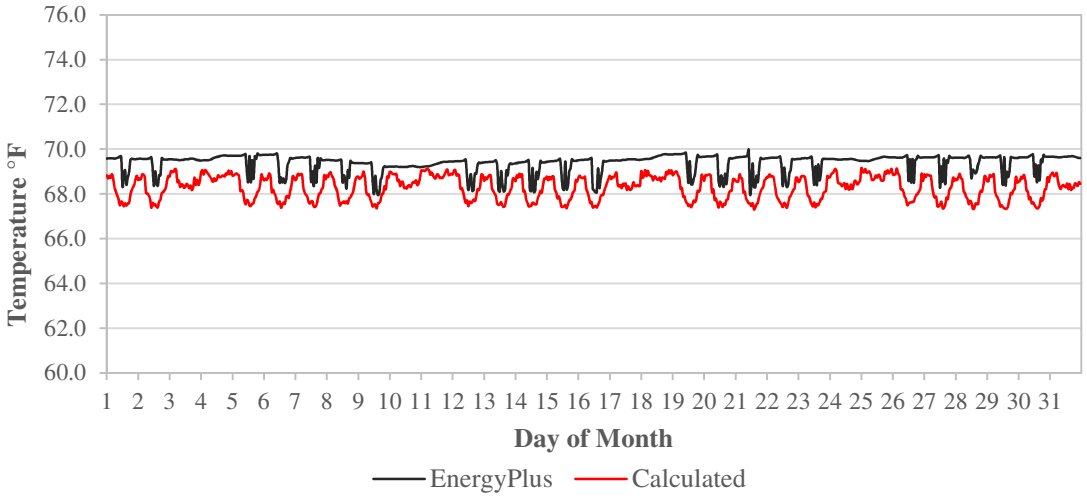

Figure 5.3: Supply Plenum Temperatures for an Interior Zone in Wing 'A' for the Month of July as Calculated by EnergyPlus and the Simplified Numerical Model

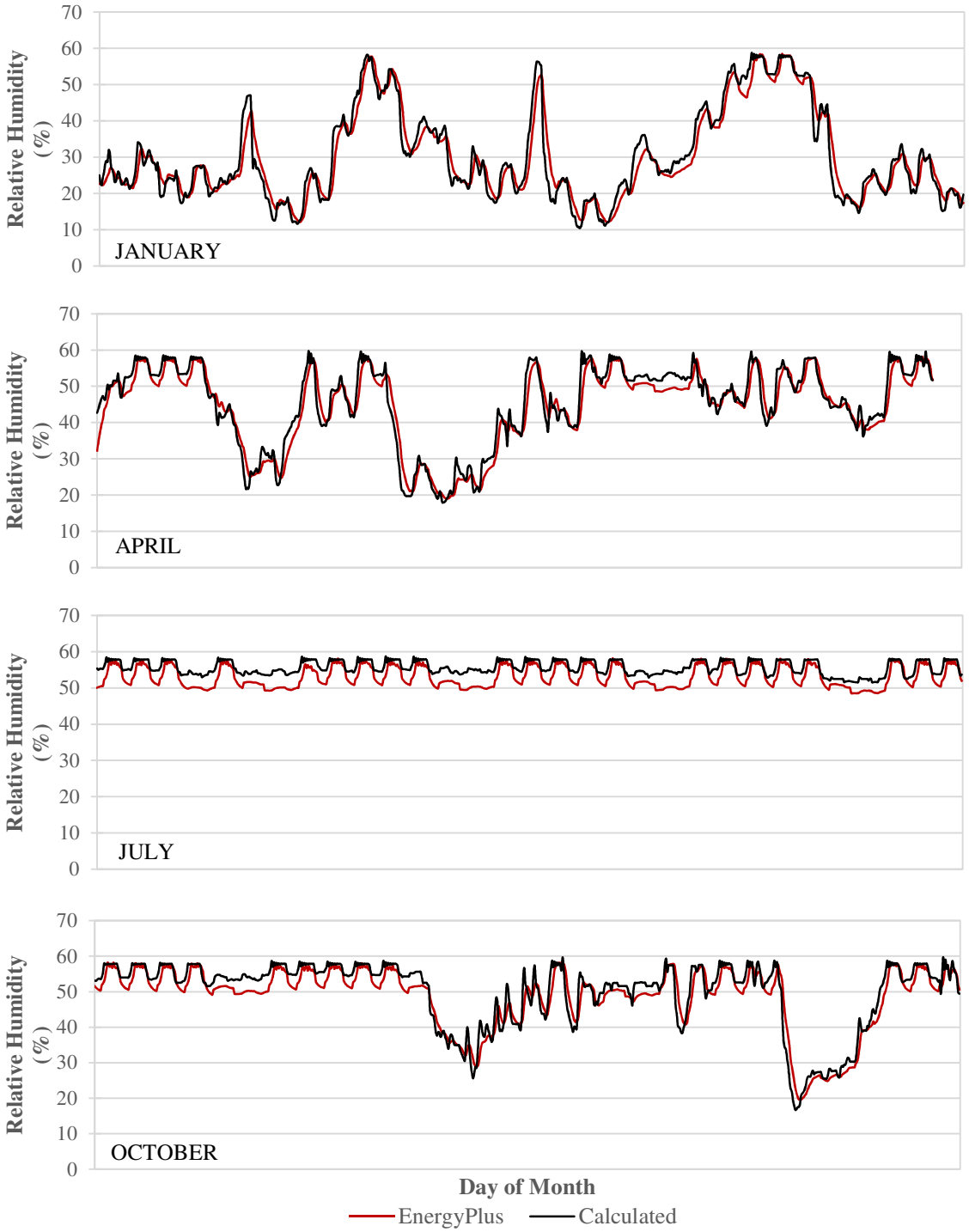

Figure 5.4: Zone Relative Humidity in an Interior Zone in Wing 'A' for the Months of January, April, July and October as Calculated by EnergyPlus and the Simplified Numerical Model

Figure 5.4 shows the relative humidity in an interior zone in Wing 'A' as calculated by the numerical model and EnergyPlus for the months of January, April, July and October. It shows that the numerical model consistently over-predicts the zone relative humidity but on an average only by 4% or less. Figure 5.5 shows the monthly cooling energy for the ventilation system as calculated by the numerical model and EnergyPlus.

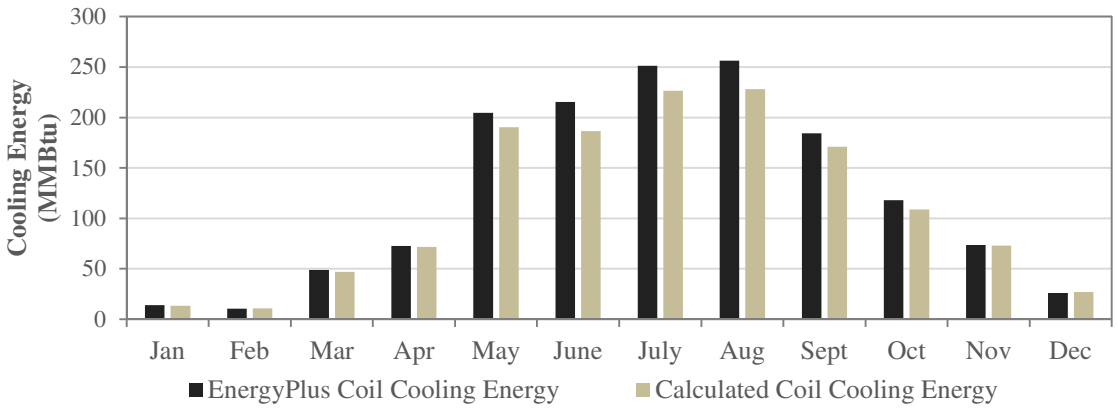

Figure 5.5: Monthly Cooling Energy for the Ventilation System as Calculated by EnergyPlus and the Simplified Numerical Model

Appendix D documents the equations used in the numerical model to calculate the air flow rates, the temperatures and humidity ratios of the nodes in the airloop, the energy use for the various components in the airloop and the chilled beam water flow rates. This spreadsheet-based model is easy to setup, does not require detailed knowledge of whole-building energy analysis software and predicts flow rates, zone temperatures, humidity ratios and energy use within 5% of a detailed whole-building energy analysis software such as EnergyPlus.

CHAPTER VI

BUILDING ENERGY USE EVALUATION

In this chapter the energy use of the building as calibrated (CALIB) and the building the modified control (MCB) is evaluated and compared with an equivalent model with a VAV system (VAV) and an ASHRAE 90.1-2004 code compliant building model (ASHRAE). Section 6.1 includes the energy use for the four models discussed in Section 3.2 (see Figure 3.1 and Table 3.1). The HVAC energy savings at varying internal sensible and latent loads are also discussed. Section 6.2 summarizes the observations from the building energy use evaluation.

6.1. Building Energy Use vs Equivalent VAV System and ASHRAE 90.1 (2004) Minimum Requirements

Figure 6.1 shows the comparative end-use energy for the CALIB, MCB, VAV and ASHRAE models. It shows that the energy use in the building is dominated by the lights and equipment, due to the presence of a 24x7 data center and high lighting loads in the building. Unfortunately, the HVAC energy of the CALIB building is higher than both the equivalent VAV the ASHRAE model (10% and 5% respectively). As discussed earlier, the ventilation system in the real building is sized for twice the peak loads in the building, so the chilled beams do not supply much cooling to the zones. Additionally, due to the presence of the chilled beams, the UFAD system is unable to achieve unidirectional flow and thermal stratification. As a result, the UFAD zone air distribution system ventilation effectiveness never exceeds 1. Due to these two systems working against each other, the

building is unable to take advantage of either of the high efficiency HVAC systems installed and the resulting HVAC energy use is 10% higher than the equivalent VAV model.

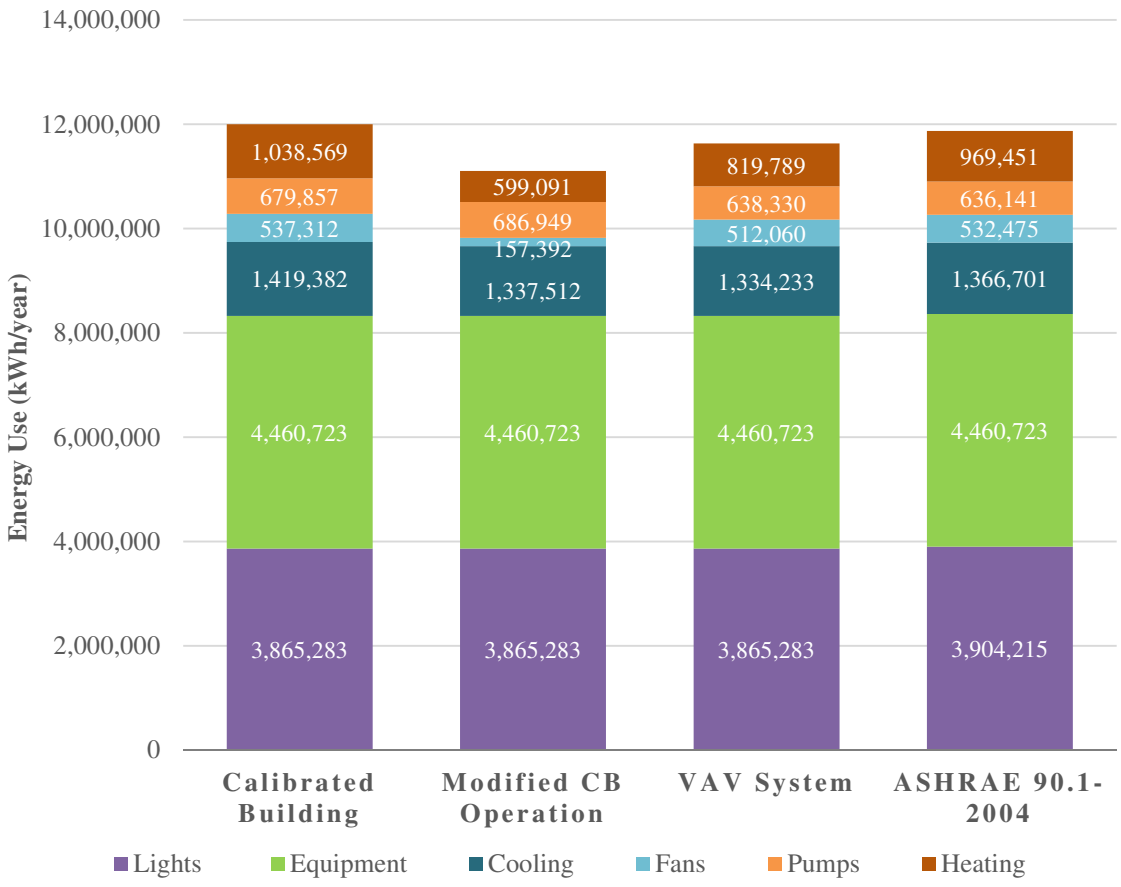

Figure 6.1: Comparative End-Use Energy Consumption for the Building with an Equivalent VAV System Model and ASHRAE 90.1 (2004) Compliant Model

The heating energy in the building as operated is also higher than the building with the VAV system because of the oversized AHUs. At low loads, the terminal boxes often operate at minimum flow and cause overcooling and reheat. The CALIB building does

have lower duct static pressure requirements, but fan energy use is 5% more than the VAV system. This is because more supply air is required to be delivered to the spaces due to the higher supply air temperature setpoint requirement for a UFAD system. Figure 6.2 shows the supply air volumes for the CALIB building, the equivalent VAV system and the MCB model. It shows that the UFAD system requires at least 25-30% more supply air than the VAV system. On the other hand, the airside system of the building with passive chilled beams supplies only 53% of the air supplied by the equivalent VAV system on.

Because of the lower quantity of supply air and the more efficient chilled beam system, the MCB building fares much better with HVAC energy use 16% and 21% lower than that of the VAV and the ASHRAE model respectively. These energy savings are consistent with chilled beam savings in hot and humid climates documented in literature. Figure 6.3 shows the detailed monthly breakdown of the HVAC energy by end-use for the MCB model and the VAV model.

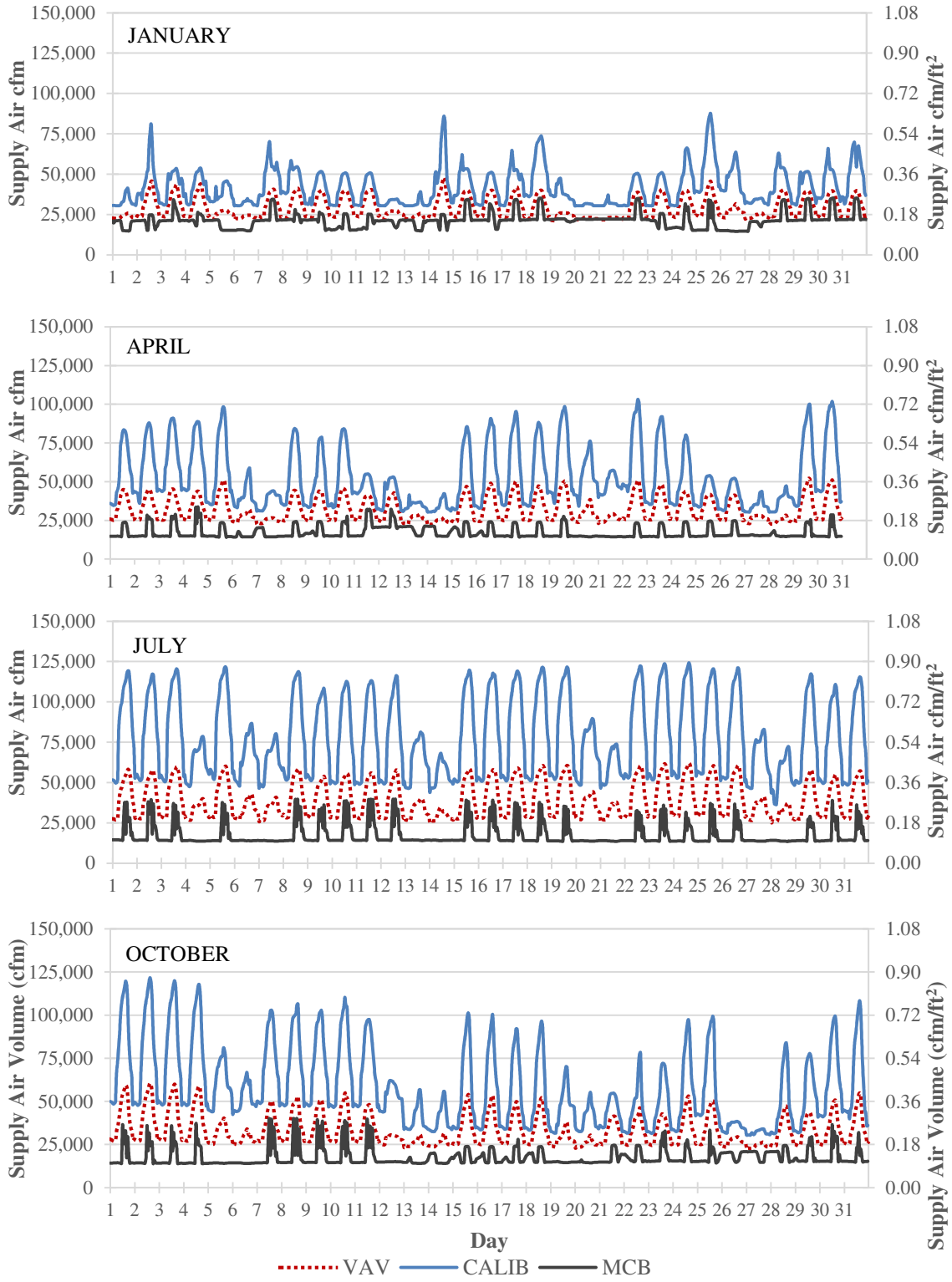

Figure 6.2: Supply Air Volume for Wing 'A' for the Months of January, April, July and October for the CALIB, VAV and MCB Model

Figure 6.3 shows that all the energy savings in the chilled beam system come from heating and fan energy reductions. Fan energy savings are substantial (69%) due to both lower static pressure requirements of the UFAD system, and the need to supply only enough air to fulfill ventilation and latent requirements (see Figure 6.2). Heating energy for the chilled beam system is also 27% lower because the smaller airside system eliminates all reheat in the building.

On the other hand, pumping energy for the chilled beam system is 7% higher, due to the need to pump chilled water to the beams in all the zones in the building. The annual cooling energy (chiller and plant) consumption for the chilled beam system is also higher than that of the VAV system. Figure 6.3 shows that at off-peak cooling seasons, the VAV system is able to take advantage of the high number of available economizer hours and uses less cooling energy than the chilled beam system. The building as currently operated has over 3,000 hours when an economizer can be potentially used. If the number of economizer hours vary due to different economizer operation or weather conditions, energy savings will be different.

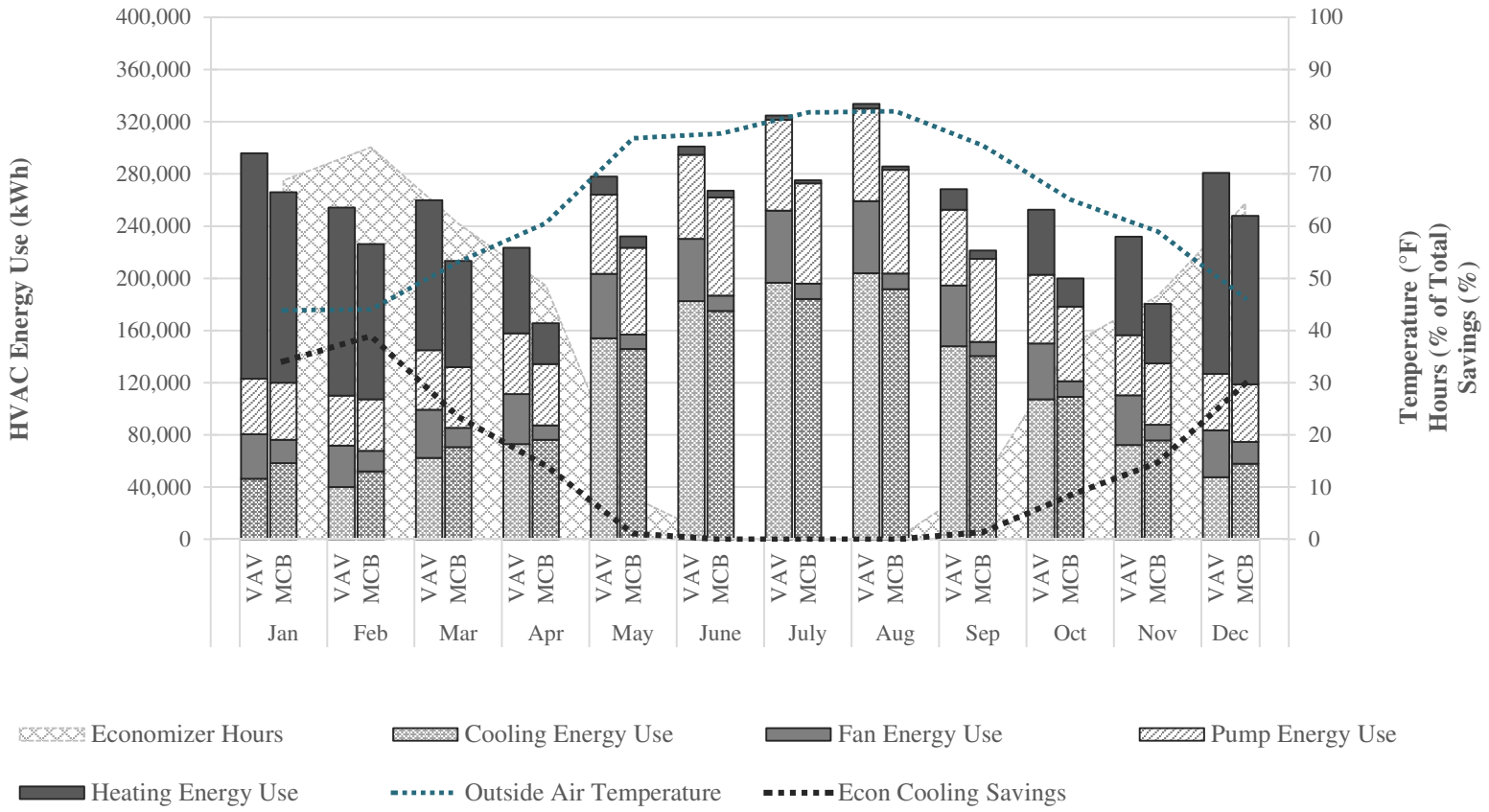

Figure 6.3: Monthly HVAC Energy Consumption for the Modified Chilled Beam (MCB) System and the Equivalent VAV System

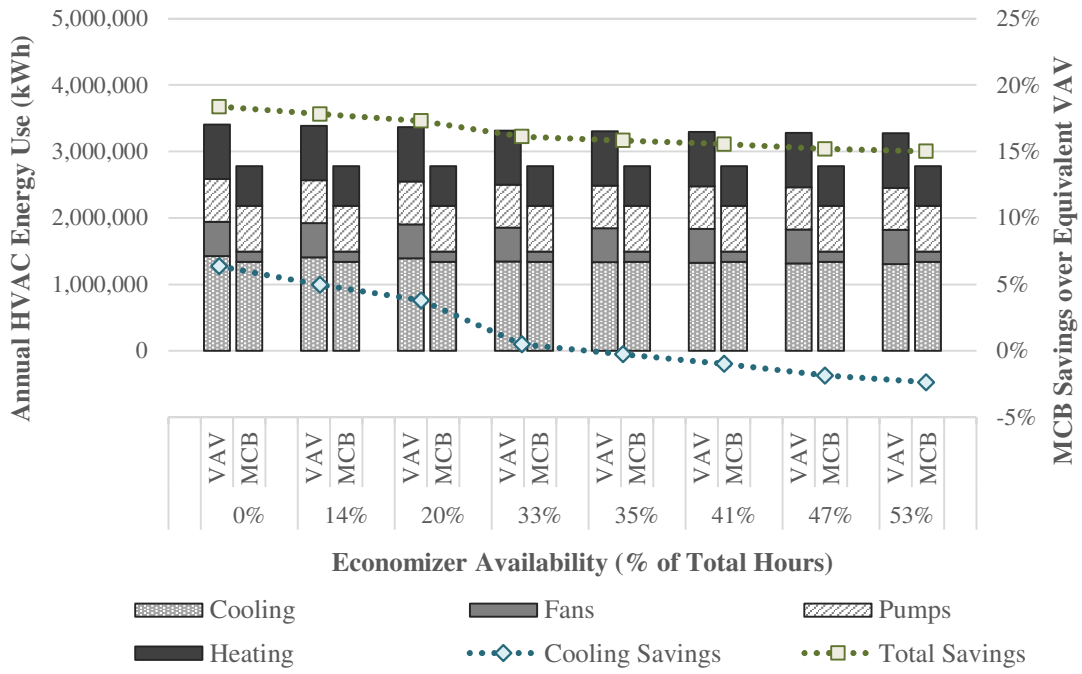

Figure 6.4: Comparative Annual HVAC Energy Use for the VAV System and the Modified Chilled Beam (MCB) System for Varying Economizer Hours

Figure 6.4 show the energy difference between the VAV system (VAV) and the chilled beam system (MCB) for varying economizer hours. It shows that even when no economizer is used with the VAV system, the actual cooling energy saved with a passive chilled beam system is modest (3-6%). This is potentially because cooling energy is wasted when the cooled dehumidified supply air is reheated by the bypass air for UFAD operation. However, as passive chilled beams require some sort of UFAD or displacement ventilation configuration, this energy waste is unavoidable unless alternate methods are used for dehumidification.

Another potential issue is the increase in plenum temperature in the UFADs when supply air volumes are low. The supply air for the building with the modified chilled beam operation is only 1/5th the air supplied in the calibrated building. While some amount of temperature increase in the supply plenum is unavoidable with UFAD operation, at the low supply air volumes associated with chilled beams, the actual supply air temperatures delivered to the zones can be 8-9°F higher than the air exiting the AHUs. Figure 6.5 shows the difference in the supply air temperatures for a zone in the calibrated building and building with the modified chilled beam operation for the month of August. Figure 6.6 shows the actual energy supplied to the zones by the various systems for wing 'A'. Figure 6.7 shows the sensible energy used by the cooling coil in the AHU vs the energy supplied to the zones.

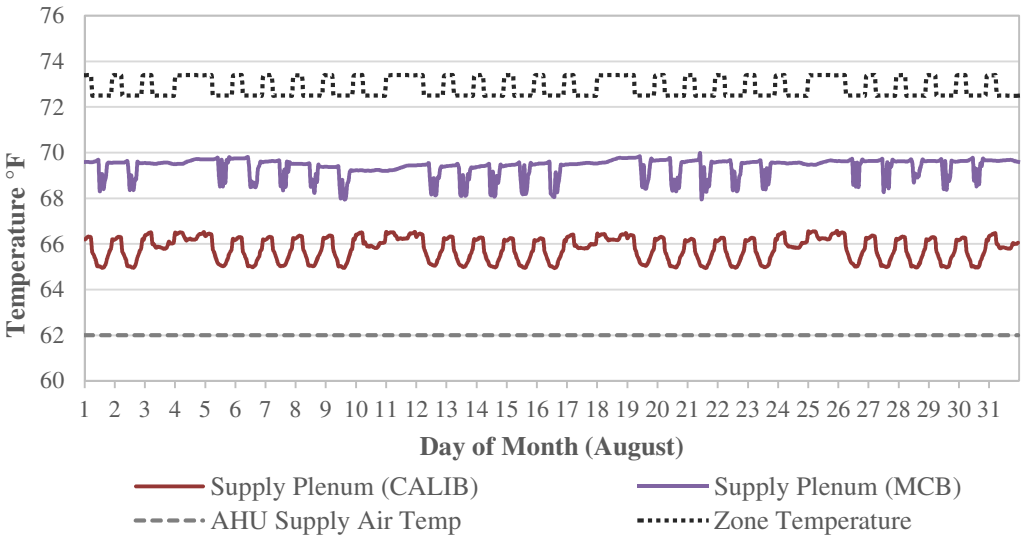

Figure 6.5: Supply Plenum Air Temperatures in Wing 'C' for the Calibrated Building and the Building with the Modified Chilled Beam Operation

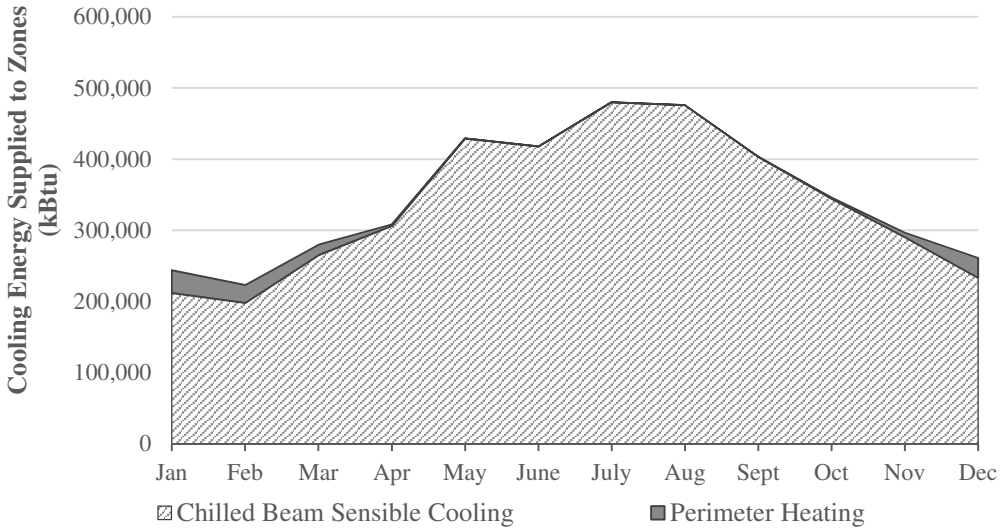

Figure 6.6: Monthly Energy Supplied to the Zones in Wing 'A' by the Ventilation System, the Chilled Beam System and the Perimeter Heating System

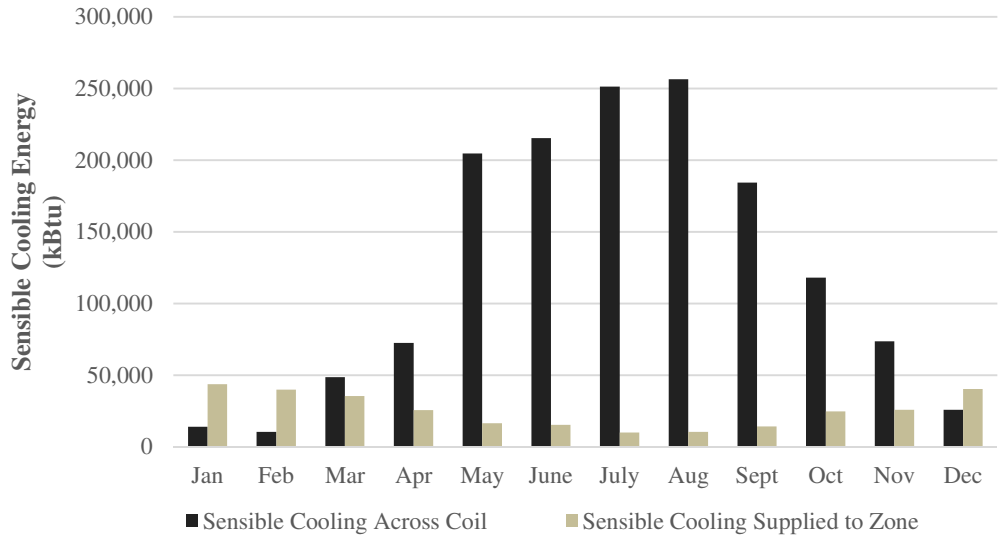

Figure 6.7: Monthly Sensible Cooling Energy Used vs Sensible Cooling Energy Supplied for the AHU4A1 Ventilation System

Figure 6.5, Figure 6.6 and Figure 6.7 reaffirm that the deep cooling of the supply air that is required for humidity control doesn't reach the zones in a passive chilled beam/UFAD configuration due to the bypass air mixing and the increase in temperature in the supply plenums. On an average, the ventilation system supplies only 7% of the annual cooling in the building. This is a very important consideration while sizing the chilled beams during the design phase. If the MCB control were to be implemented in the case-study building, the passive chilled beams would have to be sized for twice its current cooling capacity. This is possibly because the ventilation system was assumed to provide more cooling than it actually does as the increase in temperature in the supply plenums and the bypass air mixing were overlooked. Therefore it is recommended that the chilled beams be sized for the maximum sensible cooling in the zones and variable flow pumping be used to control beam capacity.

Building loads also play and important role in the energy savings potential of chilled beams. As a general rule of thumb, buildings with large sensible loads and low ventilation and latent requirements are good candidates for chilled beam systems due to the high energy savings potential they offer. A parametric study was conducted to establish energy savings under different sensible and latent load conditions. Loads were varied by

modifying internal plug loads and occupancy in the zones. The occupancy levels increase both ventilation and latent loads in the building.

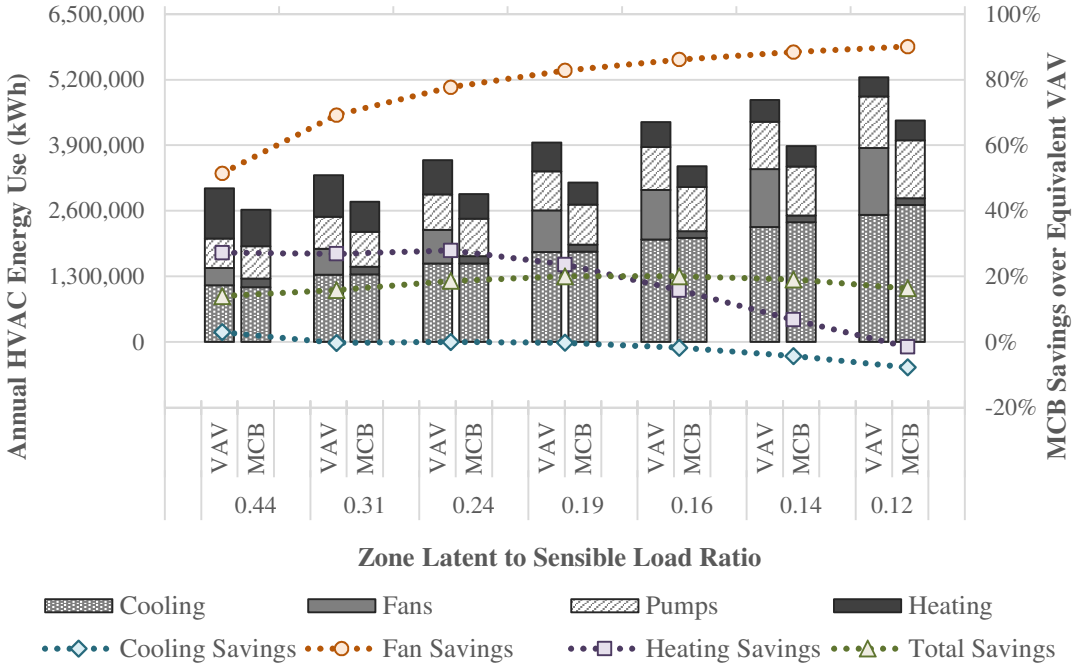

Figure 6.8: Comparative Annual HVAC Energy Use for the VAV System and the Modified Chilled Beam (MCB) System for Varying Ratios of Latent to Total Sensible Loads in the Building

Figure 6.8 shows the energy difference between the VAV system and the chilled beam system (MCB) for different latent to sensible load ratios in the building. It reaffirms that the majority of energy savings in chilled beam systems come from fan and reheat energy. Fan energy savings increase substantially (from 50% to 90%) with higher building loads but even at very high sensible loads, total HVAC energy savings potential of chilled beams doesn't exceed 20%. This is because cooling savings are minimal at any load ratios

and reheat savings degrade significantly at very high building sensible loads. Figure 6.9 shows the range of HVAC energy savings achievable from passive chilled beam systems over standard VAV systems. Energy savings are possible for a wide range of load profiles even though a chilled beam system cannot take advantage of free cooling offered by an air-side economizer cycle. Hence, in general, buildings with low latent or ventilation requirements and in locations with lower economizer opportunity are better candidates for chilled beams.

Another feature that is not included in the case-study building but needs to be addressed is a water-side economizer cycle. If a water-side plate heat exchanger is used between the condenser water loop and the chilled beam loop, the heat exchanger has the potential to be used at condenser water supply temperatures below the chilled beam water supply setpoint (58°F). This translates to over 3,500 hours when the water-side heat exchanger can be potentially used with chilled beams. In contrast, if the heat exchanger is used between the condenser water loop and the chilled water loop, as is typical with VAV systems, the heat exchanger can be used only at condenser water supply temperatures below the chilled water supply setpoint (44°F), or approximately 1,600 hours. Figure 6.10 shows the annual HVAC energy use for the MCB and VAV systems with and without a water-side heat exchanger. The cooling energy savings for the MCB system are not insignificant (7%). However, because the condenser water loop with the constant-volume pumps are used to supply chilled water to the AHUs and the chilled beams, pumping energy increases (10%) and negates all the cooling energy savings. On the other hand, cooling energy savings for the VAV system are marginal (2%) because there is very little

load on the heat-exchanger as the airside economizer supplies most of the cooling. As a result, the increase in pumping energy is also negligible (less than 1%).

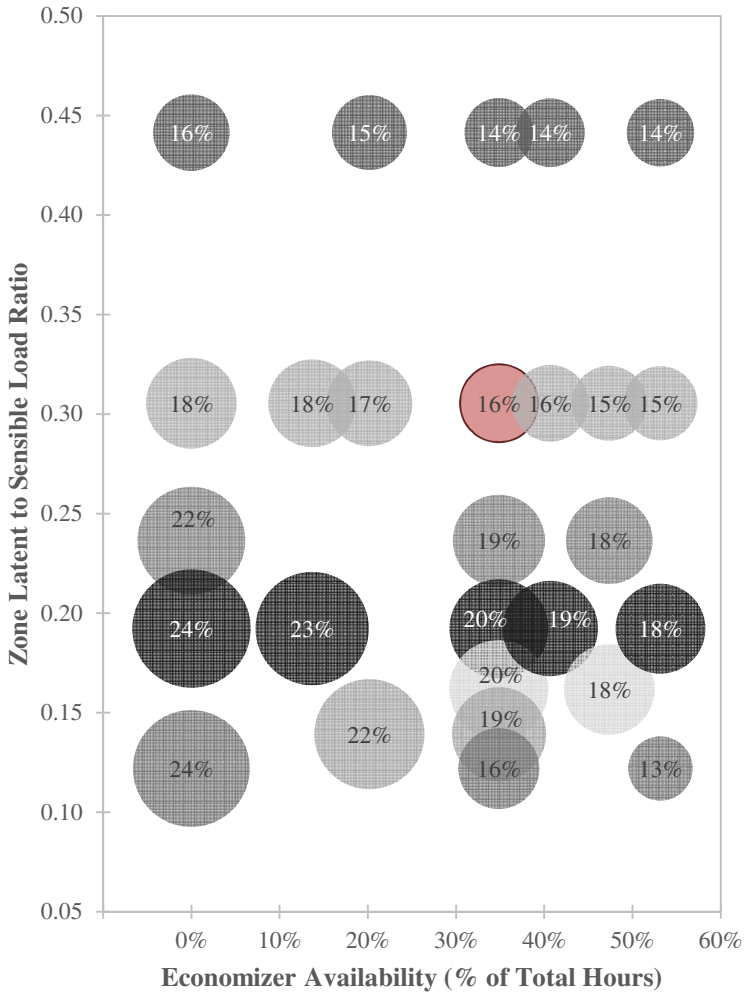

Figure 6.9: HVAC Energy Savings Potential for Passive Chilled Beam Systems over Equivalent VAV system at Varying Loads and Economizer Conditions

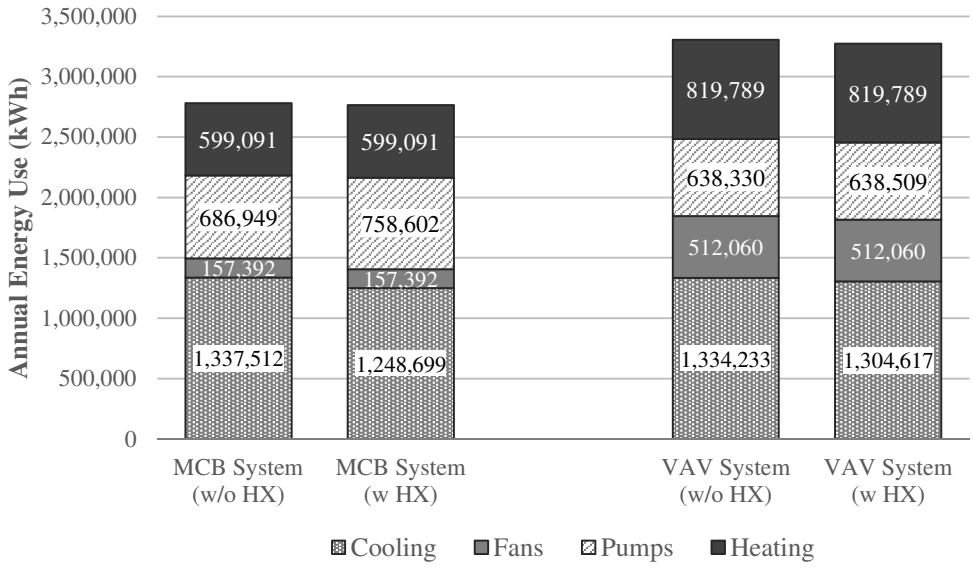

Figure 6.10: HVAC Energy Use for the MCB and VAV System with and without a Water-side Heat Exchanger

In terms of zone level thermal comfort, due to the lower volume of dehumidified supply air delivered to the zones and the added humidity from the bypass air, humidity control is poorer with a chilled beam/ventilation system than a standard VAV system. If strict humidity control is required, ventilation air volume will have to be increased, negating any energy savings achievable from the chilled beams. Figure 6.12 show the humidity levels in a typical zone for the two HVAC systems under review.

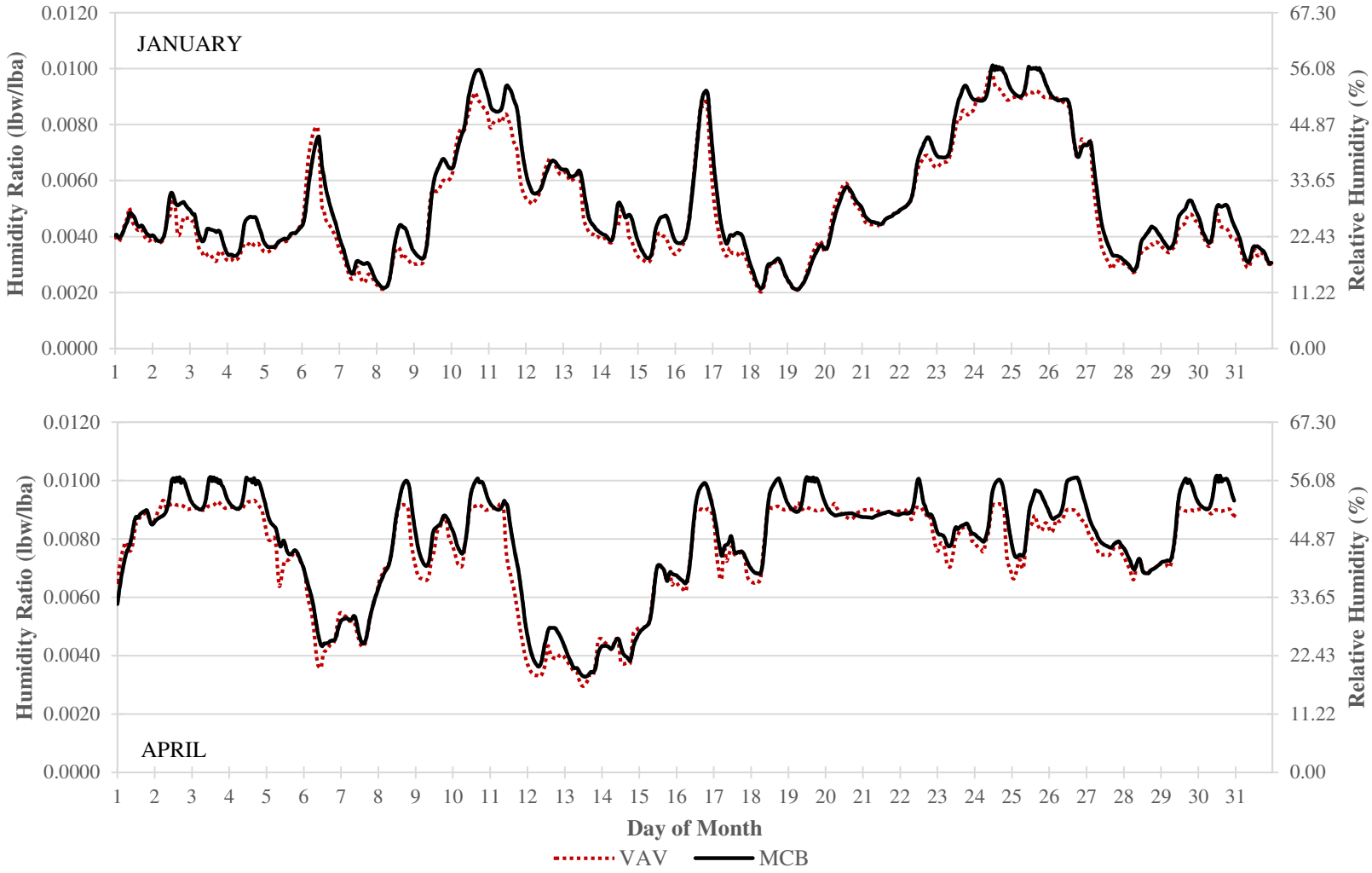

Figure 6.11: Comparative Humidity Levels in Wing 'A' Floor 2 for the VAV System (VAV) and the Modified Chilled Beam System (MCB) for the Months of January and April

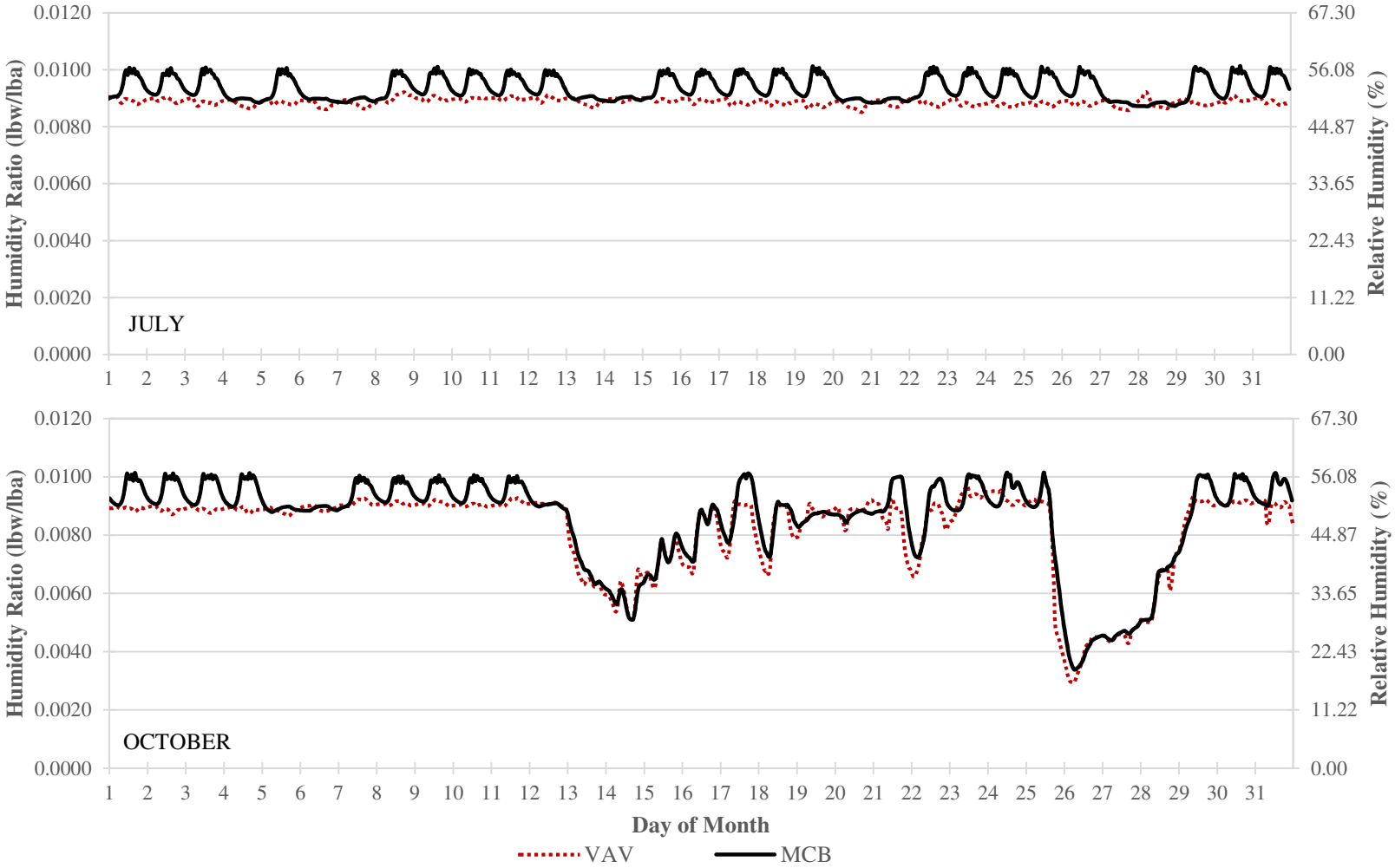

Figure 6.12: Comparative Humidity Levels in Wing 'A' Floor 2 for the VAV System (VAV) and the Modified Chilled Beam System (MCB) for the Months of July and October

6.2. Summary and Observations

In this chapter, the energy use of the building was evaluated and compared with a VAV system and an ASHRAE 90.1 (2004) code compliant building. The following observations can be drawn from the results:

- The building as operated uses 10% more energy than a comparable VAV system and 5% more energy than the minimum ASHRAE 90.1 (2004) requirements it was designed for. This is due to the improper sizing and control of the airside system in the building. The airside system in a building with chilled beams should be sized and controlled for peak ventilation and latent loads only.
- On an average, the UFAD ventilation system associated with a passive chilled beam system is approximately 50% smaller than an equivalent VAV system and almost 70% smaller than a UFAD ventilation only system.
- If properly controlled, a chilled beam system with parallel ventilation has potential for HVAC savings of 14-24% in office buildings in climate zone 3A. If latent loads and ventilation requirements are high in a building, energy savings will be lower.
- All of the energy savings by end-use are from fan and reheat energy. No cooling (chiller and plant) savings are obtained from the chilled beam system because:
    - The smaller airside system is unable to take advantage of free cooling possible through the use of an economizer. In locations when an economizer can be used for 60% or more of the time, energy savings don't exceed 15%, even in buildings with very high sensible loads. This suggests that chilled beams may not be

economically feasible in locations where an economizer can be potentially used for a large portion of the year.

  - In the UFAD operation associated with passive chilled beams, cooling energy is wasted when the cooled dehumidified supply air is reheated by the bypass air to increase supply air temperature. In addition, at the low supply air volumes, increase in temperature in the supply plenum can be substantial, i.e. the actual supply air temperatures delivered to the zones can be 8-9°F higher than the air exiting the AHUs. Due to these reasons, the ventilation system provides very little, if any sensible cooling.

- Because the ventilation system in a passive chilled beam/UFAD system provides very little sensible cooling (7-10%), it is recommended that the chilled beams be sized for maximum design day sensible cooling loads and variable speed pumping be used to regulate chilled beam capacity.
- Indoor humidity levels may be higher (approximately 60% RH) with a passive chilled beam/ventilation system than a standard VAV system (approximately 50-55% RH). This is due to the lower volume of dehumidified supply air delivered to the zones and the added humidity from the bypass air. This suggests that either a passive chilled beam system may not be appropriate in buildings with strict humidity control requirements or alternate methods of dehumidification (other than cooling and reheat) may have to be used for energy efficiency.

CHAPTER VII

BUILDING CONTROL OPTIMIZATION AND ENERGY USE

In this chapter, the results of the methods used to optimize building control and the effects on HVAC energy use and thermal comfort are presented. In Section 7.1, the results of the sensitivity analysis of operational control parameters conducted for the MCB and the VAV system are documented. Section 7.2 contains the results of the simplified rule-based optimization strategies developed for the MCB system. In Section 7.3, the results of the simulation assisted overall optimization strategy developed for the MCB system are presented. Finally, Section 7.4 summarizes the observations from the building control optimization process.

7.1. Sensitivity Analysis of Operational Control Parameters

A sensitivity analysis was conducted for the operational control used in both the MCB and the VAV model. Section 3.3 contains the details of the sensitivity analysis process. The operational parameters for the MCB model were volume of outside air (OAv), zone temperature (Tz), cooling coil leaving air temperature (Tcc), supply air temperature (Tsa) and chilled water supply temperature (Tchw). The operational parameters for the VAV model were volume of outside air (OAv), zone temperature (Tz), supply air temperature (Tsa), economizer control (Econ) and chilled water supply temperature (Tchw). Figure 7.1 and Figure 7.2 show the mean and standard deviation of the elementary effects of the operational control parameters calculated for the MCB and VAV system respectively.

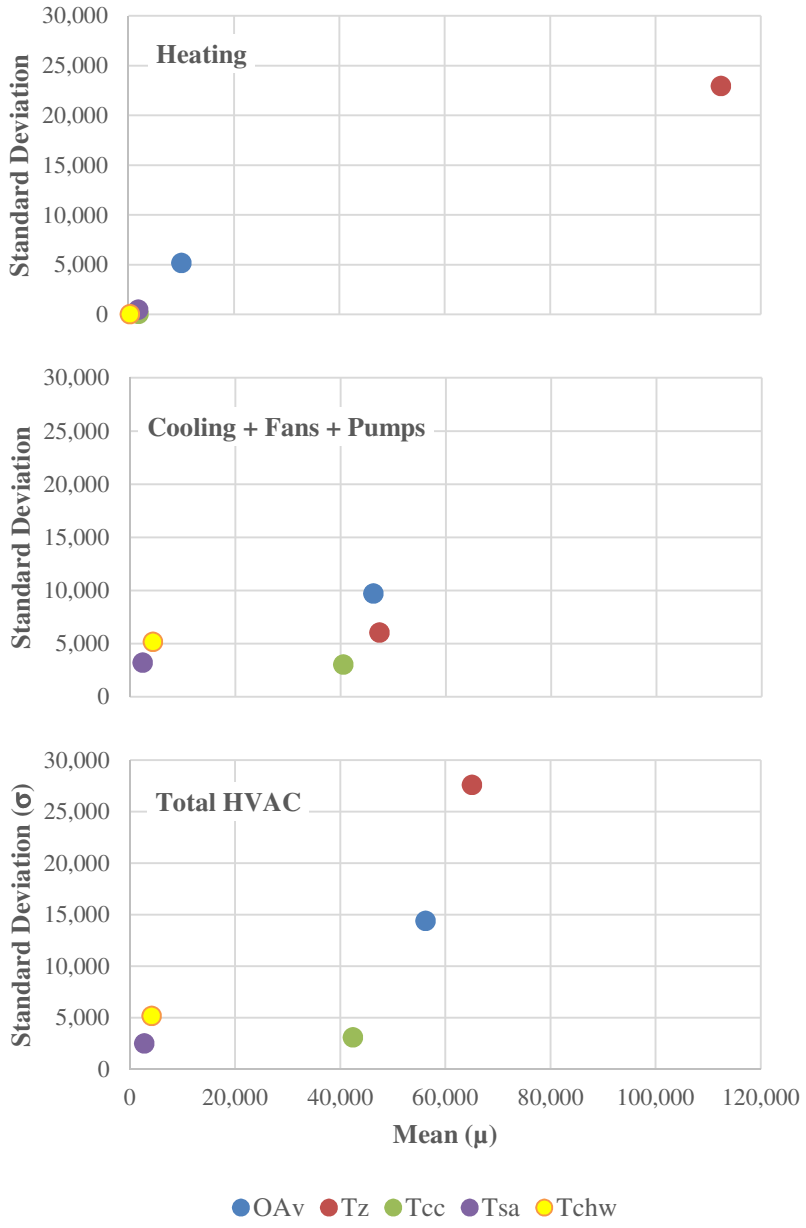

Figure 7.1: Mean and Standard Deviation of the Elementary Effects of the Operational Control Parameters calculated separately for Heating, Cooling and Total HVAC Energy Use for the MCB System

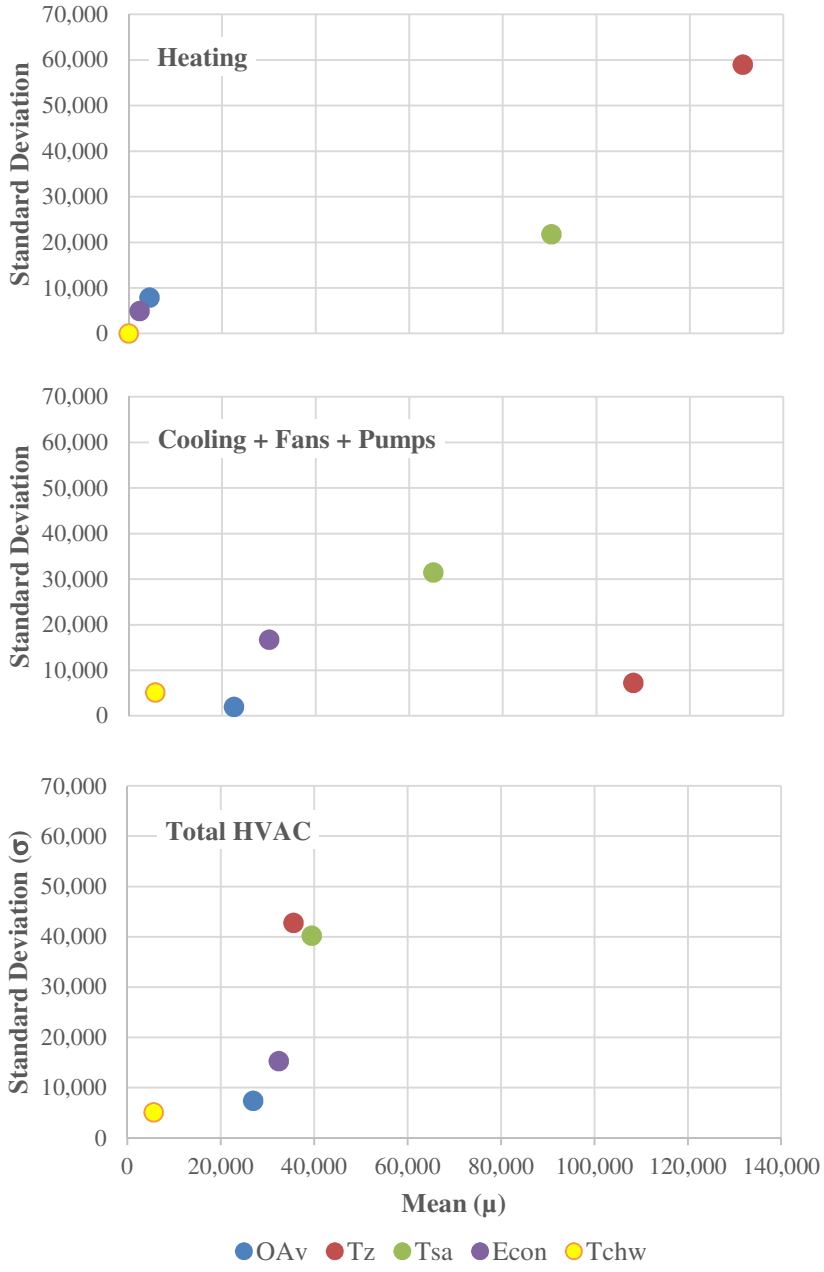

Figure 7.2: Mean and Standard Deviation of the Elementary Effects of the Operational Control Parameters calculated separately for Heating, Cooling and Total HVAC Energy Use for the VAV System

A high value of the mean implies that the input parameter has an important overall influence on the output. A high value of the standard deviation indicates that the input parameter is involved in interaction with another input or the effect of the parameter on the output is nonlinear. Figure 7.1 shows that the zone temperature by far is the most sensitive where heating energy is concerned, with the volume of outside air brought into the building a very distant second. The other parameters, such as the coil leaving temperature, supply air temperature and chilled water temperature have no influence on the heating energy use. This confirms that with an MCB system, reheat energy is almost entirely eliminated. On the other hand, Figure 7.2 shows that the cooling coil leaving temperature that directly influences reheat energy ranks second in its impact on the total heating energy in a VAV system.

In terms of cooling energy use, the three parameters that are most sensitive in the MCB system are zone temperature, outside air volume and coil leaving temperature in that order. This is true because not only the zone temperature determines the total load on the system, but also influences the efficiency of the chilled beams. The greater the temperature difference between the chilled beam water temperature and the zone temperature, the greater the heat exchange between the chilled beam and the zone. Another observation is that the quantity of outside air has a greater influence on the cooling energy use than the cooling coil leaving temperature and must be controlled more stringently. The supply air temperature and chilled water temperature do not greatly influence cooling energy use. On the VAV system side, the parameters that are most sensitive for cooling energy use are

zone temperature, supply air temperature, economizer operation, volume of outside air and chilled water temperature in that order.

For the total HVAC energy use, the ranking of the control parameters for the MCB system are; zone temperature, volume of outside air, cooling coil leaving temperature, chilled water temperature and supply air temperature. Since the zone temperature setpoint is dependent on the occupants in the space and the supply air temperature has very little impact on the total HVAC energy use, the optimization process will concentrate on the volume of outside air, cooling coil leaving temperature and chilled water temperature. The ranking of the control parameters for the VAV system are; supply air temperature, zone temperature, economizer operation, volume of outside air and chilled water temperature.

Figure 7.3 shows the actual change in total HVAC energy use for each run of the sensitivity analysis. It shows how differently a VAV and a chilled beam system respond to identical changes in control. For example, the changes in the energy use due to the changes in the coil leaving temperature are linear in the MCB system and logarithmic in the VAV system. This is because of the impact of reheat energy on total energy use in the VAV system. The changes in energy use in response to the changes in zone temperature are also different for the two systems because of the influence the ambient zone temperature has on the chilled beam heat transfer efficiency.

It is important to note that the results of the sensitivity analysis are for this HVAC system configuration. The outlined process can be repeated for other configurations and will give different results. Therefore, it is important to conduct a sensitivity analysis before developing a control strategy for implementation in the building.

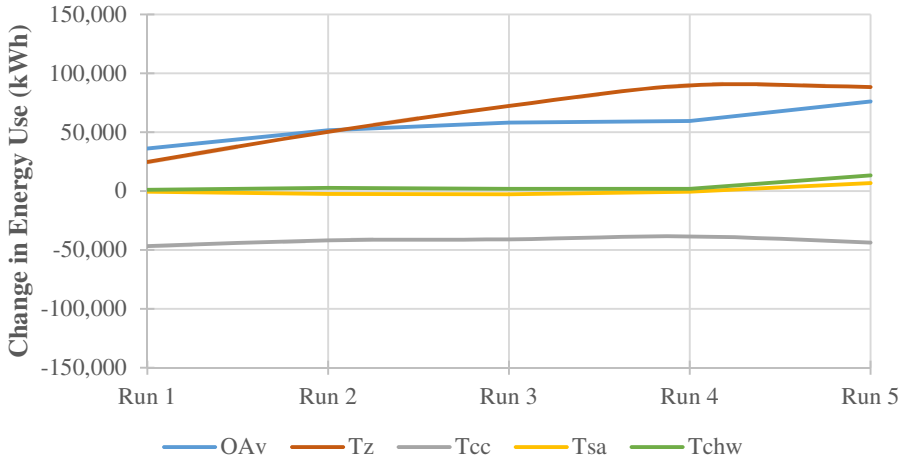

(a)

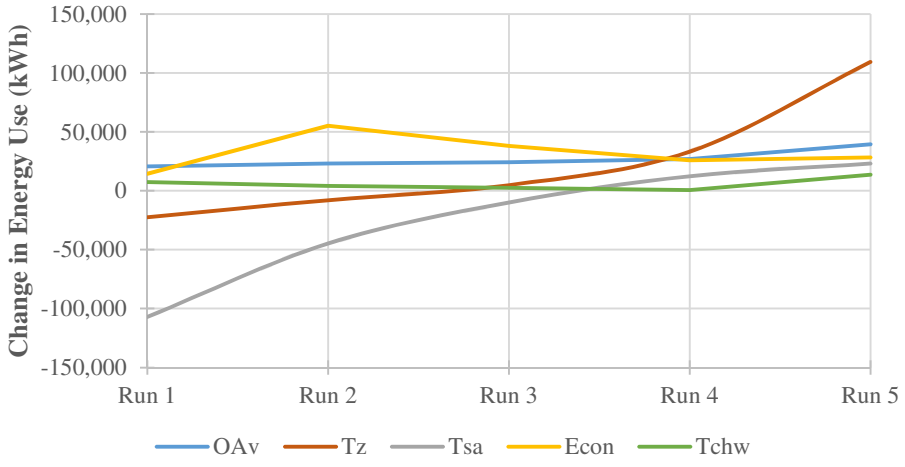

(b)

Figure 7.3: Change in Total HVAC Energy Use for Each Run of the Sensitivity Analysis for (a) the MCB System Model (b) the VAV System Model

7.2. Simplified Rule-Based Optimization

As discussed in Section 3.3, the assumption for the simplified rule-based optimization is that is that the airside system is always less efficient than the chilled beam system and is controlled only to fulfill minimum ventilation or latent load requirements,

whichever is lesser. Four possible scenarios were modeled; a constant-volume DOAS with fixed cooling coil leaving air temperature (MCB-CV-CCLT), a constant-volume DOAS with varying cooling coil leaving air temperature (MCB-CV-VCLT), a variable-volume DOAS with fixed cooling coil leaving air temperature (MCB-VAV-CCLT) and a variable-volume DOAS with varying coil leaving air temperature (MCB-VAV-VCLT). Humidity control is most important in all the configurations. Humidity control can achieved by increasing outside air volumes or reducing the cooling coil leaving air temperature. However, the sensitivity analysis for the building reveals that reducing the cooling coil leaving air temperature is less energy intensive than increasing outside air volumes. As a result, for the optimization process, the outside air volumes were sized only for ventilation control and humidity control was achieved by reducing the cooling coil leaving air temperatures.

For the constant-volume airside system with fixed cooling coil leaving air temperature (MCB-CV-CCLT), the DOAS was sized to meet ASHRAE 62.1 ventilation requirements (ASHRAE 2010b). This equaled outside air volumes of 12,540cfm for AHU4A1, 21,175cfm for AHU5B1 and 13,560cfm for AHU 5C1. The cooling coil leaving air temperature was maintained at a constant 51.5°F. The zone supply air temperature was maintained at a constant 58°F. The chilled water supply temperature was maintained at a constant 44°F. The chilled beam water temperature was maintained at 3°F above maximum zone dewpoint and subject to a minimum of 58°F. This type of system and control does not require CO_2 or relative humidity monitoring in the zones though zone dewpoint will have to be monitored for the chilled beam control. In addition, because the

DOAS is a constant-volume system, there are advantages such as an open/close two-position outside air damper, constant-volume UFAD diffusers and lower possibilities of mechanical failure. The EMCS control is also easier to implement and operate. Figure 7.4 shows the airside control sequence for the constant-volume fixed cooling coil leaving air temperature configuration as implementable in a real building. Appendix E provides the description of the DDC modules (blocks) used in the control sequence diagrams.

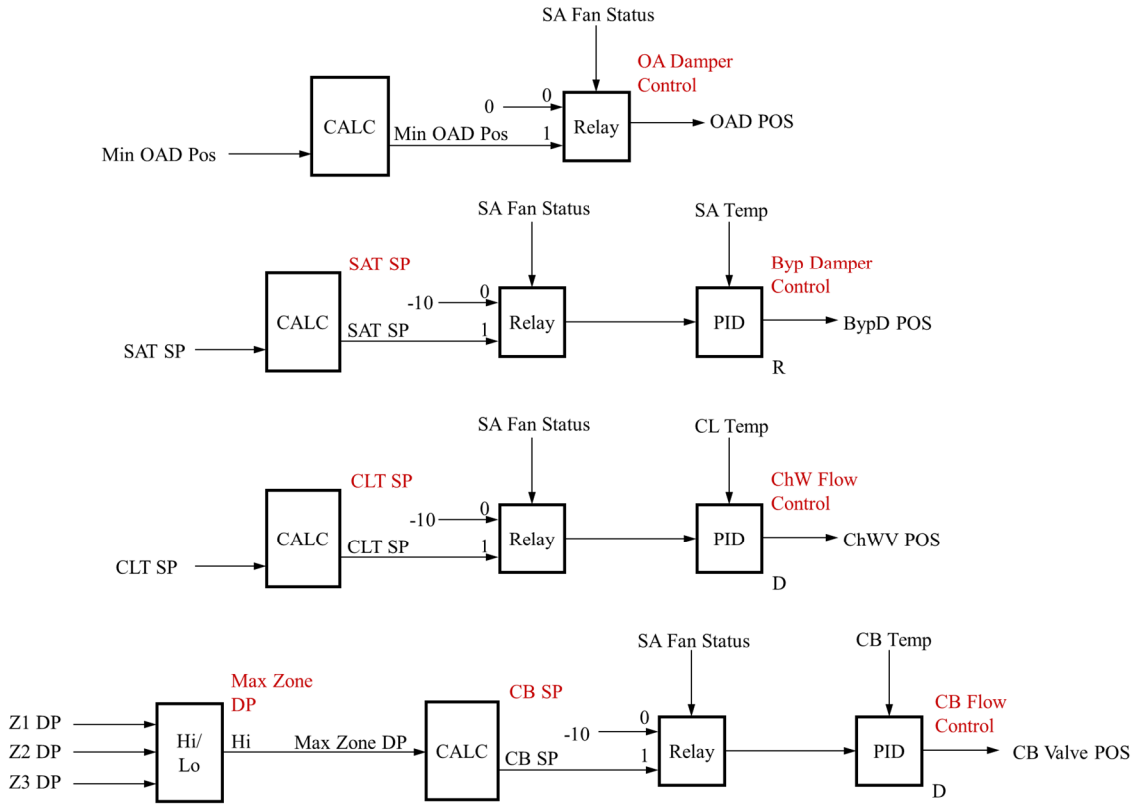

Figure 7.4: Control Diagram for the Constant-Volume Fixed Cooling Coil Leaving Air Temperature Configuration with Chilled Beams (MCB-CV-CCLT)

For the constant-volume airside system with varying cooling coil leaving air temperature (MCB-CV-VCLT), the DOAS was sized to meet ASHRAE 55 comfort requirements (ASHRAE 2010b). The building control was divided into two modes, 'no humidity control' mode and 'dehumidify' mode. If the return air zone humidity ratio was below the humidity ratio setpoint (0.01lbw/lba), no humidity control is required and the cooling coil leaving air temperature was maintained at a constant 70°F and the zone supply air temperature and volume was kept equal to the cooling coil leaving air temperature. In this mode, the chilled water supply temperature was maintained at a constant 48°F.

If the return air zone humidity ratio was above the humidity ratio setpoint (0.01lbw/lba), the 'dehumidify' mode was activated and the cooling coil leaving temperature was adjusted dynamically to meet the zone humidity setpoint. This was modeled in EnergyPlus by using the ZoneControl:Humidistat Object and the 'TemperatureandHumidityRatio' Control Variable in the Controller:WaterCoil Object. In the 'dehumidify' mode, the chilled water supply temperature was maintained at a constant 44°F. Appendix C.7 documents the EMS program for the chilled water temperature setpoint. The chilled beam water temperature in both modes was maintained at 3°F above maximum zone dewpoint and subject to a minimum of 58°F.

This type of system and control does not require CO_2 monitoring in the zones though zone humidity and dewpoint will have to be monitored for the chilled beam and supply air temperature control. The other advantages, such as an open/close two-position outside air damper and constant-volume UFAD diffusers resulting in lower possibilities of mechanical failure still apply to this configuration. Figure 7.5 shows the airside control

sequence for the constant-volume varying coil leaving air temperature configuration as implemented in a real building.

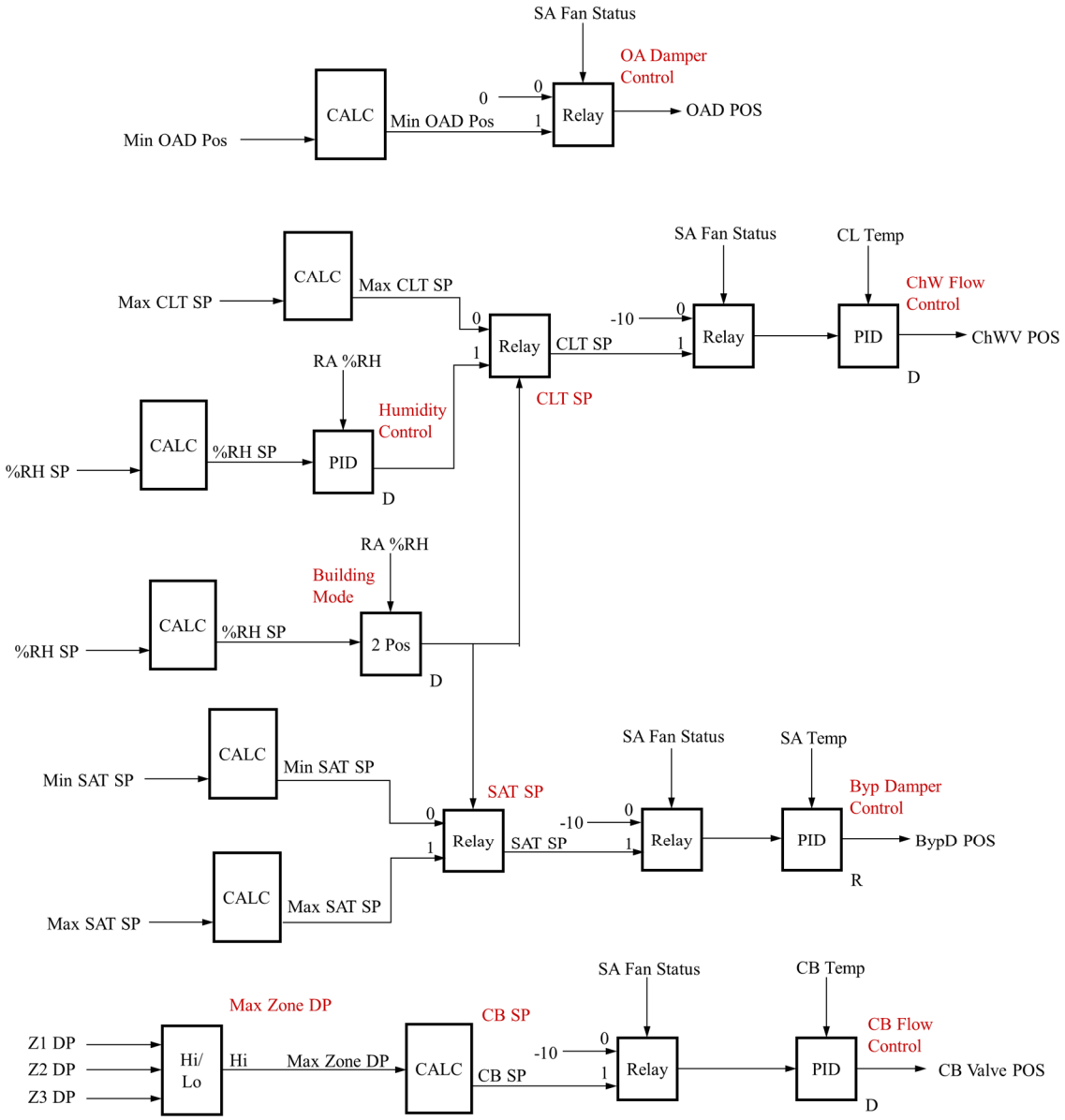

Figure 7.5: Control Diagram for the Constant-Volume Varying Cooling Coil Leaving Air Temperature Configuration with Chilled Beams (MCB-CV-VCLT)

For the variable-volume airside system with fixed cooling coil leaving air temperature (MCB-VAV-CCLT), the DOAS was a variable-volume system and sized only for ventilation requirements with demand control ventilation based on zone CO_2 levels. As compared to the MCB-CV-CCLT system, the total volume of outside air is lower and so to achieve humidity control, the cooling coil leaving air temperature was maintained at a lower setpoint of 50.5°F. The zone supply air temperature was maintained at a constant 58°F. The chilled water supply temperature was maintained at a constant 44°F. The chilled beam water temperature was maintained at 3°F above maximum zone dewpoint and subject to a minimum of 58°F. Figure 7.6 shows the control sequence for the variable-volume fixed coil leaving air temperature configuration as implementable in a real building.

The variable-volume airside system with variable cooling coil leaving air temperature (MCB-VAV-VCLT) is a combination of the MCB-VAV-CCLT and the MCB-CV-VCLT systems. The DOAS was again sized only for ventilation requirements with demand control ventilation based on zone CO_2 levels. The building control was also similarly divided into two modes, 'no humidity control' mode and 'dehumidify' mode. In the 'no humidity control' mode the cooling coil leaving air temperature was maintained at a constant 70°F and the zone supply air temperature and volume was kept equal to the cooling coil leaving air temperature. In this mode, the chilled water supply temperature was maintained at a constant 48°F. In the 'dehumidify' mode, the cooling coil leaving temperature was adjusted to meet the zone humidity setpoint. In this mode, the chilled water supply temperature was also maintained at a constant 44°F. The chilled beam water

temperature in both modes was maintained at 3°F above maximum zone dewpoint and subject to a minimum of 58°F. Figure 7.7 shows the airside control sequence for the variable-volume varying coil leaving air temperature configuration as implemented in a real building.

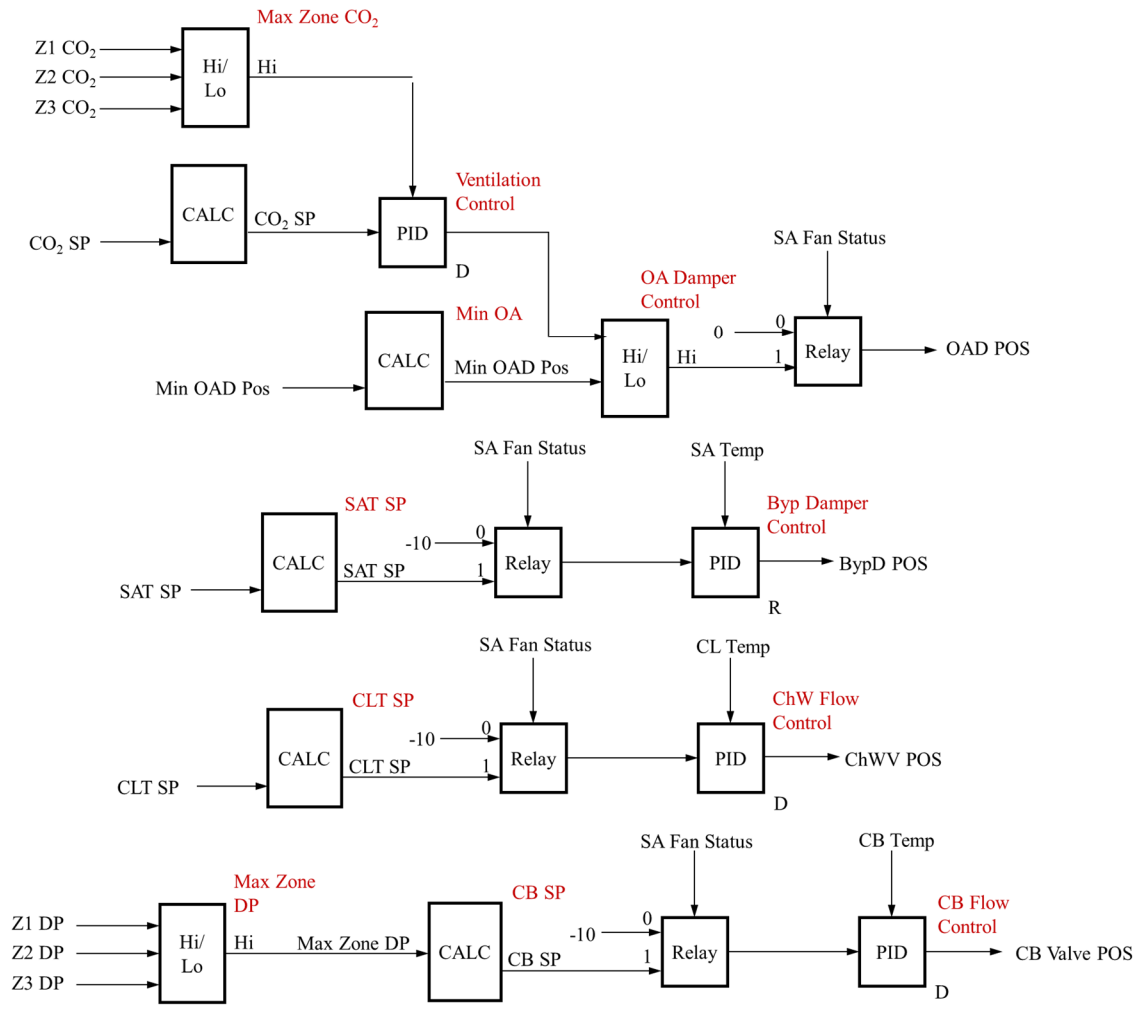

Figure 7.6: Control Diagram for the Variable-Volume Fixed Cooling Coil Leaving Air Temperature Configuration with Chilled Beams (MCB-VAV-CCLT)

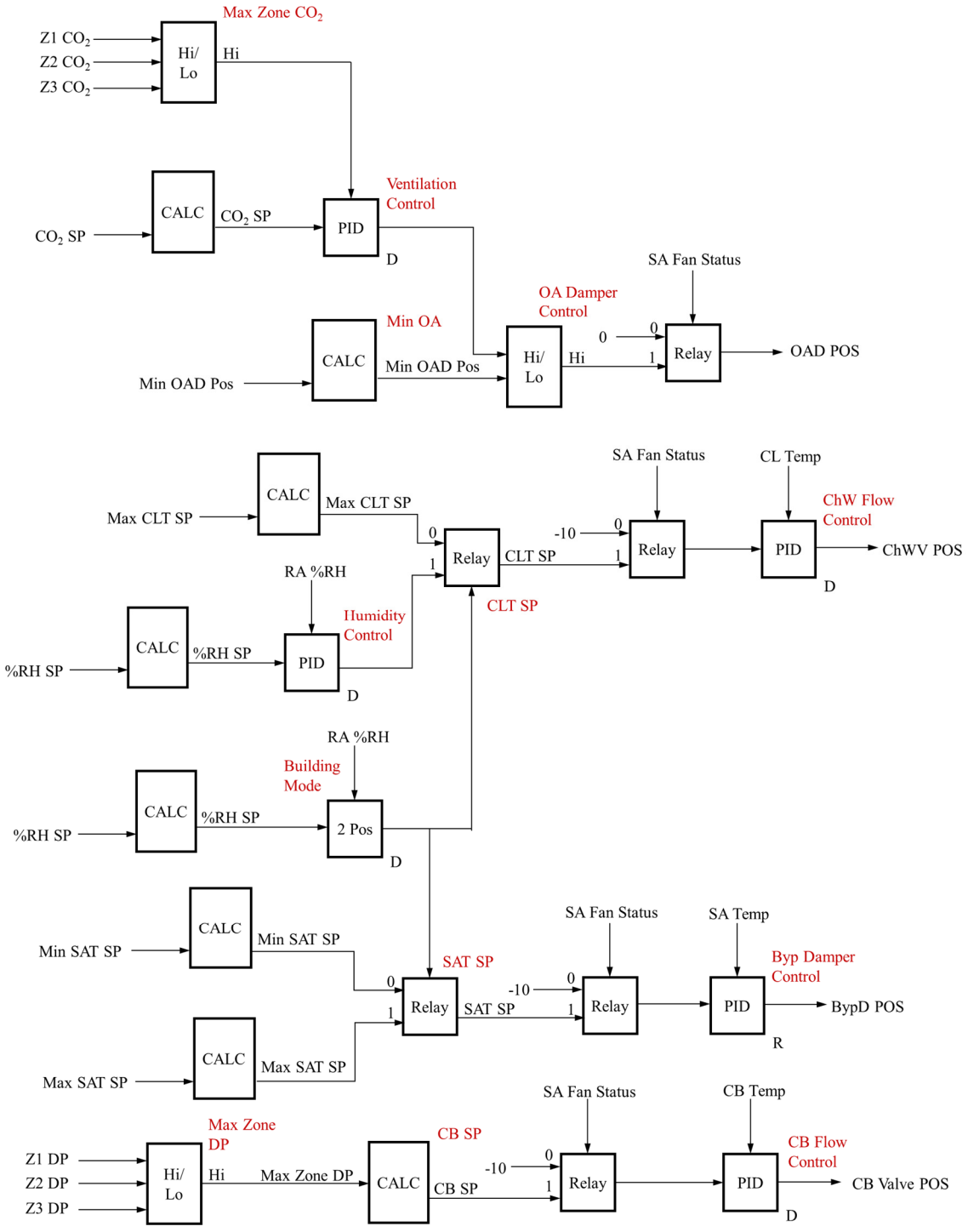

Figure 7.7: Control Diagram for the Variable-Volume Varying Cooling Coil Leaving Air Temperature Configuration with Chilled Beams (MCB-VAV-VCLT)

Figure 7.8 shows the annual HVAC energy use for the control options discussed above. As anticipated, the configurations with the fixed cooling coil leaving temperatures are the most energy intensive. The configuration with the variable-volume system and varying coil leaving temperature is the only option that shows any significant HVAC energy reduction (8%) over the initial MCB control discussed in Section 4.4. The configuration with the constant-volume ventilation system and fixed coil leaving temperature uses 6% more energy than the initial MCB control, while the other two configurations (MCB-CV-VCLT and MCB-VAV-CCLT) are almost identical in energy use to the initial MCB control configuration. Figure 7.9 and Figure 7.10 show the humidity control in a typical office zone for the four control configurations for the months of January, April, July and October. They reveal that the configurations with the fixed coil leaving temperatures are better at humidity control, but this understandably comes at an energy penalty. Thus it is important that all these factors, including ease of operation and maintenance be taken into consideration while determining the preferred control for the passive chilled beam system with UFAD ventilation.

The four MCB configurations were also compared with the VAV system that was also optimized for more efficient operation. The supply air temperature in the VAV system was reset between 55°F and 60°F at the outside air temperatures of 70°F and 30°F respectively. Similarly, the chilled water supply temperature was reset between 44°F and 48°F at the outside air temperatures of 70°F and 30°F respectively. Similar to the MCB systems, two scenarios were analyzed for the VAV system; outside air supplied to meet ASHRAE 62.1 ventilation requirements, and outside air supplied to meet zone CO_2

setpoint of 900ppm (demand control ventilation). Figure 7.11 shows the comparative annual HVAC energy use and Savings between the four MCB control options and the equivalent VAV system for the ASHRAE 62.1 (2010) ventilation requirements and the demand control ventilation requirements. It shows that a varying coil leaving temperature approach is essential to achieve the range of energy savings predicted for chilled beams (14-15%). In general, a strict control of the supply air volume and the supply air temperature is critical if any energy savings are to be achieved with chilled beam systems.

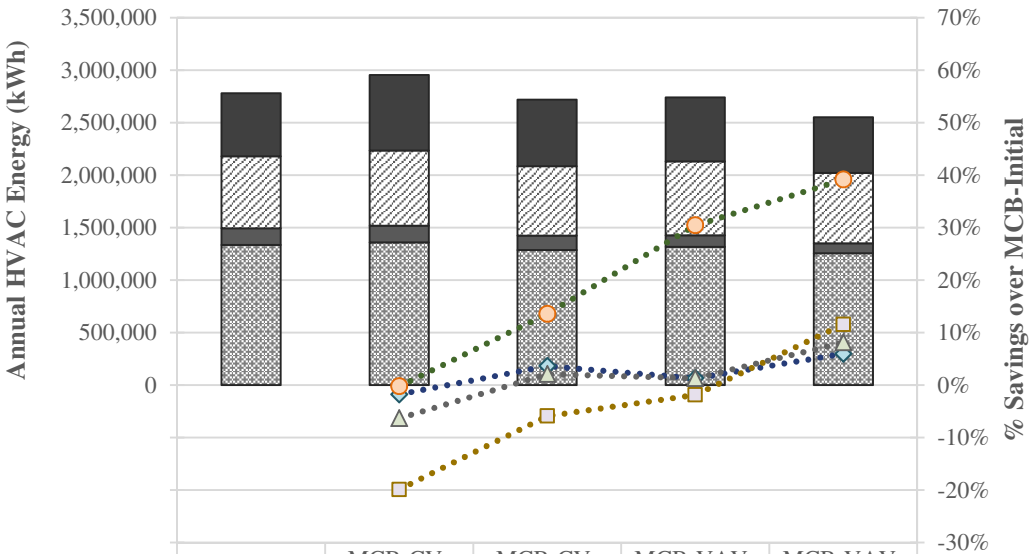

	MCB-Initial	MCB-CV-CCLT	MCB-CV-VCLT	MCB-VAV-CCLT	MCB-VAV-VCLT
Heating	599,091	717,897	634,089	609,929	529,522
Pumps	686,949	719,072	662,632	704,197	671,179
Fans	157,392	157,676	135,974	109,412	95,690
Cooling	1,337,512	1,360,689	1,288,449	1,319,417	1,256,834
Cooling Savings		-2%	4%	1%	6%
Fan Savings		0%	14%	30%	39%
Heating Savings		-20%	-6%	-2%	12%
Total Savings		-6%	2%	1%	8%

Figure 7.8: Comparative Annual HVAC Energy Use and Savings for the Four MCB Control Options

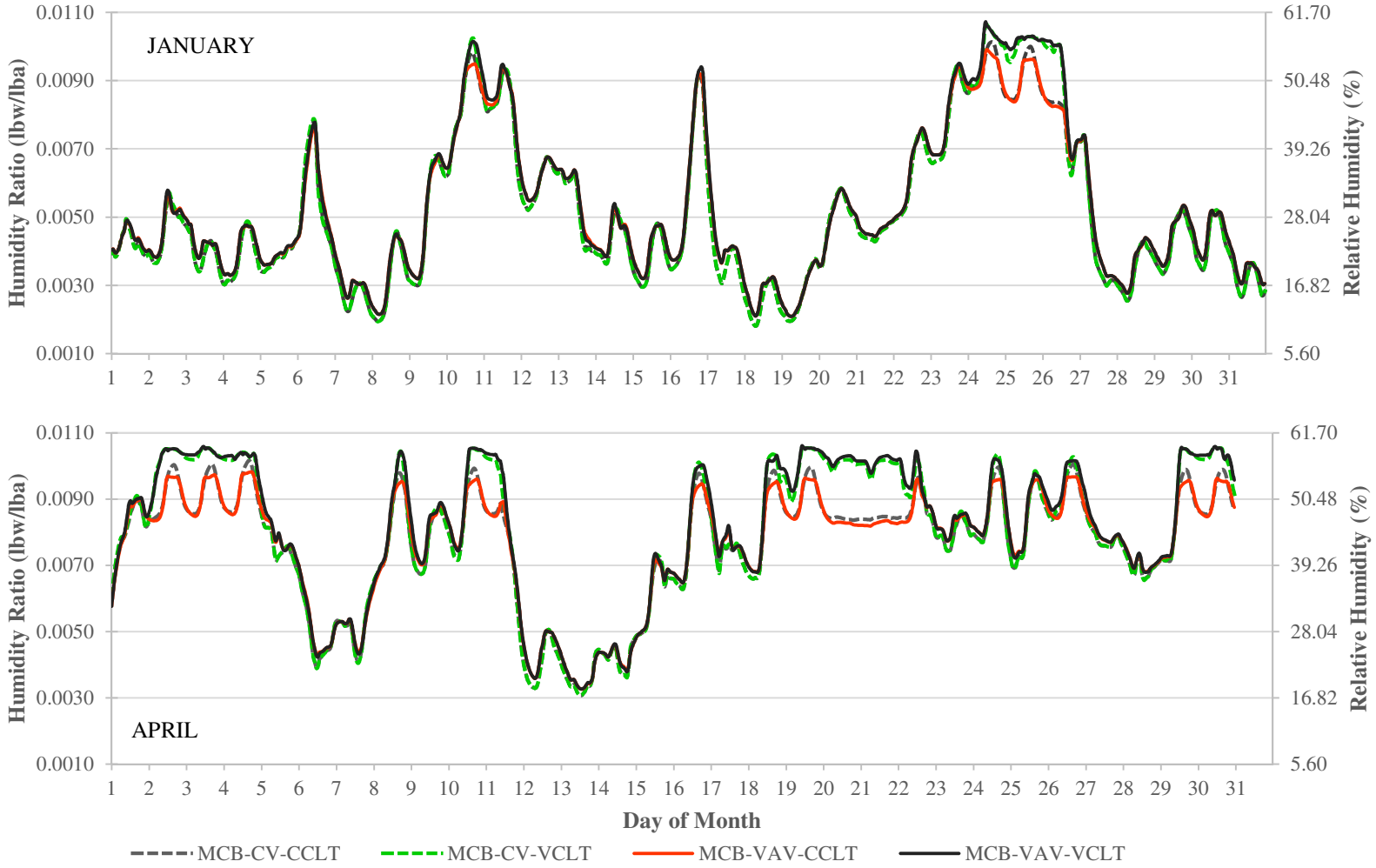

Figure 7.9: Humidity Levels in Wing 'A' Floor 2 for the Months of January and April for the Four MCB Control Options

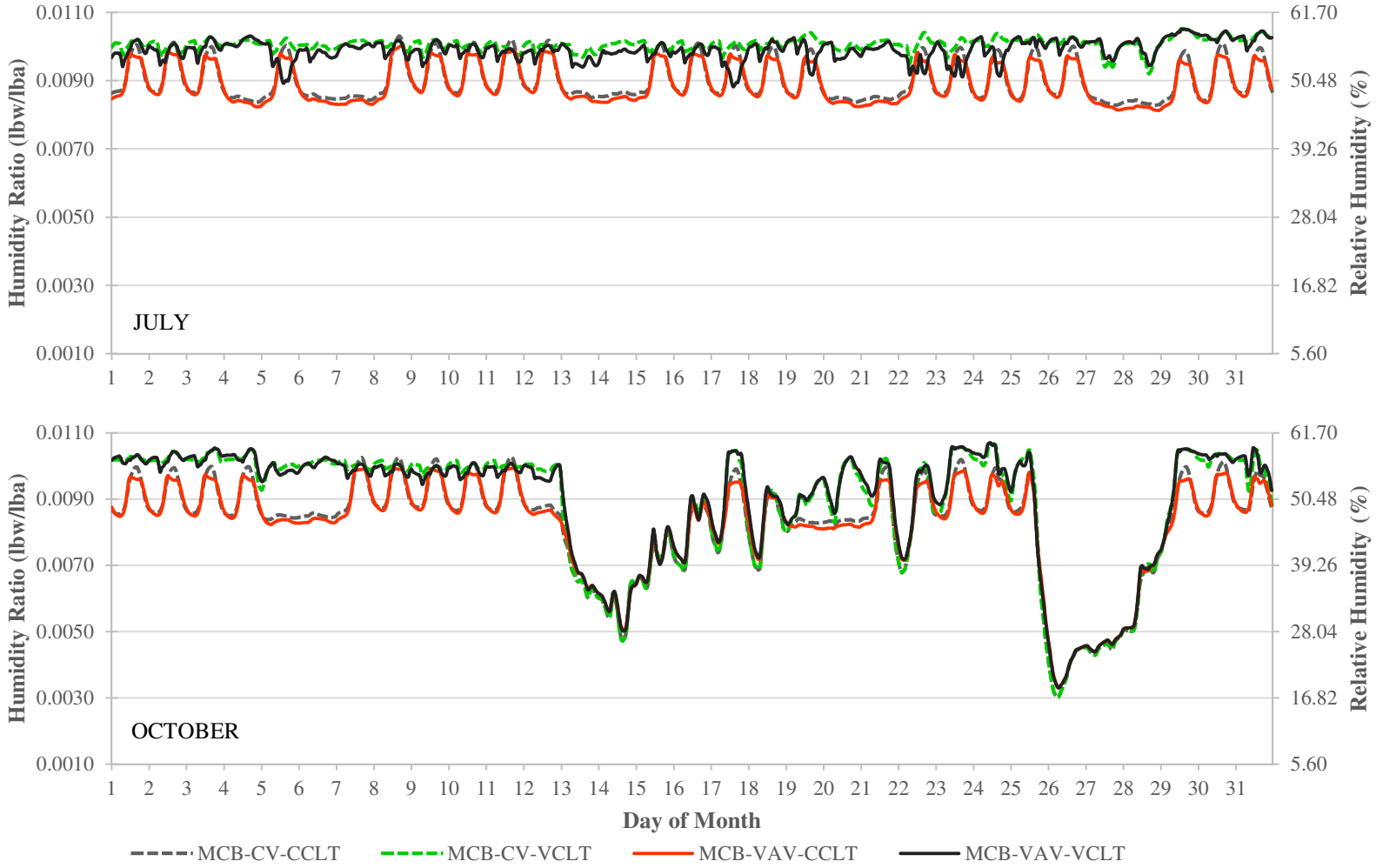

Figure 7.10: Humidity Levels in Wing 'A' Floor 2 for the Months of July and October for the Four MCB Control Options

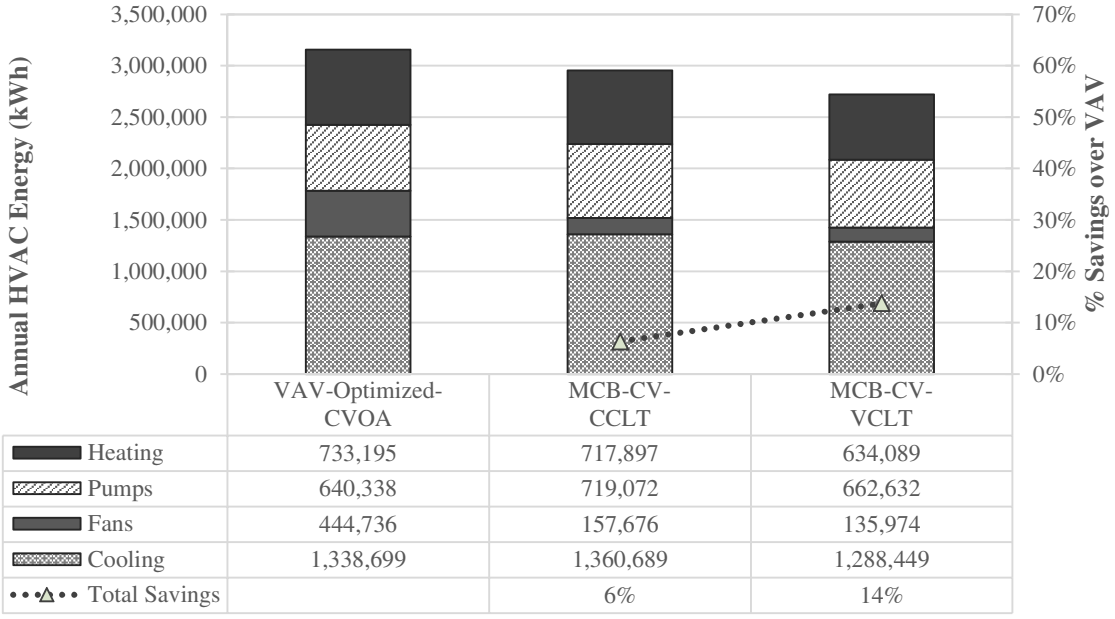

	VAV-Optimized-CVOA	MCB-CV-CCLT	MCB-CV-VCLT
Heating	733,195	717,897	634,089
Pumps	640,338	719,072	662,632
Fans	444,736	157,676	135,974
Cooling	1,338,699	1,360,689	1,288,449
Total Savings		6%	14%

(a)

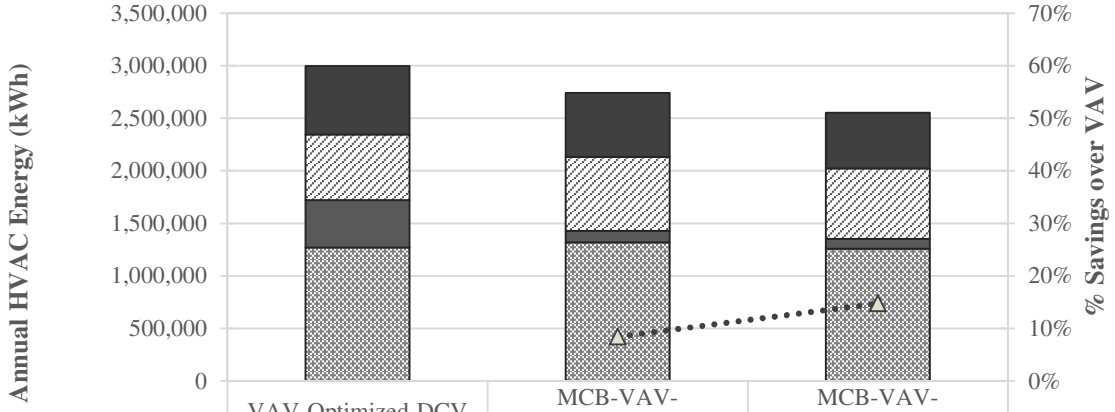

	VAV-Optimized-DCV	MCB-VAV-CCLT	MCB-VAV-VCLT
Heating	650,622	609,929	529,522
Pumps	624,830	704,197	671,179
Fans	449,492	109,412	95,690
Cooling	1,271,689	1,319,417	1,256,834
Total Savings		8%	15%

(b)

Figure 7.11: Comparative Annual HVAC Energy Use and Savings between the Four MCB Control Options and the Equivalent VAV System for the (a) ASHRAE 62.1 (2010) Ventilation Requirements (b) Demand Control Ventilation Requirements

7.3. Model Predictive Control Optimization

The model predictive control differs from the simplified rule-based optimization in that it evaluates the building loads and outside conditions and devises a comprehensive strategy for all the control points under review simultaneously. This means that if the ventilation system is more energy efficient than the chilled beam system, the optimization process will be able to predict this and the operation can be modified to take advantage of it. Similarly, the predictive control can predict if it is less energy intensive to increase the supply air volumes than reducing the cooling coil leaving temperatures. This approach makes sense in a system like the chilled beam system which is non-typical and one in which rule-based solutions are not readily available or tested.

An ideal model predictive control would be linked to the building energy management system and run a live simulation at each timestep to predict optimized control points. However, this approach is very computationally intensive and not entirely feasible to be implemented in real buildings. Therefore, a modified predictive control based on Coffey (2011) was tested for the building. It involved developing a control strategy for a matrix that would cover a range of possible conditions that one would encounter in an office building in a year. In this study, the matrix of inputs were the outside air temperature, humidity and the internal gains in the building. The control points that were optimized were the outside airflow rate, cooling coil leaving temperature and chilled water temperature. Section 3.3 documents the details of the model predictive control process. The cost function used for the optimization was the total HVAC energy use with a

substantial penalty added to the energy use if temperature and humidity setpoints were not met.

Figure 7.12 shows the optimization iterations in GenOpt® to predict cooling coil leaving temperatures, chilled water temperatures and outside air flow volume in order to minimize the HVAC energy use. It also shows the significant penalty that is added to the actual HVAC energy use when temperature and humidity setpoints in the zones are not met. The equations used for calculating the thermal comfort penalty will affect the setpoint predictions in the optimization process.

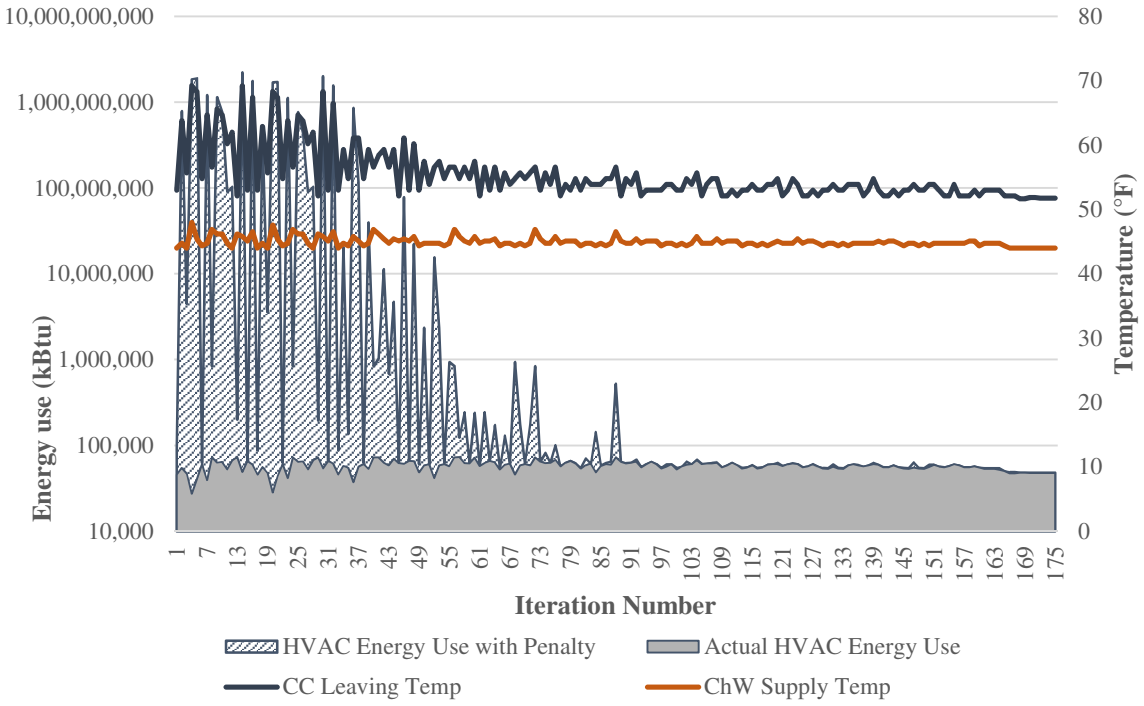

Figure 7.12: The Optimization Iterations in GenOpt® for a Warm-Humid Day at Maximum Internal Load Conditions

Table 7.1 shows the results of the GenOpt® optimization for the grid of operating conditions discussed in Section 3.3. These results align closely with the control strategies developed in Section 7.2. Cooling coil leaving air temperatures are lowest when outside air humidity levels are high and at off-peak office occupancy levels and internal gains due to the lower supply air volumes. This is true even with chilled water supply temperatures. The chilled water temperature setpoint that supplies both the AHU cooling coils and the chilled beams never exceeds 49°F even when the AHU cooling coils are off. This is because the same chilled water loop also supplies chilled water to the two VAV AHU cooling coils that require cooling. Therefore it might be beneficial to design the UFAD/chilled beam AHUs and the VAV AHUs with separate chilled water loops so that different chilled water setpoints can be allowed.

Outside air volumes predicted by GenOpt® are almost identical to the approach proposed in Section 7.2, with the exception of cool (40-60°F) and dry (<0.0065lbw/lba humidity) days when a larger quantity of outside air provides free cooling and lowers the HVAC energy use. However, this strategy doesn't work on cold days (<40°F) because it increases preheat energy use. Figure 7.13 and Figure 7.14 show the optimized cooling coil leaving air temperature and chilled water temperature setpoints for both the rule-based optimization and the model-based optimization for the months of January, April, July and October. They also show that the outside air humidity ratio is a good proxy for zone humidity levels. So if it is not desired to constantly monitor zone or return air humidity, an alternative control approach can be specified in which at outdoor air humidity ratios below 0.0085 lbw/lba, the coil leaving temperatures can be set to the maximum setpoint

(70°F in this case). At outdoor air humidity ratios above 0.015 lbw/lba, the coil leaving temperatures can be set to the minimum setpoint (48°F in this case). The coil leaving temperatures can then be linearly reset at outdoor air humidity ratios between 0.0085 and 0.015 lbw/lba.

Table 7.1: Results of the GenOpt® Optimization for the Grid of Operating Conditions in the Building

OA Temp	OA Humidity	Office Loads	Coil Leaving Temp	Volume of Outside Air			ChW Temp
				4A1	5B1	5C1	
°F	lbw/lba		°F	cfm			°F
< 40	-	Max	X	14,050	22740	15,170	48.0
		Mid	X	10,750	18,500	12,000	48.0
		Min	X	8,300	13,000	10,000	49.0
40 - 60	< 0.0065	Max	X	14,565	23,315	15,390	47.7
		Mid	X	10,750	18,500	12,000	47.8
		Min	X	8,300	13,000	10,000	47.8
60 - 80	< 0.0065	Max	61.2	14,050	22740	15,170	45.1
		Mid	70.0	10,750	18,500	12,000	45.9
		Min	70.0	8,300	13,000	10,000	48.0
	0.0065 - 0.0098	Max	51.7	14,050	22740	15,170	45.8
		Mid	50.8	10,750	18,500	12,000	44.0
		Min	52.7	8,300	13,000	10,000	46.4
> 80	0.0065 - 0.0098	Max	50.4	14,050	22740	15,170	44.0
		Mid	48.7	10,750	18,500	12,000	44.4
		Min	52.7	8,300	13,000	10,000	46.4
	> 0.0098	Max	50.2	14,050	22740	15,170	44.0
		Mid	48.7	10,750	18,500	12,000	44.0
		Min	52.7	8,300	13,000	10,000	46.4

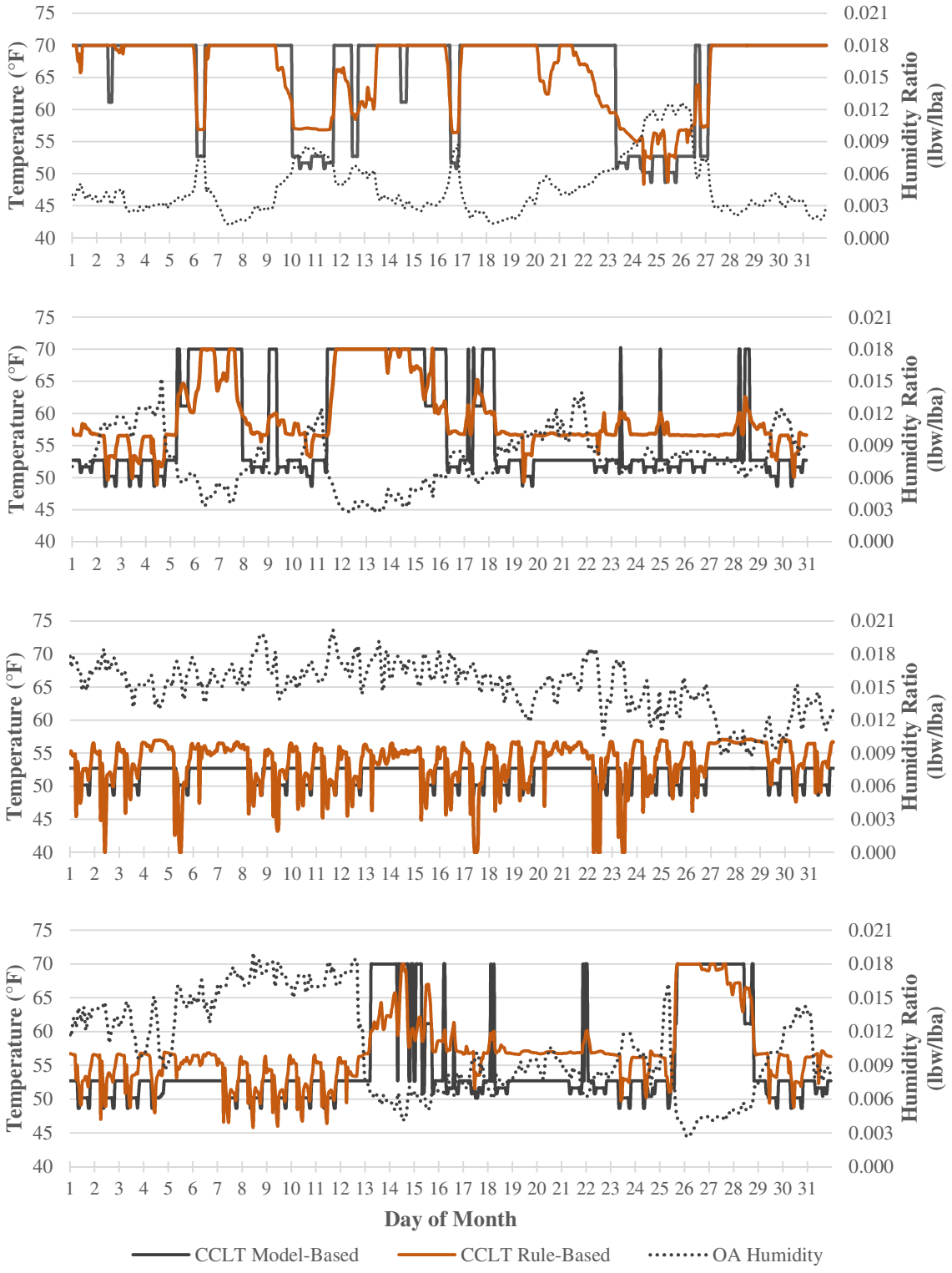

Figure 7.13: Optimized Cooling Coil Leaving Air Temperature Setpoints for the Rule-Based and Model-Based Optimization

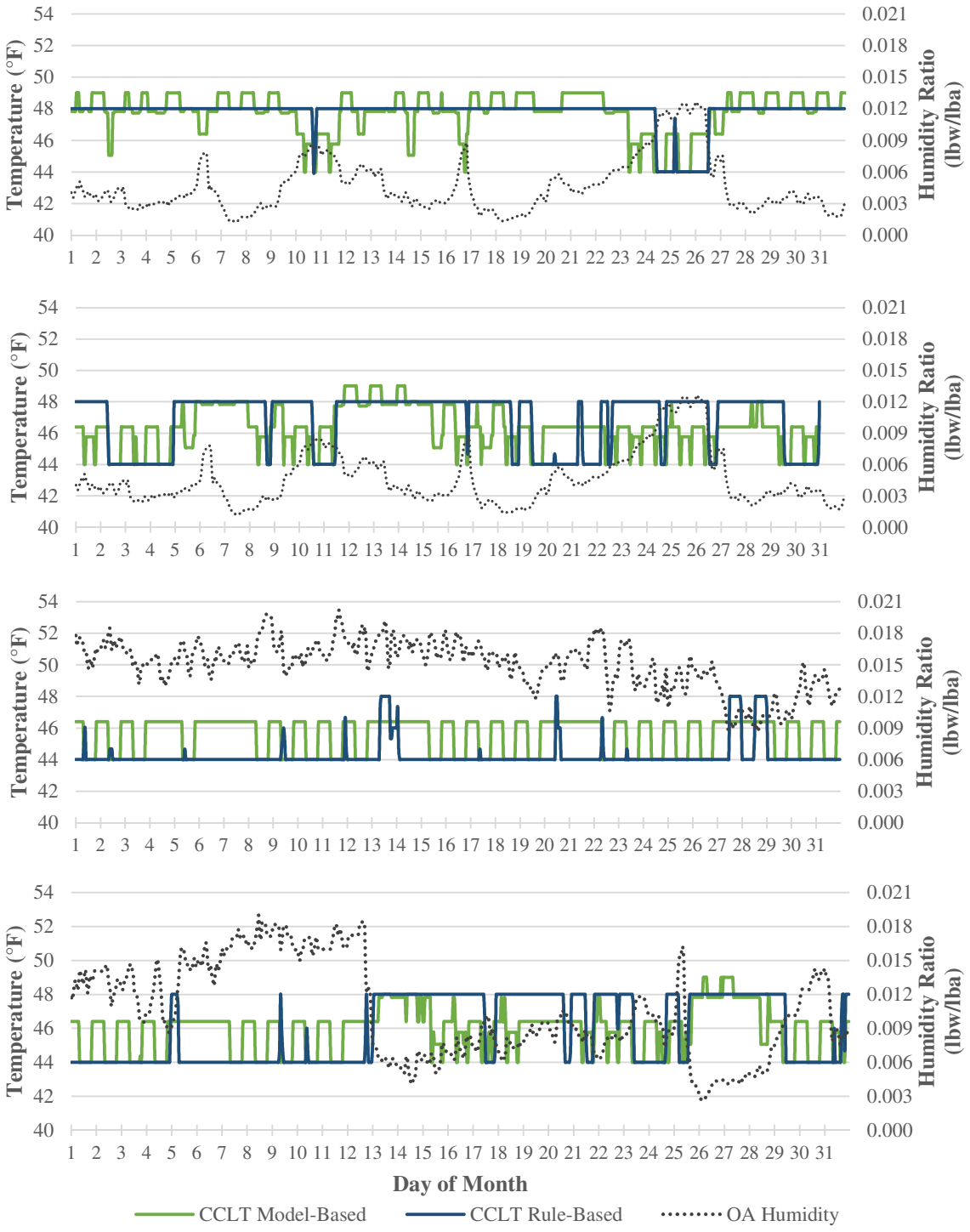

Figure 7.14: Optimized Chilled Water Supply Temperature Setpoints for the Rule-Based and Model-Based Optimization

Figure 7.15 shows the comparative annual energy use for the optimized VAV system with demand controlled ventilation, the chilled beam system with the rule-based optimization (MCB-VAV-VCLT), and the chilled beam system with the model-based optimization. Figure 7.16 and Figure 7.17 show the humidity levels in wing 'A' floor 2 for the months of January and April for the rule-based and model-based MCB control options. They show that humidity control is superior with the model predictive control even though energy use is very similar to the MCB-VAV-VCLT system.

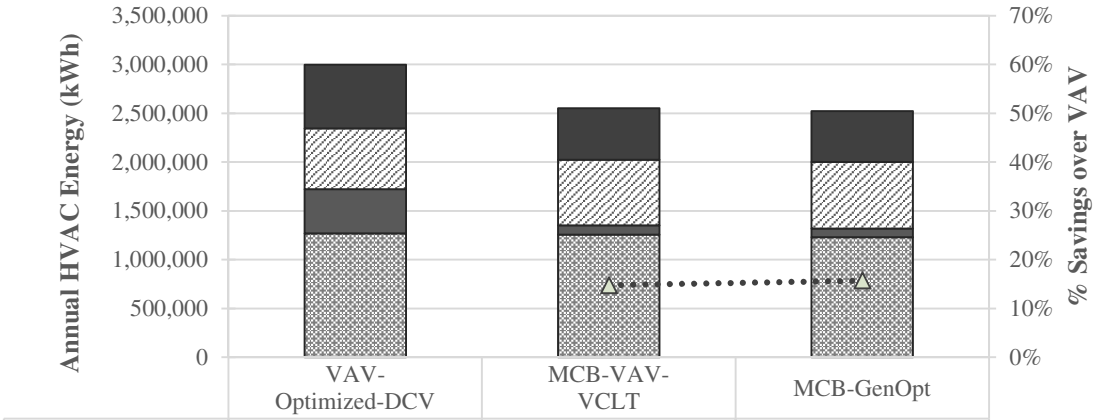

	VAV-Optimized-DCV	MCB-VAV-VCLT	MCB-GenOpt
Heating	650,622	529,522	522,627
Pumps	624,830	671,179	681,151
Fans	449,492	95,690	90,277
Cooling	1,271,689	1,256,834	1,230,283
Total Savings		15%	16%

Figure 7.15: Comparative Annual HVAC Energy Use and Savings for the Optimized VAV System, the MCB system with the Rule-Based Optimization and the MCB System with the Model-Based Optimization

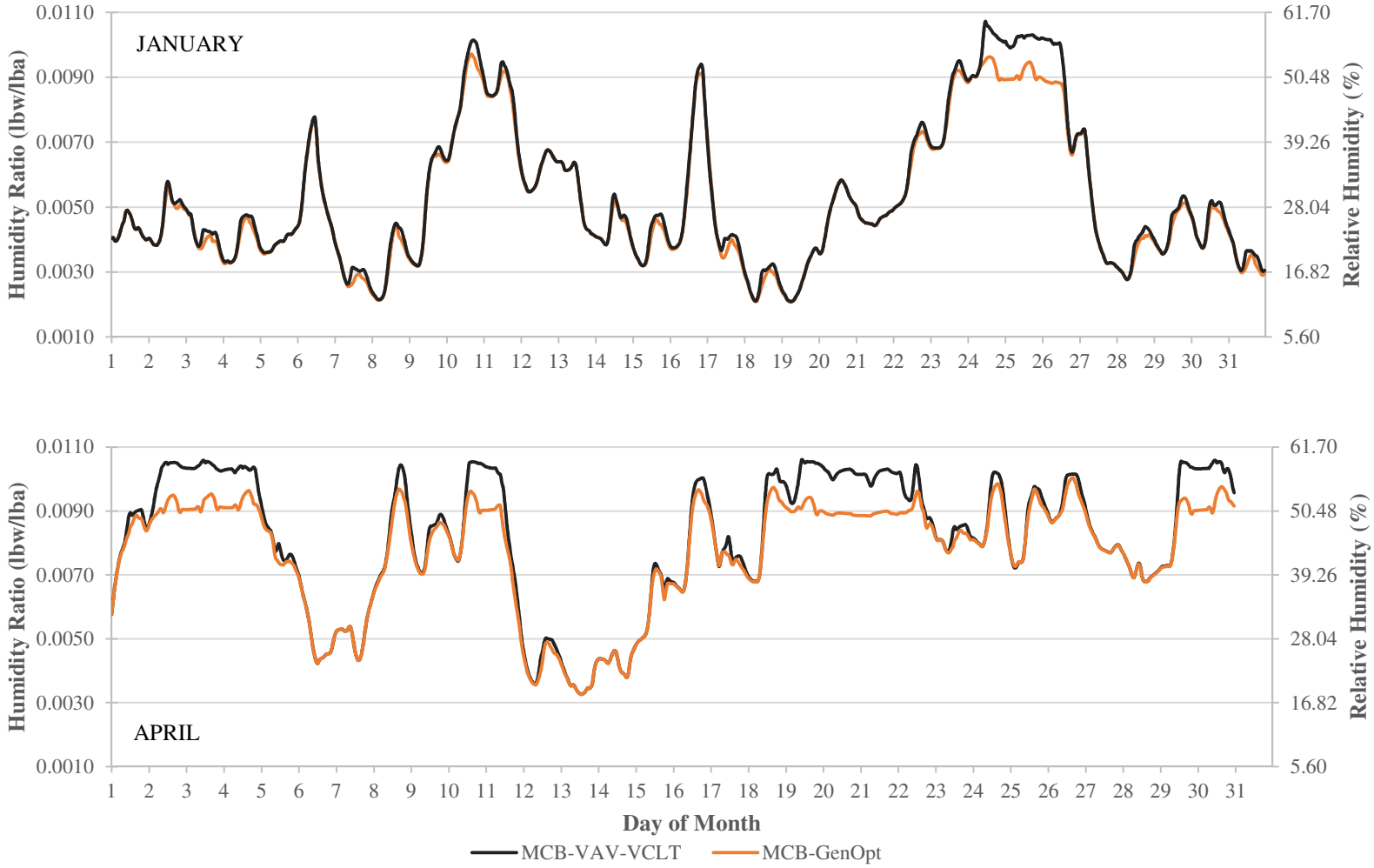

Figure 7.16: Humidity Levels in Wing 'A' Floor 2 for the Months of January and April for the Rule-Based and Model-Based MCB Control Options

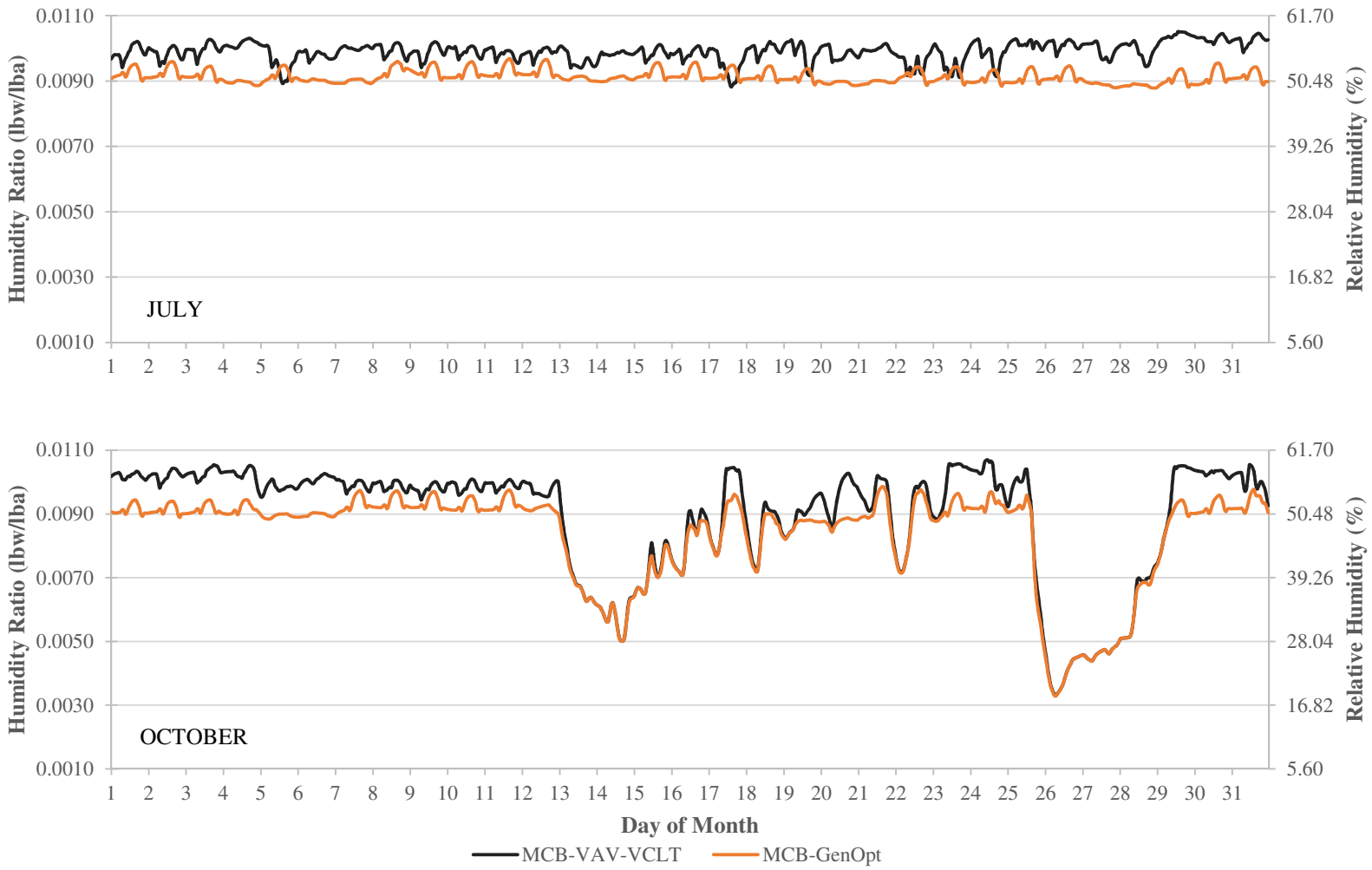

Figure 7.17: Humidity Levels in Wing 'A' Floor 2 for the Months of July and October for the Rule-Based and Model-Based MCB Control Options

7.4. Summary and Observations

In this chapter, the results of the optimization strategies for operational control of the chilled beam system was presented. In the first step, a sensitivity analysis was conducted on both the MCB and the VAV models to rank the operational control parameters based on their influence on the energy use of the building. The operational control parameters for the MCB model were the outside air flow rate, cooling coil leaving temperature, supply air temperature, chilled water temperature and zone temperatures. For the VAV model, the control parameters were outside air flow rate, supply air temperature, supply air flow rate, chilled water temperature, economizer operation and zone temperatures.

The next step in the building control optimization was the development of simplified rule-based optimization strategies that are implementable in a real building. Four possible scenarios were modeled; a constant-volume DOAS with fixed cooling coil leaving air temperature (MCB-CV-CCLT), a constant-volume DOAS with varying cooling coil leaving air temperature (MCB-CV-VCLT), a variable-volume DOAS with fixed cooling coil leaving air temperature (MCB-VAV-CCLT) and a variable-volume DOAS with varying coil leaving air temperature (MCB-VAV-VCLT).

The final step in the building control optimization was the development of a model-based predictive control strategy for a matrix of possible operating conditions encountered in the office building in a year. This step involved coupling an external optimization program with the EnergyPlus model of the building in order to optimize the

outside airflow rate, cooling coil leaving temperature and chilled water temperature and minimize the HVAC energy use.

The following observations were made from the sensitivity analysis:

- For the MCB system, the zone temperatures are the only significant parameter affecting heating energy use. For the cooling energy use, the three parameters that are most sensitive are the zone temperature, outside air volume and coil leaving temperature in that order. For total HVAC energy use, the ranking of the control parameters are; zone temperature, volume of outside air, cooling coil leaving air temperature, chilled water temperature and supply air temperature.
- For the VAV system, the zone temperatures and supply air temperatures are the significant parameters affecting heating energy use. For the cooling energy use, the three parameters that are most sensitive are zone temperature, supply air temperature, economizer control and outside air volume in that order. For total HVAC energy use, the ranking of the control parameters are; supply air temperature, zone temperature, economizer operation and volume of outside air.
- For the MCB system, the quantity of outside air has a greater influence on the cooling energy use than the cooling coil leaving temperature which leads us to deduct that reducing the cooling coil leaving air temperature can be less energy intensive than increasing outside air volumes for humidity control.
- For the MCB system, the supply air temperature and chilled water temperature do not greatly influence cooling energy use.

- The sensitivity analysis confirms that in an MCB system, reheat energy is entirely eliminated and the changes in the energy use due to the changes in the coil leaving air temperature are linear for the MCB system. It also confirms that the control of the zone thermostats setpoints is important because the ambient zone temperatures directly influence the efficiency of the chilled beam system.

The following observations were made from the simplified rule-based optimization:

- The advantages of the MCB-CV-CCLT system are that it does not require CO_2 or relative humidity monitoring in the zones. In addition, because the DOAS is a constant-volume system, a two-position open/close outside air damper and constant-volume UFAD diffusers can be used which lower the possibilities of mechanical failure. This type of control is also effective at stricter humidity control in the zones. The control is also easier to implement and operate in a building EMCS. However, this type of control is more energy intensive with energy savings of only 6% over an equivalent optimized VAV system.
- The advantages of the MCB-CV-VCLT system are that it does not require CO_2 monitoring in the zones. In addition, similar to the MCB-CV-CCLT system, a two-position open/close outside air damper and constant-volume UFAD diffusers can be used. However, this type of control is the poorest of the four configurations at humidity control in the zones. With this type of control, energy savings of approximately 14% over an equivalent optimized VAV system can be expected.

- The MCB-VAV-CCLT configuration is typically the best of the four configurations at zone humidity control. The HVAC energy use from this configuration is approximately 8% lower than an equivalent optimized VAV system.
- The MCB-VAV-VCLT configuration is typically the most energy efficient of the four configurations. HVAC energy savings from this configuration is approximately 15% over an equivalent optimized VAV system. Zone humidity control for this configuration is marginally better than that of the MCB-CV-VCLT system.
- In general, the varying coil leaving temperature along with a strict control of the supply air volume is essential to achieve the range of energy savings predicted for chilled beams (14-15%).

The following observations were made from the model predictive control optimization:

- The optimization setpoints predicted by the model predictive control align closely with the rule-based control strategies developed.
    - Cooling coil leaving air temperatures are lowest when outside air humidity levels are high and at off-peak office occupancy levels and internal gains due to the lower supply air volumes.
    - Chilled water supply temperatures are also lowest when outside air humidity levels are high and at off-peak office occupancy levels.
    - The chilled water temperature setpoint never exceeds 49°F even when the AHU cooling coils are off. This is because the same chilled water loop also supplies chilled water to the two VAV AHU cooling coils that require cooling. Therefore

it is recommended that UFAD/chilled beam AHUs and the VAV AHUs are designed with separate chilled water loops so that different chilled water setpoints can be allowed.

  - Outside air volumes predicted by GenOpt® are almost identical to the approach proposed by the rule-based optimization, with the exception of cool (40-60°F) and dry (<0.0065lbw/lba humidity) days when a larger quantity of outside air provides free cooling and lowers the HVAC energy use.

- Energy use for the model-predictive control system is within 2% of the MCB-VAV-VCLT system. Humidity control with the model predictive control is better than that of the MCB-VAV-VCLT system.
- For the optimization, a penalty function was added to the HVAC energy use if the zone temperature and humidity setpoints were not being maintained. The equations used for calculating this penalty affects the setpoint predictions.
- Since outdoor air humidity is a good representation of zone humidity, an alternative control approach can be specified in which the cooling coil leaving temperatures can be linearly reset at outdoor air humidity ratios between 0.0085 and 0.015 lbw/lba.

CHAPTER VIII

ZONE LEVEL COMFORT ANALYSIS

This chapter documents the results of the zone level comfort analysis conducted in the office spaces. The analysis included stratification measurements taken in the offices to establish temperature profiles in the zones and a CFD model of an interior zone showing the temperature and airflow patterns.

8.1. Temperature Measurements in the Zones

Summertime stratification measurements were taken for two scenarios, one when both the ventilation system and the chilled beams were operational and one when only the ventilation system was operational. Measurements were taken separately for the interior and exterior zones. The results are presented separately for day and night. Trends were also collected from the building EMCS system for the AHU supply air temperature and setpoints, chilled beam water temperature and zone thermostat setpoints and have been superimposed on the results to understand the operating conditions that are responsible for the temperature profiles in the zones.

Figure 8.1 shows the temperature profiles in an interior office zone with both the chilled beams and UFAD ventilation system operational. Figure 8.2 shows the temperature profiles in the interior office zone with only the UFAD ventilation system operational. Figure 8.3 shows the temperature profiles in an exterior office zone with both the chilled beams and UFAD ventilation system operational. Figure 8.4 shows the temperature profiles in the exterior office zone with only the UFAD ventilation system operational.

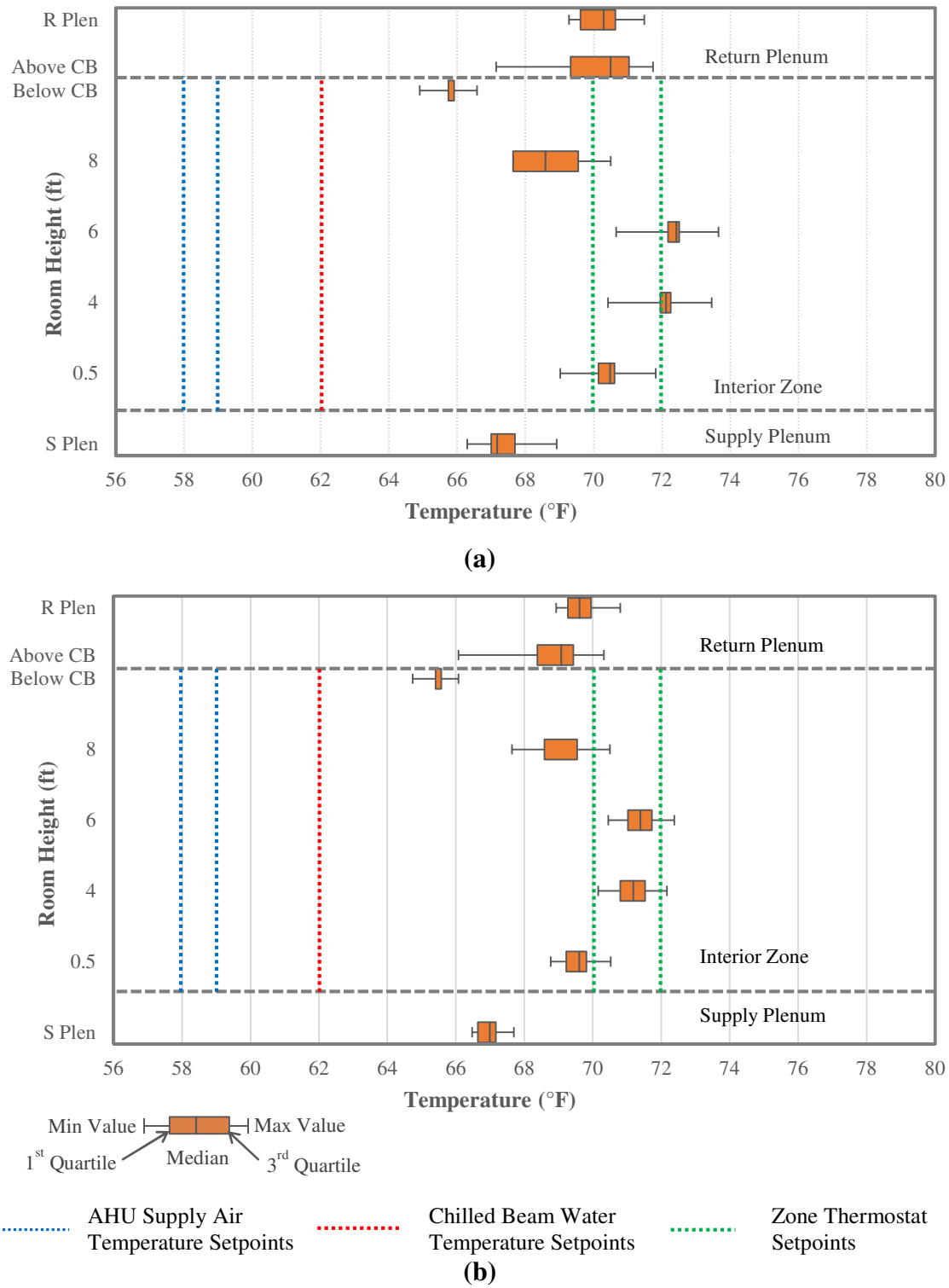

Figure 8.1: (a) Day and (b) Night Temperature Measurements in an Interior Office Zone with the Chilled Beams and the UFAD Ventilation System Operational

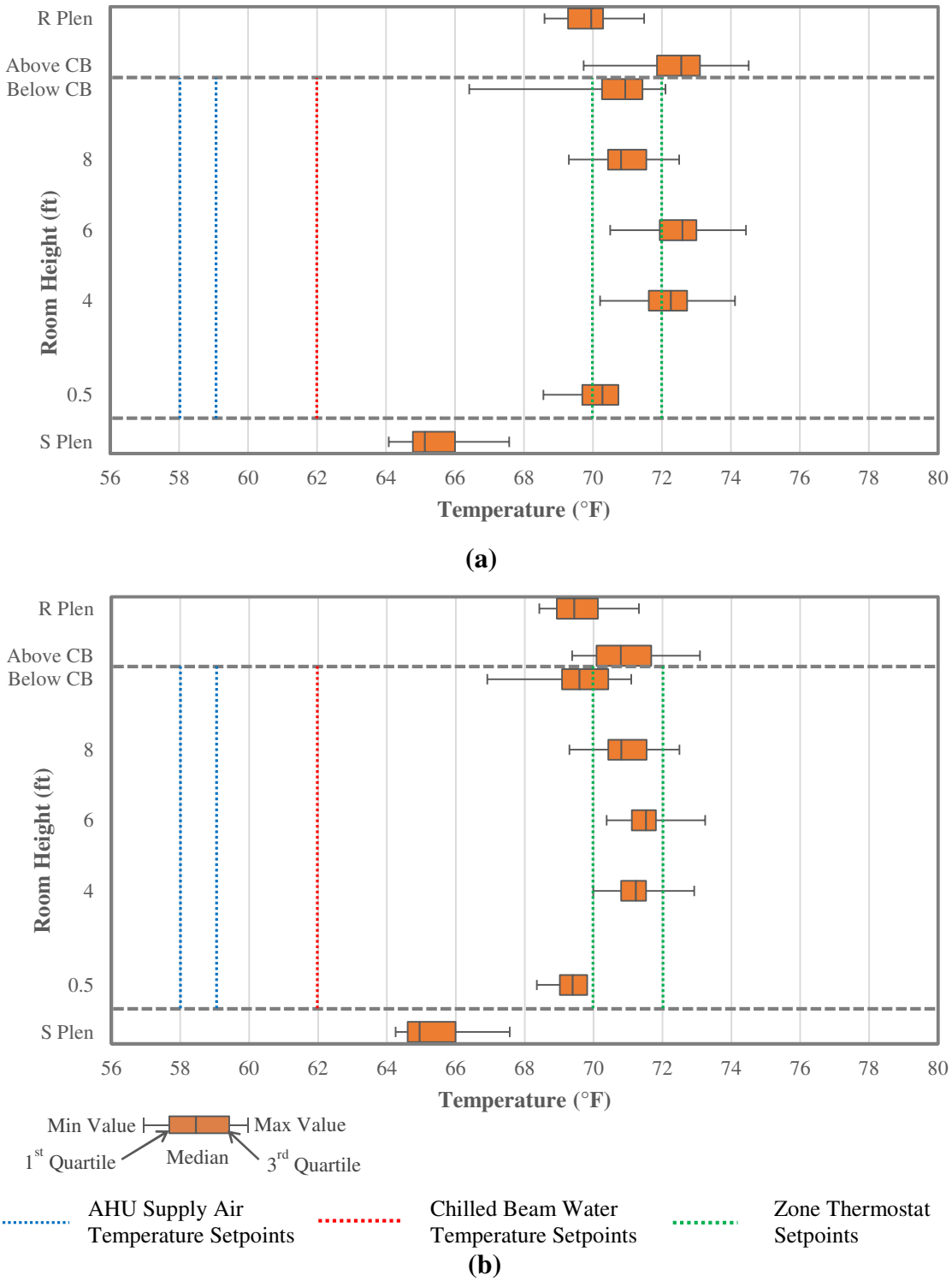

Figure 8.2: (a) Day and (b) Night Temperature Measurements in an Interior Office Zone with only the UFAD Ventilation System Operational

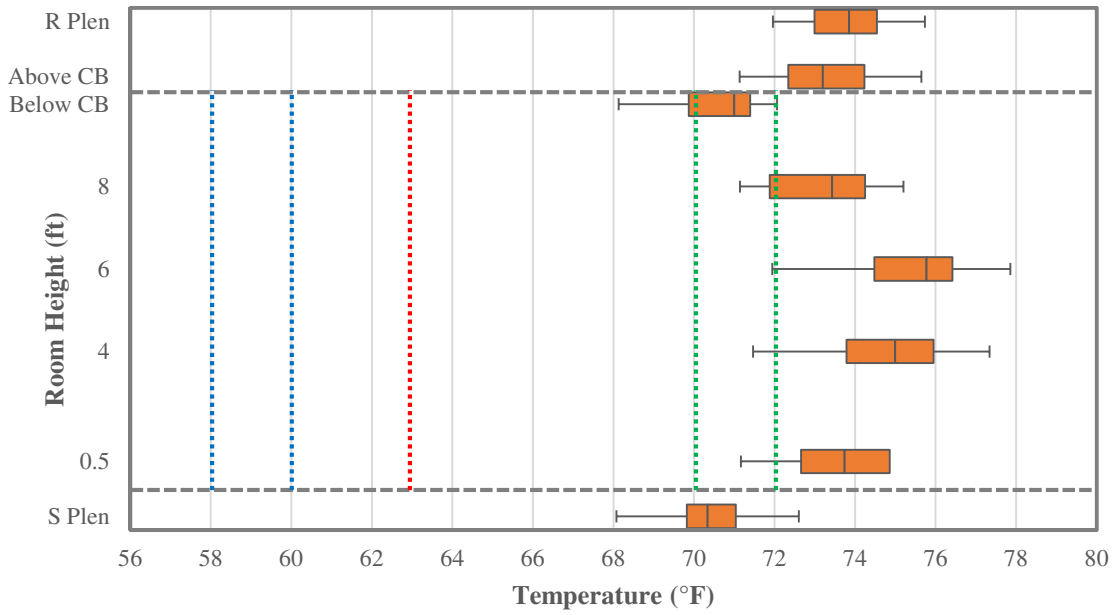

(a)

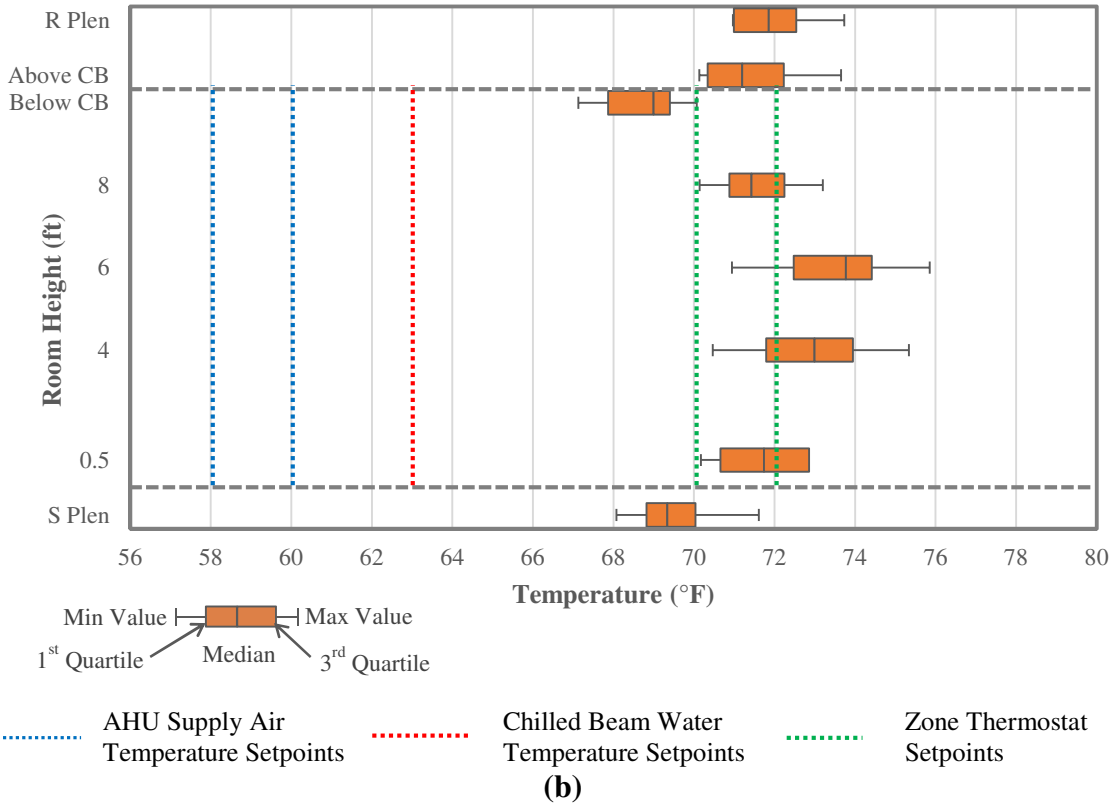

(b)

Figure 8.3: (a) Day and (b) Night Temperature Measurements in an Exterior Office Zone with the Chilled Beams and the UFAD Ventilation System Operational

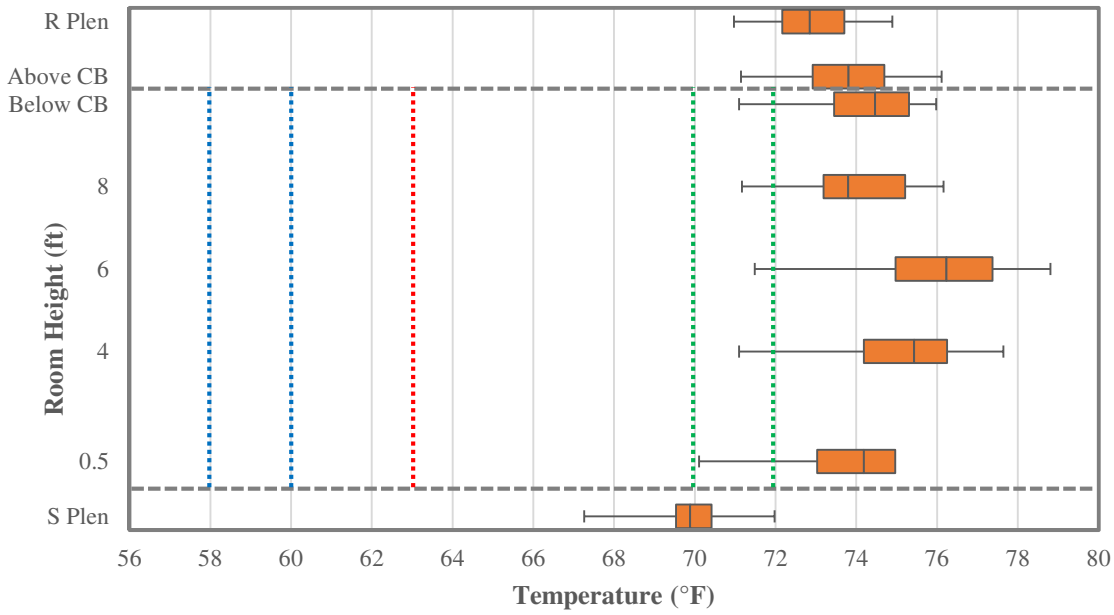

(a)

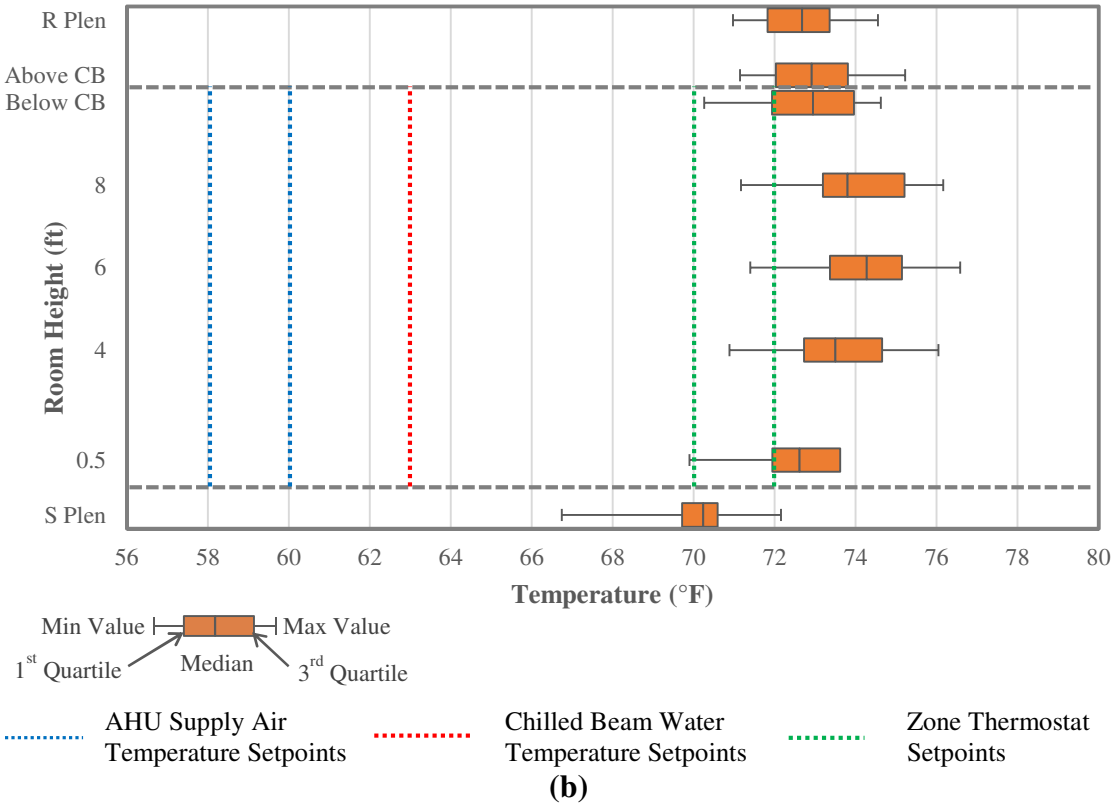

(b)

Figure 8.4: (a) Day and (b) Night Temperature Measurements in an Exterior Office Zone with only the UFAD Ventilation System Operational

The observations from the summertime zone temperature measurements are:

- The interior zone sees stable temperatures while the exterior zone temperatures vary substantially through the day. This is understandable because of the fluctuating solar gain from the windows in the exterior zone.
- The temperatures in the supply plenum are approximately 8-9°F higher than the supply air temperature leaving the AHUs when the chilled beams are operational. The temperatures in the supply plenum are lower (6-7°F more than the supply air temperature leaving the AHUs) when only the UFAD system is on. This is because the supply air volumes are lower when the chilled beams are on which increases the temperatures in the supply plenum.
- The daytime temperatures in the exterior zones are consistently 4-5°F higher than the zone thermostat setpoints, i.e. the zone thermostat setpoints are not met in the exterior zones. This is because the chilled beams in both the interior and exterior zones are piped in series and controlled to a single chilled beam water flow rate. As a result, the beam flow is controlled to the interior zone loads and the exterior zone is undercooled. When only the ventilation system is operational, the supply air temperatures are almost equal to the zone thermostat temperatures due to the heat gain from the windows to the supply plenum. As a result, the system is unable to provide cooling even at full capacity and the thermostat setpoints in the exterior zone cannot be met.
- The temperatures in the return plenum are consistently 2-4°F lower than the zone temperatures in all the scenarios monitored. This is because of the heat exchange between the return plenum and the adjacent cooler supply plenum on the floor above.

It also implies that some cooling from the chilled beams escapes to the return plenum instead of being delivered to the zones.

- The vertical temperature gradient between the floor and head height (occupied zone) in the UFAD only configuration is on an average about 2-3°F which is consistent with supply airflows of approximately 0.5-0.7cfm/ft^2. This is also below the maximum limit of 5°F (3°C) specified in ASHRAE Standard 55 (ASHRAE 2010b) so thermal comfort is not compromised.
- Even when the chilled beams are off, the unoccupied upper zone (6'-0" to 10'-0") sees temperatures that are 2-3°F lower than the occupied zone temperatures. A possible reason for this could be leaky chilled beam valves.
- In terms of operation, the chilled beam water setpoint temperatures were 62-63°F. The zone thermostat setpoints were 70-72°F. Since the temperature difference between the zone air and the chilled beam water affects the beam cooling capacity, a temperature difference of 8-10°F translates to a cooling capacity of 65-90Btu/hr-ft even at peak flow rates. This is far lower than the maximum capacity of the beam (250Btu/hr-ft). Therefore a minimum temperature difference of 15°F is recommended between the zone air and the chilled beam water to increase cooling capacity and efficiency of the chilled beam.
- The chilled beam exiting air temperatures in the interior zone are 65-66°F in the interior zones and 69-71°F in the exterior zones. The values for the interior zone are consistent with the recommended values discussed in literature (Virta et al. 2007). In the exterior zone, the location and size of the windows reduce the capacity of the

beams and result in the higher temperatures seen below the beams. Therefore, steps should be taken to minimize the effect of the windows through blinds or other shading devices.

- The temperatures above the chilled beams were observed to be consistently lower (1-2°F) than that of the return plenum when the chilled beams were on. This implies that some portion of the cooling from the beam is lost to the return plenum.

8.2. CFD Simulations of the Temperature and Airflows in the Zone

A CFD model of a single interior zone was also developed in Star CCM+ 9.04 to supplement the zone temperature measurements and to estimate the zone airflows. The CFD model uses the standard k-ε model to calculate the turbulent flows. The zone was modeled with walls with a surface temperature of 73°F, zone floor and return plenum ceilings with surface temperatures of 68°F, three velocity inlets with velocities of 50ft/min. and a pressure outlet in the return plenum. Four persons were modeled in the zone with heat fluxes of 409 Btu/hr each. Eight computer monitors were also modeled with heat fluxes of 137 Btu/hr each.

Figure 8.5 shows the temperature profiles for three sections in the zone. They reveal that the zone does not see much variation in temperature within the zone. On the other hand, the return plenum temperatures are 2-3°F below the ambient zone temperatures. The temperature above the chilled beam is also equal to that below the chilled beam indicating that some portion of the cooling from the beam is lost to the return

plenum. Stratification in the occupied zone due to the UFAD inlets and a clear downward thermal plume from the chilled beam is also not observed in the temperature profiles.

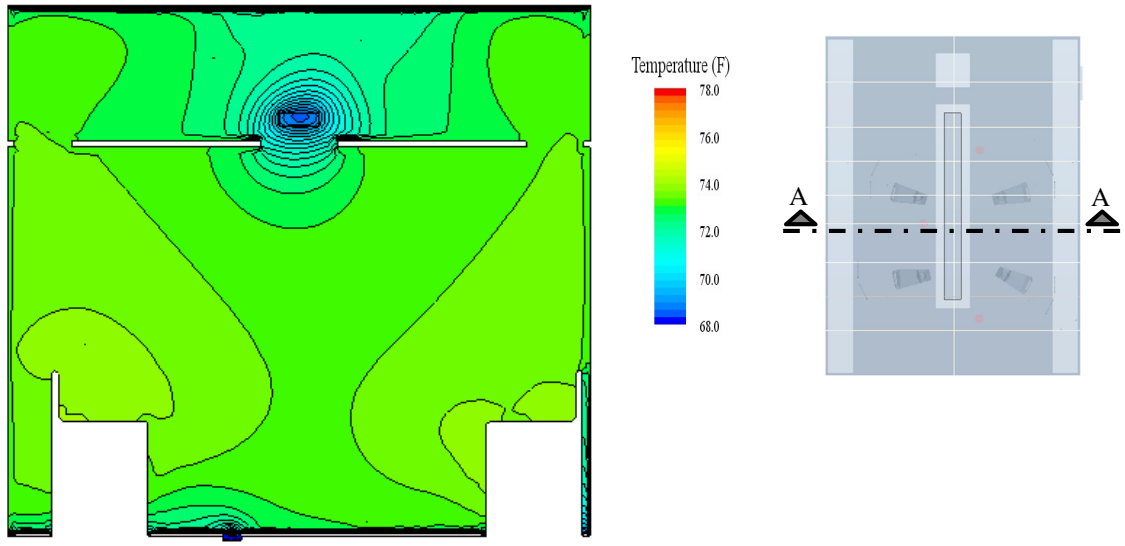

(a)

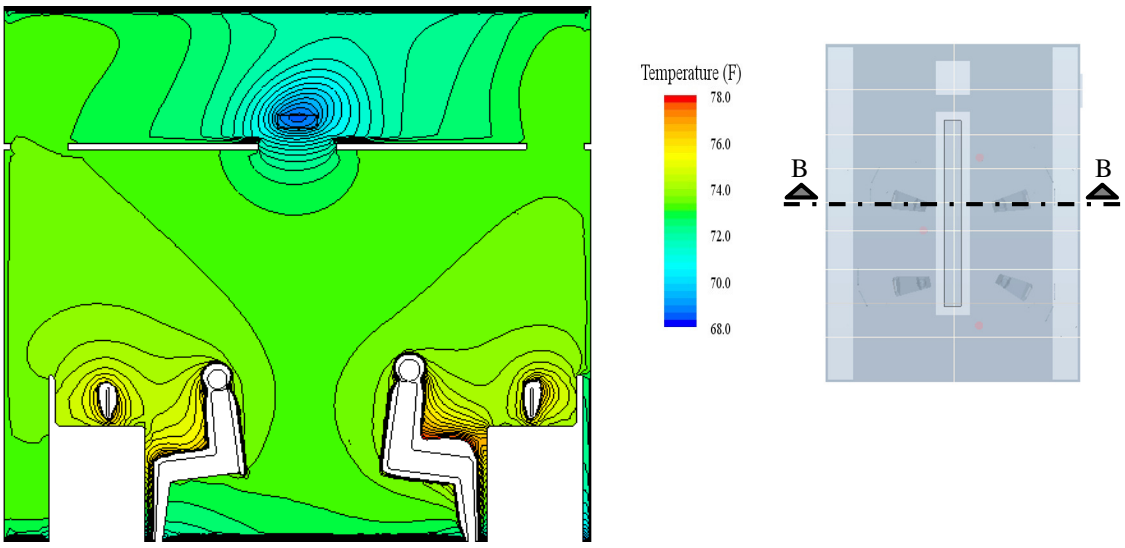

(b)

Figure 8.5: CFD Temperature Profiles for (a) Section A and (b) Section B of the Interior Office Zone

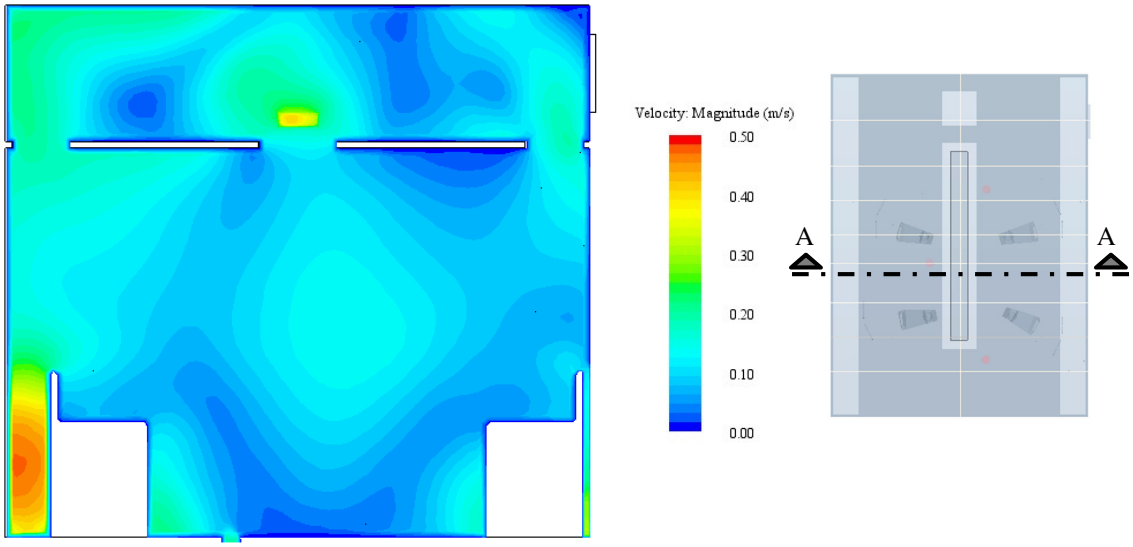

(a)

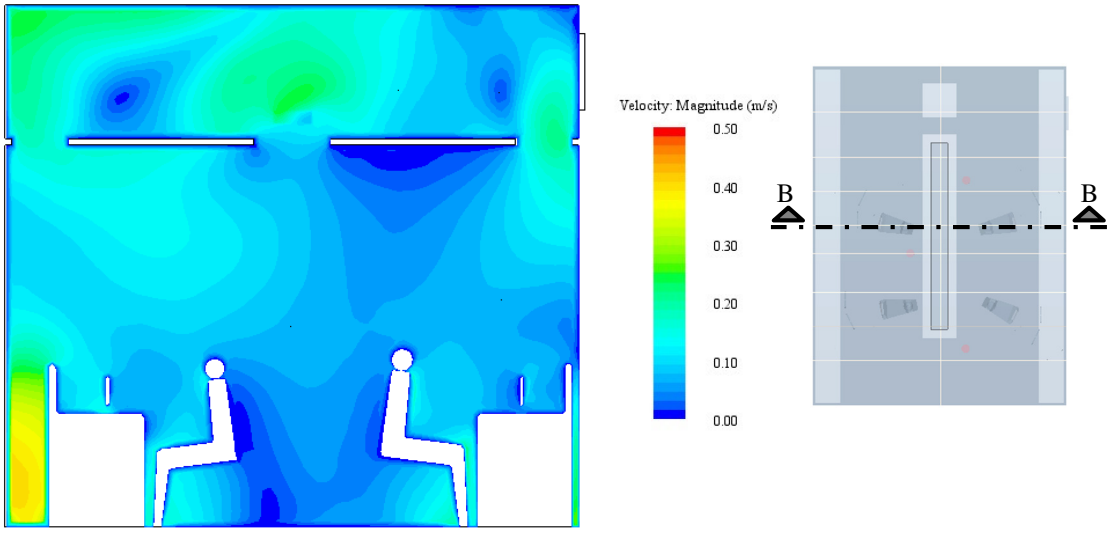

(b)

Figure 8.6: CFD Velocity Scalar Profiles for (a) Section A and (b) Section B of the Interior Office Zone

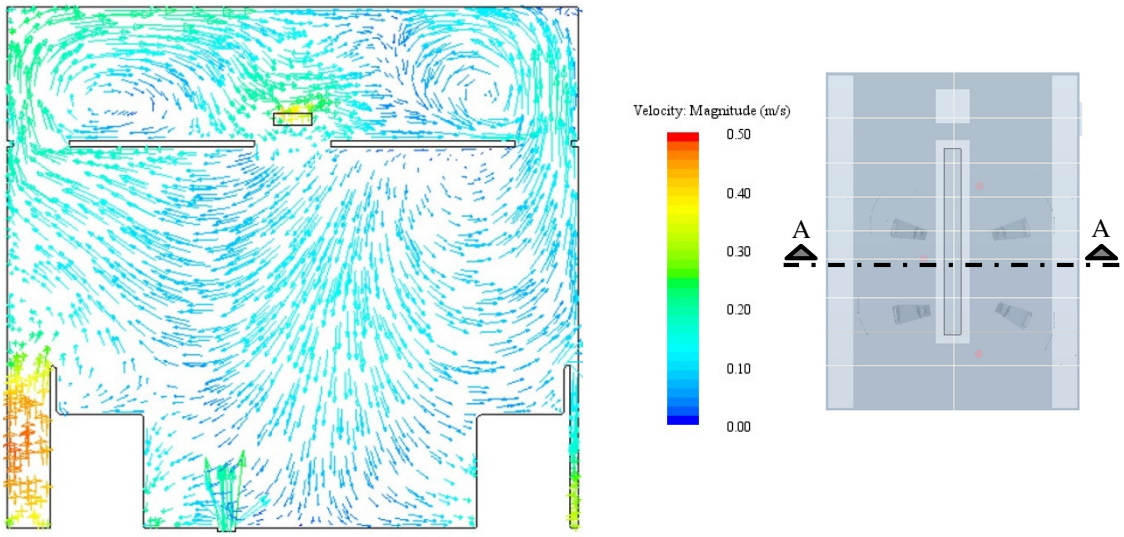

(a)

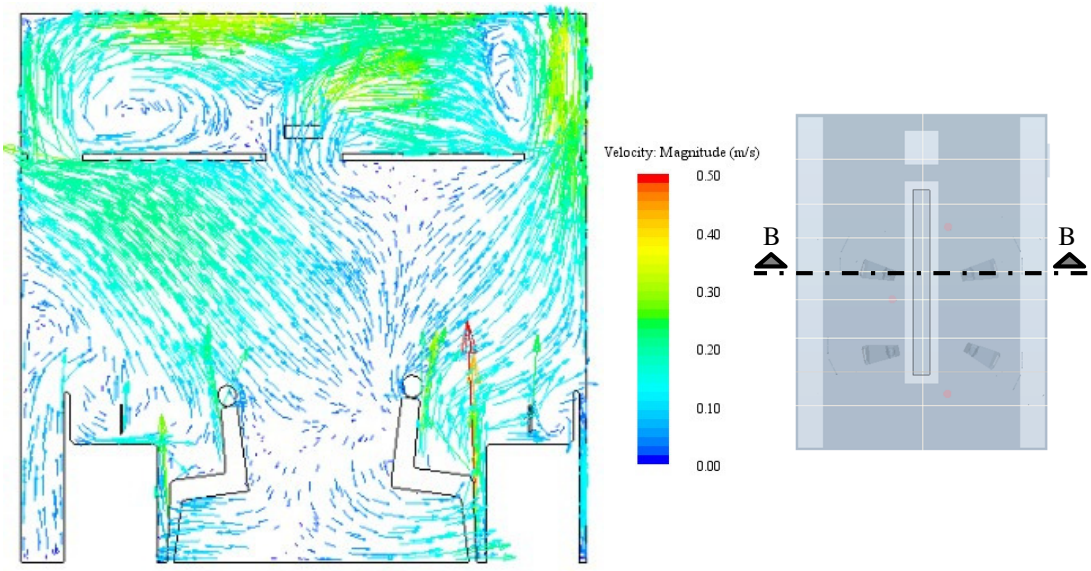

(b)

Figure 8.7: CFD Velocity Vector Profiles for (a) Section A and (b) Section B of the Interior Office Zone

Figure 8.6 and Figure 8.7 show the velocity profiles in the space. They show that velocities in the zone are within the maximum recommendations of 0.5m/s to avoid draughts and thermal discomfort in the space. This is because the loads in the zone are low. The general direction of the airflow is downward below the chilled beams and upward near the walls, but an upward trend above the chilled beam is also observed. This replicates the observations seen during the temperature measurements in the zone and could possibly be due to the negatively pressurized return plenum outlets drawing return air away from the zones to the AHUs. However, additional modeling, or measured data collection is required to ascertain the cause of the upward flow from the chilled beam and steps that need to be taken to avoid the subsequent energy waste.

8.3. Summary and Observations

In summary, the summertime zone level comfort analysis revealed that supply plenum temperatures are higher (+2°F) when the chilled beams are on because supply air volumes are lower. Return plenum temperatures are also lower (-2°F) than zone temperatures. Intermittently, the temperatures above the chilled beam are lower (1-2°F) than that of the return plenum. This phenomenon is also observed in the CFD model of the zone and shows that some cooling from the chilled beam is lost to the return air. The CFD model also shows that the temperatures in the zone doesn't see much vertical variation suggesting that no significant stratification occurs in the occupied zone. A clear downward thermal plume from the chilled beam is also not observed in the temperature profiles. These observations suggest that the presence of the UFAD ventilation system

hinders the natural downward plumes from the chilled beams and the presence of the chilled beam system inhibits stratification in the zones.

On the thermal comfort side, the occupied zone temperature difference for the UFAD system is within the ASHRAE comfort recommendations. The temperatures below the chilled beams are also consistent with chilled beam application recommendations. The velocities below the chilled beam predicted by the CFD model are within the maximum recommended to avoid draughts and thermal discomfort. Exterior zone temperatures are consistently higher than thermostat setpoints in summer suggesting that the system is unable to meet comfort requirements in the exterior zones. It is important to note that the zone level comfort analysis was conducted in July-August and these observations are valid only for summer. A separate set of stratification measurements should be taken in winter to understand comfort conditions in winter.

CHAPTER IX

SUMMARY AND CONCLUSIONS

This chapter documents the findings from the research, presents the conclusions and provides recommendations for the modeling, implementation and operation of passive chilled beams in humid climates. In addition, based on the limitations of this study, opportunities for future research are presented. Section 9.1 summarizes the research methodology and the results of the study. It also presents the recommendations for the implementation and operation of passive chilled beams. Finally, in Section 9.2 opportunities for future research are proposed.

9.1. Summary of Research and Conclusions

The research was conducted in four major steps. At first, an office building with passive chilled beams and UFADs was selected as the case-study for the research. Building data was collected and inputs were established in order to develop a calibrated EnergyPlus 8.1 simulation model of the building. A process for modeling the operation of the passive chilled beams and the UFAD system in EnergyPlus was developed. A simplified steady state model was also developed for validation of the EnergyPlus model and energy use predictions.

In the next step, the energy use of the building was compared to an equivalent VAV system baseline and an ASHRAE 90.1 code-compliant building. A parametric study was then conducted by varying the latent and sensible loads in the space to understand their effect on the energy savings potential of the chilled beam system. Optimization

strategies for operational control of passive chilled beams were then developed. This step involved conducting a sensitivity analysis of operational control parameters and the equivalent VAV system. Simplified rule-based optimization strategies were then developed for the operational control of the chilled beams. A process was then outlined to develop and model a simulation assisted optimization strategy that can be eventually implemented in the building. The results of this strategy was compared with the simplified rule-based optimization strategies developed. Lastly, summertime stratification measurements were taken in the offices to establish temperature profiles in the zones. These measurements were taken for the cooling season only and provided insight into the zone airflow patterns and the thermal effect of the chilled beam and UFAD system on each other.

Several lessons were learned from the operation and energy evaluation of the case-study building. The ventilation system was sized for twice the total building loads and was controlled by the zone thermostats. On the other hand, the chilled beam system was undersized and the beam water flow rate was controlled to a loop pressure setpoint. This leads to overcooling of the zones, instable operation and inadequate use of both the high-efficiency systems. As a result, in the building the chilled beams were used for only two (2) months in the year and the energy use of the building was 10% more than an equivalent VAV system and 5% more than the ASHRAE 90.1 (2004) baseline it was designed to comply with. The chilled beams for an entire floor in the building were controlled by a single valve to a single water flow rate. As a result of this incorrect zoning, there were hot

and cold spaces in the building. On the maintenance side, the variable-volume UFAD diffusers are prone to frequent leakage and failure.

Lessons learned from the modeling of the chilled beam system are that even though many widely available whole-building energy analysis software such as EnergyPlus, TRACE and IDA-ICE contain a chilled beam model, the operation is incorrectly simulated leading to inaccurate energy use results. In spaces with UFADs, if heat gain in the supply plenum is not modeled, it can result in predicted cooling, fan and heating consumption that is lower than the actual energy use. EnergyPlus does model heat gains/losses in the supply and return plenum, but can only model chilled beams with constant volume supply air and overhead distribution in the zones. EnergyPlus also lacks an option to control the air and water systems in the zones separately. Default values provided in EnergyPlus for the chilled beam model yield cooling capacities that are less than 50% of the capacities provided by the chilled beam manufacturer. Therefore, a process for modeling the operation of the passive chilled beams and the UFAD system within EnergyPlus was developed. A simplified steady state model was also developed for validation of the EnergyPlus model and energy use predictions.

On the control optimization side, the results of the sensitivity analysis show that zone temperature setpoints, quantity of outside air and the temperature of the cooling coil leaving at temperature are the most significant to the energy use of the chilled beam system. The quantity of outside air has a greater influence on the cooling energy use than the cooling coil leaving temperature. This means that reducing the cooling coil leaving air temperature for humidity control is less energy intensive than increasing outside air

volumes. Therefore, independent control of the outside air volume for ventilation and the cooling coil leaving air temperature to control zone humidity yields the most efficient system with the lowest energy use. A demand control ventilation approach can be used even in a DOAS type of application but would require zone CO_2 monitoring and variable-volume UFAD diffusers. However, the demand controlled ventilation system supplies more ventilation air than minimum ASHRAE 62.1 (2013) ventilation requirements at peak occupancy levels. This results in better humidity control at peak occupancy since people are the primary source of latent loads in office buildings. Increasing the zone thermostat setpoints also improves the cooling capacity of the chilled beams. Two types of control optimization were proposed, a rule-based control and a model-predictive control. Of the two, the model-predictive control yielded better humidity control in the zones, but energy use was very similar to that of the developed rule-based control system.

The energy use evaluation of the building reveals that if properly controlled, a chilled beam system with parallel ventilation has potential for HVAC savings of 14-24% over VAV systems in office buildings in climate zone 3A. If latent loads and ventilation requirements are high in a building, energy savings will be on the lower side. All of the energy savings by end-use are from fan and reheat energy. Reheat energy is entirely eliminated with chilled beam systems. However, no cooling (chiller and plant) savings are obtained from the chilled beam system because the smaller airside system is unable to take advantage of free cooling possible through the use of an economizer. This suggests that chilled beams may not be economically feasible in locations where an economizer can be potentially used for a large portion of the year.

Indoor humidity levels are higher (approximately 60% RH) with a passive chilled beam/ventilation system than a standard VAV system (approximately 50-55% RH). This suggests that either a passive chilled beam system may not be appropriate in buildings with strict humidity control requirements or alternate methods of dehumidification may have to be used for energy efficiency.

The summertime zone level comfort analysis revealed that supply plenum temperature is higher (+2°F) when the chilled beams are on because supply air volumes are lower. Return plenum temperatures are also lower (-2°F) than zone temperatures. Because the perimeter heating coils are located in the return plenum, this increases the heating energy use. Intermittently, the temperatures above the chilled beam were also found to be lower (1-2°F) than that of the return plenum implying that some cooling from the chilled beam is lost to the return air. Stratification in the zones equipped with UFAD is also low because of the presence of the chilled beam system. These observations suggest that the two systems adversely affect the performance of each other though thermal comfort in the zones is not affected.

Based on the results obtained, the following recommendations are proposed for the design, implementation and operation of passive chilled beams with underfloor air distribution of ventilation air:

- Size the ventilation system only to meet outside air requirements. Size the chilled beams for maximum sensible cooling loads in the zones. Zone the chilled beams based on loads, i.e. in an open-office plan, the chilled beams in the exterior zone should be piped and controlled separately from the chilled beams in the interior zone.

- Control the quantity of outside air for ventilation loads only and independent of zone humidity. Control the cooling coil leaving air temperatures for zone humidity only and independent of zone temperature. In humid climates, this may require cooling coil leaving air temperatures as low as 48°F. Control the chilled beam water flow rate for zone temperatures.
- If humidity control in the zones is a concern, use other solutions (such as a run-around coil) to reheat the air leaving the cooling coil instead of a bypass air UFAD AHU configuration. In buildings which require stringent humidity control, chilled beam systems may be energy intensive.
- If the building contains both UFAD/chilled beam and VAV AHU types, they would benefit from separate chilled water loops so that the UFAD AHUs can be controlled to a higher chilled water supply temperature setpoint when humidity control is not an issue in the zones.
- Chilled beam systems are most efficient in buildings with high sensible loads, low latent loads and low ventilation requirements. However, in locations where an economizer can be potentially used for a large portion of the year, the ventilation systems associated with chilled beams cannot take advantage of the free cooling which may render this type of system economically unfeasible.
- Supply plenum temperature increase is significant because of the low supply air volumes associated with chilled beams. Therefore, steps should be taken to reduce heat exchange between the adjacent supply and return plenums. Similarly, low supply

air velocities and low plenum pressures are important to ensure heat exchange between the chilled beam and the zone air.

9.2. Recommendations for Future Work

Recommendations for future work based on the findings of this research include:

- Using the simplified building model for the model-based optimization. This will speed up the simulation time and allow for more variables to be included in the grid of operating conditions and for hourly or live online optimization. Compare the results from this optimization to the proposed rule-based optimization to verify if there are advantages to the model-based optimization.
- Obtaining wintertime zone temperature stratification measurements to understand the effect of the perimeter heating system on chilled beams and zone airflows.
- Implementation of the recommended optimization strategies in the case-study building and monitoring measured energy savings and comfort conditions in the zones.
- Conducting sub-hourly dynamic simulations to understand the interactions between the HVAC components and the time-responses required for stable operation.
- Evaluating other HVAC configurations such as temperature and enthalpy recovery for the airside system, other methods of dehumidification, run-around coils for bypass air mixing, displacement ventilation and water-side economizers.
- Conducting a similar study for other building types and climatic conditions. Developing a range of recommendations for situations when chilled beams are more energy efficient than VAV systems.

- Conducting an economic analysis to provide payback estimates for different HVAC configurations, building loads and climatic conditions. This will help in informed decision-making during the design process.
- Conducting a similar study for active chilled beams. Active chilled beams are equipped with overhead ventilation and so unlike a passive chilled beam with underflow ventilation, the ventilation system will provide cooling to the zones. However, drastically reducing the ventilation volumes reduces the heat transfer capacity of active chilled beams. As a results a different approach to the control of active chilled beams may be required.
- Development of a detailed CFD analysis that includes temperature and airflow modeling in the office spaces. The analysis can include the influence of control parameters such as velocity and temperature of supply air and temperature of chilled beam water on thermal plumes and airflow.
- Conduct a CFD contaminant modeling analysis for the zones. Contaminant and dust control for chilled beam systems is an important aspect that needs to be addressed since the beams recirculate zone air without filtering. This is a disadvantage over air-terminal units in overhead ventilation systems which filter the return plenum air before redistributing it back to the zones.
- Development of a detailed CFD analysis that explains the effect of the drop ceiling with embedded chilled beams on chilled beam capacity and heat transfer.

- Development of a mathematical model for estimating the energy use and cooling capacity of a passive chilled beam system. The model should take into consideration changes in capacity based on heat sources in the spaces.
- Development of an empirical model to estimate stratification temperatures and airflows in the spaces equipped with a passive chilled beam/UFAD configuration.

REFERENCES

Alexander, D. and M. Rourke. (2008). Design Considerations for Active Chilled Beams. ASHRAE Journal, 50(9): 50-58.

Antonopoulos, K. A., M. Vrachopoulos and C. Tzivanidis. (1998). Experimental Evaluation of Energy Savings in Air-Conditioning using Metal Ceiling Panels. Applied Thermal Engineering, 18(11): 1129-1138.

Ardehali, M. M. and T. F. Smith. (1997). Evaluation of HVAC System Operational Strategies for Commercial Buildings. Energy Conversion and Management, 38(3): 225-236.

ASHRAE. (2002). ASHRAE Guideline 14-2002 for Measurement of Energy and Demand Savings. Atlanta, GA: American Society of Heating, Refrigerating and Air-Conditioning Engineers.

ASHRAE. (2004). ANSI/ASHRAE/IESNA Standard 90.1-2004: Energy Standard for Buildings Except Low-Rise Residential Buildings. Atlanta, GA: American Society of Heating, Refrigerating and Air-Conditioning Engineers.

ASHRAE. (2010a). ANSI/ASHRAE Standard 62.1-2010: Ventilation for Acceptable Indoor Air Quality. Atlanta, GA: American Society of Heating, Refrigerating and Air-Conditioning Engineers.

ASHRAE. (2010b). ANSI/ASHRAE Standard 55-2010: Thermal Environmental Conditions for Human Occupancy. Atlanta, GA: American Society of Heating, Refrigerating and Air-Conditioning Engineers.

ASHRAE. (2012). ASHRAE Handbook: HVAC Systems and Equipment. Atlanta, GA: American Society of Heating, Refrigerating and Air-Conditioning Engineers.

ASHRAE. (2013). ANSI/ASHRAE Standard 62.1-2013: Ventilation for Acceptable Indoor Air Quality. Atlanta, GA: American Society of Heating, Refrigerating and Air-Conditioning Engineers.

Babiak, J., B. W. Olesen and D. Petráš. (Eds.) (2009). Low Temperature Heating and High Temperature Cooling: Embedded Water Based Surface Heating and Cooling Systems. REHVA Low Temperature Heating and High Temperature Cooling Guidebook. Brussels, Belgium: REHVA, Federation of European Heating and Air-Conditioning Associations.

Bahman, A., R. Saade, W. Chakroun, K. Ghali and N. Ghaddar. (2009). Performance Comparison of Conventional and Chilled Ceiling/Displacement Ventilation Systems in Kuwait. ASHRAE Transactions, 115(1): 587-594.

Bauman, F. (2003). Underfloor Air Distribution (UFAD) Design Guide. Atlanta, GA: American Society of Heating, Refrigerating and Air-Conditioning Engineers.

Bauman, F., K. H. Lee and I. C. Nelson. (2011). Testing and Modeling Energy Performance of Active Chilled Beam Systems: Research Topic Acceptance Request (1629-RTAR). Atlanta, GA: American Society of Heating, Refrigerating and Air-Conditioning Engineers.

Bauman, F. and T. Webster. (2001). Outlook for Underfloor Air Distribution. ASHRAE Journal, 43(6): 18-27.

Bauman, F., T. Webster and D. Dickerhoff. (2008). Air Leakage Test Report: EPA Region 8 Headquarters, Denver, CO. Berkeley, CA: Center for the Built Environment, University of California, Berkeley.

Bengea, S., A. Kelman, F. Borrelli, R. Taylor and S. Narayanan. (2013). Implementation of Model Predictive Control for an HVAC System in a Mid-Size Commercial Building. HVAC&R Research, 20(1): 121-135.

Betz, F., J. McNeill, B. Talbert, H. Thimmanna and N. Repka. (2012). Issues Arising from the Use of Chilled Beams in Energy Models. Proceedings from the 5th National Conference of IBPSA-USA, Madison, WI.

Brandemuehl, M. J. and T. Katejanekarn. (2004). Dehumidification Characteristics of Commercial Building Applications. ASHRAE Transactions, 110(2): 65.

Campolongo, F., J. Cariboni, A. Saltelli and W. Schoutens. (2004). Enhancing the Morris Method. Proceedings from the 4th International Conference on Sensitivity Analysis of Model Output (SAMO), Santa Fe, NM.

Cehlin, M. and B. Moshfegh. (2002). Numerical and Experimental Investigations of Air Flow and Temperature Patterns of a Low Velocity Diffuser. Proceedings from the 9th International Conference on Indoor Air Quality and Climate, Monterey, CA.

Ceylan, H. T. and G. E. Myers. (1980). Long-Time Solutions to Heat-Conduction Transients with Time-Dependent Inputs. Journal of Heat Transfer, 102(1): 115.

Chamberlin, G. A., K. S. Maki, Z. Li, D. M. Schwenk and L. L. Christianson. (1999). VAV Systems and Outdoor Air. ASHRAE Journal, 41(10): 39-47.

Chen, Q. and W. Xu. (1998). A Zero-Equation Turbulence Model for Indoor Airflow Simulation. Energy and Buildings, 28(2): 137-144.

Chen, Q., Z. Zhang and W. Zuo. (2007). Computational Fluid Dynamics for Indoor Environment Modeling: Past, Present and Future. Proceedings from the 25th UIT National Heat Transfer Conference, Trieste, Italy.

Chowdhury, A. A., M. G. Rasul and M. M. K. Khan. (2008). Thermal Comfort Analysis and Simulation for Various Low-Energy Cooling Technologies Applied to an Office Building in a Subtropical Climate. Applied Energy, 85(6): 449-462.

Coffey, B. (2011). Using Building Simulation and Optimization to Calculate Lookup Tables for Control. Ph.D. Dissertation, University of California, Berkeley, Berkeley, CA.

Crawley, D. B., J. W. Hand, M. Kummert and B. T. Griffith. (2008). Contrasting the Capabilities of Building Energy Performance Simulation Programs. Building and Environment, 43(4): 661-673.

Dai, Y. J., R. Z. Wang, H. F. Zhang and J. D. Yu. (2001). Use of Liquid Desiccant Cooling to Improve the Performance of Vapor Compression Air Conditioning. Applied Thermal Engineering, 21(12): 1185-1202.

Deru, M., K. Field, D. Studer, K. Benne, B. Griffith, P. Torcellini, B. Liu, M. Halverson, D. Winiarski, M. Rosenberg, M. Yazdanian, J. Huang and D. Crawley. (2011). U.S. Department of Energy Commercial Reference Building Models of the National Building Stock. NREL/TP-5500-46861. Golden, CO: National Renewable Energy Laboratory.

Deru, M., P. Torcellini, S. M. and A. Lau. (2005). Analysis of the Design and Energy Performance of the Pennsylvania Department of Environmental Protection Cambria Office Building. NREL/TP-550-34931. Golden, CO: National Renewable Energy Laboratory.

Eberhart, R. C. and J. Kennedy. (1995). A New Optimizer using Particle Swarm Theory. Proceedings from the 6th International Symposium on Micro Machine and Human Science, Nagoya, Japan.

Effinger, M., J. Anthony and L. Webster. (2009). Case Studies in Using Whole Building Interval Data to Determine Annualized Electrical Savings. Proceedings from the 9th International Conference for Enhanced Building Operations, Austin, TX.

Ellis, P. G., B. T. Griffith, N. Long, P. A. Torcellini and D. Crawley. (2006). Automated Multivariate Optimization Tool for Energy Analysis. NREL/CP-550-40353. Golden, CO: National Renewable Energy Laboratory.

Emmerich, M. T., C. J. Hopfe, R. Marijt, J. L. M. Hensen, C. Struck and P. Stoelinga. (2008). Evaluating Optimization Methodologies for Future Integration in Building Performance Tools. Proceedings from the 8th International Conference on Adaptive Computing in Design and Manufacture (ACDM), Clifton, Bristol UK.

Engdahl, F. and D. Johansson. (2004). Optimal Supply Air Temperature with Respect to Energy Use in a Variable Air Volume System. Energy and Buildings, 36(3): 205-218.

EQUA. (2012). IDA Indoor Climate and Energy 4.0. Retrieved October 2, 2014, from http://www.equa.se/eng.ice.html

Ge, G. M., F. Xiao and X. H. Xu. (2011). Model-Based Optimal Control of a Dedicated Outdoor Air Chilled Ceiling System using Liquid Desiccant and Membrane-Based Total Heat Recovery. Applied Energy, 88(11): 4180-4190.

Ghaddar, N., R. Saadeh, K. Ghali and A. Keblawi. (2008). Design Charts for Combined Chilled Ceiling Displacement Ventilation System. ASHRAE Transactions, 114(2).

Grondzik, W. T. (Ed.) (2007). Air-Conditioning System Design Manual. Atlanta, GA: American Society of Heating, Refrigerating and Air-Conditioning Engineers.

Hanafy, R. M. (2012). Energy Efficient Management and Optimization Strategies in Office Buildings. M.S. Thesis, University of Kassel and Cairo University, Cairo, Egypt.

Hao, X., G. Zhang, Y. Chen, S. Zou and D. J. Moschandreas. (2007). A Combined System of Chilled Ceiling, Displacement Ventilation and Desiccant Dehumidification. Building and Environment, 42(9): 3298-3308.

Hirsch & Associates, J. J. (2010). eQuest Introductory Tutorial, version 3.64.

Hooke, R. and T. A. Jeeves. (1961). 'Direct Search' Solution of Numerical and Statistical Problems. Journal of the Association for Computing Machinery (JACM), 8(2): 212-229.

Hopfe, C. J. (2009). Uncertainty and Sensitivity Analysis in Building Performance Simulation for Decision Support and Design Optimization. Ph.D. Dissertation, Eindhoven University, Eindhoven, Netherlands.

Hottel, H. C. (1967). Radiative Transfer: New York: McGraw-Hill.

Huang, J. (2014). White Box Technologies: Weather Data for Energy Calculations. Retrieved April 25, 2014, from http://weather.whiteboxtechnologies.com

Imanari, T., T. Omori and K. Bogaki. (1999). Thermal Comfort and Energy Consumption of the Radiant Ceiling Panel System: Comparison with the Conventional All-Air System. Energy and Buildings, 30(2): 167-175.

Joo, I.-S. and M. Liu. (2003). Economizer Application in Dual-Duct Air-Handling Units. Journal of Architectural Engineering, 9(4): 126-133.

Khattar, M. K. and M. J. Brandemuehl. (2002). Separating the V in HVAC: A Dual-Path Approach. ASHRAE Journal, 44(5): 37-43.

Kim, S. (2006). An Analysis of International Energy Conservation Code (IECC) Compliant Single Family Residential Building Energy Use. Ph.D. Dissertation, Texas A&M University, College Station, TX.

Koskela, H., H. Haggblom, R. Kosonen and M. Ruponen. (2010). Air Distribution in Office Environment with Asymmetric Workstation Layout using Chilled Beams. Building and Environment, 45(9): 1923-1931.

Kreider, J. F. (2010). Heating and Cooling of Buildings: Design for Efficiency. Dubuque, IA: McGraw-Hill.

Launder, B. E. and D. B. Spalding. (1974). The Numerical Computation of Turbulent Flows. Computer Methods in Applied Mechanics and Engineering, 3(2): 269-289.

Lechner, N. (2001). Heating, Cooling, Lighting: Design Methods for Architects. New York: J. Wiley.

Lee, K. H., S. Schiavon, F. Bauman and T. Webster. (2012). Impact of Plenum Thermal Decay on Underfloor Air Distribution (UFAD) System Performance. Applied Energy, 92(1): 197-207.

Lin, Y. and P. F. Linden. (2005). A Model for an Underfloor Air Distribution System. Energy and Buildings, 37(4): 399-409.

Liu, M., M. Abbas, Y. Zhu and D. E. Claridge. (2001). Terminal Box Airflow Reset: An Effective Operation and Control Strategy for Comfort Improvement and Energy Conservation. ESL-HH-02-05-10. College Station, TX: Energy Systems Laboratory, Texas A&M University.

Liu, M., D. E. Claridge and W. D. Turner. (2002). Continuous Commissioning Guidebook: Maximizing Building Energy Efficiency and Comfort: Federal Energy Management Program, Office of Energy Efficiency and Renewable Energy, US Department of Energy.

Liu, Q. (2006). The Fluid Dynamics of an Underfloor Air Distribution System. Ph.D. Dissertation, University of California, San Diego, San Diego, CA.

Liu, X. H., Z. Li, Y. Jiang and B. R. Lin. (2006). Annual Performance of Liquid Desiccant Based Independent Humidity Control HVAC System. Applied Thermal Engineering, 26(11-12): 1198-1207.

Livchak, A. and C. Lowell. (2012). Don't Turn Active Beams Into Expensive Diffusers. ASHRAE Journal, 54(4): 52-60.

Loudermilk, K. (2009). Designing Chilled Beams for Thermal Comfort. ASHRAE Journal, 51(10): 58-64.

Lowenstein, A., S. Slayzak, J. Ryan and A. Pesaran. (1998). Advanced Commercial Liquid-Desiccant Technology Development Study. NREL/TP-550-24688. Golden, CO: National Renewable Energy Laboratory.

Matsuki, N., Y. Nakano, T. Miyanaga, N. Yokoo and T. Oka. (1999). Performance of Radiant Cooling System Integrated with Ice Storage. Energy and Buildings, 30(2): 177-183.

McGuinness, W. J. (1960). Valance System Both Heats and Cools. Progressive Architecture, 41: 13.

McGuinness, W. J. (1964). Valance Cooling. Progressive Architecture, 45: 148.

Melikov, A., B. Yordanova, L. Bozkhov, V. Zboril and R. Kosonen. (2007). Impact of the Airflow Interaction On Occupants' Thermal Comfort in Rooms with Active Chilled Beams. Proceedings from the 6th International Conference on Indoor Air Quality, Sendai, Japan.

Morris, M. D. (1991). Factorial Sampling Plans for Preliminary Computational Experiments. Technometrics, 33(2): 161-174.

Morris, W. (2003). The ABCs of DOAS Dedicated Outdoor Air Systems. ASHRAE Journal, 45(5): 24-29.

Mossolly, M., K. Ghali, N. Ghaddar and L. Jensen. (2008). Optimized Operation of Combined Chilled Ceiling Displacement Ventilation Systems using Genetic Algorithm. ASHRAE Transactions, 114(2): 541-554.

Mumma, S. A. (2001). Dedicated Outdoor Air in Parallel with Chilled Ceiling System. ASHRAE Transactions, 108(2): 220-231.

Mumma, S. A. and J. W. Jeong. (2005). Direct Digital Temperature, Humidity, and Condensate Control for a Dedicated Outdoor Air Ceiling Radiant Cooling Panel System. ASHRAE Transactions, 111(1): 547-558.

Nelson, I. C. (2012). A Numerical Simulations Method of Thermal Load Configuration Effect for Passive Chilled Beams. Ph.D. Dissertation, Texas A&M University, College Station, TX.

Nielsen, P. V. (1998). The Selection of Turbulence Models for Prediction of Room Airflow. ASHRAE Transactions, 104: 1119-1127.

Niu, J., J. VanderKooi and H. VanderRee. (1995). Energy Saving Possibilities with Cooled-Ceiling Systems. Energy and Buildings, 23(2): 147-158.

Novoselac, A. and J. Srebric. (2002). A Critical Review on the Performance and Design of Combined Cooled Ceiling and Displacement Ventilation Systems. Energy and Buildings, 34(5): 497-509.

Ouyang, K. and F. Haghighat. (1991). A Procedure for Calculating Thermal Response Factors of Multi-Layer Walls: State Space Method. Building and Environment, 26(2): 173-177.

Penny, J. (2012). Helping Chilled Beams to Fit Humid Climates. Buildings, 106(3): 28.

Persily, A. K. (1998). Airtightness of Commercial and Institutional Buildings. Proceedings from the ASHRAE Thermal Envelopes VII Conference, Atlanta, GA.

Pless, S. D. and P. A. Torcellini. (2005). Energy Performance Evaluation of a Low Energy Academic Building. NREL/CP-550-38962. Golden, CO: National Renewable Energy Laboratory.

Powell, G. L. (1982). ASHRAE Clear Sky Model: An Evaluation. ASHRAE Journal, 24: 32-34.

Rasouli, M., C. J. Simonson and R. W. Besant. (2010). Applicability and Optimum Control Strategy of Energy Recovery Ventilators in Different Climatic Conditions. Energy and Buildings, 42(9): 1376-1385.

Roth, K., J. Dieckmann, R. Zogg and J. Brodrick. (2007). Chilled Beam Cooling. ASHRAE Journal, 49(9): 84-86.

Roth, K. W., D. Westphalen, J. Dieckman, S. D. Hamilton and W. Goetzler. (2002). Energy Consumption Characteristics of Commercial Building HVAC Systems Volume III: Energy Savings Potential. Cambridge, MA: Building Technologies Program, U.S. Department of Energy.

Rumsey, P. (2010). Chilled Beams. Heating, Piping, Air-Conditioning Engineering, 82(1): 46-49.

Rumsey, P. and J. Weale. (2007). Chilled Beams in Labs: Eliminating Reheat & Saving Energy on a Budget. ASHRAE Journal, 49(1): 18-25.

Schiavon, S., K. H. Lee, F. Bauman and T. Webster. (2011). Simplified Calculation Method for Design Cooling Loads in Underfloor Air Distribution (UFAD) Systems. Energy and Buildings, 43(2-3): 517-528.

Schurk, D. (2012). Chilled Beam Application & Control: Hot & Humid Climates. Houston, TX: Heat Transfer Solutions.

Seidl, R. (2008). Using Demand-Based Reset Strategies. Consulting-Specifying Engineer, 44(1): 33-38.

Skistad, H., E. Mundt, P. V. Nielsen, K. Hagstrom and J. Railio. (Eds.) (2002). Displacement Ventilation in Non-Industrial Premises. Brussels, Belgium: REHVA, Federation of European Heating and Air-Conditioning Associations.

Srebric, J. and Q. Chen. (2002). Simplified Numerical Models for Complex Air Supply Diffusers. HVAC&R Research, 8(3): 277-294.

Srebric, J., V. Vukovic, G. He and X. Yang. (2008). CFD Boundary Conditions for Contaminant Dispersion, Heat Transfer and Airflow Simulations Around Human Occupants in Indoor Environments. Building and Environment, 43(3): 294-303.

Stein, J. and S. T. Taylor. (2005). It's in the Details: Engineering for Low Cost and High Efficiency. ASHRAE Journal, 47(10): 50-53.

Stein, J. and S. T. Taylor. (2013). VAV Reheat Versus Active Chilled Beams & DOAS. ASHRAE Journal, 55(5): 18-32.

Stetiu, C. (1998). Radiant Cooling in US Office Buildings: Towards Eliminating the Perception of Climate-Imposed Barriers. Ph.D. Dissertation, University of California, Berkeley, Berkeley, CA.

Sun, Y. and J.-C. Baltazar. (2013). Analysis and Improvement on the Estimation of Building Energy Savings Uncertainty. ASHRAE Transactions, 119(2): 1-8.

TRANE. (2014). TRACE 700 (Version 6.3.1). Retrieved October 2, 2014, from http://www.trane.com/commercial/north-america/us/en/products-systems/design-and-analysis-tools/analysis-tools/trace-700.html#21

U.S.DOE. (2012b). EnergyPlus Energy Simulation Software 8.1. Retrieved October 2, 2014, from http://apps1.eere.energy.gov/buildings/energyplus/

Ugursal, A. (2010). Thermal Comfort Under Transient Metabolic and Dynamic Localized Airflow Conditions Combined with Neutral and Warm Ambient Temperatures. Ph.D. Dissertation, Texas A&M University, College Station, TX.

UWM. (2012). A TRanNsient SYstems Simulation Program (Version 17). Retrieved October 2, 2014, from http://sel.me.wisc.edu/trnsys/

Vangtook, P. and S. Chirarattananon. (2006). An Experimental Investigation of Application of Radiant Cooling in Hot Humid Climate. Energy and Buildings, 38(4): 273-285.

Virta, M., D. Butler, J. Graslund, J. Hogeling, E. L. Kristiansen, M. Reinikainen and G. Svensson. (Eds.) (2007). Chilled Beam Application Guidebook. Brussels, Belgium: REHVA, Federation of European Heating and Air-Conditioning Associations.

Walton, G. N. (1983). Thermal Analysis Research Program Reference Manual. Springfield, VA: U.S. Dept. of Commerce, National Bureau of Standards.

Wang, S. (2010). Intelligent Buildings and Building Automation. London; New York: Spon Press.

Webster, T., F. Bauman, D. Dickerhoff and Y. S. Lee. (2008). Case Study of Environmental 1793 Protection Agency (EPA) Region 8 Headquarters Building, Denver, Colorado. Berkeley, CA: Center for the Built Environment, University of California, Berkeley.

Webster, T., F. Bauman and J. Reese. (2002). Underfloor Air Distribution: Thermal Stratification. ASHRAE Journal, 44(5): 28-36.

Wei, G., D. E. Claridge and M. Liu. (2000). Optimize the Supply Air Temperature Reset Schedule for a Single-Duct VAV System. ESL-HH-00-05-19. College Station, TX: Energy Systems Laboratory, Texas A&M University.

Weidner, S., J. Doerger and M. Walsh. (2009). Cooling With Less Air Using Underfloor Air Distribution and Chilled Beams. ASHRAE Journal, 51(12): 34-40.

Wetter, M. (2011). GenOpt(R) Generic Optimization Program User Manual Version 3.1.0. Berkeley, CA: Ernest Orlando Lawrence Berkeley National Laboratory.

Wetter, M. and E. Polak. (2005). Building Design Optimization using a Convergent Pattern Search Algorithm with Adaptive Precision Simulations. Energy and Buildings, 37(6): 603-612.

Wilcox, S. and W. Marion. (2008). User's Manual for TMY3 Data Sets. NREL/TP-581-43156. Golden, CO: National Renewable Energy Laboratory.

Yıldız, Y. and Z. D. Arsan. (2011). Identification of the Building Parameters that Influence Heating and Cooling Energy Loads for Apartment Buildings in Hot-Humid Climates. Energy, 36(7): 4287-4296.

Zboril, V., A. Melikov, B. Yordanova, L. Bozkhov and R. Kosonen. (2007). Airflow Distribution in Rooms with Active Chilled Beams. Proceedings from the 10th International Conference on Air Distribution in Rooms (Roomvent), Helsinki, Finland.

Zhang, Q., J. Huang and S. Lang. (2002). Development of Typical Year Weather Data for Chinese Locations. ASHRAE Transactions, 108(2): 1063-1078.

Zhou, J., G. Wei, W. D. Turner and D. E. Claridge. (2010). Airside Economizer: Comparing Different Control Strategies and Common Misconceptions. ESL-IC-08-10-54. College Station, TX: Energy Systems Laboratory, Texas A&M University.

Zhou, Y. P., J. Y. Wu and R. Z. Wang. (2007). Performance of Energy Recovery Ventilator with Various Weathers and Temperature Setpoints. Energy and Buildings, 39(12): 1202-1210.

Zhu, Y., M. Liu, D. E. Claridge, W. D. Turner and T. Powell. (1998). A Novel Procedure to Determine Optimal Air Static Pressure Setpoints and Reset Schedules in VAV Air Handling Units. ESL-HH-98-06-29. College Station, TX: Energy Systems Laboratory, Texas A&M University.

APPENDIX A

Appendix A contains the measurements conducted during the initial walkthrough of the building and the mechanical systems. It includes the AHU points verification checks and comfort baseline (temperature and CO_2) measurements in the zones.

Date: 08/10/2013 Time: 1:00pm

Table A.1: AHU points verification check

Point Description	Measured/ Observed	BAS	Notes
AHU 4A1-1			
SYSTEM WAS SWITCHED OFF			
AHU 4A1-2			
CC Leaving Temp	53.0°F	52.5°F	
SA Temp	56.7°F	56.6°F	
SA Fan Speed / SA Static Pressure	-	54% 0.43 in.W.G.	Responds to override in EMCS
AHU 4A2-1			
CC Leaving Temp	52.5°F	52.7°F	
SA Temp	58.0°F	56.3°F	
OA Damper Position	Partially open	10%	OA flow station / EMCS point seems to be malfunctioning
CHW Valve Position	-	91%	Responds to override in EMCS
SA Fan Speed / SA Static Pressure	-	53% 0.66 in.W.G	Responds to override in EMCS
AHU 4A2-2			
CC Leaving Temp	56°F	56.9°F	
SA Temp	60°F	59.5°F	
AHU 4A1-3			
SA Temp	55°F	55.1°F	
AHU 4A1-4			
SA Temp	55°F	54.1°F	
OA Damper Position			Responds to override in EMCS
CHW Valve Position			Responds to override in EMCS
AHU 5B1-1			
CC Leaving Temp	58°F	57.5°F	
SA Temp	58°F	57.1°F	SAT is lower than CCLT in BAS

Table A.1 (continued): AHU points verification check

Point Description	Measured/ Observed	BAS	Notes
AHU 5B1-1 (continued)			
OA Damper Position	Partially open	20%	OA flow station / EMCS point seems to be malfunctioning
CHW Valve Position		100%	Responds to override in EMCS
AHU 5B1-2			
CC Leaving Temp	55.5°F	54.7°F	
SA Temp	58.5°F	57.4°F	
OA Damper Position			Responds to override in EMCS
SA Fan Speed / SA Static Pressure		78% 0.71in.W.G.	Responds to override in EMCS
AHU 5B2-1			
CC Leaving Temp	55.5°F	55.5°F	
SA Temp	59.0°F	59.2°F	SAT setpoint is lower than CCLT setpoint
OA Damper Position	Closed	0%	
CHW Valve Position			Responds to override in BAS
AHU 5B2-2			
CC Leaving Temp	56.5°F	56.0°F	
SA Temp	57.5°F	57.3°F	SAT setpoint is lower than CCLT setpoint
OA Damper Position			OA damper seems to be stuck
AHU 5C1-1			
CC Leaving Temp	55.0°F	54.4°F	
SA Temp	61.0°F	61.0°F	
OA Damper Position	Partially open	40%	Responds to override in EMCS
CHW Valve Position		100%	Responds to override in EMCS
SA Fan Speed / SA Static Pressure		92% 0.7 in.W.G.	Responds to override in EMCS
AHU 5C1-2			
SYSTEM WAS SWITCHED OFF			
AHU 5C2-1			
CC Leaving Temp	56.0°F	55.4°F	
SA Temp	60.8°F	60.7°F	
SA Fan Speed / SA Static Pressure		49% 0.6 in.W.G.	Responds to override in EMCS
AHU 5C2-2			
CC Leaving Temp	57.0°F	56.6°F	
SA Temp	61.0°F	60.7°F	
OA Damper Position	Partially open	40%	OA flow station / EMCS point seems to be malfunctioning
SA Fan Speed / SA Static Pressure		49% 0.61 in.W.G.	Responds to override in BAS

Table A.1 (continued): AHU points verification check

Point Description	Measured/ Observed	BAS	Notes
AHU 5C1-3			
SA Temp	51.8°F	52.7°F	
OA Damper Position	Partially open	0%	OA flow station / EMCS point seems to be malfunctioning
CHW Valve Position		100%	CHW valve seems to stuck
SA Fan Speed / SA Static Pressure		72% 1.96 in.W.G.	

Date: 10/14/2013 Time: 2:00pm

Table A.2: Zone Temperature and CO_2 Measurements

Location	Zone Temp	UFAD Supply Temp	CO_2 Levels
Cafeteria/Kitchen/Lobby Area			
Cafeteria (North-West End)	71.0°F	N/A	674ppm
Cafeteria (South-West End)	74.0°F	N/A	
Cafeteria (South-East End)	74.3°F	N/A	
Cafeteria (Interior Zone)	71.0°F	N/A	750ppm
Serving Area 1	70.9°F	N/A	
Serving Area 2	69.7°F	N/A	
Cafeteria Lobby/Stairs	69.9°F	N/A	
Ground Floor Lobby	71.5°F	N/A	630ppm
Wing C, Floor 1			
Interior Zone (NW End)	72.0°F	65.9°F	730ppm
Exterior Zone (NW End)	69.7°F	65.3°F	677ppm
Interior Zone (SW End)	70.9°F	69.2°F	685ppm
Exterior Zone (SW End)	73.3°F		
Interior Zone (SE End)	73.3°F	68.5°F	694ppm
Exterior Zone (SE End)	74.5°F	68.9°F	
Wing C, Floor 3			
Interior Zone (NW End)	71.8°F	64.6°F	675ppm
Exterior Zone (NW End)	70.6°F		692ppm
Interior Zone (SW End)	72.9°F	68.7°F	
Exterior Zone (SW End)	74.8°F	69.1°F	671ppm
Interior Zone (SE End)	72.9°F	68.5°F	720ppm
Exterior Zone (SE End)	75.1°F	69.5°F	
Wing B, Floor 2			
Interior Zone (South End)	72.1°F	67.0°F	863ppm
Exterior Zone (South End)	74.2°F		791ppm
Exterior Zone (East End)	72.1°F	66.2°F	875ppm
Interior Zone (East End)	72.8°F		
Exterior Zone (East End)	72.5°F	66.5°F	735ppm
Wing B, Floor 4			
Interior Zone (South End)	71.8°F	68.2°F	740ppm
Exterior Zone (South End)	70.6°F		
Interior Zone (East End)	73.5°F	67.9°F	791ppm

Table A.2 (continued): Zone Temperature and CO_2 Measurements

Location	Zone Temp	UFAD Supply Temp	CO_2 Levels
Wing B, Floor 4 (continued)			
Exterior Zone (East End)	70.7°F	67.1°F	805ppm
Interior Zone (East End)	71.6°F	67.0°F	797ppm
Exterior Zone (East End)	72.8°F		
Wing A, Floor 2			
Interior Zone (SW End)	73.5°F		
Exterior Zone (SW End)	74.3°F	68.7°F	598ppm
Interior Zone (NW End)	71.4°F		
Exterior Zone (NW End)	73.1°F	69.9°F	763ppm
Interior Zone (NE End)	72.2°F		973ppm
Exterior Zone (NE End)	73.4°F	68.0°F	663ppm

APPENDIX B

Appendix B contains the calibration offset charts for the RTD sensors and the portable data loggers.

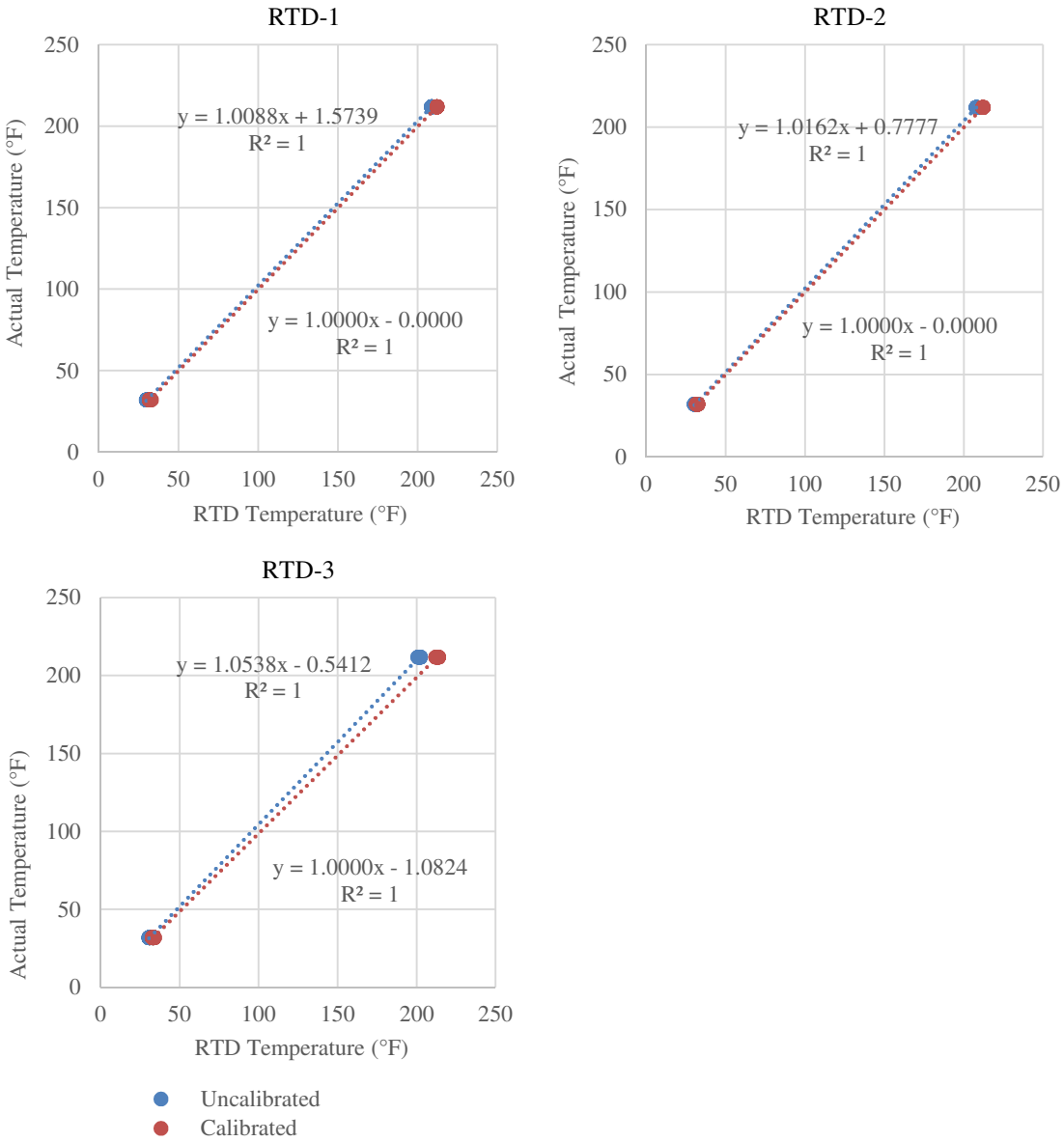

Figure B.1: Calibration Offset Graphs for the RTD Sensors Calculated from Ice-Point and Boiling Point Measurements

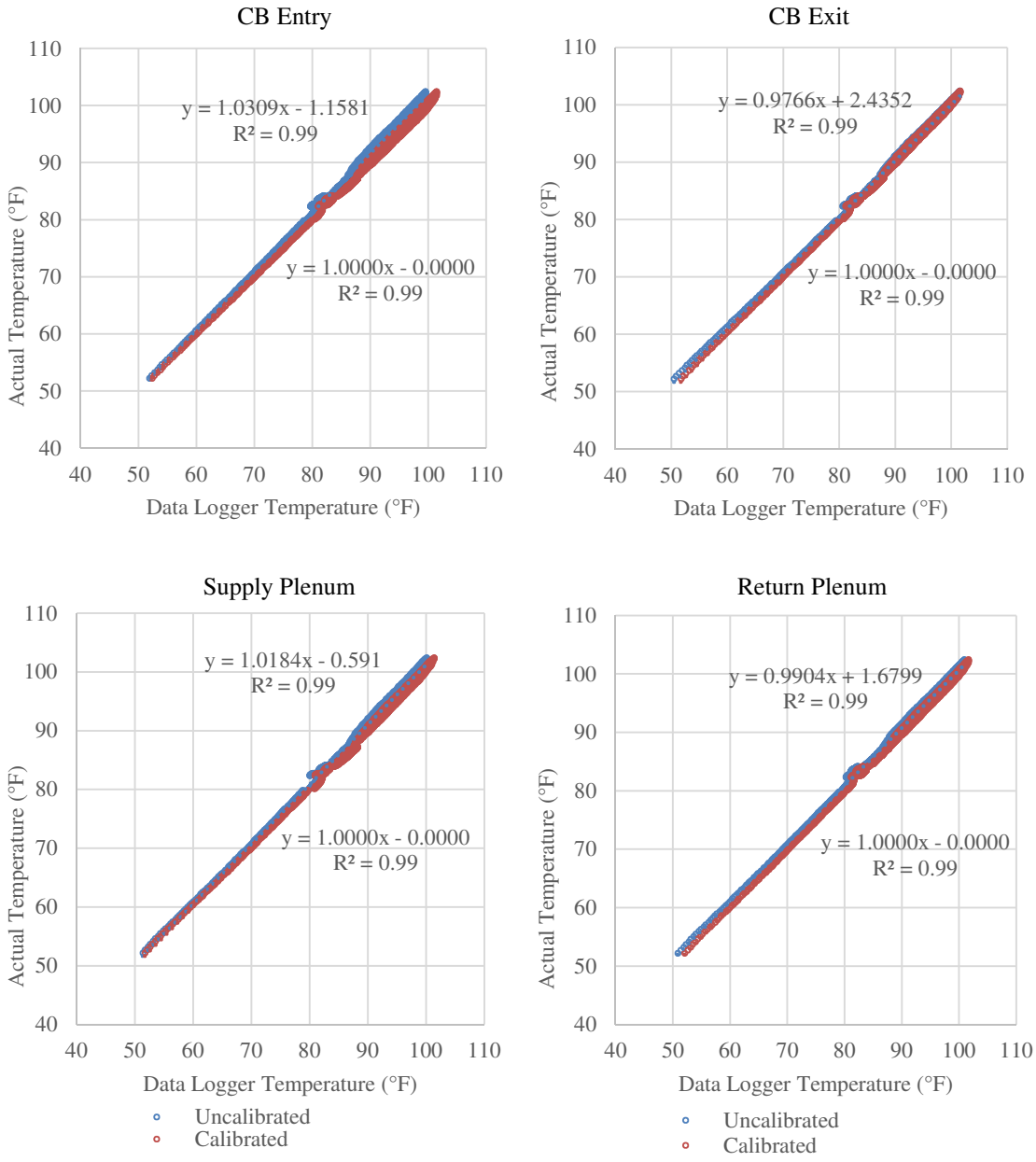

Figure B.2: Calibration Offset Graphs for the Portable Data Loggers Calculated from Cold, Ambient, Warm and Hot Measurements

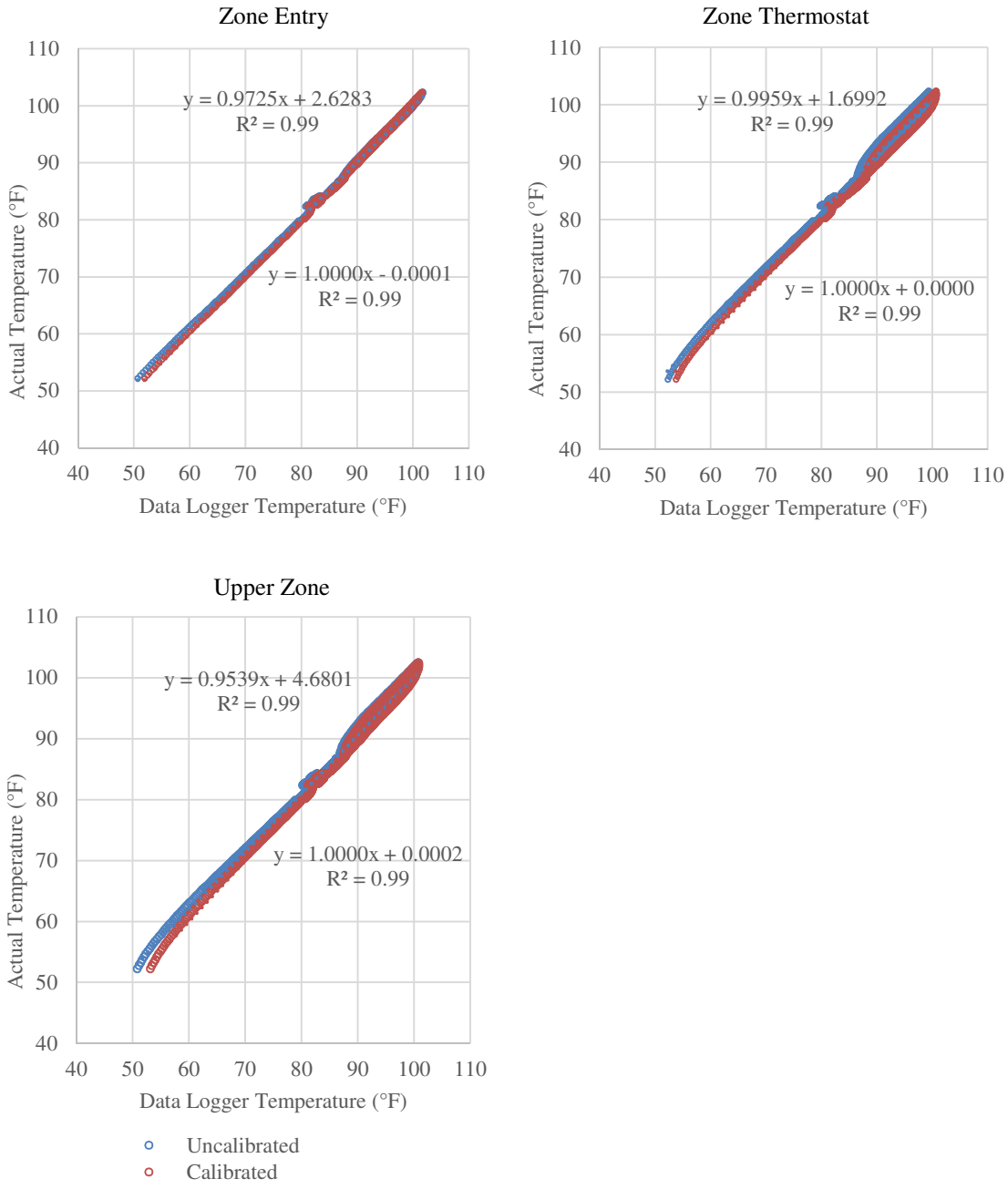

Figure B.2 (continued): Calibration Offset Graphs for the Portable Data Loggers Calculated from Cold, Ambient, Warm and Hot Measurements

APPENDIX C

Appendix C contains the code for the GenOpt® optimization program and the EnergyPlus Energy Management System used in the simulation.

C.1: Command file for GenOpt® optimization

```
/* GenOpt command file
*/
Vary{
  Parameter{    // Cooling Coil Leaving Temperature
    Name    = ClLeavTemp;
    Min     =  9.00;
    Ini     =  11.67;
    Max     =  21.11;
    Step    =   0.5;
  }
  Parameter{    // Outside Air Volume
    Name    = OAMinSched;
    Min     = 500;
    Ini     = 900;
    Max     = 900;
    Step    = 15;
  }
  Parameter{    // CHW Temperature
    Name    = ChWTemp;
    Min     = 6.67;
    Ini     = 6.67;
    Max     = 9.00;
    Step    = 0.2;
  }
}

OptimizationSettings{
  MaxIte = 500;
  MaxEqualResults = 20;
  WriteStepNumber = false;
  UnitsOfExecution = 0;
}

Algorithm{
  Main = GPSPSOCCHJ;
  NeighborhoodTopology = vonNeumann;
```

```
  NeighborhoodSize = 5;
  NumberOfParticle = 10;
  NumberOfGeneration = 10;
  Seed = 1;
  CognitiveAcceleration = 2.8;
  SocialAcceleration = 1.3;
  MaxVelocityGainContinuous = 0.5;
  MaxVelocityDiscrete = 4;
  ConstrictionGain = 0.5;
  MeshSizeDivider = 2;
  InitialMeshSizeExponent = 0;
  MeshSizeExponentIncrement = 1;
  NumberOfStepReduction = 4;
}
```

C.2: Objective function for GenOpt® optimization

```
  ObjectiveFunctionLocation
  {
     Name1      = Q_total;
      Function1  = "add( %Q_heat%, %Q_plant%, %Q_fans%, %Temp_constraint%,
      %Humidity_constraint%)";

     Name2            = Q_heat;
     Delimiter2       = "3424,";
     FirstCharacterAt2 = 1;

     Name3            = Q_plant;
     Delimiter3       = "3784,";
     FirstCharacterAt3 = 1;

     Name4            = Q_fans;
     Delimiter4       = "3671,";
     FirstCharacterAt4 = 1;

     Name5            = Temp_constraint;
     Delimiter5       = "907,";
     FirstCharacterAt5 = 1;

     Name6            = Humidity_constraint;
     Delimiter6       = "908,";
     FirstCharacterAt6 = 1;

     Name7            = CCLT;
     Function7        = %ClLeavTemp%;

     Name8            = OAF;
     Function8        = %OAMinSched%;

     Name9            = CHWST;
```

```
    Function9        = %ChWTemp%;
  }
} // end of section Simulation
```

C.3: EnergyPlus Energy Management System temperature and humidity constraint calculation program (for GenOpt® optimization)

```
EnergyManagementSystem:Sensor,
   F_WINGA_EXT_Temp,       !- Name
   F_WINGA_EXT,            !- Output:Variable or Output:Meter Index Key Name
   Zone Air Temperature;   !- Output:Variable or Output:Meter Name

EnergyManagementSystem:Sensor,
   F_WINGA_INT_Temp,       !- Name
   F_WINGA_INT,            !- Output:Variable or Output:Meter Index Key Name
   Zone Air Temperature;   !- Output:Variable or Output:Meter Name

EnergyManagementSystem:Sensor,
   S_WINGA_INT_Temp,       !- Name
   S_WINGA_INT,            !- Output:Variable or Output:Meter Index Key Name
   Zone Air Temperature;   !- Output:Variable or Output:Meter Name

EnergyManagementSystem:Sensor,
   S_WINGA_EXT_Temp,       !- Name
   S_WINGA_EXT,            !- Output:Variable or Output:Meter Index Key Name
   Zone Air Temperature;   !- Output:Variable or Output:Meter Name

EnergyManagementSystem:Sensor,
   T_WINGA_EXT_Temp,       !- Name
   T_WINGA_EXT,            !- Output:Variable or Output:Meter Index Key Name
   Zone Air Temperature;   !- Output:Variable or Output:Meter Name

EnergyManagementSystem:Sensor,
   T_WINGA_INT_Temp,       !- Name
   T_WINGA_INT,            !- Output:Variable or Output:Meter Index Key Name
   Zone Air Temperature;   !- Output:Variable or Output:Meter Name

EnergyManagementSystem:Sensor,
   F_WINGA_EXT_Hum,        !- Name
   F_WINGA_EXT,            !- Output:Variable or Output:Meter Index Key Name
   Zone Air Relative Humidity;  !- Output:Variable or Output:Meter Name

EnergyManagementSystem:Sensor,
   F_WINGA_INT_Hum,        !- Name
   F_WINGA_INT,            !- Output:Variable or Output:Meter Index Key Name
   Zone Air Relative Humidity;  !- Output:Variable or Output:Meter Name

EnergyManagementSystem:Sensor,
   S_WINGA_EXT_Hum,        !- Name
   S_WINGA_EXT,            !- Output:Variable or Output:Meter Index Key Name
```

```
   Zone Air Relative Humidity;  !- Output:Variable or Output:Meter Name

EnergyManagementSystem:Sensor,
   S_WINGA_INT_Hum,         !- Name
   S_WINGA_INT,             !- Output:Variable or Output:Meter Index Key Name
   Zone Air Relative Humidity;  !- Output:Variable or Output:Meter Name

EnergyManagementSystem:Sensor,
   T_WINGA_EXT_Hum,         !- Name
   T_WINGA_EXT,             !- Output:Variable or Output:Meter Index Key Name
   Zone Air Relative Humidity;  !- Output:Variable or Output:Meter Name

EnergyManagementSystem:Sensor,
   T_WINGA_INT_Hum,         !- Name
   T_WINGA_INT,             !- Output:Variable or Output:Meter Index Key Name
   Zone Air Relative Humidity;  !- Output:Variable or Output:Meter Name

EnergyManagementSystem:ProgramCallingManager,
   Max Zone Temp Humidity Calculations,  !- Name
   EndOfZoneTimestepBeforeZoneReporting,  !- EnergyPlus Model Calling Point
   Zone_Max_Temp,           !- Program Name 1
   Zone_Max_Humidity;       !- Program Name 2

EnergyManagementSystem:Program,
   Zone_Max_Temp,           !- Name
   SET MaxZoneTemp = @MAX F_WINGA_EXT_Temp F_WINGA_INT_Temp,  !- Program Line 1
   SET MaxZoneTemp = @MAX MaxZoneTemp S_WINGA_INT_Temp,  !- Program Line 2
   SET MaxZoneTemp = @MAX MaxZoneTemp S_WINGA_EXT_Temp,  !- A4
   SET MaxZoneTemp = @MAX MaxZoneTemp T_WINGA_INT_Temp,  !- A5
   SET MaxZoneTemp = @MAX MaxZoneTemp T_WINGA_EXT_Temp,  !- A6
   SET MaxZoneTemp = @MAX MaxZoneTemp F_WINGB_INT_Temp,  !- A7
   SET MaxZoneTemp = @MAX MaxZoneTemp F_WINGB_EXT_Temp,  !- A8
   SET MaxZoneTemp = @MAX MaxZoneTemp S_WINGB_INT_Temp,  !- A9
   SET MaxZoneTemp = @MAX MaxZoneTemp S_WINGB_EXT_Temp,  !- A10
   SET MaxZoneTemp = @MAX MaxZoneTemp FO_WINGB_INT_Temp,  !- A11
   SET MaxZoneTemp = @MAX MaxZoneTemp FO_WINGB_EXT_Temp,  !- A12
   SET MaxZoneTemp = @MAX MaxZoneTemp F_WINGC_INT_Temp,  !- A13
   SET MaxZoneTemp = @MAX MaxZoneTemp F_WINGC_EXT_Temp,  !- A14
   SET MaxZoneTemp = @MAX MaxZoneTemp S_WINGC_INT_Temp,  !- A15
   SET MaxZoneTemp = @MAX MaxZoneTemp S_WINGC_EXT_Temp,  !- A16
   SET MaxZoneTemp = @MAX MaxZoneTemp FO_WINGC_EXT_Temp,  !- A17
   SET MaxZoneTemp = @MAX MaxZoneTemp FO_WINGC_INT_Temp,  !- A18
   IF MaxZoneTemp < 22.5,   !- A19
   SET TempConstraint = 0,  !- A20
   ELSE,                    !- A21
   SET TempConstraint = 50 * (MaxZoneTemp - 22.5)^5,  !- A22
   ENDIF;                   !- A23

EnergyManagementSystem:Program,
   Zone_Max_Humidity,       !- Name
   SET MaxZoneHumidity = @MAX F_WINGA_EXT_Hum F_WINGA_INT_Hum,  !- Program Line 1
   SET MaxZoneHumidity = @MAX MaxZoneHumidity S_WINGA_INT_Hum,  !- Program Line 2
   SET MaxZoneHumidity = @MAX MaxZoneHumidity S_WINGA_EXT_Hum,  !- A4
```

```
   SET MaxZoneHumidity = @MAX MaxZoneHumidity T_WINGA_INT_Hum,  !- A5
   SET MaxZoneHumidity = @MAX MaxZoneHumidity T_WINGA_EXT_Hum,  !- A6
   SET MaxZoneHumidity = @MAX MaxZoneHumidity F_WINGB_INT_Hum,  !- A7
   SET MaxZoneHumidity = @MAX MaxZoneHumidity F_WINGB_EXT_Hum,  !- A8
   SET MaxZoneHumidity = @MAX MaxZoneHumidity S_WINGB_INT_Hum,  !- A9
   SET MaxZoneHumidity = @MAX MaxZoneHumidity S_WINGB_EXT_Hum,  !- A10
   SET MaxZoneHumidity = @MAX MaxZoneHumidity FO_WINGB_INT_Hum,  !- A11
   SET MaxZoneHumidity = @MAX MaxZoneHumidity FO_WINGB_EXT_Hum,  !- A12
   SET MaxZoneHumidity = @MAX MaxZoneHumidity F_WINGC_INT_Hum,  !- A13
   SET MaxZoneHumidity = @MAX MaxZoneHumidity F_WINGC_EXT_Hum,  !- A14
   SET MaxZoneHumidity = @MAX MaxZoneHumidity S_WINGC_INT_Hum,  !- A15
   SET MaxZoneHumidity = @MAX MaxZoneHumidity S_WINGC_EXT_Hum,  !- A16
   SET MaxZoneHumidity = @MAX MaxZoneHumidity FO_WINGC_EXT_Humm,  !- A17
   SET MaxZoneHumidity = @MAX MaxZoneHumidity FO_WINGC_INT_Hum,  !- A18
   IF MaxZoneHumidity < 60, !- A19
   SET HumidityConstraint = 0,  !- A20
   ELSE,                    !- A21
   SET HumidityConstraint = 50 * (MaxZoneHumidity - 60)^5,  !- A22
   ENDIF;                   !- A23

EnergyManagementSystem:GlobalVariable,
   TempConstraint,          !- Erl Variable 1 Name
   HumidityConstraint,      !- Erl Variable 2 Name
   MaxZoneTemp,             !- Erl Variable 3 Name
   MaxZoneHumidity;         !- A4

EnergyManagementSystem:OutputVariable,
   Temperature Constraint Penalty,  !- Name
   TempConstraint,          !- EMS Variable Name
   Averaged,                !- Type of Data in Variable
   ZoneTimestep;            !- Update Frequency

EnergyManagementSystem:OutputVariable,
   Humidity Constraint Penalty,  !- Name
   HumidityConstraint,      !- EMS Variable Name
   Averaged,                !- Type of Data in Variable
   ZoneTimestep;            !- Update Frequency
```

C.4: EnergyPlus Energy Management System chilled beam water temperature setpoint program

```
EnergyManagementSystem:Sensor,
   F_WINGA_EXT_DP,          !- Name
   F_WINGA_EXT,             !- Output:Variable or Output:Meter Index Key Name
   Zone Mean Air Dewpoint Temperature;  !- Output:Variable or Output:Meter Name

EnergyManagementSystem:Sensor,
   F_WINGA_INT_DP,          !- Name
   F_WINGA_INT,             !- Output:Variable or Output:Meter Index Key Name
   Zone Mean Air Dewpoint Temperature;  !- Output:Variable or Output:Meter Name
```

```
EnergyManagementSystem:Sensor,
   S_WINGA_INT_DP,          !- Name
   S_WINGA_INT,             !- Output:Variable or Output:Meter Index Key Name
   Zone Mean Air Dewpoint Temperature;  !- Output:Variable or Output:Meter Name

EnergyManagementSystem:Sensor,
   S_WINGA_EXT_DP,          !- Name
   S_WINGA_EXT,             !- Output:Variable or Output:Meter Index Key Name
   Zone Mean Air Dewpoint Temperature;  !- Output:Variable or Output:Meter Name

EnergyManagementSystem:Sensor,
   T_WINGA_INT_DP,          !- Name
   T_WINGA_INT,             !- Output:Variable or Output:Meter Index Key Name
   Zone Mean Air Dewpoint Temperature;  !- Output:Variable or Output:Meter Name

EnergyManagementSystem:Sensor,
   T_WINGA_EXT_DP,          !- Name
   T_WINGA_EXT,             !- Output:Variable or Output:Meter Index Key Name
   Zone Mean Air Dewpoint Temperature;  !- Output:Variable or Output:Meter Name

EnergyManagementSystem:Actuator,
   WINGA_CB_STPT,           !- Name
   Wing A CB Supply Outlet Node,  !- Actuated Component Unique Name
   System Node Setpoint,    !- Actuated Component Type
   Temperature Setpoint;    !- Actuated Component Control Type

EnergyManagementSystem:ProgramCallingManager,
   EMS CB Setpoints,        !- Name
   AfterPredictorAfterHVACManagers,  !- EnergyPlus Model Calling Point
   WingA_CB_StptCALC,       !- Program Name 1
   WingB_CB_StptCALC,       !- Program Name 2
   WingC_CB_StptCALC;       !- Program Name 3

EnergyManagementSystem:Program,
   WingA_CB_StptCALC,       !- Name
   SET Tmax = @MAX F_WINGA_EXT_DP F_WINGA_INT_DP,  !- Program Line 1
   SET Tmax = @MAX Tmax S_WINGA_EXT_DP,  !- Program Line 2
   SET Tmax = @MAX Tmax S_WINGA_INT_DP,  !- A4
   SET Tmax = @MAX Tmax T_WINGA_INT_DP,  !- A5
   SET Tmax = @MAX Tmax T_WINGA_EXT_DP,  !- A6
   IF Tmax > 12.8,          !- A7
   SET WINGA_CB_STPT = Tmax + 1.67,  !- A8
   ELSE,                    !- A9
   SET WINGA_CB_STPT = 14.5,!- A10
   ENDIF;                   !- A11
```

C.5: EnergyPlus Energy Management System AHU outside air quantity calculation program

```
EnergyManagementSystem:Sensor,
   F_A_EXT_Lat,           !- Name
   F_WINGA_EXT,           !- Output:Variable or Output:Meter Index Key Name
   Zone Total Internal Latent Gain Rate;  !- Output:Variable or Output:Meter Name

EnergyManagementSystem:Sensor,
   F_A_INT_Lat,           !- Name
   F_WINGA_INT,           !- Output:Variable or Output:Meter Index Key Name
   Zone Total Internal Latent Gain Rate;  !- Output:Variable or Output:Meter Name

EnergyManagementSystem:Sensor,
   S_A_EXT_Lat,           !- Name
   S_WINGA_EXT,           !- Output:Variable or Output:Meter Index Key Name
   Zone Total Internal Latent Gain Rate;  !- Output:Variable or Output:Meter Name

EnergyManagementSystem:Sensor,
   S_A_INT_Lat,           !- Name
   S_WINGA_INT,           !- Output:Variable or Output:Meter Index Key Name
   Zone Total Internal Latent Gain Rate;  !- Output:Variable or Output:Meter Name

EnergyManagementSystem:Sensor,
   T_A_EXT_Lat,           !- Name
   T_WINGA_EXT,           !- Output:Variable or Output:Meter Index Key Name
   Zone Total Internal Latent Gain Rate;  !- Output:Variable or Output:Meter Name

EnergyManagementSystem:Sensor,
   T_A_INT_Lat,           !- Name
   T_WINGA_INT,           !- Output:Variable or Output:Meter Index Key Name
   Zone Total Internal Latent Gain Rate;  !- Output:Variable or Output:Meter Name

EnergyManagementSystem:Sensor,
   F_A_EXT_InfLat,        !- Name
   F_WINGA_EXT,           !- Output:Variable or Output:Meter Index Key Name
   Zone Infiltration Latent Heat Gain Energy;  !- Output:Variable or Output:Meter Name

EnergyManagementSystem:Sensor,
   S_A_EXT_InfLat,        !- Name
   S_WINGA_EXT,           !- Output:Variable or Output:Meter Index Key Name
   Zone Infiltration Latent Heat Gain Energy;  !- Output:Variable or Output:Meter Name

EnergyManagementSystem:Sensor,
   T_A_EXT_InfLat,        !- Name
   T_WINGA_EXT,           !- Output:Variable or Output:Meter Index Key Name
   Zone Infiltration Latent Heat Gain Energy;  !- Output:Variable or Output:Meter Name

EnergyManagementSystem:Sensor,
   AHU4A1_RA_Hum,         !- Name
   AHU4A1 Return Fan Outlet Node,  !- Output:Variable or Output:Meter Index Key Name
   System Node Humidity Ratio;  !- Output:Variable or Output:Meter Name
```

```
EnergyManagementSystem:Sensor,
   AHU4A1_SA_Hum,          !- Name
   AHU4A1 Supply Fan Outlet Node,  !- Output:Variable or Output:Meter Index Key Name
   System Node Humidity Ratio;  !- Output:Variable or Output:Meter Name

EnergyManagementSystem:Actuator,
   AHU4A1_OA_Cntl,         !- Name
   AHU4A1 OA Controller,    !- Actuated Component Unique Name
   Outdoor Air Controller,  !- Actuated Component Type
   Air Mass Flow Rate;      !- Actuated Component Control Type

EnergyManagementSystem:ProgramCallingManager,
   AHU4A1 OA Flow Setpoints,!- Name
   InsideHVACSystemIterationLoop,  !- EnergyPlus Model Calling Point
   AHU4A1_OA_Flow_Stpt,     !- Program Name 1
   AHU5B1_OA_Flow_Stpt,     !- Program Name 2
   AHU5C1_OA_Flow_Stpt;     !- Program Name 3

EnergyManagementSystem:Program,
   AHU4A1_OA_Flow_Stpt,     !- Name
   SET AHU4A1_OA_Cntl = NULL,  !- Ventilation OA Requirements
   IF AHU4A1_RA_Hum > 0.01, !- Program Line 2
   SET F_A = F_A_EXT_Lat + F_A_INT_Lat + ((F_A_EXT_InfLat)/600),  !- A4
   SET S_A = S_A_EXT_Lat + S_A_INT_Lat + ((S_A_EXT_InfLat)/600),  !- A5
   SET T_A = T_A_EXT_Lat + T_A_INT_Lat + ((T_A_EXT_InfLat)/600),  !- A6
   SET A_LAT_TOT = F_A + S_A + T_A,  !- A7
          SET A_OA_Cntl_Lat = 0.58 * (A_LAT_TOT / (2257000 * (0.01 - AHU4A1_SA_Hum))),  !-
          Latent OA Requirements
   SET A_OA_Cntl_Vent = 4.59,  !- Minimum OA Requirements
   SET AHU4A1_OA_Cntl = @MAX A_OA_Cntl_Lat A_OA_Cntl_Vent,  !- A10
   ENDIF;                  !- A11
```

C.6: EnergyPlus Energy Management System AHU supply air quantity calculation program

```
EnergyManagementSystem:Sensor,
   AHU4A1_OA_Flow,         !- Name
   AHU4A1 CC Air Outlet Node,  !- Output:Variable or Output:Meter Index Key Name
   System Node Mass Flow Rate;  !- Output:Variable or Output:Meter Name

EnergyManagementSystem:Sensor,
   AHU4A1_CC_Temp,         !- Name
   AHU4A1 CC Air Outlet Node,  !- Output:Variable or Output:Meter Index Key Name
   System Node Temperature; !- Output:Variable or Output:Meter Name

EnergyManagementSystem:Sensor,
   AHU4A1_RA_Temp,         !- Name
   AHU4A1 Return Fan Outlet Node,  !- Output:Variable or Output:Meter Index Key Name
   System Node Temperature; !- Output:Variable or Output:Meter Name
```

```
EnergyManagementSystem:Sensor,
   AHU4A1_FanDT,           !- Name
   AHU4A1 Supply Fan,      !- Output:Variable or Output:Meter Index Key Name
   Fan Rise in Air Temperature;  !- Output:Variable or Output:Meter Name

EnergyManagementSystem:Actuator,
   AHU4A1_SA_Flow,         !- Name
   AHU4A1 Supply Fan,      !- Actuated Component Unique Name
   Fan,                    !- Actuated Component Type
   Fan Air Mass Flow Rate;  !- Actuated Component Control Type

EnergyManagementSystem:ProgramCallingManager,
   AHU4A1 SA Flow Setpoints,!- Name
   InsideHVACSystemIterationLoop,  !- EnergyPlus Model Calling Point
   AHU4A1_SA_Flow_Stpt,    !- Program Name 4
   AHU5B1_SA_Flow_Stpt,    !- Program Name 5
   AHU5C1_SA_Flow_Stpt;    !- Program Name 6

EnergyManagementSystem:Program,
   AHU4A1_SA_Flow_Stpt,    !- Name
   SET A = (AHU4A1_RA_Temp - AHU4A1_CC_Temp) * AHU4A1_OA_Flow,  !- Program Line 1
   SET B = AHU4A1_RA_Temp - (16.67 - AHU4A1_FanDT),  !- Program Line 2
   SET AHU4A1_SA_Flow = A / B;  !- A4
```

C.7: EnergyPlus Energy Management System ChW temperature setpoint calculation program for the MCB-CV-VCLT and MCB-VAV-VCLT systems

```
EnergyManagementSystem:Sensor,
   AHU4A1_Hum,             !- Name
   AHU4A1 Return Fan Outlet Node,  !- Output:Variable or Output:Meter Index Key Name
   System Node Humidity Ratio;  !- Output:Variable or Output:Meter Name

EnergyManagementSystem:Sensor,
   AHU5B1_Hum,             !- Name
   AHU5B1 Return Fan Outlet Node,  !- Output:Variable or Output:Meter Index Key Name
   System Node Humidity Ratio;  !- Output:Variable or Output:Meter Name

EnergyManagementSystem:Sensor,
   AHU5C1_Hum,             !- Name
   AHU5C1 Return Fan Outlet Node,  !- Output:Variable or Output:Meter Index Key Name
   System Node Humidity Ratio;  !- Output:Variable or Output:Meter Name

EnergyManagementSystem:Actuator,
   CHW_TEMP_STPT,          !- Name
   ChW Supply Outlet Node,  !- Actuated Component Unique Name
   System Node Setpoint,   !- Actuated Component Type
   Temperature Setpoint;   !- Actuated Component Control Type

EnergyManagementSystem:ProgramCallingManager,
```

```
    CHW Temp Setpoint,       !- Name
    InsideHVACSystemIterationLoop,  !- EnergyPlus Model Calling Point
    ChW_Temp_StptCALC;       !- Program Name 1

EnergyManagementSystem:Program,
    ChW_Temp_StptCALC,       !- Name
    IF AHU4A1_Hum > 0.01,    !- Program Line 1
    SET X = 6.67,            !- Program Line 2
    ELSE,                    !- A4
    SET X = 8.89,            !- A5
    ENDIF,                   !- A6
    IF AHU5B1_Hum > 0.01,    !- A7
    SET Y = 6.67,            !- A8
    ELSE,                    !- A9
    SET Y = 8.89,            !- A10
    ENDIF,                   !- A11
    IF AHU5C1_Hum > 0.01,    !- A12
    SET Z = 6.67,            !- A13
    ELSE,                    !- A14
    SET Z = 8.89,            !- A15
    ENDIF,                   !- A16
    SET A = @MIN X Y,        !- A17
    SET B = @MIN A Z,        !- A18
    SET CHW_TEMP_STPT = B;   !- A19
```

APPENDIX D

Appendix D documents the equations in the simplified spreadsheet-based numerical model. These equations are set up for the HVAC configuration in the case-study building and may need to be modified for other building HVAC configurations.

OA Volume for Ventilation = IF (((CO$_2$ generation * people activity * number of people) / (space CO$_2$ concentration setpoint – OA CO$_2$ concentration)) < minimum OA volume), min OA volume, ((CO$_2$ generation * people activity * number of people) / (space CO$_2$ concentration setpoint – OA CO$_2$ concentration)))

Infiltration Latent Load = IF ((OA humidity < zone humidity setpoint), 0, (4840 * Infiltration Volume * (OA humidity – zone humidity setpoint)))

Latent Load due to People = number of people * people latent heat generation

Total Latent Loads = infiltration latent load + latent load due to people

SA Volume for Ventilation = (cooling coil leaving air temperature – return air temperature) * OA volume for ventilation / ((SA temperature setpoint – temperature rise across supply fan) – return air temperature)

BA Volume for Ventilation = SA volume for ventilation – OA volume for ventilation

SA Volume for Latent Requirements = total latent loads / (4840 * (humidity setpoint – SA humidity ratio))

OA Volume for Latent Requirements = (OA volume for ventilation / SA volume for ventilation) * SA volume for latent requirements

BA Volume for Latent Requirements = SA volume for latent requirements – OA volume for latent requirements

Actual SA Volumes = MAX (SA volume for ventilation, SA volume for latent requirements)

Actual OA Volumes = MAX (OA volume for ventilation, OA volume for latent requirements)

Actual BA Volumes = MAX (BA volume for ventilation, BA volume for latent requirements)

Heat Gain across Fans = (0.00153 + 0.0052 * (volume of air across fan / total design volume) + (1.1086 * (volume of air across fan / total design volume)^2) – (0.1164 * (volume of air across fan / total design volume)^3) * peak heat gain across fan

Temperature Rise across Fans = motor efficiency * heat gain across fan / (1.08 * volume of air across fan)

Return Air Temperature = zone temperature + temperature rise across return fan

Cooling Coil Leaving Temperature = IF (OA temperature < pre-heat coil temperature setpoint, pre-heat coil temperature setpoint, IF (AND (OA temperature > 45, OA temperature < cooling coil leaving temperature setpoint), OA temperature, cooling coil leaving temperature setpoint))

RA Humidity Ratio
when coil is wet = SA humidity ratio when coil is wet + (zone latent loads / (4840 * SA volume))

when coil is dry = SA humidity ratio when coil is dry + (zone latent loads / (4840 * SA volume))

SA Humidity Ratio
when coil is wet = ((OA volume * cooling coil leaving humidity ratio) + (BA * RA humidity ratio when coil is wet)) / SA volume

when coil is dry = ((OA volume * OA humidity ratio) + (BA * RA humidity ratio when coil is dry)) / SA volume

Actual RA Humidity Ratio = MIN (RA humidity ratio when coil is wet, RA humidity ratio when coil is dry)

Actual SA Humidity Ratio = MIN (SA humidity ratio when coil is wet, SA humidity ratio when coil is dry)

Pre-heat Coil Heating Energy = IF (OA temperature > 45, 0, 1.08 * OA volume * (preheat coil temperature setpoint – OA temperature))

Cooling Coil Sensible Cooling Energy = IF (OA temperature < cooling coil leaving temperature setpoint, 0, 1.08 * OA volume * (OA temperature - cooling coil leaving temperature setpoint))

Cooling Coil Latent Cooling Energy = IF (OA humidity ratio < cooling coil leaving humidity ratio, 0, 1.08 * OA volume * (OA humidity ratio - cooling coil leaving humidity ratio))

Zone Cooling Supplied by the Ventilation System = 1.08 * zone SA volume * (zone temperature setpoint – SA temperature)

Zone Cooling Supplied by the Chilled Beam System = IF (zone sensible load – zone cooling supplied by the ventilation system < 0, 0, zone sensible load – zone cooling supplied by the ventilation system)

Zone Heating Required = IF (zone cooling supplied by the ventilation system > zone cooling load, zone cooling supplied by the ventilation system – zone cooling load + zone heating load, zone heating load)

Zone Humidity Ratio = (atmospheric pressure * RA humidity ratio) / ((0.622 * saturated vapor pressure) + (RA humidity ratio * saturated vapor pressure))

Zone Dewpoint Temperature = 243.04 * (LN (zone RH / 100) + ((17.625 * zone temperature) / (243.04 + zone temperature))) / (17.625 – LN (zone RH/100) - ((17.625 * zone temperature) / (243.04 + zone temperature)))

APPENDIX E

Appendix E contains the DDC modules used in the EMCS control diagrams. These modules are based on the modules used in the Schneider TAC I/NET Seven EMCS system.

Relay Module	
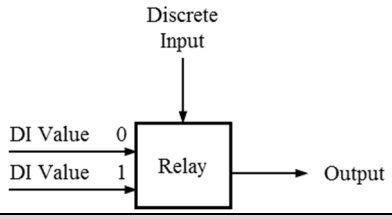	When the discrete input is 0, the state/value from the DI=0 is passed on as the output. When the discrete input is 1, the state/value from the DI=1 is passed on as the output.
CALC Module	
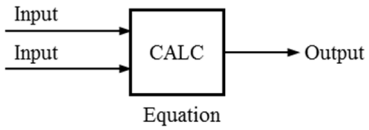	The inputs are used in the user-defined equation to calculate the outputs. The inputs can be constants or parameters.
PID Module	
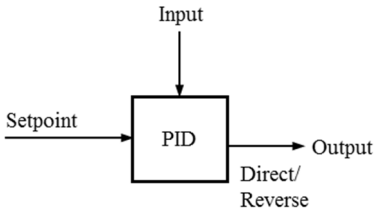	This module compares the input with the setpoint and adjusts the output to reduce the error between the input and the setpoint. Depending on the module type (direct or reverse), the output is either increased or decreased to reduce the error.
Hi/Lo Module	
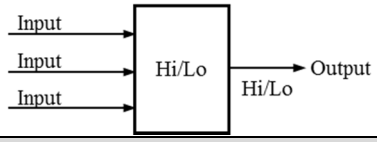	Depending on the module type (Hi or Lo), the highest or the lowest input is passed on as the output.
Two-Position Module	
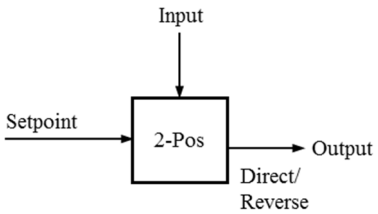	The 2-Position module compares the input to the setpoint and delivers an on/off signal as an output. In the direct mode, if the input is above the setpoint, an 'on' signal is passed on as an output. The reverse occurs in the reverse mode.